DISSERTATION

Spatially Distributed Model to Assess Watershed Contaminant Transport and Fate

Submitted by:
Mark L. Velleux
Department of Civil Engineering

In partial fulfillment of the requirements
For the Degree Doctor of Philosophy
Colorado State University
Fort Collins, Colorado
Fall 2005

COLORADO STATE UNIVERSITY

October 14, 2005

WE HEREBY RECOMMEND THAT THE DISSERTATION PREPARED UNDER OUR SUPERVISION BY MARK L. VELLEUX ENTITLED SPATIALLY DISTRIBUTED MODEL TO ASSESS WATERSHED CONTAMINANT TRANSPORT AND FATE BE ACCEPTED AS FULFILLING IN PART REQUIREMENTS FOR THE DEGREE DOCTOR OF PHILOSOPHY.

Committee on Graduate Work

Dr. Brian P. Bledsoe

Dr. Kenneth H. Carlson

Dr. William E. Sanford

Dr. Pierre Y. Julien

(Advisor)

Dr. Luis A. Garcia

(Department Head)

ABSTRACT OF DISSERTATION

SPATIALLY DISTRIBUTED MODEL TO ASSESS WATERSHED CONTAMINANT TRANSPORT AND FATE

Unmanaged contaminant releases from upland areas, transport across the land surface, and delivery to stream networks can have adverse impacts on water quality and stream ecology. Environmental management agencies need high resolution, quantitative tools to assess chemical transport and fate to formulate effective plans to address chemical impacts. To meet this need a spatially distributed, physically-based model was developed to simulate chemical transport and fate at the watershed scale. In addition to runoff and sediment transport, this new model simulates: (1) chemical erosion, advection, and deposition; (2) chemical partitioning and phase distribution; and (3) chemical infiltration and redistribution. Floodplain interactions for water, sediment, and chemicals are also simulated.

The ability of the model to simulate chemical transport and fate is demonstrated by a site-specific application to the California Gulch watershed in Colorado. Using a database of observations for the period 1984-2004, hydrology, sediment transport, and chemical transport and fate were simulated for a calibration event in June, 2003 and a validation event in September, 2003. The model accurately simulates flow volumes, peak flows, and times to peak. Average relative percent differences for flow volume were -8.6% for the calibration event and +11.3% for the validation event. The model also successfully simulated observed ranges of total suspended solids and total metals concentrations for cadmium, copper, and zinc.

Model applicability is further demonstrated for a 1-in-100-year rainfall event. Simulated flows were within the range of other estimated values. The simulated dissolved zinc load was also within the range of values extrapolated from field observations. The model was used to assess the relative impact upstream sources have on downstream areas. The chemical source tracking features of the model were demonstrated for zinc transport. The

primary source of zinc export was the lower gulch floodplain. Model results indicate that the lower gulch floodplain zinc inventory increased due to redistribution during the flood and that 76% of the imported zinc originates from nearby areas of the lower gulch watershed and 23% from the upper gulch.

Mark L. Velleux
Civil Engineering Department
Colorado State Univerity
Fort Collins, CO 80523
Fall 2005

ACKNOWLEDGEMENTS

Thank you to Dr. Pierre Julien, my advisor, for your guidance, direction, encouragement, and the opportunity to make this happen.

Thank you also to my committee: Dr. Brian Bledsoe, Dr. Ken Carlson, and Dr. Bill Sanford. Your input helped me refine my thought and think about my research in a more complete and holistic way.

I would like to especially thank John England. His knowledge, exploration of new ideas, and constant encouragement helped keep me going when the work in front of me seemed like more than I could handle. Thanks, John! We accomplished quite a bit, didn't we?

During my time at CSU, I had the honor of working with a truly amazing group of fellow students. Not least among them were Bill Annable, Bret Jordan, Mike Sixta, Jason Albert, Seema Shah, Susan Novak, Un Ji, and Max (Hui-Ming) Shih. Many others also deserve mention, especially Jamis Darrow, Lisa and Pete Fardal, Steve Sanborn, Jen Morgan, Liz Fagen, John Meyer, Elaina Holburn and Drew, Laura Girard, Paul Schmidt, Kristophe Kinzli, Amanda Lee, Chris Cuhaciyan, and Andy Darrow. If I have left anyone off this list it was unintentional.

Many thanks go to Jenifer Davis, Gloria Garza, and Mary Casey. They are the glue that keeps the ERC running.

Funding for this research was provided by the U.S. Environmental Protection Agency Region VIII Rocky Mountain Regional Hazardous Substance Research Center and the Department of Defense Center for Geosciences/Atmospheric Research. Field data for my project were provided courtesy of Dr. Carmen King and Don Stephens of the Colorado Mountain College Natural Resources Management Institute and Mike Holmes and Stan Christensen (USEPA Region VIII). Rosalia Rojas-Sanchez graciously shared her research and computer code with me.

Many friends along the way helped me more than they may realize, especially: Steve and Kirsten Westenbroek, Jim Killian, Bill Fitzpatrick, Ed Lynch, Bob Schaefer, Jo Mercurio and Terry Donovan, Carol Holden, Jim Witthuhn, Brian Burger and Sherry Gibson, and Kirk and Emmarie Burger. Thanks also to the FOTD Contra crowd in Fort Collins.

Special thanks go to Sharon Harris. Your steadfast friendship helped me stay the course and keep an even keel as I navigated the sometimes stormy waters of life in Fort Collins.

Among all my friends who helped me through this, T. Matt Boyington deserves special mention. Thank you for being there, above and beyond the call!

My family is never far from thought and has helped me in ways I cannot fully express. I thank you all, especially: the Schleden family, David and Julie Velleux, and Keith and Tyler and Lauren Velleux. Piranha Man: bite, bite!

To Diana and Charles Berndt: your boundless strength and compassion make the world a better place.

To Louis and Prudence DePaul, my grandparents, without whom none of this would have been possible. Nan and Pa, I dedicate this to you!

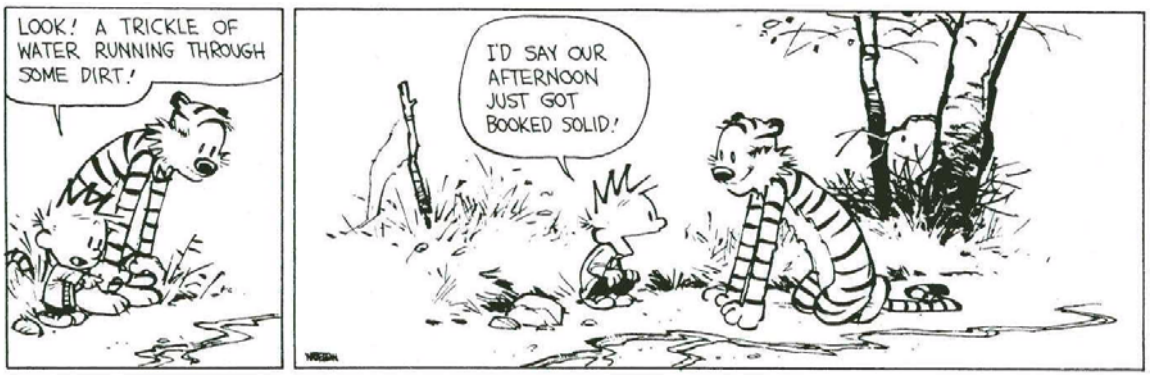

TABLE OF CONTENTS

LIST OF TABLES

LIST OF FIGURES

LIST OF SYMBOLS

a	experimentally determined constant for flocculation
A_c	cross sectional area of flow [L^2]
A_s	surface area [L^2]
B_e	width of eroding surface in flow direction [L]
B_x , B_y	flow width in the x- or y-direction [L]
$\hat{C}$	USLE soil cover factor [dimensionless]
C_c , C_{c1}	total chemical concentration in the water column [M/L^3]
C_{cb} , C_{c2}	total chemical concentration in the soil or sediment bed [M/L^3]
C_s	concentration of sediment particles in the water column [M/L^3]
C_{sb}	concentration of sediment particles in the soil or sediment bed [M/L^3]
C_t	concentration of entrained sediment particles at the transport capacity [M/L^3]
C_w	concentration of entrained sediment particles by weight at the transport capacity [dimensionless]
d_f	median floc diameter (μm) [L]
d_p	particle diameter [L]
d_*	dimensionless particle diameter [dimensionless]
D	diffusion coefficient [L^2/T]
D_e	DOC-binding effectiveness coefficient [dimensionless]
$D\frac{\partial C_s}{dx}$	diffusive flux the x-direction [M/L^2T]
$D\frac{\partial C_s}{dy}$	diffusive flux the y-direction [M/L^2T]
E	evaporation rate [L/T]

f	infiltration rate [L/T]
F	cumulative (total) infiltrated water depth [L]
f_b	fraction of the total chemical in the bound phase [dimensionless]
f_{b1}	fraction of the total chemical in bound phase in the water column [dimensionless]
f_d	fraction of the total chemical in dissolved phase [dimensionless]
f_{d1}	fraction of the total chemical in dissolved phase in the water column [dimensionless]
f_{m1}	fraction of the total chemical in the mobile phase in the water column [dimensionless] = $f_{d1} + f_{b1}$
f_{oc_D}	fraction organic carbon of DOC [dimensionless]
f_{oc_n}	fraction organic carbon of particle "n" [dimensionless]
f_{p_n}	fraction of the total chemical in the particulate phase associated with particle "n" [dimensionless]
f_{p1_n}	fraction of the total chemical in particulate phase associated with particle "n" in the water column [dimensionless]
f_{p2_n}	fraction of the total chemical in particulate phase associated with particle "n" in the sediment column [dimensionless]
g	gravitation acceleration [L/T^2]
G	particle specific gravity [dimensionless]
h	surface water depth (flow depth of water column) [L]
H_c	capillary pressure (suction) head at the wetting front [L]
H_w	hydrostatic pressure head of water (depth of water in channel) [L]
$[H^+]$	hydronium ion concentration (activity)
i_e	excess precipitation rate [L/T]
i_g	gross precipitation rate [L/T]
i_n	net (effective) rainfall rate at the surface [L/T]

J_c	sediment transport capacity areal flux [M/L^{2}T]
J_d	deposition flux [M/L^2/T]
J_{dc}	chemical deposition flux [M/L^{2}T]
$\hat{J}_d$	sediment deposition volumetric flux [M/L^{3}T]
J_e	erosion flux [M/L^{2}T]
J_{ec}	chemical erosion flux [M/L^{2}T]
$\hat{J}_e$	sediment erosion volumetric flux [M/L^{3}T]
J_{ic}	chemical infiltration flux [M/L^{2}T]
$\hat{J}_n$	net sediment transport volumetric flux [M/L^{3}T]
J_{xc} , J_{yc}	chemical advective flux in the x- or y-direction [M/L^{2}T]
$\hat{K}$	USLE soil erodibility factor [dimensionless]
K_d	chemical distribution coefficient [L^3/M]
K_h	effective hydraulic conductivity [L/T]
K_p	chemical partition coefficient [L^3/M]
K_{oc}	organic carbon normalized partition coefficient [L^3/M]
L_c	length of channel in flow direction [L]
m	experimentally determined constant for flocculation
m_n	concentration of particle "n" [M/L^3]
n	Manning roughness coefficient [T/L$^{1/3}$]
P	probability integral for the Gaussian distribution
P_c	wetted perimeter of channel flow [L]
$\hat{P}$	USLE soil management practice factor [dimensionless]
P_{dep}	probability of deposition [dimensionless]
pH	-log[H$^+$]

q	unit flow rate of water = $v_a\, h$ [L^2/T]
Q	total discharge [L^3/T]
q_c	critical unit flow for erosion (for the aggregate soil matrix) [L^2/T]
q_l	lateral unit flow from overland plane to channel (floodplain) [L^2/T]
q_s	total sediment transport capacity (kg/m s) [M/LT]
q_x , q_y	unit discharge in the x- or y-direction = Q_x/B_x , Q_y/B_y [L^2/T]
Q_x , Q_y	flow in the x- or y-direction [L^3/T]
$\hat{q}_{tx}$, $\hat{q}_{ty}$	total sediment transport areal flux in the x- or y-direction [M/L^2T]
R	Retardation factor [dimensionless]
R_h	hydraulic radius of flow = A_c/P [L]
R_x , R_y	dispersion (mixing) coefficient the x- or y-direction [L^2/T]
$R_x \frac{\partial C_s}{dx}$	dispersive flux the x-direction [M/L^2T]
$R_y \frac{\partial C_s}{dy}$	dispersive flux the y-direction [M/L^2T]
S_e	effective soil saturation [dimensionless]
S_f	friction slope [dimensionless]
S_{fx} , S_{fy}	friction slope (energy grade line) in the x- or y-direction [dimensionless]
S_i	interception capacity of projected canopy per unit area [L^3/L^2]
S_0	ground surface slope [dimensionless]
S_{0x} , S_{0y}	ground surface slope in the x- or y-direction [dimensionless]
t	time [T]
T	cumulative (total) depth of water transported by transmission loss [L]
t_l	transmission loss rate [L/T]
t_R	precipitation event duration [T]

u_*	shear velocity [L/T]
v_a	advective (flow) velocity (in the x- or y-direction) [L/T]
v_c	critical velocity for for soil or sediment erosion [L/T]
v_f	flow velocity between overland plane and channel (floodplain) [L/T]
V_g	gross precipitation water volume [L^3]
v_i	infiltration rate or transmission loss velocity of water [L/T]
V_i	interception volume [L^3]
V_n	net precipitation volume reaching the surface [L^3]
v_r	resuspension (erosion) velocity [L/T]
v_s	quiescent settling velocity [L/T]
v_{se}	effective settling (deposition) velocity [L/T]
v_{sf}	floc settling velocity (cm/s) [L/T]
v_r	resuspension (erosion) velocity [L/T]
v_x , v_y	advective (flow) velocity in the x- or y-direction [L/T]
$v_x C_s$	advective flux in the x-direction = J_x [M/L^2T]
$v_y C_s$	advective flux in the y-direction = J_y [M/L^2T]
V_s	volume of sediments [L^3]
V_w	volume of water [L^3]
W	unit discharge from/to a point source/sink [L^2/T]
$\hat{W}_s$	sediment point source/sink volumetric flux [M/L^3T]
$W_{w,s,c}$	material point source/sink: water [L^3/T], solids, or chemical [M/T]
z	elevation of the soil surface or sediment bed [L]
α_x , α_y	resistance coefficient for flow in the x- or y-direction [$L^{1/3}/T$]
β	resistance exponent = 5/3 (assuming Manning resistance) [dimensionless]
ν	kinematic viscosity of water [L^2/T]

ν_x	particle interaction parameter [dimensionless]
ω_0	settling velocity [L/T]
ρ_b	bulk density of soil or bed sediments [M/L^3]
τ_0	bottom shear stress (M/LT^2)
$\tau_{cd,c}$	critical shear stress for deposition of cohesive particles, defined as the shear stress at which 100% of the particles deposit (M/LT^2)
$\tau_{cd,n}$	critical shear stress for deposition of non-cohesive particles, defined as the shear stress at which 50% of particles deposit (M/LT^2)
φ	total soil porosity [dimensionless]
θ_e	effective soil or sediment porosity = (φ-θ_r) [dimensionless]
θ_r	residual soil or sediment moisture content [dimensionless]
σ	experimentally determined constant for deposition
$¶_b$	equilibrium binding coefficient [L^3/M]
$¶_{p_n}$	equilibrium partition (distribution) coefficient for particle "n" [L^3/M]
$¶_{px_n}$	particle-dependent partition coefficient [L^3/M]
$s\big\|_{t+dt}$	value of model state variable at time $t+dt$ [L] or [M/L^3]
$s\big\|_t$	value of model state variable at time t [L] or [M/L^3]
$\left.\frac{\partial s}{\partial t}\right\|_t$	value of model state variable derivative at time t [L/T] or [M/L^{3}T]

1.0 INTRODUCTION

1.1 OVERVIEW

The unmanaged release of contaminants from upland source areas, their transport across the land surface, and delivery to stream networks can have adverse water quality and ecological impacts. Examples include the transport of acid mine drainage and metals from mining areas and metals and organic chemicals from military training ranges. Environmental management agencies need high resolution, quantitative tools to assess chemical transport and fate at the watershed scale to formulate effective management plans that address chemical impacts. The need for high resolution is driven by the fact that contaminant occurrence and transport conditions are often highly heterogeneous and can differ significantly across small spatial and temporal scales. Existing watershed models do not meet this need because they generally lack the spatial resolution and sediment and chemical transport features needed to accurately represent contaminant source heterogeneity and transport.

To meet this need a fully distributed, physically-based numerical modeling framework to simulate chemical transport and fate at the watershed scale was developed. In addition to hydrology and sediment transport, this new framework simulates chemical partitioning and phase distribution, advection, erosion, deposition, and dissolved phase infiltration in surface water, soil, and sediment. Floodplain interactions are also simulated and include the bi-directional exchange of water, sediment, and chemicals between upland areas and stream channels. The ability of this numerical modeling framework to simulate chemical transport and fate is demonstrated by a site-specific model application to the California Gulch watershed. Located in the mountains surrounding Leadville, Colorado, this watershed is contaminated with wastes from mining activities. More than 2,000 mine waste piles are scattered across the land surface of the site. Chemicals of specific concern include cadmium (Cd), copper (Cu), and zinc (Zn).

1.2 OBJECTIVES

The objectives of this research were to:

1. Develop a fully distributed, physically-based numerical model to simulate the watershed-scale transport and fate of chemicals;
2. Calibrate and validate the model by a site-specific application to the California Gulch (Leadville, Colorado) watershed; and
3. Demonstrate model applicability by simulation of an extreme storm, the 1-in-100-year event, at the California Gulch site.

1.3 APPROACH AND METHODOLOGY

The approach used entailed: 1) computer modeling of processes that affect sediment and chemical transport across land surfaces and delivery to receiving surface waters; 2) use of field data for model parameterization, calibration, and validation by a case study application; and 3) demonstration of model applicability to assess the relative impacts that chemical transport from upland sources have on downstream areas.

The CASC2D (CASC2D-SED) watershed model (Johnson et al. 2000; Julien and Rojas, 2002) was selected as the initial basis to develop a fully distributed watershed chemical transport and fate modeling framework. The basic CASC2D framework is an event-based model that provides mechanisms to simulate overland flow, surface erosion and deposition, channel flow and sediment transport through stream channels. As part of model development efforts, the hydrologic and sediment transport components of CASC2D were significantly expanded and enhanced to support the addition of chemical transport features. Chemical transport and fate components were formulated based on those found in the USEPA WASP/IPX series of stream water quality models (Ambrose et al. 1993; Velleux et al. 2001). These chemical transport and fate components were the added to an expanded CASC2D chassis to create a new, fully distributed model to simulate contaminant transport and fate at the watershed scale.

The ability of the new watershed modeling framework to simulate chemical transport and fate is demonstrated by a site-specific model application to the California Gulch watershed. The conditions simulated include surface hydrology, sediment transport, and chemical transport and fate for three metals: cadmium (Cd), copper (Cu), and zinc (Zn). A database of field observations collected between 1984 and 2004 as part of characterization and remediation efforts for the site was compiled. These data were used to define initial and boundary conditions, especially the physical and chemical characteristics of soil and sediment. The model was parameterized based on observed storm conditions. A June 2003, storm event was used for model calibration. A September 2003, event was used for model validation. The parameterized model was then used to simulate an extreme storm: the 1-in-100-year, 2-hour duration event. Results of the extreme storm simulation were used to assess the relative impacts that contaminants from different upland source areas have on downstream conditions.

2.0 LITERATURE REVIEW

2.1 WATERSHED MODELS

A brief review of watershed models was conducted to select a basic structure for development of a fully distributed watershed chemical transport and fate modeling framework. This review was conducted with the goal of developing a framework with metals as specific chemicals of consideration applicable to high gradient, mountain watershed environments. A range of watershed modeling methods and frameworks exist. Methods include unit hydrograph/lumped parameter, advanced lumped parameter/semi-distributed, and fully distributed, physically based approaches.[1] Singh (1995) presents descriptions of numerous watershed models. As part of initial screening, unit hydrograph/lumped parameter models such as HEC-1 (USACE, 1998) and TR-55 (USDA, 1986) were not considered viable for development as watershed chemical transport models because these frameworks lack sediment transport features and do not permit the needed degree of spatial variation of model parameters (the spatial properties of soil and sediment are expected to vary widely, as are metals concentrations, as a function of the spatial distribution of chemical sources such as mine wastes).

After initial screening, a range of potential models remained for further review. In particular, HSPF (Johanson et al. 1980; Donigian et al. 1984; Bicknell et al. 1997; Bicknell et al. 2001), KINEROS (Woolhiser et al. 1990), SWAT (Neitsch et al. 2002), SHETRAN (Ewen et al. 2000), and CASC2D (CASC2D-SED) (Johnson et al. 2000; Julien and Rojas, 2002) were more closely examined. Brief reviews of these frameworks are presented. Based on these reviews, CASC2D was selected as the basic structure for

[1] Absolute distinctions between approaches are somewhat subjective. For example, lumped parameter models that can treat a watershed as a number of sub-basins can be considered equivalent to semi-distributed models while fully distributed models with limited spatial variation of parameters can approach the performance of lumped parameter models.

development of the new watershed chemical transport and fate modeling framework. The basis for this selection follows the reviews.

2.1.1 HSPF

HSPF (Hydrologic Simulation Program–Fortran) (Johanson et al. 1980; Donigian et al. 1984; Bicknell et al. 1997; Bicknell et al. 2001) has its origins in the Stanford Watershed Model (Crawford and Linsley, 1966) and can be classified as an advanced lumped parameter or semi-distributed model. Among its processes and state variables, HSPF simulates interception, infiltration, soil moisture, surface runoff, interflow, base flow, snowpack depth and water content, snowmelt, evapotranspiration, groundwater recharge, dissolved oxygen (DO) and biochemical oxygen demand (BOD), temperature, pesticides, fecal coliform bacteria, sediment detachment and transport, sediment routing by particle size, channel routing, reservoir routing, constituent routing, pH, nitrogen and phosphorus compounds, and plankton. Hydrologic processes are represented as flows and storages. Routing is performed using a modified form of the kinematic wave equation. Generally, flow is a one-dimensional outflow from storage, expressed as a function of the present storage amount and the physical characteristics of the subsystem. Although the overall model is physically based, many of the flows and storages are represented in a simplified or conceptual manner. This requires use of calibrated parameters but has the advantage of avoiding the need to explicitly specify all physical dimensions and characteristics of the flow system.

HSPF has been used for a wide variety of spatial scales from the Chesapeake Bay watershed (160,000 km^2) to small (a few acres) experimental plots near Watkinsville, Georgia. The model is best used for continuous simulation of hydrology and water quality in watersheds. To simulate chemical transport, HSPF incorporates the watershed-scale NonPoint Source (NPS) (Donigian and Crawford, 1976a) Agricultural Runoff Management (ARM) (Donigian and Crawford, 1976b; Donigian et al. 1977), and Sediment and Radionuclides Transport (SERATRA) (Onishi and Wise, 1979) models into a framework that includes fate and transport in one dimensional stream channels. HSPF simulates three sediment types (sand, silt, and clay) in addition to a single organic

chemical and transformation products of that chemical. However, it does not simulate metals. HSPF (Version 11.0) source code is publicly available.

2.1.2 KINEROS

KINEROS (Kinetic Runoff and Erosion) (Woolhiser et al. 1990) is a semi-distributed, physically based, event-oriented model that simulates rainfall, interception, infiltration, surface runoff and erosion. A rainfall record is used to describe the spatial and temporal distribution of rainfall to simulate runoff for a catchment. A watershed is represented by a (cascading) series of planes and channels (open channels or pipes). The kinematic wave approximation and the Manning equation are used for one-dimensional flow routing. Infiltration is determined using the Smith-Parlange (1978) equation. KINEROS does not include groundwater flow processes other than infiltration and overland flow is Hortonian. Erosion overland is represented by splash and hydraulic rate components and a transport capacity relation of the form summarized by Julien and Simons (1985), such as tractive force (Meyer and Wischmeier, 1969), unit stream power (Yang, 1973), Ackers and White (1973), and Engelund and Hansen (1967). Erosion in channels is similar with the exception that splash erosion is neglected and lateral inflow is not. Deposition is computed from particle fall velocity for the particle concentration in excess of the concentration computed from the transport capacity equation. Sediment transport is represented for a single effective grain size (d_{50}) that can vary by element in the model domain. KINEROS (Version 2) source code is publicly available.

2.1.3 SWAT

SWAT (Soil and Water Assessment Tool) (Neistch et al. 2002) is an advanced lumped/semi-distributed, physically based, continuous simulation model that simulates rainfall, infiltration, flow routing through basin streams and reservoirs (including lateral flow, groundwater flow, and transmission losses), and sediment and chemical transport through ponds, reservoirs, and streams. Simulated watersheds can be divided into sub-basins or hydrologic response units. SWAT was developed to predict the impact of land management practices on water, sediment and agricultural chemical yields in large complex watersheds with varying soils, land use and management conditions over long

periods of time. Major components model include weather, hydrology, erosion, soil temperature, crop growth, nutrients, pesticides, subsurface flow, and agricultural management. Instream chemical transport in SWAT is based on algorithms adapted from the QUAL2E (Brown and Barnwell, 1987) stream water quality model and includes first-order decay relationships for algae, dissolved oxygen (DO), carbonaceous biochemical oxygen demand (CBOD), as well as nitrogen and phosphorus compounds. However, it does not simulate metals. Bian et al. (1996) linked SWAT with the Arc/Info geographic information system (GIS).

Soil profiles can be divided into ten layers. Infiltration is computed as precipitation minus runoff (SCS curve number approach) or using the Green and Ampt (1911) relationship. Infiltration moves into the soil profile and is routed through the soil layers. A storage routing coefficient is used to compute flow through each layer, with flow occurring when a layer exceeds field capacity. When water percolates past the bottom layer of the soil profile, it enters the shallow aquifer zone (Arnold et al. 1993). Channel transmission losses and pond/reservoir seepage replenish the shallow aquifer layer, which can interact directly with the stream. Flow to the deep aquifer system is lost and cannot return (Arnold et al. 1993). An irrigation algorithm allows water transfers from any reach or reservoir to any other in the watershed. Based on surface runoff calculated using the SCS runoff equation, excess surface runoff not lost to other pathways is delivered to the channel network and is routed downstream. Sediment erosion for stream transport is determined with the Modified Universal Soil Loss Equation (MUSLE) (Williams, 1975). For sediment routing, deposition is based on fall velocities for various sediment sizes. Channel degradation rates are determined using the Bagnold (1977) stream power equation. Sediment size is estimated from the primary particle size distribution (Foster et al. 1980) for soils the described in the STATSGO database (USDA, 1991). Stream power is also used in the sediment routing routine to calculate re-entrainment of loose and deposited material in the system until all of the material has been removed. SWAT is a continuous time (long-term yield) model and is not designed to simulate detailed, single-event flood routing (Neistch et al. 2002). SWAT (Version 2000) source code is publicly available.

2.1.4 SHETRAN

SHETRAN (Ewen et al. 2000; Ewen et al. 2002) has its origins in the Système Hydrologique Europèen (SHE) (Abbott et al. 1986a,b) and is a fully distributed, physically based model. Among its processes and state variables are interception, infiltration, surface runoff, groundwater flow in saturated and unsaturated zones including aquifers, snowpack and snowmelt, evapotranspiration, channel transmission losses, sediment erosion and deposition for multiple particle classes, and chemical transport and fate including advection, dispersion, erosion, deposition, partitioning, and decay. For surface waters, flow routing is performed using the diffusive wave approximation and is two-dimensional overland and one-dimensional in channels. For the subsurface, flow is variably saturated and three-dimensional.

SHETRAN can be applied to a wide variety of spatial scales from large (2,500 km^2) contiguous river basins with multiple sub-basins, to single or partial watersheds, to individual hillslopes and catchments (0.94 km^2) (Bathurst et al. 2004). However, most applications summarized in the literature are for small catchment areas (<2 km^2). Sediment transport processes in SHETRAN are derived from those in the earlier SHESED framework (Wicks and Bathurst, 1996). Overland erosion is computed based on raindrop impact and hydraulic erosion rates similar to the approach used in KINEROS. Channel erosion is computed using the Ackers and White (1973), Engelund and Hansen (1967), and Day (1980) (a modification to the Ackers and White approach) methods. Unfortunately, SHETRAN model source code (and documentation) could not be obtained and is not publicly available.

2.1.5 CASC2D

CASC2D (CASC2D-SED) (Julien and Saghafian, 1991; Julien et al. 1995; Johnson et al. 2000; Ogden and Julien, 2002; Rojas, 2002; Julien and Rojas, 2002) is a fully distributed, physically based, event-oriented model that simulates rainfall, interception, infiltration, overland flow, channel flow, as well as sediment erosion and deposition. For surface waters, flow routing is performed using the diffusive wave approximation and is two-dimensional overland and one-dimensional in channels. CASC2D does not include groundwater flow processes other than infiltration and overland flow is Hortonian.

However, it can be directly coupled with GIS-based site characterization data obtained from remote sensing sources.

CASC2D has been applied at a wide variety of spatial scales from large river basins (12,000 km^2) to moderate watersheds (560 km^2) (Molnár and Julien, 2000) to small watersheds (20-30 km^2) (Rojas, 2002). Overland erosion is computed using a modified form of the Kilinc-Richardson (1973) method (Johnson et al. 2000). Channel erosion is computed using the Engelund and Hansen (1967) method. Up to three solids classes can be simulated (Rojas, 2002). Chemical transport and fate is not simulated. CASC2D source code is publicly available.

It should be noted that variants of CASC2D exist (Ogden, 1997), including the Gridded Surface Subsurface Hydrologic Analysis (GSSHA) model (Downer and Ogden, 2004). These variants may offer some improvement relative to CASC2D in terms of representation of subsurface flows. However, source codes for GSSHA or other variants are not publicly available.

2.1.6 Basis for Selection of CASC2D as the Framework for Further Development

The criteria for selection of a framework for further development were:

1. Availability of source code;
2. Model support for fully distributed parameters;
3. Compatibility with raster GIS to facilitate model use;
4. Support for a two-dimensional overland routing approach;
5. Support for multiple solids and chemical types in a single simulation; and
6. Ability to simulate event hydrology.

HSPF is a capable and well-proven tool and has some chemical transport components. However, the sub-basin approach used for segmentation may prevent the model from being used with fully distributed parameters. As a result, HSPF is not expected to be fully compatible with raster GIS without loss of spatial detail because raster cells would likely

need to be aggregated into the sub-basin units the model supports. While the model source code is modular, it is limited to three solids state variables (sand, silt, and clay) and just one chemical. As the intended use of the final watershed chemical transport and fate modeling framework is to simulate multiple solids and chemical types (i.e. many solids and chemical types are needed for particle and chemical source tracking applications), the level of effort needed to expand the sediment and chemical transport features of HSPF was judged to be excessive. Further, the one-dimensional overland routing approach used in the model may not be adequate to resolve transport over terrain with very large slopes. Finally, the minimum model numerical integration time step that can be used during a simulation is one minute. This time step is too large to support high intensity rainfall events at fine spatial scales (e.g. 30 m by 30 m cells). Because of these potential limitations, HSPF was not judged to be an adequate framework for further chemical transport and fate model development.

KINEROS is in several respects similar to CASC2D. It is event-oriented and physically based. Like HSPF, the sub-basin approach used in KINEROS for segmentation may prevent the model from being used with fully distributed parameters. However, the biggest limitations to KINEROS are that it is limited to a single solids type, does not have chemical transport components, and uses a one-dimensional overland routing approach. Given these potential limitations, KINEROS was not judged to be an adequate framework for further chemical transport and fate model development.

SWAT is also a capable tool and has some chemical transport components. One of its more interesting features is that has been coupled to standard GIS tools (i.e. ArcSWAT) to facilitate model use. Unfortunately, SWAT also used a sub-basin approach for segmentation and so is not fully distributed. As a result, despite the model coupling to GIS tools, some loss of spatial detail is expected because raster cells would likely need to be aggregated into the sub-basin units the model supports. However, the biggest limitation to use of SWAT is that it is not designed to simulate detailed, single-event flood routing (Neistch et al. 2002). Consequently, despite its other qualities, SWAT was not judged to be an adequate framework for further chemical transport and fate model development.

In many respects, SHETRAN appears to be a good choice for selection as a framework for further development because it has some chemical transport and fate components, allows for detailed representation of the soil column with depth, has extensive groundwater flow features, and supports fully distributed model parameters. Further, it uses a two-dimensional overland routing approach. Unfortunately, SHETRAN source code is not publicly available and therefore cannot be used for further development.

CASC2D (CASC2D-SED) was the best overall choice for selection as a framework for further watershed chemical transport and fate model development. Beyond its history of development and use at Colorado State University, CASC2D is event-oriented, fully distributed, can be directly coupled with outputs from GIS sources, and use a two-dimensional overland routing approach. Unfortunately, sediment transport is limited to just three solids types. However, the CASC2D source code can be easily modified to support an unlimited number of solids types. Also, although it lacks chemical transport components, the CASC2D source code is amenable to restructuring to support incorporation of chemical transport and fate processes modules based on those present in the USEPA WASP/IPX series of stream water quality models. It is again worth noting CASC2D derivatives, such as GSSHA, cannot be used for development because source code is not readily available.

2.2 WATERSHED MODEL PROCESSES

A review of hydrologic and sediment transport process descriptions is informative to illustrate the physics behind individual model process representations. The processes reviewed are specific to those needed to formulate a fully distributed watershed chemical transport and fate model framework applicable to contaminants such as metals. The major components of the framework are hydrology, sediment transport, and chemical transport and fate. Each of the major components can be viewed as submodels within the overall framework. The reviews that follow are grouped by submodel.

2.3 HYDROLOGIC PROCESSES

The main processes in the hydrologic submodel are: (1) rainfall and interception; (2) infiltration and transmission loss; (3) storage; and (4) overland and channel flow.

2.3.1 Rainfall and Interception

The hydrologic cycle begins with precipitation reaching the near surface of the land or water. Precipitation includes both rainfall and snowfall. Since snowfall can be represented as an equivalent depth (or volume) of water, it may be expressed as equivalent precipitation. The gross volume of water reaching the near surface is:

$$\frac{\partial V_g}{\partial t} = i_g A_s \tag{2.1}$$

where: V_g = gross precipitation water volume [L^3]

i_g = gross precipitation rate [L/T]

A_s = surface area over which precipitation occurs [L^3]

t = time [T]

Interception is the reduction in the volume of gross precipitation due to water retention by vegetative cover. As precipitation falls to the surface, a portion of the gross precipitation at the surface may contact vegetative canopy and may be held on foliage by surface tension (Eagleson, 1970). Much of the precipitation falling during the early period of an event may be stored on vegetative surfaces (Linsley et al. 1982). Intercepted water can return to the atmosphere by evaporation. Alternatively, intercepted water may reach the land surface when the force of gravity acting of water drops exceeds the surface tension force holding water to plant surfaces. Conceptually, interception may be represented as a volume. The net rainfall volume equals the gross rainfall volume minus the volume lost to interception (Linsley et al. 1982):

$$V_i = \left(S_i + Et_R\right)A_s \tag{2.2}$$

$$V_n = V_g - V_i \qquad for: V_g > V_i$$
$$V_n = 0 \qquad for: V_g \le V_i \tag{2.3}$$

where: V_i = interception volume [L^3]

S_i = interception capacity of projected canopy per unit area [L^3/L^2]

E = evaporation rate [L/T]

t_R = precipitation event duration [T]

V_n = net precipitation volume reaching the surface [L^3]

Note that when the cumulative gross rainfall volume that occurs during an event is less than the interception volume, the net rainfall volume (or depth) reaching the land surface is zero. For single storm events, recovery of interception volume by evaporation can be neglected. The net precipitation volume may also be expressed as a net (effective) precipitation rate:

$$i_n = \frac{1}{A_s}\frac{\partial V_n}{\partial t} \tag{2.4}$$

where: i_n = net (effective) rainfall rate at the surface [L/T]

2.3.2 Infiltration and Transmission Loss

Infiltration is the downward transport of water from the surface to the subsurface. The rate at which infiltration occurs may be affected by several factors including hydraulic conductivity, capillary action and gravity (percolation) as the soil matrix reaches saturation. Many relationships have been used to describe infiltration including expressions presented by Green and Ampt (1911), Richards (1931), Philip (1957), and Smith and Parlange (1978). The Green and Ampt relationship is often used because of its ease of application. This relationship assumes a sharp wetting front exists between the infiltration zone and soil at the initial water content (piston flow) and that the length of the wetted zone increases as infiltration progresses. Neglecting the depth of ponding at the surface (i.e. assuming that the pressure head is much smaller than the suction head),

the general equation showing the Green and Ampt relationship can be expressed as (Li et al. 1976; Julien, 2002):

$$f = K_h\left(1 + \frac{H_c(1 - S_e)\theta_e}{F}\right) \tag{2.5}$$

where: f = infiltration rate [L/T]

K_h = effective hydraulic conductivity [L/T]

H_c = capillary pressure (suction) head at the wetting front [L]

θ_e = effective soil porosity = (φ-θ_r) [dimensionless]

φ = total soil porosity [dimensionless]

θ_r = residual soil moisture content [dimensionless]

S_e = effective soil saturation [dimensionless]

F = cumulative (total) infiltrated water depth [L]

Similar to infiltration in overland areas, water in stream channels may be lost to the subsurface by transmission loss. The rate at which transmission loss occurs in a channel may be affected by several factors, particularly hydraulic conductivity. For ephemeral streams, capillary suction head may be significant when stream sediments are unsaturated. Relationships to describe the volume of transmission loss are presented by Lane (1983). Abdullrazzak and Morel-Seytoux (1983) and Freyberg (1983) use the Green and Ampt (1911) relationship to assess transmission loss. Following the form of the Green and Ampt relationship and accounting for the depth of (ponded) water in the stream channel (hydrostatic head), the transmission loss rate may be expressed as:

$$t_l = K_h\left(1 + \frac{(H_w + H_c)(1 - S_e)\theta_e}{T}\right) \tag{2.6}$$

where: t_l = transmission loss rate [L/T]

K_h = effective hydraulic conductivity [L/T]

H_w = hydrostatic pressure head (depth of water in channel) [L]

H_c = capillary pressure (suction) head at the wetting front [L]

θ_e = effective sediment porosity = (φ-θ_r) [dimensionless]

φ = total sediment porosity [dimensionless]

θ_r = residual sediment moisture content [dimensionless]

S_e = effective sediment saturation [dimensionless]

T = cumulative (total) depth of water transported by transmission loss [L]

For single storm events, recovery of infiltration capacity by evapotranspiration and percolation can be neglected. Similarly, recovery of transmission loss capacity by evaporation or other processes can also be neglected for single storm events.

2.3.3 Storage

Water may be stored in depressions on the land surface as small, discontinuous surface pools. Precipitation retained in such small surface depressions is depression storage (Linsley et al. 1982). Water in depression storage may be conceptualized as a volume or, when normalized by surface area, a depth. In effect, the depression storage depth represents a threshold limiting the occurrence of overland flow. When the water depth is below the depression storage threshold, overland flow is zero. Note that water in depression storage is still subject to infiltration and evaporation.

Similar to depression storage in overland areas, water in channels may be stored in depressions in the stream bed (as the channel water depth falls below some critical level, flow is zero and the water surface discontinuous but individual pools of water remain). This mechanism is termed dead storage. Note that water in dead storage is still subject to transmission loss and evaporation.

For single storm events, recovery of depression storage volume by evaporation can be neglected. Similarly, recovery of dead storage volume by evaporation can also be neglected for single storm events.

2.3.4 Overland and Channel Flow

Overland flow can occur when the water depth on the overland plane exceeds the depression storage threshold. Overland flow is governed by conservation of mass (continuity) and conservation of momentum. The two-dimensional (vertically integrated) continuity equation for gradually-varied flow over a plane in rectangular (x, y) coordinates is (Julien et al. 1995; Julien, 2002):

$$\frac{\partial h}{dt} + \frac{\partial q_x}{dx} + \frac{\partial q_y}{dy} = i_n - f + W = i_e \tag{2.7}$$

where: h = surface water depth [L]

q_x , q_y = unit discharge in the x- or y-direction = Q_x/B_x , Q_y/B_y [L^2/T]

Q_x , Q_y = flow in the x- or y-direction [L^3/T]

B_x , B_y = flow width in the x- or y-direction [L]

W = unit discharge from/to a point source/sink [L^2/T]

i_e = excess precipitation rate [L/T]

Momentum equations for the x- and y-directions may be derived by relating the net forces per unit mass to flow acceleration (Julien et al. 1995; Julien, 2002). In full form, with all terms retained, these equations can be expressed in dimensionless form as the friction slope and are known as the Saint Venant equations. The full Saint Venant equations may be simplified by neglecting small terms that describe the local and convective acceleration components of momentum, resulting in the diffusive wave approximation (of the friction slope) for the x- and y-directions:

$$S_{fx} = S_{0x} - \frac{\partial h}{dx} \tag{2.8}$$

$$S_{fy} = S_{0y} - \frac{\partial h}{dy} \tag{2.9}$$

where: S_{fx} , S_{fy} = friction slope (energy grade line) in the x- or y-direction [dimensionless]

S_{0x} , S_{0y} = ground surface slope in the x- or y-direction [dimensionless]

To solve the overland flow equations for continuity and momentum, five hydraulic variables must be defined in terms of a depth-discharge relationship to describe flow resistance. Assuming that flow is turbulent and resistance can be described using the Manning formulation (in S.I. units), the depth-discharge relationships are (Julien et al. 1995; Julien, 2002):

$$q_x = \alpha_x h^{\beta} \tag{2.10}$$

$$q_y = \alpha_y h^{\beta} \tag{2.11}$$

$$\alpha_x = \frac{S_{fx}^{1/2}}{n} \tag{2.12}$$

$$\alpha_y = \frac{S_{fy}^{1/2}}{n} \tag{2.13}$$

where: α_x , α_y = resistance coefficient for flow in the x- or y-direction [$L^{1/3}/T$]

β = resistance exponent = 5/3 [dimensionless]

n = Manning roughness coefficient [$T/L^{1/3}$]

Similarly, channel flow can occur when the water depth in the channel exceeds the dead storage threshold. Channel flow is also governed by conservation of mass (continuity) and conservation of momentum. At the watershed it is convenient to represent channel flows in a watershed as one-dimensional (along the channel in the down-gradient direction). The one-dimensional (laterally and vertically integrated) continuity equation for gradually-varied flow along a channel is (Julien et al. 1995; Julien, 2002):

$$\frac{\partial A_c}{dt} + \frac{\partial Q}{dx} = q_l \tag{2.14}$$

where: A_c = cross sectional area of flow [L^2]

Q = total discharge [L^3/T]

q_l = lateral unit flow (into or out of the channel) [L^2/T]

W = unit discharge from/to a point source/sink [L^2/T]

Based on the momentum equation for the down-gradient direction and again neglecting terms for local and convective acceleration, the diffusive wave approximation may be used for the friction slope (see Eq. 2.7). To solve the channel flow equations for continuity and momentum, the Manning relationship may be used to describe flow resistance (Julien et al. 1995; Julien, 2002):

$$Q = \frac{1}{n} A_c R_h^{2/3} S_f^{1/2} \tag{2.15}$$

where: R_h = hydraulic radius of flow = A_c/P_c [L]

P_c = wetted perimeter of channel flow [L]

2.4 SEDIMENT TRANSPORT PROCESSES

The movement of water across the overland plane or through a channel network can transport and redistribute soil and sediment throughout a watershed. The main processes in the sediment transport submodel are: (1) advection-diffusion; (2) erosion; (3) deposition; and (4) bed processes (bed elevation response to erosion and deposition).

2.4.1 Advection-Diffusion

For the overland plane in two-dimensions (vertically integrated), the concentration of particles is governed by conservation of mass (sediment continuity) (Julien, 1998):

$$\frac{\partial C_s}{dt} + \frac{\partial \hat{q}_{tx}}{dx} + \frac{\partial \hat{q}_{ty}}{dy} = \hat{J}_e - \hat{J}_d + \hat{W}_s = \hat{J}_n \tag{2.16}$$

where: C_s = concentration of sediment particles in the flow [M/L^3]

$\hat{q}_{tx}$, $\hat{q}_{ty}$ = total sediment transport areal flux in the x- or y-direction [M/L^{2}T]

$\hat{J}_e$ = sediment erosion volumetric flux [M/L^{3}T]

$\hat{J}_d$ = sediment deposition volumetric flux [M/L^{3}T]

$\hat{W}_s$ = sediment point source/sink volumetric flux [M/L^{3}T]

$\hat{J}_n$ = net sediment transport volumetric flux [M/L^{3}T]

The total sediment transport flux in any direction has three components, advective, dispersive (mixing), and diffusive, and may be expressed as (Julien, 1998):

$$\hat{q}_{tx} = v_x C_s - (R_x + D)\frac{\partial C_s}{dx} \tag{2.17}$$

$$\hat{q}_{ty} = v_y C_s - (R_y + D)\frac{\partial C_s}{dy} \tag{2.18}$$

where: v_x , v_y = flow (advective) velocity in the x- or y-direction [L/T]

R_x , R_y = dispersion (mixing) coefficient the x- or y-direction [L^2/T]

D = diffusion coefficient [L^2/T]

$v_x C_s$ = advective flux in the x-direction = J_x [M/L^{2}T]

$v_y C_s$ = advective flux in the y-direction = J_y [M/L^{2}T]

$R_x \frac{\partial C_s}{dx}$ = dispersive flux the x-direction [M/L^{2}T]

$R_y \frac{\partial C_s}{dy}$ = dispersive flux the y-direction [M/L^{2}T]

$D\frac{\partial C_s}{dx}$ = diffusive flux the x-direction [M/L^{2}T]

$D\frac{\partial C_s}{dy}$ = diffusive flux the y-direction [M/L^{2}T]

The dispersive and diffusive flux terms in Eqs. (2.16) and (2.17) are negatively signed to indicate that mass is transported in the direction of decreasing concentration gradient. Note that both dispersion and diffusion are represented in forms that follow Fick's Law. However, dispersion represents a relatively rapid turbulent mixing process while diffusion represents a relatively slow a Brownian motion, random walk process (Holley, 1969). In turbulent flow, dispersive fluxes are typically several orders of magnitude larger than diffusive fluxes. Further, flow conditions for intense precipitation events are usually advectively dominated as dispersive fluxes are typically one to two orders smaller than advective fluxes. As a result, both the dispersive and diffusive terms may be neglected.

Similarly, for the channel plane in one-dimension (laterally and vertically integrated), the concentration of particles is governed by conservation of mass (sediment continuity) (Julien, 1998):

$$\frac{\partial C_s}{dt} + \frac{\partial \hat{q}_{tx}}{dx} = \hat{J}_e - \hat{J}_d + \hat{W}_s = \hat{J}_n \tag{2.19}$$

Individual terms for the channel advection-diffusion equation are identical to those defined for the overland plane. Similarly, the diffusive flux term can be neglected. The dispersive flux is expected to be larger than the corresponding term for overland flow. However, the channel dispersive flux still may be negligible relative to the channel advective flux during intense runoff events.

2.4.2 Erosion

Erosion is the entrainment (gain) of material from a bottom boundary into a flow by the action of water. The erosion flux may be expressed as a mass rate of particle removal from the boundary over time and the concentration (bulk density) of particles at the boundary:

$$J_e = v_r C_{sb} \tag{2.20}$$

where: J_e = erosion flux [M/L^{2}T]

v_r = resuspension (erosion) velocity [L/T]

C_{sb} = concentration of sediment at the bottom boundary (in the bed) [M/L^3]

Entrained material may be transported as either bedload or suspended load. However, for overland sheet and rill flows, bedload transport by rolling and sliding may predominate as the occurrence of saltation and full suspension may be limited (Julien and Simons, 1985). Entrainment rates may be estimated from site-specific erosion rate studies or, in general, from the difference between sediment transport capacity and advective fluxes:

$$v_r = \begin{cases} \dfrac{J_c - v_a C_s}{\rho_b} & for \quad J_c > v_a C_s \\ 0 & for \quad J_c \le v_a C_s \end{cases} \tag{2.21}$$

where: v_r = resuspension (erosion) velocity [L/T]

J_c = sediment transport capacity areal flux [M/L^{2}T]

v_a = advective (flow) velocity (in the x- or y-direction) [L/T]

C_s = concentration of sediment entrained in the flow [M/L^3]

ρ_b = bulk density of bed sediments [M/L^3]

In the overland plane, particles can be detached from the bulk soil matrix by raindrop (splash) impact and entrained into the flow by hydraulic action when the exerted shear stress exceeds the stress required to initiate particle motion (Julien and Frenette, 1985; Julien and Simons, 1985). The overland erosion process is influenced by many factors including precipitation (rainfall) intensity and duration, runoff length, surface slope, soil characteristics, vegetative cover, exerted shear stress, and particle size. Raindrop impact may generally be neglected when flow depths are greater than three times the average

raindrop diameter (Julien, 2002). Julien and Simons (1985) summarize numerous relationships to describe the transport capacity of overland flow. Julien (1998, 2002) recommends a modified form of the Kilinc and Richardson (1973) relationship that includes soil erodibility, cover, and management practice terms from the Universal Soil Loss Equation (USLE) (Meyer and Weischmeier, 1969) to estimate the total overland sediment transport capacity (for both the x- and y-directions):

$$q_s = 1.542 \times 10^8 \, q^{2.035} S_f^{1.66} \hat{K} \hat{C} \hat{P} \tag{2.22}$$

$$J_c = \frac{q_s}{B_e} \tag{2.23}$$

where:
- q_s = total sediment transport capacity (kg/m s) [M/LT]
- q = unit flow rate of water = $v_a \, h$ [L^2/T]
- S_f = friction slope [dimensionless]
- $\hat{K}$ = USLE soil erodibility factor [dimensionless]
- $\hat{C}$ = USLE soil cover factor [dimensionless]
- $\hat{P}$ = USLE soil management practice factor [dimensionless]
- B_e = width of eroding surface in flow direction [L]

In channels, sediment particles can be entrained into the flow when the exerted shear stress exceeds the stress required to initiate particle motion. For non-cohesive particles, the channel erosion process is influenced by factors such as particle size, particle density and bed forms. For cohesive particles, the erosion process is significantly influenced by inter-particle forces (such as surface charges that hold grains together and form cohesive bonds) and consolidation. Total (bed material) load transport capacity relationships account for the both bedload and suspended load components of sediment transport. Yang (1996) and Julien (1998) provide summaries of numerous total load transport relationships. The Engelund and Hansen (1967) relationship is considered a reasonable estimator of the total load:

$$C_w = 0.05\left(\frac{G}{G-1}\right)\frac{v_a S_f}{\left[(G-1)gd_p\right]^{0.5}}\left[\frac{R_h S_f}{(G-1)d_p}\right]^{0.5} \tag{2.24}$$

$$J_c = \frac{v_a C_t}{A_c} \tag{2.25}$$

where: C_w = concentration of entrained sediment particles by weight at the transport capacity [dimensionless]

G = particle specific gravity [dimensionless]

v_a = advective (flow) velocity (in the down-gradient direction) [L/T]

S_f = friction slope [dimensionless]

R_h = hydraulic radius of flow [L]

g = gravitation acceleration [L/T^2]

d_p = particle diameter [L]

A_c = cross sectional area of flow [L^2]

C_t = concentration of entrained sediment particles at the transport capacity = $10^6 GC_w/\left[G+(1-G)C_w\right]$ (g/m^3) [M/L^3]

It is worth noting that one feature common to both the Kilinc and Richardson (1973) and Engelund and Hansen (1967) relationships is that the implicit threshold for incipient motion is zero. This means that the transport capacity of any particle will always be greater than zero, regardless of particle size or the exerted shear stress, as long as the unit flow or flow velocity and friction slope are non-zero. This can lead to inconsistent results when erosion rates are computed from sediment transport capacities. The inferred erosion rate will almost always be greater than zero because the difference between the transport capacity and advective flux will nearly always be greater than zero. Consequently, a non-zero erosion rate can be computed even when the exerted shear stress is far less than the incipient motion threshold for the material. To address this limitation, an incipient motion threshold can be added to the modified Kilinc and Richardson (1973) and Engelund and Hansen (1967) relationships:

$$q_s = 1.542 \times 10^8 (q - q_c)^{2.035} S_f^{1.66} \hat{K} \hat{C} \hat{P} \tag{2.26}$$

$$C_w = 0.05 \left(\frac{G}{G-1} \right) \frac{(v_a - v_c) S_f}{\left[(G-1) g d_p \right]^{0.5}} \left[\frac{R_h S_f}{(G-1) d_p} \right]^{0.5} \tag{2.27}$$

where: q_c = critical unit flow for erosion (for aggregate the soil matrix) = $v_c h$ [L^2/T]

v_c = critical velocity for erosion [L/T]

h = surface water depth [L]

Further detail regarding the addition of erosion thresholds to the Kilinc and Richardson (1973) and Engelund and Hansen (1967) relationships is presented in Appendix A.

2.4.3 Deposition

Deposition is the sedimentation (loss) of material entrained in a flow to a bottom boundary by gravity. The deposition process is influenced by many factors including particle density, diameter, and shape, and fluid turbulence. The deposition flux may be expressed as a mass rate of particle removal from the water column over time and the concentration of sediment particles that are entrained in the flow:

$$J_d = v_{se} C_s \tag{2.25}$$

where: J_d = deposition flux [$M/L^2/T$]

v_{se} = effective settling (deposition) velocity [L/T]

C_s = concentration of sediment particles in the flow [M/L^3]

Coarse particles (>62 μm) are typically inorganic and non-cohesive and generally have large settling velocities under quiescent conditions. Numerous empirical relationships to describe the non-cohesive particle settling velocities are available. Summaries of relationships and settling velocities are presented by Yang (1996) and Julien (1998). For non-cohesive (fine sand) particles with diameters from 62 μm to 500 μm, the settling velocity can be computed as (Cheng, 1997):

$$v_s = \frac{\nu}{d_p}\left[\left(25 + 1.2{d_*}^2\right)^{0.5} - 5\right]^{-1.5} \tag{2.26}$$

$$d_* = d_p\left[\frac{(G-1)g}{\nu^2}\right]^{1/3} \tag{2.27}$$

where: v_s = quiescent settling velocity [L/T]

ν = kinematic viscosity of water [L^2/T]

d_* = dimensionless particle diameter [dimensionless]

Medium particles (10 μm < d_p <62 μm) can vary in character. Inorganic particles may behave in a non-cohesive manner. In contrast, organic particles (potentially including particles with organic coatings) may behave in a cohesive manner. Fine particles (<10 μm) often behave in a cohesive manner. If behavior is largely non-cohesive, settling velocities may be estimated as described by Julien (1998). If the behavior is cohesive, flocculation may occur. Floc size and settling velocity depend on the conditions under which the floc was formed (Burban et al. 1990; Krishnappan, 2000; Haralampides et al. 2003). When flocculation occurs, settling velocities of cohesive particles can be approximated by relationship of the form (Burban et al. 1990):

$$v_{sf} = a{d_f}^m \tag{2.28}$$

where: v_{sf} = floc settling velocity (cm/s) [L/T]

a = experimentally determined constant = 8.4×10^{-3}

d_f = median floc diameter (μm) [L]

m = experimentally determined constant = 0.024

However, depending on fluid shear, particle surface charge, and other conditions, fine particles may not flocculate. Under conditions that limit floc formation, fine particles can have very small, near zero settling velocities.

As a result of turbulence and other factors, not all particles settling through a column of flowing water will necessarily reach the sediment-water interface or be incorporated into the sediment bed (Krone, 1962). Beuselinck et al. (1999) suggest this process also occurs for the overland plane. As a result, effective settling velocities in flowing water can be much less than quiescent settling velocities. The effective settling velocity of a particle can be described as a reduction in the quiescent settling velocity by the probability of deposition (Krone 1962; Mehta et al. 1989):

$$v_{se} = P_{dep} v_s \tag{2.29}$$

where: v_{se} = effective settling velocity [L/T]

v_s = quiescent settling velocity [L/T]

P_{dep} = probability of deposition [dimensionless]

The probability of deposition varies with shear stress near the sediment bed and particle size. As particle size decreases or shear stress increases, the probability of deposition decreases. For non-cohesive particles, the probability of deposition has been described as a function of bottom shear stress (Gessler, 1965; Gessler 1967; Gessler, 1971):

$$P_{dep} = P = \frac{1}{\sqrt{2\pi}} \int_{-\infty}^{Y} e^{-0.5x^2} dx \tag{2.30}$$

$$Y = \frac{1}{\sigma}\left(\frac{\tau_{cd,n}}{\tau} - 1\right) \tag{2.31}$$

where: P = probability integral for the Gaussian distribution

σ = experimentally determined constant = 0.57

τ_0 = bottom shear stress (M/LT^2)

$\tau_{cd,n}$ = critical shear stress for deposition of non-cohesive particles, defined as the shear stress at which 50% of particles deposit (M/LT^2)

For coarse particles, the critical shear stress for deposition can be computed from a force balance following the method of van Rijn (1984a,b) as summarized by QEA (1999), with the particle diameter equal to the mean diameter for a range of particle size in a class (i.e. $d_p = d_{50}$).

For cohesive particles, the probability of deposition has also been described as a function of bottom shear stress (Partheniades, 1992):

$$P_{dep} = 1 - P = 1 - \frac{1}{\sqrt{2\pi}} \int_{-\infty}^{Y} e^{-0.5x^2} dx \tag{2.32}$$

$$Y = \frac{1}{\sigma} \ln \left[0.25 \left(\frac{\tau_{cd,c}}{\tau} - 1 \right) e^{1.27 \tau_{cd}} \right] \tag{2.33}$$

where: σ = experimentally determined constant = 0.49

τ_0 = bottom shear stress (M/LT^2)

$\tau_{cd,c}$ = critical shear stress for deposition of cohesive particles, defined as the shear stress at which 100% of particles deposit (M/LT^2)

The probability integrals in Equations 2.30 and 2.32 can be approximated as (Abramowitz and Stegun, 1972):

$$\begin{aligned} P &= 1 - F(Y)\left(0.4362X - 0.1202X^2 + 0.9373X^3\right) && \text{for } Y > 0 \\ P &= 1 - P(|Y|) && \text{for } Y < 0 \end{aligned} \tag{2.34}$$

$$F(Y) = \frac{1}{\sqrt{2\pi}} e^{-0.5Y^2} \tag{2.35}$$

$$X = \left(1 + 0.3327Y\right)^{-1} \tag{2.36}$$

2.4.4 Soil and Sediment Bed Processes

In response to the difference between bedform transport, erosion, and deposition fluxes, the net addition (burial) or net loss (scour) of particles from the bed causes the bed

surface elevation to increase or decrease. The rise or fall of the bed surface is governed by the sediment continuity (conservation of mass) equation, various forms of which are attributed to Exner (1925) (see Simons and Sentürk, 1992). Julien (1998) presents a derivation of the bed elevation continuity equation for an elemental control volume that includes vertical and lateral (x- and y-direction) transport terms. Neglecting bed consolidation and compaction processes, and assuming that only vertical mass transport processes (erosion and deposition) occur, the sediment continuity equation for the change in elevation of the soil or sediment bed surface may be expressed as:

$$\rho_b \frac{\partial z}{dt} = v_{se} C_s - v_r C_{sb} \tag{2.37}$$

where:
- z = elevation of the soil surface or sediment bed [L]
- ρ_b = bulk density of soil or bed sediments [M/L^3]
- v_{se} = effective setting (deposition) velocity [L/T]
- C_s = concentration of sediment particles in the water column [M/L^3]
- v_r = resuspension (erosion) velocity [L/T]
- C_{sb} = concentration of sediment particles in the soil or sediment bed [M/L^3]

2.5 CHEMICAL TRANSPORT AND FATE PROCESSES

The movement of water and sediment across the overland plane or through a channel network can also transport and redistribute chemicals throughout a watershed. On the land surface and in channel environments, chemical typically exist in three phases: (1) dissolved in water, (2) bound with dissolved organic compounds (DOC) or other binding ligands or complexation agents; and (3) particle-associated. The pathways that affect chemical movements and interactions in the environment depend on the phase in which the chemicals are present. The main processes in the chemical transport and fate submodel are: (1) chemical partitioning and phase distribution; (2) advection-diffusion; (3) erosion; (4) deposition; (5) infiltration; and (6) mass transfer and transformation processes (chemical reactions).

2.5.1 Chemical Partitioning and Phase Distribution

Many chemicals are hydrophobic and readily partition between dissolved, bound, and particle-associated (particulate) phases. Partitioning to bound and particulate phases is a function of chemical affinity for surfaces and ion exchange (ionic chemicals) or organic carbon (neutral chemicals) (Karichoff et al. 1979; Schwarzenbach et al. 1993; Chapra, 1997). The equilibrium distribution of chemicals between phases is described by the partition (distribution) coefficient, concentration and binding effectiveness of binding agents, and the concentration of particles or organic carbon. Mechanistically, partitioning is a function of the equilibrium rate at which chemicals sorb (move out of the dissolved phase) and desorb (move back into the dissolved phase). If the rates at which chemicals partition are much faster than the rates of other mass transfer processes, local equilibrium is assumed to exist and the dissolved, bound and particulate phase chemical concentrations can be expressed in terms of the total chemical concentration (sum of phases) (Thomann and Mueller, 1987; Chapra, 1997).

Chemicals may partition to all particle types (sorbents) present in a solution. The equilibrium partition (distribution) coefficient to any particle is defined as (Thomann and Mueller, 1987):

$$\P_{p_n} = K_{p_n} = f_{oc\,n} K_{oc} \tag{2.38}$$

where: $\P_{p_n}$ = equilibrium partition (distribution) coefficient for particle "*n*" [L^3/M]

K_{p_n} = equilibrium partition (distribution) coefficient for particle "*n*" [L^3/M]

f_{oc_n} = fraction organic carbon of particle "*n*" [dimensionless]

K_{oc} = organic carbon normalized partition coefficient [L^3/M]

For particulate phases in the water column, equilibrium partition coefficients vary with the concentration of suspended solids as a result of particle interactions. Particle-dependent partition coefficients are described as (DiToro, 1985):

$$\P_{px_n} = \frac{\P_{p_n}}{1 + \sum_{n=1}^{N} m_n \P_{p_n} / \nu_x} = \frac{f_{oc} K_{oc}}{1 + \sum_{n=1}^{N} f_{oc_n} m_n K_{oc} / \nu_x} \quad (2.39)$$

where: $\P_{px_n}$ = particle-dependent partition coefficient [L^3/M]

n = particle index = 1, 2, 3, etc.

m_n = concentration of particle "n" [M/L^3]

ν_x = particle interaction parameter [dimensionless]

For the bound phase, the equilibrium binding coefficient is defined as:

$$\P_b = D_e f_{oc_D} K_{oc} \quad (2.40)$$

where: $\P_b$ = equilibrium binding coefficient [L^3/M]

f_{oc_D} = fraction organic carbon of DOC [dimensionless]

D_e = DOC-binding effectiveness coefficient [dimensionless]

Conceptually, dissolved organic compounds are composed entirely of organic carbon (f_{oc_D} = 1). Under those conditions, the equilibrium binding coefficient would equal the organic carbon partition coefficient. However, at least for neutral organic chemical binding in some surface waters (the Great Lakes), observed binding coefficients were up to 100 times smaller than K_{oc} (Eadie et al. 1990; Eadie et al. 1992). Also, in sediment observed binding coefficients were up to 10 times smaller than K_{oc} (Landrum et al. 1985; Landrum et al. 1987; Capel and Eisenreich, 1990). One explanation for decreased binding efficiency is photobleaching of DOC by ultraviolet (UV-B) radiation (Kashian et al. 2004).

The equilibrium partition coefficient can be used to describe the fraction of the total chemical that is associated with each phase as follows (Thomann and Mueller, 1987; Chapra, 1997):

$$f_d = \frac{1}{1 + D_{oc} \P_b + \sum_{n=1}^{N} m_n \P_{px_n}} \quad (2.41)$$

$$f_b = \frac{D_{oc} \P_b}{1 + D_{oc} \P_b + \sum_{n=1}^{N} m_n \P_{px_n}} \quad (2.42)$$

$$f_{p_n} = \frac{m_n \P_{px_n}}{1 + D_{oc} \P_b + \sum_{n=1}^{N} m_n \P_{px_n}} \quad (2.43)$$

$$f_d + f_b + \sum_{n=1}^{N} f_{p_n} = 1 \quad (2.44)$$

where: f_d = fraction of the total chemical in the dissolved phase [dimensionless]

f_b = fraction of the total chemical in the DOC-bound phase [dimensionless]

n = particle index = 1, 2, 3, etc.

f_{pn} = fraction of the total chemical in the particulate phase associated with particle "n" [dimensionless]

Equations 2.41-2.43 are presented for the water column. For the sediment bed, $\P_{p_n}$ is used in place of $\P_{px_n}$.

Lu and Allen (2001) present extensive assessments of copper partitioning onto suspended particulate matter in river water. They performed a series of adsorption experiments and found that many factors may influence the partition coefficient including pH, total suspended solids concentration, total copper concentration, dissolved organic matter, particulate organic matter, hardness, and ionic strength. Graphs showing variation of the copper partition coefficient as a function of key environmental conditions are presented in Figure 2-1. Their results suggest that adsorption to organic matter binding sites in aqueous and solid phases plays the biggest role in controlling the extent of copper partitioning. However, Lu and Allen (2001) found that the most significant

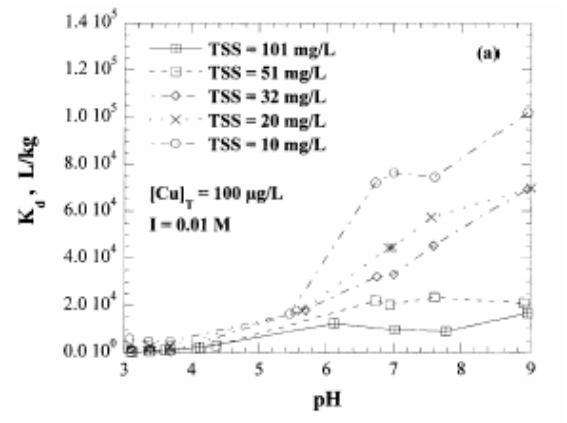

a) K_d as a function of pH and TSS concentration

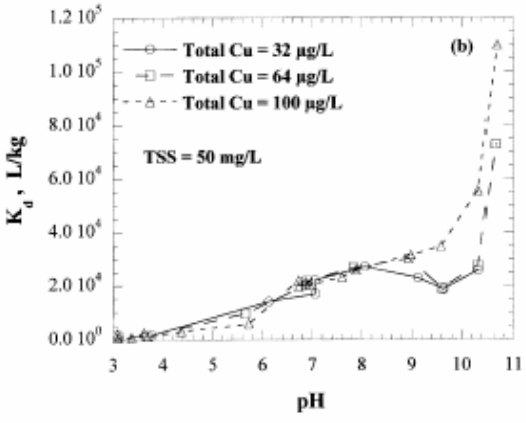

b) K_d as a function of pH and Cu concentration

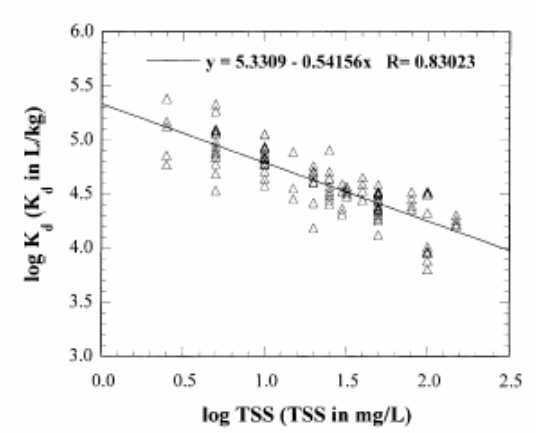

c) K_d as a function of TSS concentration

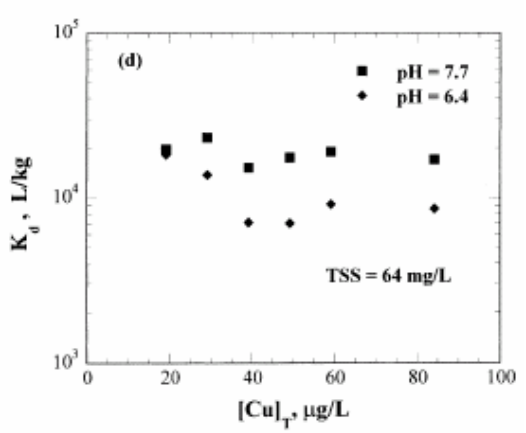

d) K_d as a function of Cu concentration and pH

Figure 2-1. Copper partitioning vs. environmental conditions (Lu and Allen, 2001).

environmental factors affecting the value of the partition coefficient were the total suspended solids (TSS) concentration and pH. Holm et al. (2003) found that cadmium partitioning, like copper, was highly correlated with soil cation exchange capacity, which is largely determined by organic carbon and clay content. Also, cadmium partition coefficients were found to decrease by an order of magnitude as soil pH decreased from 6.7 to 5.3. Similar behavior is also expected for zinc because, like copper and cadmium, it is divalent. Sauvé et al. (2000, 2003) noted that distribution coefficients for cadmium, copper, and zinc and other divalent metals are sensitive to pH. Sauvé et al. (2003) reported distribution coefficients (log K_d) values for acidic (pH 4.4) soils were low: Cd log K_d = 3.05; Cu log K_d = 2.98; and Zn log K_d = 2.75. While pH may be the most

important variable for partitioning, Sauvé et al. (2000, 2003) also noted the importance of organic matter as, after being normalized for pH, sorptive capacities for organic soils were reported to be up to 30 times larger than those observed for mineral soils.

2.5.2 Chemical Advection

Advection transports all chemical phases. For two-dimensional flow in the overland plane, a chemical continuity (conservation of mass) equation analogous the sediment continuity equation can be written as:

$$J_{xc} = v_x \left(f_d + f_b + \sum_{n=1}^{N} f_{p_n} \right) C_c = v_x C_c \tag{2.45}$$

$$J_{yc} = v_y \left(f_d + f_b + \sum_{n=1}^{N} f_{p_n} \right) C_c = v_y C_c \tag{2.46}$$

where: J_{xc} , J_{yc} = chemical advective flux in the x- or y-direction [M/L^{2}T]

v_x , v_y = advective velocity in the x- or y-direction [L/T]

n = particle index = 1, 2, 3, etc.

v_{r_n} = resuspension (erosion) velocity of particle "n" [L/T]

f_d = fraction of the total chemical in dissolved phase in the water column [dimensionless]

f_b = fraction of the total chemical in the bound phase in the water column [dimensionless]

f_{pn} = fraction of the total chemical in particulate phase associated with particle "n" in the sediment column [dimensionless]

C_c = total chemical concentration in the water column [M/L^3]

Similarly, for one-dimensional flow in channels a chemical continuity (conservation of mass) equation analogous the sediment continuity equation is identical to Equation 2.45.

2.5.3 Erosion and Deposition of Particulate Phase Chemicals

Chemicals associated with particles in the water column will enter the sediment bed if those particles settle. Similarly, chemicals associated with particles in the sediment bed will return to the water column if those particles are entrained (resuspend). The factors that control particle transport between the water column and sediment bed were described in Section 2.2.2. Since particle phase chemicals move with the particles transported, the erosion and deposition fluxes of chemicals are described as (Thomann and Mueller, 1987):

$$J_{ec} = \sum_{n=1}^{N} v_{rn} f_{p2_n} C_{c2} \tag{2.47}$$

$$J_{dc} = \sum_{n=1}^{N} v_{sen} f_{p1_n} C_{c1} \tag{2.48}$$

where:

J_{ec} = chemical erosion flux [M/L^{2}T]

J_{dc} = chemical deposition flux [M/L^{2}T]

n = particle index = 1, 2, 3, etc.

v_{r_n} = resuspension (erosion) velocity of particle "n" [L/T]

v_{se_n} = effective settling velocity of particle "n" [L/T]

f_{p1_n} = fraction of the total chemical in particulate phase associated with particle "n" in the water column [dimensionless]

f_{p2_n} = fraction of the total chemical in particulate phase associated with particle "n" in the sediment column [dimensionless]

C_{c1} = total chemical concentration in the water column [M/L^3]

C_{c2} = total chemical concentration in the soil/sediment column [M/L^3]

2.5.4 Chemical Infiltration and Subsurface Transport

Chemicals associated with the dissolved and bound phase in the water column will enter the soil or sediment bed if the water transporting those chemicals infiltrates. When chemical partition coefficients are low and a significant fraction of the total chemical

mass is in a mobile form, chemical infiltration may be significant. To account for this process, the chemical infiltration flux can be computed from the water infiltration flux as:

$$J_{ic} = v_i \left(f_{d1} + f_{b1} \right) C_{c1} = v_i f_{m1} C_{c1} \tag{2.49}$$

where: J_{ic} = chemical infiltration flux [M/L^{2}T]

v_i = infiltration rate or transmission loss of water [L/T], previously defined as f in Eq. (2.5) or t_l in Eq. (2.6)

f_{d1} = fraction of the total chemical in dissolved phase in the water column [dimensionless]

f_{b1} = fraction of the total chemical in bound phase in the water column [dimensionless]

f_{m1} = fraction of the total chemical in the mobile phase in the water column [dimensionless] = $f_{d1} + f_{b1}$

C_{c1} = total chemical concentration in the water column [M/L^3]

Once in the subsurface, infiltrated chemicals would be subject to repartitioning with the chemical mass associated with porewater and particles in the soil column and transport via groundwater. The flow of groundwater through the soil also has the potential to leach chemicals from the soil column. Due to adsorption and the comparatively high bulk density of particles in the soil, subsurface chemical transport is subject to retardation (Fetter, 2001). Chemicals subject to retardation travel trough the subsurface at rates less than the average linear velocity of water. The retardation factor for a chemical in the subsurface is computed as (Fetter, 2001):

$$R = 1 + \frac{\rho_b}{\theta_e} K_p \tag{2.50}$$

where: R = Retardation factor [dimensionless]

ρ_b = soil bulk density [M/L^3]

θ_e = effective soil porosity (volume of voids/total volume of particles and voids) [dimensionless]

K_p = chemical equilibrium partition (distribution) coefficient [L^3/M]

2.5.5 Other Chemical Mass Transfer and Transformation Processes

Beyond partitioning and mass transport processes, the fate of chemicals is potentially influenced by a number of other processes such as biodegradation, hydrolysis, oxidation, photolysis, and volatilization, and dissolution. However, for general simulation of elemental metals such as cadmium, copper, and zinc, volatilization, biodegradation, and photolysis do not occur. Hydrolysis and oxidation can affect the ionic speciation and phase distribution of metallic chemicals but do not affect the total chemical concentration. The effect that possible hydrolysis or oxidation reactions have on phase distributions of metals can be represented in terms of the chemical distribution (partitioning) coefficient.

3.0 TREX WATERSHED MODEL

A fully distributed numerical modeling framework to simulate the transport and fate of chemicals across watersheds was developed. This new modeling framework is the Two-dimensional, Runoff, Erosion, and Export (TREX) watershed model. An overview of TREX features and numerical implementation follows. A manual describing TREX model theory, inputs, outputs, and a programming guide is presented in Appendix B.

3.1 GENERALIZED CONCEPTUAL MODEL

A generalized conceptual framework for TREX is presented in Figure 3-1. At present, framework development focuses on the event transport of metals in surface waters. Consequently, several possible processes in the general conceptual framework can be neglected because storm events are short-lived, lasting no more than a few hours. In particular, mass transfer and reactions processes such as volatilization, biodegradation, hydrolysis, and photodegradation can be neglected because of the short time scale for simulations or because these processes do not occur for metals. Other processes, such as dispersion and diffusion can also be neglected because at the time scale of event simulations transport processes are reasonable expected to be dominated by advection. At the event time scale, subsurface transport is also neglected. As a result, the transport and fate processes most important for the event simulation of metals are:

- Advective water column transport;
- chemical partitioning between water (truly dissolved), dissolved organic compounds (DOC) (or other binding agents) (bound), and solid (particulate) phases;
- Transport (erosion, deposition, net burial) of solids and particulate chemicals;
- Infiltration of dissolved and bound (mobile) phase chemicals;

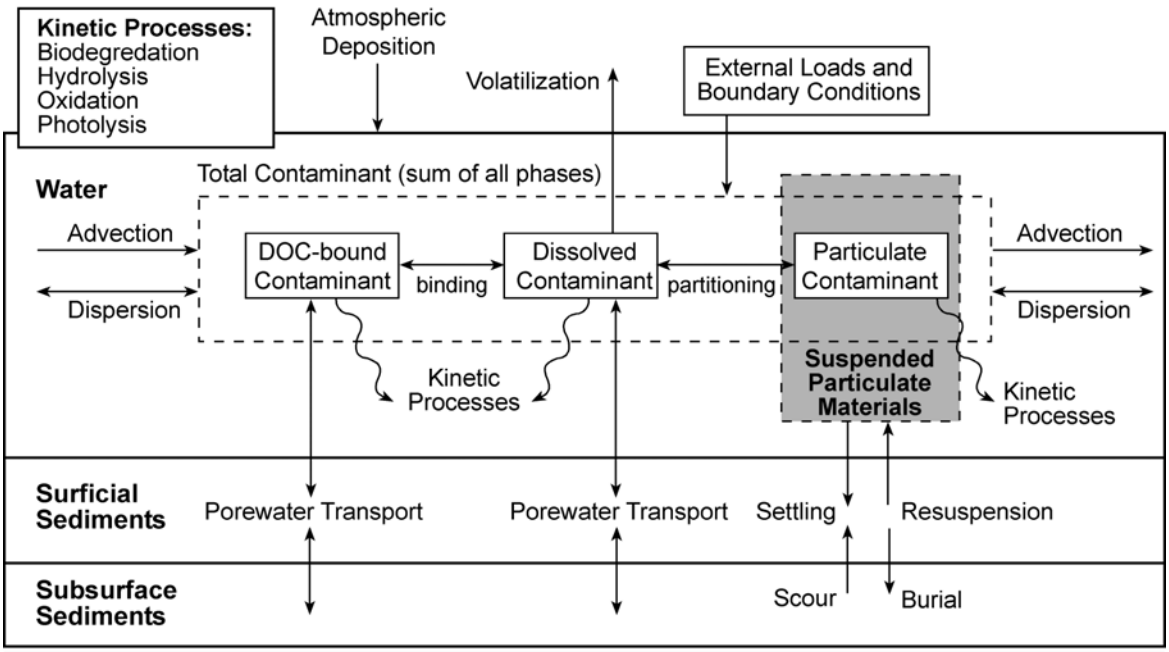

Figure 3-1. Generalized conceptual model framework.

- External sources and sinks of water, solids and chemicals.

Dynamic mass balance equations were developed based on the process descriptions presented in Section 2.0. In their most general form, these mass balance equations form a system of coupled partial differential equations that are functions of time and space.

These equations describe the relationship between material inputs (precipitation or loads) and mass (water depth or constituent concentrations). To solve these equations, three simplifying assumptions were made and the equations expressed in finite difference form (Thomann and Mueller, 1987; Chapra, 1997):

1. Water column volumes are constant with respect to time during any interval ($\partial V/\partial t = 0$);
2. Surficial sediments do not move horizontally within the sediment bed; and

3. Chemical partitioning to solids and binding is rapid relative to other processes (local equilibrium).

The state variables in the model framework for the overland plane (denoted with the subscript "ov") and channel network (denoted with the subscript "ch") are: water depth (h), solids concentration (C_s), and chemical concentration (C_c). The corresponding equations for the water column and bed are:

Water Depth in the Overland Plane and Channel Network

$$\frac{\partial h_{ov}}{\partial t} = i_e - \frac{1}{B_x}\frac{\partial Q_{ovx}}{\partial x} - \frac{1}{B_y}\frac{\partial Q_{ovy}}{\partial y} - \frac{q_l}{L_c} + \frac{W_w}{A_c} \tag{3.1}$$

$$\frac{\partial (h_{ch} B_c)}{\partial t} = q_l - \frac{\partial Q_{ch}}{\partial x} + \frac{W_w}{L_c} \tag{3.2}$$

Solids in the Water Column of the Overland Plane and Channel Network

$$\frac{\partial C_{s,ov}}{\partial t} = v_r C_{sb,ov}\frac{A_s}{V_w} - v_{se} C_{s,ov}\frac{A_s}{V_w} - v_x C_{s,ov}\frac{A_c}{V_w} - v_y C_{s,ov}\frac{A_c}{V_w} - v_f C_{s,ov}\frac{A_c}{V_w} + \frac{W_s}{V_w} \tag{3.3}$$

$$\frac{\partial C_{s,ch}}{\partial t} = v_r C_{sb,ch}\frac{A_s}{V_w} - v_{se} C_{s,ch}\frac{A_s}{V_w} - v_x C_{s,ch}\frac{A_c}{V_w} + v_f C_{s,ov}\frac{A_c}{V_w} + \frac{W_s}{V_w} \tag{3.4}$$

Solids in the Soil and Sediment Bed

$$\frac{\partial C_{sb,ov}}{\partial t} = v_{se} C_{s,ov}\frac{A_s}{V_s} - v_r C_{sb,ov}\frac{A_s}{V_s} \tag{3.5}$$

$$\frac{\partial C_{sb,ch}}{\partial t} = v_{se} C_{s,ch}\frac{A_s}{V_s} - v_r C_{sb,ch}\frac{A_s}{V_s} \tag{3.6}$$

Total Chemical in the Water Column of the Overland Plane and Channel Network

$$\begin{aligned}\frac{\partial C_{c,ov}}{\partial t} = {} & v_r C_{cb,ov} f_{pb}\frac{A_s}{V_w} - v_{se} C_{c,ov} f_p \frac{A_s}{V_w} - v_x C_{c,ov}\frac{A_c}{V_w} - v_y C_{c,ov}\frac{A_c}{V_w} - v_f C_{c,ov}\frac{A_c}{V_w} \\ & - v_{i,ov} C_{c,ov}(f_d + f_b)\frac{A_s}{V_w} + \frac{W_c}{V_w}\end{aligned} \tag{3.7}$$

$$\frac{\partial C_{c,ch}}{\partial t} = v_r C_{cb,ch} f_{pb} \frac{A_s}{V_w} - v_{se} C_{c,ch} f_p \frac{A_s}{V_w} - v_x C_{c,ch} \frac{A_c}{V_w} + v_f C_{c,ov} \frac{A_c}{V_w} - v_{i,ch} C_{c,ch} \left(f_d + f_b\right) \frac{A_s}{V_w} + \frac{W_c}{V_w} \tag{3.8}$$

Total Chemical in the Soil and Sediment Bed

$$\frac{\partial C_{cb,ov}}{\partial t} = v_{se} C_{c,ov} f_p \frac{A_s}{V_s} - v_r C_{cb,ov} f_{pb} \frac{A_s}{V_s} \tag{3.9}$$

$$\frac{\partial C_{cb,ch}}{\partial t} = v_{se} C_{c,ch} f_p \frac{A_s}{V_s} - v_r C_{cb,ch} f_{pb} \frac{A_s}{V_s} \tag{3.10}$$

where:

h	=	flow depth of water column [L]
C_s , C_{sb}	=	solids concentration in water column and bed [M/L^3]
C_c , C_{cb}	=	total chemical concentration in water column and bed [M/L^3]
Q_x , Q_y	=	flow in the x- or y-direction [L^3/T]
q_l	=	lateral unit flow from overland plane to channel (floodplain) [L^2/T]
L_c	=	length of channel in flow direction [L]
A_c , A_s	=	cross sectional area in flow direction, bed surface area [L^2]
V_w , V_s	=	volume of water and sediments [L^3]
v_x , v_y , v_f	=	flow velocity in the x- or y-direction and between overland plane and channel (floodplain) [L/T]
v_r , v_{se} , v_i	=	resuspension (erosion), effective settling (deposition), and infiltration (or transmission loss) velocities [L/T]
f_d , f_b , f_p	=	dissolved, bound, and particulate chemical fractions [dimensionless]
$W_{w,s,c}$	=	material point source/sink: water [L^3/T], solids, or chemical [M/T]

Each term in the mass balance equations represents a process in the conceptual framework. The variables in each term represent model parameters. Thomann and Mueller (1987) and Chapra (1997) provide more detailed presentations of mass balance equations for chemical transport.

3.2 NUMERICAL IMPLEMENTATION

To simulate hydrologic, sediment, and chemical transport, values must be assigned to each model parameter and the mass balance equations defined by the conceptual model framework must be solved. Numerical integration techniques are needed to solve the model equations. TREX uses a finite difference control volume implementation of the generalized mass balance equation. To generate solutions, the framework computes dynamic mass balances for each state variable and accounts for all material that enters, accumulates within, or leaves a control volume through precipitation excess, external loads, advection, erosion, and deposition. TREX also features a "semi-Lagrangian" soil/sediment bed layer submodel to account for the vertical distribution of the physical and chemical properties of the overland soil and channel sediment columns (see Section 3.3). These equations are solved using Euler's method for numerical integration (Chapra and Canale, 1985):

$$s\big|_{t+dt} = s\big|_{t} + \left.\frac{\partial s}{\partial t}\right|_{t} dt \tag{3.11}$$

where: $s\big|_{t+dt}$ = value of model state variable at time $t+dt$ [L] or [M/L^3]

$s\big|_{t}$ = value of model state variable at time t [L] or [M/L^3]

$\left.\frac{\partial s}{\partial t}\right|_{t}$ = value of model state variable derivative at time t [L/T] or [M/L^{3}T]

dt = time step for numerical integration [T]

3.3 TREX FRAMEWORK FEATURES

The starting point for TREX development was CASC2D. As part of TREX development, CASC2D's underlying hydrologic and sediment transport submodels were significantly enhanced before chemical transport and fate components were added to create the TREX framework. An overview of TREX features is presented in Table 3-1. The entire body of TREX source code is organized to significantly improve code structure and modularity and includes line-by-line documentation. Beyond allowing development of basic chemical transport and fate features, TREX is structured so future categories of model features can be added to the framework without having to reconstruct the basic code. As presented in Figure 3-2, the code is designed so that the calculations for each process at any time level are independent and information is carried forward from hydrology to sediment transport to chemical transport in order to generate a solution. At any time level, flow is assumed to be unaffected by sediment and chemical transport and sediment transport is affected by chemical transport, so calculations for these three components have a natural hierarchy. The organization of hydrologic, sediment, and chemical transport and fate process functional units within TREX is presented in Figure 3.3.

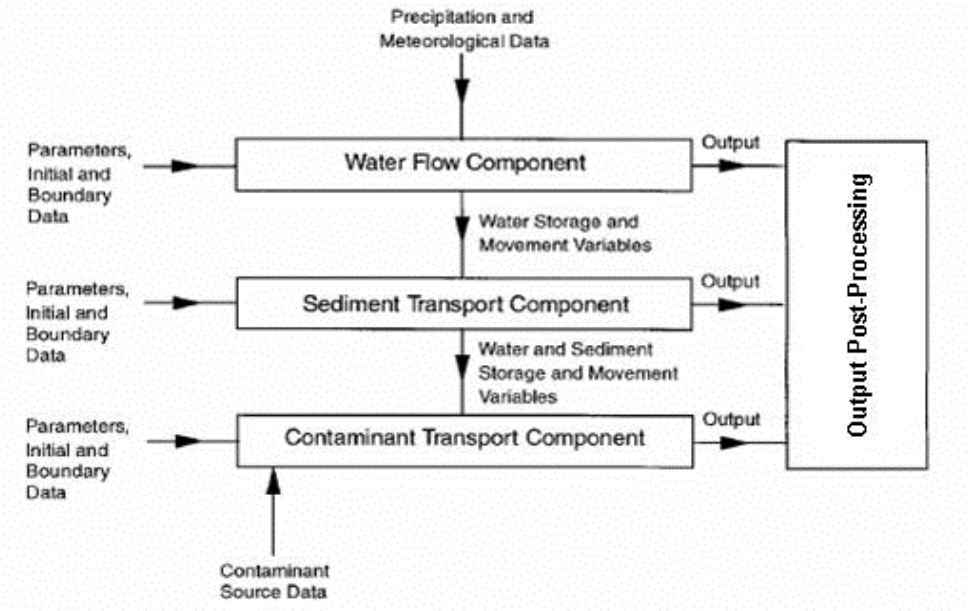

Figure 3-2. TREX Hierarchy and information flow (after Ewen et al 2000).

Table 3-1. Comparative overview of TREX features.

Model Component	*Prior CASC2D Code*	*TREX Code*
General Model Controls		
Numerical integration time step	One time step limited to critical value regardless of flow	Series of time step values that can be optimized based on flow
Hydrologic Submodel		
Water depth initial condition	Assumed to be zero but recent code allowed a non-zero flow depth in channels (dry start)	User can specify any value for depth overland, in channels, or infiltrated (wet or dry start)
Flow outlets and downstream boundary conditions	Limited to one outlet, assumed normal depth	Any number of outlets possible, downstream control or normal depth can be specified
Floodplain interaction	Present in initial code (Julien et al. 1995) but not in recent code (Rojas, 2002).	Restored feature and enhanced to compute flooding from water surface elevations
Channel topology: orientation	Channel connections limited to four (N-S or E-W) directions	Channel connections in all eight raster grid directions
Channel topology: branching	Converging branches only, limited to two branches upstream	Converging and diverging branches with 2-7 branches
Flow point sources and sinks	None	Point sources for overland plane and channel network
Sediment Transport Submodel		
Number of particle types	Limited to three: sand, silt, clay	Unlimited
Floodplain sediment transport	None: solids passing through overland part of a floodplain cell instantly move to channel	Occurs whenever water depth in overland part of floodplain cell exceeds zero
Channel erosion	Limited: only solids deposited during simulation erode; net bed elevation change never < 0	Not restricted; channels can incise and net change in bed elevation can be < 0
Solids point sources and sinks	None	Point sources for overland plane and channel network
Chemical Transport Submodel		
Number of chemical types	None	Unlimited
Chemical transport and fate	None	Three-phase partitioning with advection, erosion, deposition
Chemical point sources and sinks	None	Point sources for overland plane and channel network

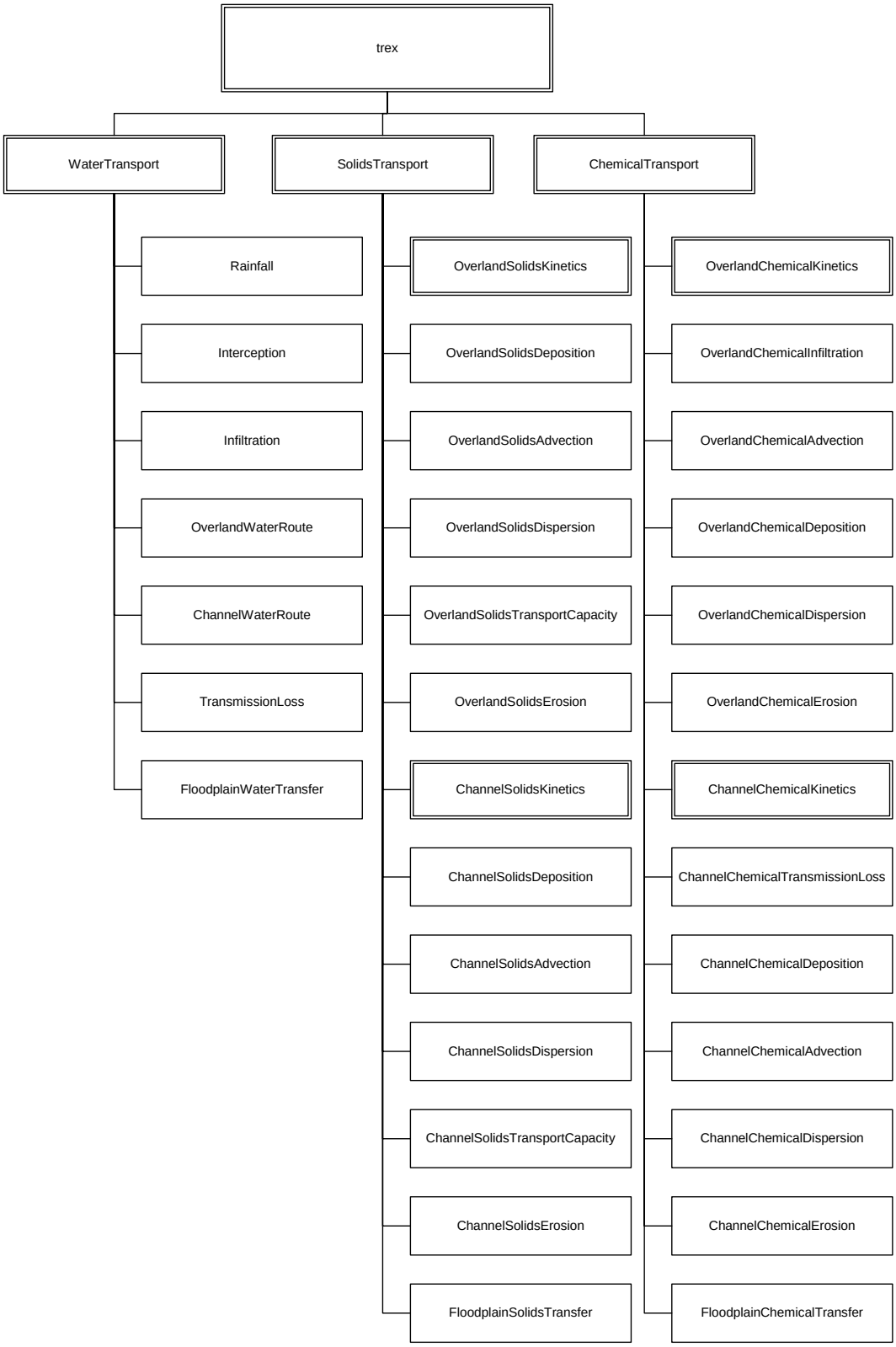

Figure 3-3. Organization of transport and fate process functional units in TREX.

As part of TREX development, many features of the original CASC2D code were significantly enhanced and many entirely new features were added. In particular, the TREX code is designed to simulate multiple watershed outlets and to also allow channel network branching in the upstream and downstream directions. This permits simulation of braided tributaries and distributary flows that might occur around alluvial fans or where a stream system on a high slope meets a large receiving waterbody on a low slope. Another significant enhancement is the addition of flow point sources and sinks. Note that TREX does not consider groundwater flow processes other than water loss at the surface by infiltration or channel transmission loss. However, to account for other water losses or gains, groundwater interactions could be represented as a series of time-variable point sources and sinks. In effect, this feature allows TREX to be externally coupled with groundwater flow and transport modeling tools such as MODFLOW (Harbaugh et al. 2000), HST3D (Kipp, 1997), and MT3DMS (Zheng and Wang, 1999).

Another key feature of TREX is the representation of the bed and bed processes. The bed itself is presented as a vertical stack (layers). Typical water quality modeling approaches use an Eulerian (fixed) frame of reference for all compartments. In contrast, TREX uses what is termed a "semi-Lagrangian" (floating) frame of reference (Velleux et al. 2001). In the semi-Lagrangian approach, the control volume of the surface bed layer is allowed to expand or contract in response to erosion or deposition. This allows for improved simulation of the dynamics of chemical distributions in soils and sediment. Velleux et al. (2001) and Imhoff et al. (2003) present further descriptions of the semi-Lagrangian approach and its details. The approach allows for dynamic simulation of both transport capacity limited and supply limited sediment and chemical transport.

Beyond these enhancements, TREX is fully-distributed and is designed to be compatible with data from raster GIS sources. In particular, data describing elevation, soil types, land use, and contaminant distributions can be processed in a GIS and used as model inputs. Model outputs are also designed to be compatible for use with a GIS. Descriptions of TREX features specifically designed to visualize chemical transport and fate outputs are described in Section 3.4.

3.4 FEATURES TO VISUALIZE CHEMICAL TRANSPORT AND FATE

TREX has a number of features specifically designed to aid visualization of chemical transport and fate simulation results. Expanding on the approach described by Rojas (2002), TREX can provide outputs in several different formats including point-in-time, point-in-space, cumulative-time, and mass balance reports. An overview of these reports is provided below. Full detail is provided in the TREX user's manual in Appendix B.

The point-in-time grid format reports model conditions across all points in the entire spatial domain at specified time intervals. This format can be directly imported to GIS software where images can be displayed in sequence, creating animations to visualize changes in conditions in both space and time. The model can report point-in-time grids to display rainfall intensity and depth, infiltration rate and depth, flow rate and depth, suspended solids concentrations in surface water and soil, chemical concentrations by phase in surface water and sediment, chemical phase distribution, and the dissolved phase chemical infiltration flux.

The point-in-space format reports model conditions over time at select points in space in a table. This format can be directly imported to spreadsheet software to create graphs of model results over time for visual comparison to observations. The model can report point-in-space tables to display water flow or depth, solids concentration or flux, and chemical concentration or flux by phase.

The cumulative-time grid format reports model conditions for all points in the spatial domain accumulated over the entire time of the simulation. This format can also be directly imported to GIS software to create static maps that show differences in results over the model domain. The model can report cumulative-time grids to display the elevation changes as well as gross erosion, gross deposition, and net accumulation (erosion minus deposition) for all solids and chemical types simulated.

Two types of mass balance reports are provided. The first type is the summary statistics report. This report provides brief summaries of simulation statistics for water volume, solids mass, and chemical mass inputs and outputs as well as other statistics. For

example, the hydrologic summary reports all water sources and sinks including rainfall inputs, the total volume lost to infiltration and transmission loss, and the volume exiting the model domain at outlets. Summaries for solids and chemicals are similar and also include mass reports for erosion and deposition. Summary reports for solids are provided for each individual state variable as well as for the sum of all solids types simulated. The second type is the detailed mass balance report. This report provides detailed, cell-by-cell and node-by-node summaries of mass transported into and out of each cell or node in the model domain. The detailed mass balance file is directly importable to spreadsheet software (tab-delimited format) and can be used to track water, solids, and chemical movement from point to point across the model domain. By summing ranges of cells or nodes, mass can be tracked across more broadly defined areas such as sub-basins within a larger watershed.

3.5 TREX COMPUTER SOURCE CODE AND PROGRAM OPERATION

The TREX source code is written in C and conforms to ANSI C99 conventions. The code is divided into 181 C source files and 10 header files. TREX has been compiled and simulations executed on several computing systems to ensure a degree of portability.

TREX is operated from a command line interface (the command prompt for the Windows operating system). TREX requires that the user specify one argument. This argument is the path and file name of the TREX main input file. The main input file provides the basic model input parameters that control a simulation including the names of ancillary model input files. Ancillary input files specify characteristics of the modeled system such as the watershed boundary mask, elevations, soil classes, and land use, etc. When run from the command prompt under the Windows operating system, the command stream to begin execution of a TREX simulation is of the form:

C:\>trex.exe *inputfilename.inp*

During execution, TREX generates a series of output files. The files generated depend on options specified in the main input file.

4.0 CALIFORNIA GULCH WATERSHED

4.1 BACKGROUND

The watershed transport of chemicals from mining wastes is representative of a large class of water quality problems that can be assessed using watershed models. Environmental impairments attributable to contamination from inactive and abandoned mine (IAM) sites are widespread. Across the western U.S., contaminants associated with acid mine drainage (AMD) from more than 100,000 IAM sites affect more than 500,000 acres of land and several thousand miles of streams and other surface waters (IMCC, 1992; USEPA 1996). USEPA and other authorities (e.g. Bureau of Land Management, state agencies, etc.) manage remediation of IAM sites. However, the scale of IAM problem is so extensive that not all areas of all contaminated sites can necessarily be rehabilitated. As a result, priorities must be established to maximize the cleanup that can be achieved with limited resources. USEPA and others needs a methodology to screen sites, assess how much different contaminated areas contribute to the overall site impairments, and prioritize areas for cleanup.

Each individual contaminated area of an IAM site will not necessarily contribute equally to site impairment. Cleanup priorities must be based on the transport potential and delivery mechanism of a contaminant of concern from each source area. For IAM sites, metals such as copper (Cu), cadmium (Cd), and zinc (Zn) are typical contaminants of concern due to their toxicity to aquatic organisms. The transport of metals from a source area is complex because they partition between dissolved, bound, and particulate phases in response to differences in environmental conditions over time (i.e. changes in pH or suspended solids concentrations, reactions with other compounds, etc.). As a result, metals initially transported from a waste pile in one phase may ultimately be delivered to a receiving water body in a different phase. Rehabilitation measures for a site must be designed to account for these differences.

4.2 SITE DESCRIPTION

California Gulch (CG) is part of a historical mining district located near Leadville, Colorado. The site covers an area of approximately 30 km^2 (11.8 mi^2) and lies within the headwaters of the Arkansas River watershed (Figures 4-1 and 4-2). Mining and related activities such as ore milling and smelting have occurred in the gulch since 1859 (HDR, 2002). One legacy of mining activities is extensive contamination of the CG watershed and adjacent areas by a variety of mining wastes including waste rock, tailings, and slag. Approximately 2,000 waste piles are present across the site (USEPA, 1987a; WCC, 1993a-c; HDR, 2002). Environmental impacts attributable to these wastes include surface and ground water contamination from AMD (low pH), elevated metals concentrations on the land surface and stream channels (water column and sediment bed), and ecological impairments (toxicity to fish and benthos) (USEPA 1987a-c; Walsh, 1992; WWC, 1993a-d; Walsh, 1993; CDM, 1994). Metals of particular concern due to their toxicity to wildlife are Cu, Cd, and Zn (Clements et al. 2002). In response to rainfall, surface erosion, and subsequent sediment transport, these contaminants are exported from CG and harm water quality and habitat in downstream regions, particularly the CG confluence with the Arkansas River (USEPA, 1987a; Techlaw, 2001). Efforts to remediate CG began in 1983 when USEPA placed the site on the National Priority List (NPL) under the Comprehensive Environmental Response, Compensation, and Liability Act (CERCLA) (Superfund) (USEPA, 1987a). The USEPA Region VIII Superfund Division manages these efforts. The goal of remediation efforts is to prevent or reduce the release of harmful materials from sources such as waste rock piles, tailings areas, slag, and soils (HDR, 2002). It is worth noting that remediation efforts are so complex and costly that USEPA classifies this site as a Superfund megasite.[2]

The CG Superfund project area is presented in Figure 4-2. The site includes the California Gulch watershed, including Stray Horse Gulch, portions of South Evans Gulch, and a portion of the Arkansas River downstream of the California Gulch

[2] A site is considered to be a megasite if removal and remedial action costs incurred by USEPA or by Potentially Responsible Parties (PRPs) exceed $50 million. (USEPA, 2003).

a) United States and State of Colorado

b) State of Colorado and Leadville

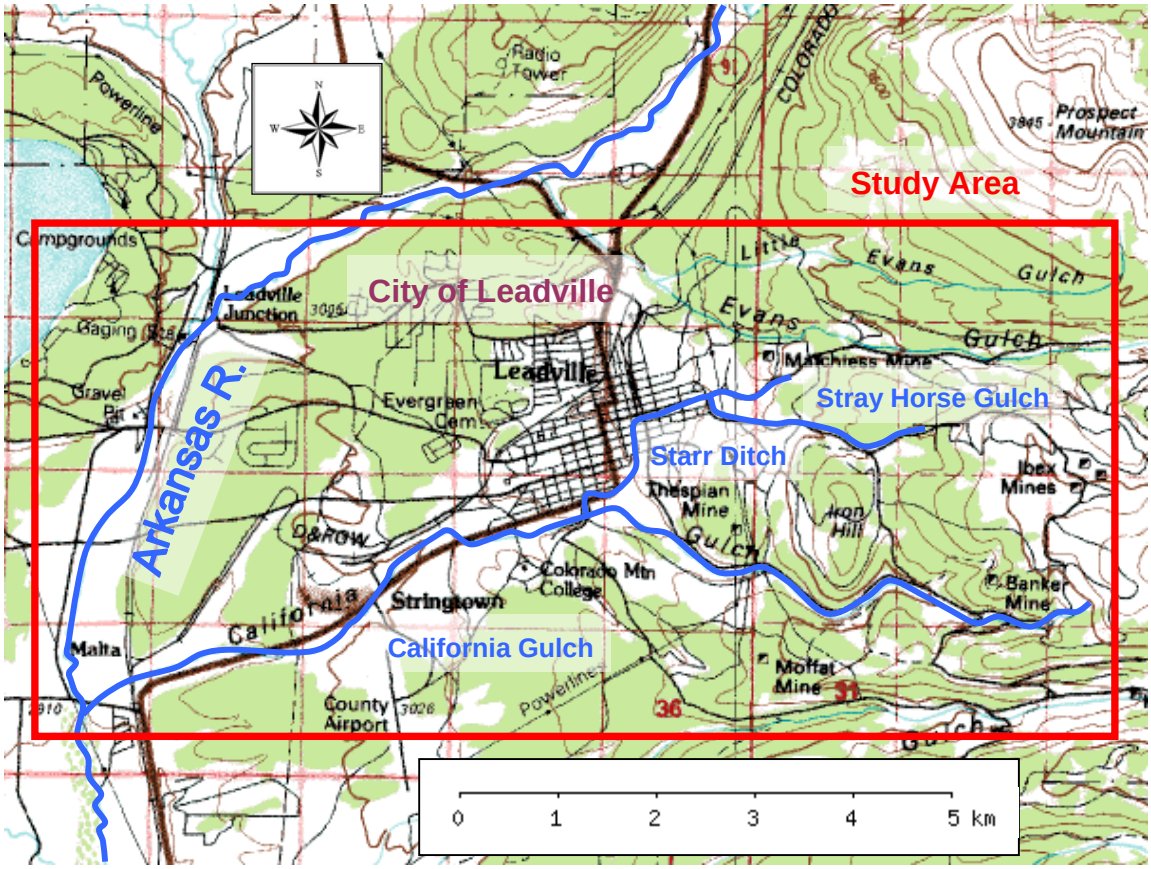

c) Leadville, California Gulch, East Fork Arkansas River

Figure 4-1. Location of California Gulch Watershed, Colorado.

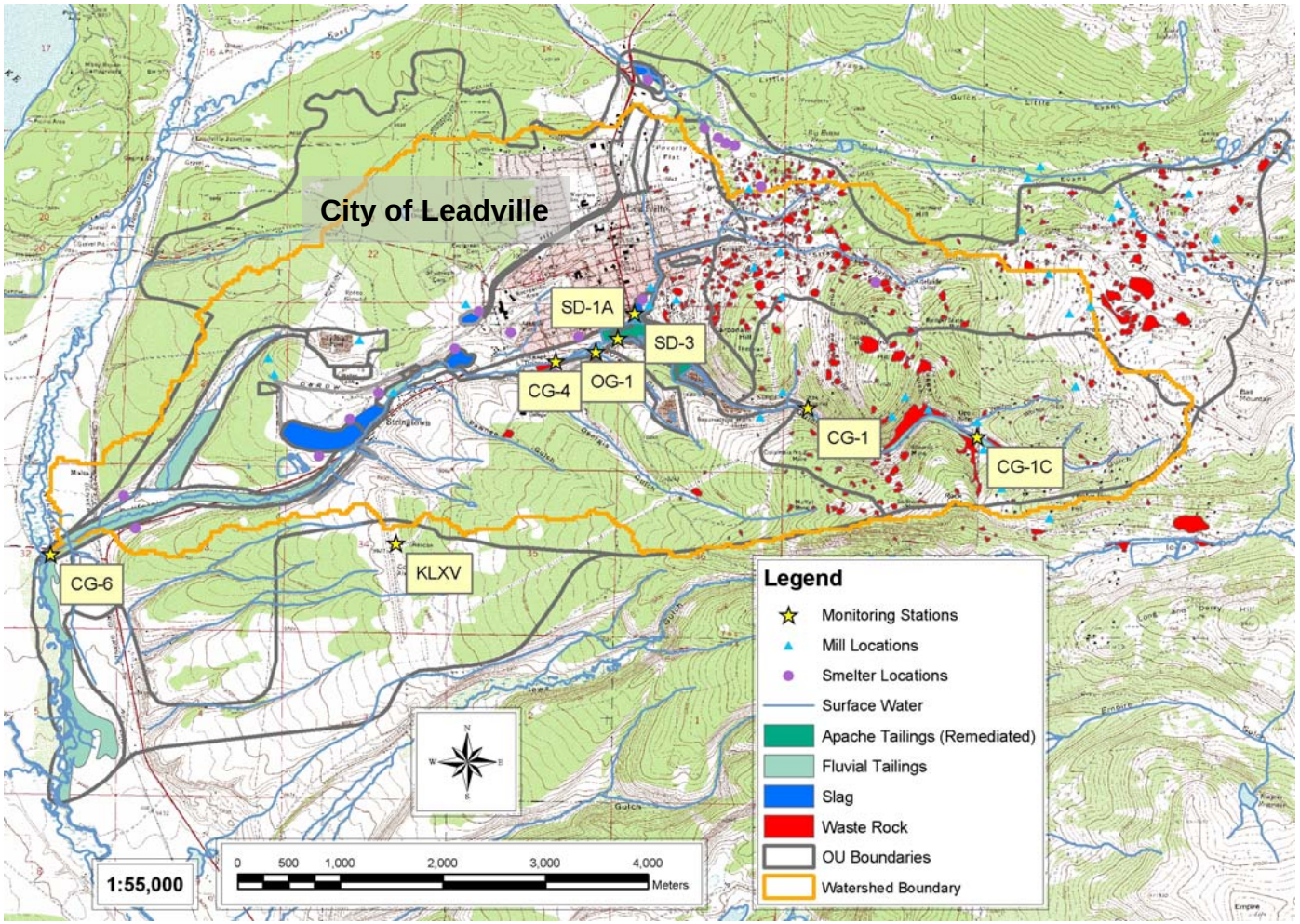

Figure 4-2. California Gulch Superfund project area: site boundaries, waste distribution, and monitoring stations.

confluence (USEPA, 1987a). The project area is divided into 12 Operable Units (OUs). Descriptions of the OUs are presented in Table 4-1. The locations of the most extensive waste rock piles, fluvial tailings, and slag piles are shown. These wastes are widely distributed across the site. The locations of mill and smelter sites are also shown. Operable Unit 6 (OU6) covers the area immediately east and north of the City of Leadville and includes Stray Horse Gulch and Starr Ditch. Operable Unit 4 (OU4) covers the area south and east of the city and includes the upper CG area. Several stream monitoring stations are also shown: (1) CG-1c and CG-1 (upper CG); (2) SD3 and SD-1A (Starr Ditch/Stray Horse Gulch confluence with CG); (3) OG1 (Oregon Gulch confluence with CG); (4) CG-4 (middle CG); and (5) CG-6 (CG confluence with the Arkansas River). The location of the KLXV weather station at the Lake County Airport is also shown. Through upper California Gulch, the stream is narrow, high slope, and ephemeral. In its lower reaches, the stream meanders, has a milder slope, and is perennial, receiving water from ephemeral drainages, the Yak Tunnel mine water treatment works, the Leadville wastewater treatment plant (WWTP), and recharge from the shallow alluvial aquifer that underlies the stream.

4.3 DATA ANALYSIS AND SYNTHESIS

A database of field observations collected as part of characterization and remediation efforts for California Gulch was compiled to support watershed model development. Numerous studies were completed by groups working on behalf of USEPA, Resurrection Mining Company, American Smelting and Refining Company (ASARCO), Denver and Rio Grande Railroad Company, and Colorado Department of Public Health and Environment (CDPHE). These studies were conducted between 1984 and 2004 and delineate the extent of chemical contamination across the site for soils, stream sediment, surface water, and groundwater.

The types of waste present in each OU and related field investigations are summarized in Table 4-1. The locations and spatial distributions of the major waste types and sites and monitoring stations are shown in Figure 4-2. To augment the database, CSU collected

Table 4-1. California Gulch Superfund site Operable Unit (OU) descriptions.

OU	*Description*	*Waste Types Present*					*Investigation*
		Waste Rock	*Tailings*	*Slag*	*Residential Soils*	*Other*	
1	Yak Tunnel outlet and immediately downstream reach of California Gulch	NA	NA	NA	NA	Yak Tunnel	HSI (1986) USEPA (1987)
2	Malta Gulch	?	Yes	?	No	Smelter Soil	USEPA (1987) WCC (1993b)
3	Denver & Rio Grande Railroad Slag	No	No	Yes	No	No	MKC (1993)
4	Upper California Gulch (Garibaldi Mine)	Yes	Yes	No	No	Smelter Soil	USEPA (1987) WCC (1993a)
5	Smelter Sites	Yes	No	Yes	No	Yes	Walsh (1993)
6	Stray Horse Gulch (and Starr Ditch)	Yes	Yes	No	No	Smelter Soil	USEPA (1987) WWC (1993a) HDR (2002)
7	Apache Tailings	No	Yes	No	No	No	USEPA (1987) WCC (1993b) Golder (1997)
8	Colorado Zinc-Lead (Lower California Gulch fluvial tailings)	No	Yes	No	No	Smelter Soil	USEPA (1987) USEPA (1987) WCC (1993b)
9	Leadville (residential and commercial soils)	Yes	No	Yes	Yes	Smelter Soil	USEPA (1987) Walsh (1992) CDM (1994)
10	Oregon Gulch sediments (tailings ponds)	No	Yes	No	No	No	USEPA (1987) WCC (1993b)
11	Arkansas River floodplain	No	Yes	No	No	No	USEPA (1987) WCC (1993b)
12	Surface and groundwater	NA	NA	NA	NA	Surface water and bed sediments, and groundwater	USEPA (1987) WCC (1993c,d) Golder (1996) RMC (2001) RMC (2002) TTRMC (2003) CMC (2004)

Abbreviations: CDM = Camp Dresser and McKee; CMC = Colorado Mountain College; Golder = Golder Associates, Inc.; HDR = HDR Engineering; HSI = Hydro-Search, Inc.; MKC = Morrison-Knudsen Corp.; Walsh = Walsh and Associates, Inc.; WCC = Woodward-Clyde Consultants; RMC = Rocky Mountain Consultants; TTRMC = Tetra-Tech RMC.

soil samples at four locations during July 2002 and contracted with Colorado MountainCollege (CMC) to collect additional water quality samples at four long-term monitoring stations in May 2004. The database was further augmented with digital elevation and land use data obtained from the U.S. Geological Survey (USGS) and soil survey data (USDA, 1975) from the STATSGO (USDA, 1991) and SSURGO (USDA, 1995) databases. These data were used to define watershed characteristics, boundary conditions, and initial conditions, especially the physical and chemical characteristics of soil and sediment for the watershed. With respect to chemical contamination, a summary of conditions by waste type for each operable unit is presented in Table 4-2. Elevation data for the watershed are presented in Figure 4-3. Further descriptions of data describing site surface hydrology (precipitation and flow), soil and sediment properties, and chemical distributions are presented in the sections that follow.

4.3.1 Surface Hydrology: Precipitation and Flow

As part of site monitoring efforts USEPA began to operate a series of automonitors in California Gulch starting in 2002. The automonitors measure stream flow (stage) and precipitation, as well as specific conductivity, water temperature, and pH. During 2002, data were collected at CG-1 and CG-6, initially at a 15-minute interval and later at a 10-minute interval. During 2003, data were collected at CG-1, SD-3, OG-1, CG-4, and CG-6 at a 10-minute interval. Not all parameters are reported at each station. However, flow was reported at CG-1, SD-3, OG-1, CG-4, and CG-6 and precipitation at CG-1, CG-4, and CG-6. It is worth noting that since the time this database was compiled, USEPA has continued to operate the automonitors and even more recent data may be available. The precipitation and flow data from the automonitors provide the most detailed description available of the site surface hydrologic conditions over time. Also note that precipitation was reported for the KLXV weather station at the Lake County Airport.

Automonitor precipitation data were reviewed to determine the intensity and duration of recorded rainfall events. The largest rainfall events the automonitors recorded occurred June 12-13, 2003 and September 5-8, 2003. The June event delivered 18.5 mm (0.73

Table 4-2. Summary of California Gulch field conditions at surface by waste type for each operable unit.

OU	*1*	*2*	*3*	*4*	*5*	*6*	*7*	*8*	*9*	*10*	*11*	*12*	*Investigation*
Waste Rock (mg/kg)													
Cd				60	60	108			25				USEPA (1987a,b,c) WWC (1993a)
Cu				332	206	782			59				
Zn				11100	4502	14200			4040				
Tailings (mg/kg)													
Cd		61		52		81	12	55		13	55		USEPA (1987a,b,c) WWC (1993b) Golder (1997)
Cu		160		271		300	183	344		826	344		
Zn		7250		11300		12200	859	6320		1740	6320		
Slag (mg/kg)													
Cd			5		5				5				USEPA (1987a,b,c) MKC (1993)
Cu			570		570				570				
Zn			66000		66000				66000				
Soils (Residential Areas, Smelter Site "Disturbed Soils") (mg/kg)													
Cd	31	15				26		15	65	4			USEPA (1987a,b,c) Walsh (1992) CDM (1994)
Cu	110	250				206		247	175	118			
Zn	4568	2850				3291		3132	2163	573			
Other Soils (Smelter Site "Undisturbed Soils") (mg/kg)													
Cd	15		15	15	15		15		15				USEPA (1987a,b,c) Walsh (1992) Walsh (1993) CDM (1994)
Cu	159		159	159	159		159		159				
Zn	590		590	590	590		590		590				

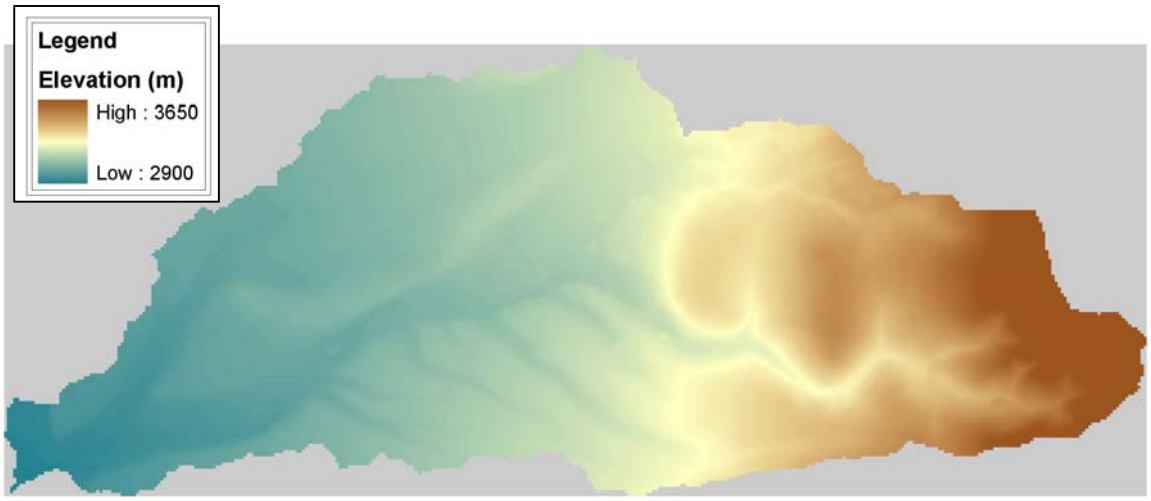

Figure 4-3. Elevations within the California Gulch watershed.

inches) of rain at Station CG-6 with a maximum intensity of approximately 11 mm/hr. The September event delivered 20.3 mm (0.8 inches) of rain at Station CG-6 with a maximum intensity of roughly 9 mm/hour but was spread out as three distinct pulses over roughly 48 hours. The spatial and temporal distributions of rainfall for these events are markedly different. For example, at Station CG-1 the June event delivered less than 14 mm of rain while the September event delivered more than 35 mm. The rainfall time series at Stations CG-1, CG-4, and CG-6 are, in general, weakly correlated. Correlation coefficients (r) range from 0.46 to 0.85. The degree of correlation decreased considerably with increasing distance between stations.

For the June and September 2003 events, automonitor data were reported at a 10-minute interval. In contrast, rainfall data from KLXV is only reported on an hourly basis. The automonitor data indicate that rainfall distributions are highly variable in time. Rainfall pulse durations are generally more intense and much shorter in duration than the hourly reporting interval of the KLXV station. As a consequence of time averaging, rainfall intensities inferred from hourly precipitation data are much lower than the intensities from automonitor data. Although considerable research into the temporal and spatial variability of rainfall patterns has been conducted in recent years (Lanza et al. 2001; Mackay et al. 2001; Fiorucci et al. 2001; Kandel et al. 2005), no reliable procedure to disaggregate hourly rainfall data to a 10-minute interval could be identified. Therefore,

KLXV rainfall data were not further considered in the analysis and all areal rainfall extrapolations were based on the 10-minute automonitor data.

Stream flows across the site are also highly variable. Base flow conditions around the times of the June and September storm events were quite different. The June event occurred at the very end of the snowmelt season. The September event occurred at the end of a relatively dry summer. As inferred from automonitor data, base flow at CG-6 was 0.05 m^3/s (1.8 cfs) during the June event and less than 0.30 m^3/s (1.0 cfs) during the September event. Differences in base flows in the upper portions of the gulch were also observed. Base flow at CG-1 in upper California Gulch was 0.002 m3/s (0.08 cfs) during June and was zero during September. Similarly, base flow at SD-3 in Stray Horse Gulch was 0.005 m3/s (0.18 cfs) during June and was zero during the September. In addition to flow differences over time, annual synoptic survey sampling reports (RMC, 2001; RMC, 2002; TTRMC, 2003) document the patchy occurrence of water influx from seeps and other sources while also documenting flow transmission loss through different reaches of the stream bed. Note that the inferred base flows at CG-6 include effluent discharged from the Leadville WWTP. Data provided by the Leadville Sanitation district indicate that effluent flows from the plant are typically 360,000 gallons/day (0.016 m^3/s or 0.56 cfs). Also note that the Yak Tunnel treatment works can discharge effluents on an intermittent basis. However, during the June and September events no effluents were discharged from the Yak Tunnel facility.

4.3.2 Soil and Sediment Properties

Within the watershed, the NRCS SSURGO database defines 14 soil classifications and the USGS National Land Cover Database (NLCD) defines 13 land uses. To better resolve conditions within the City of Leadville, soil classifications for urban and commercial areas were further subdivided by land use resulting in 17 total soil types. Soil type and land use data for the watershed are presented in Figures 4-4 and 4-5. The NRCS SSURGO database also includes reports of grain size distribution with depth and surface erodibility (USLE K) factors for each soil type. The NLCD, in combination with SSURGO data, also includes more detailed descriptions of ground cover from which

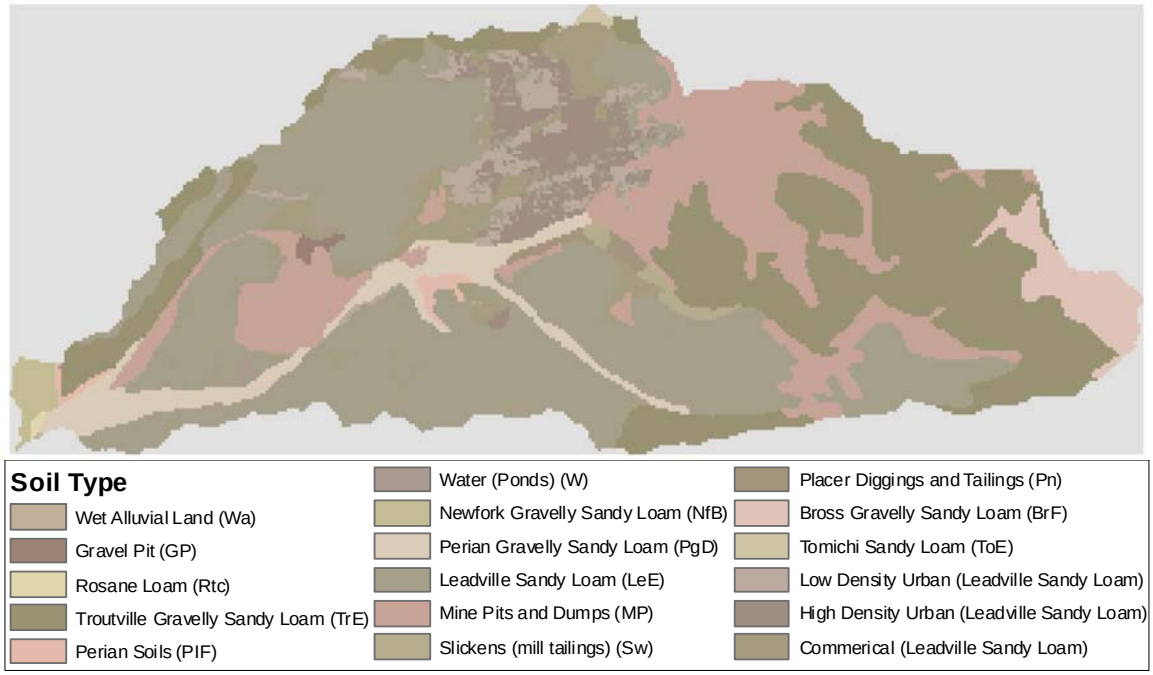

Figure 4-4. Soil types within the California Gulch watershed.

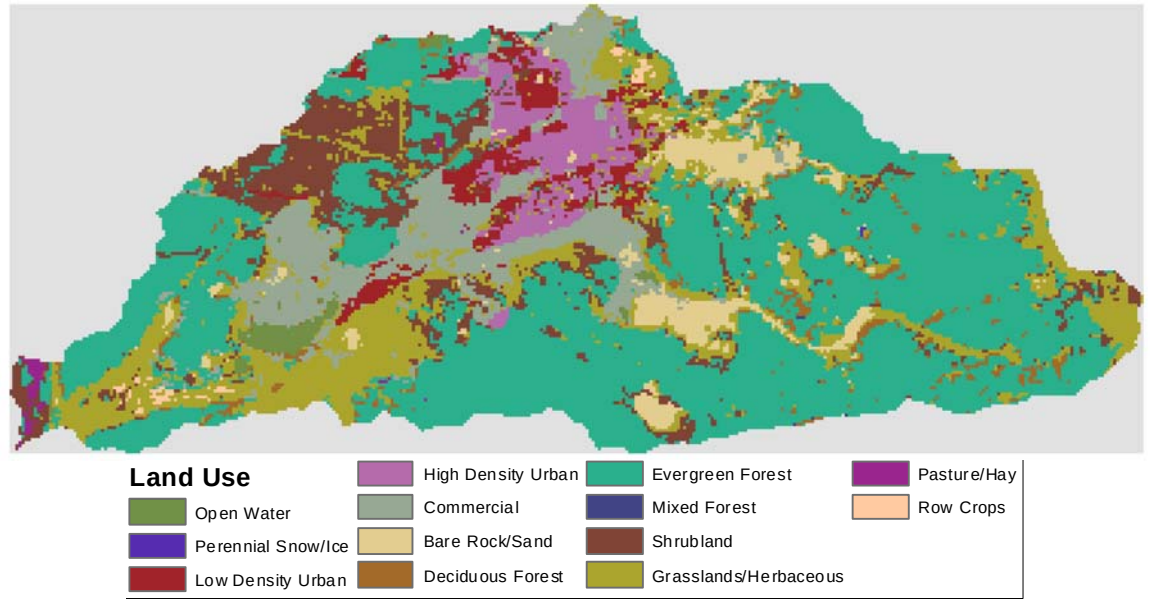

Figure 4-5. Land use within the California Gulch watershed.

cover (USLE C) factors, surface roughness (Manning n), and typical vegetative interception depth can be estimated for each land use. In addition to grain size and erodibility, the SSURGO data also describes soil texture and reports hydraulic conductivity. This information can be used to estimate the infiltration properties of each soil type. As noted in Table 4-1, site characterization reports present grain size distribution, porosity, hydraulic conductivity, and other information for waste rock, tailings, slag piles, soil, and sediment (USEPA, 1987; WCC, 1993a-d; Walsh 1992; Walsh 1993; CDM, 1994; Golder, 1996). The project reports also provide suspended solids concentration and other surface water quality data (WCC, 1993c; Golder, 1996; RMC, 2001; RMC, 2002; TTRMC, 2003; CMC, 2004). Water quality data for upper CG (Stations CG-1C and CG-1), Starr Ditch (Stations SD-1A and SD-3), middle CG (Station CG-4), and lower CG (Station CG-6) are presented in Tables 4-3 to 4-6.

4.3.3 Metals Concentrations

Within the watershed, three basic types of mine waste are defined: waste rock, tailings, and slag. Metals concentrations in representative waste rock, tailings, and slag piles were measured during site characterization efforts (USEPA, 1987a,b,c; WCC, 1993a,b; MKC, 1993; Golder, 1997). In addition, metal concentrations in soils (USEPA, 1987a,b,c; Walsh, 1992; Walsh, 1993; CDM, 1994) were measured at thousands of locations across the site as presented in Figure 4-6. These soil samples identify typical concentrations in disturbed areas where mined rock was processes (e.g. mill and smelter sites), residential areas, and undisturbed area to determine background levels. Stream sediments were also sampled (WCC 1993c,d). Typical metals concentrations across the site are summarized in Table 4-2. These field measurements were further augmented by the surface distributions of pyritic mineral decomposition products (pyrite, goethite, jarosite, and hematite) across the site determined using the Airborne Visible/Infrared Imaging spectrometer (AVIRIS) (Swayze et al. 2000). The AVIRIS data are useful for identifying areas beyond limits of identified waste piles where chemicals from wastes have been transported over time. The project reports also provide metals concentration and other surface water quality data (WCC, 1993c; Golder, 1996; RMC, 2001; RMC, 2002; TTRMC, 2003; CMC, 2004). These surface water data are summarized in Tables 4-3 to 4-6.

Table 4-3. Water quality data for upper California Gulch (Stations CG-1C and CG1).

Date	*Data Source ID*	*Q (m3/s)*	*TSS (mg/L)*	*DOC (mg/L)*	*TOC (mg/L)*	*pH (su)*	*dissolved Cd (µg/L)*	*total Cd (µg/L)*	*dissolved Cu (µg/L)*	*total Cu (µg/L)*	*dissolved Zn (µg/L)*	*total Zn (µg/L)*
11/16/1984	SW-1, USEPA	8.778E-03				8.1	12	11	25	44	1506	1823
3/25/1985	SW-1, USEPA	Dry										
6/17/1985	SW-1, USEPA	7.561E-02	3		0.71	3.4	81	75	644	600	12700	11600
9/9/1985	SW-1, USEPA	Dry										
11/11/1985	SW-1, USEPA	Dry										
5/3/1991	CG-1, WCC	0	152	3.5		4.93	122	97.5	31.1	94	12400	10300
6/12/1991	CG-1, WCC	8.495E-03	1	630		3.47	225	198	713	639	30500	26100
7/24/1991	CG-1, WCC	Dry										
9/17/1991	CG-1, WCC	Dry										
3/24/1992	CG-1, WCC	Dry										
5/15/2001	CG-1C, RMC	5.324E-02	386			2.75	90.1	98.2	1020	1110	16800	17400
5/23/2001	CG-1C, RMC	2.973E-02	9			3.33	52.4	52.2	523	532	9580	9570
4/23/2002	CG-1C, RMC	Dry										
5/22/2003	CG-1C, TTRMC	2.124E-02	326			3.23	156	160	1480	1390	25800	24700
5/21/2004	CG-1C, CMC	5.663E-03	37.3	U	2.2	3.5	110	100	550	510	17000	16000

Q = flow; TSS = total suspended solids; DOC = dissolved organic carbon; TOC = total organic carbon; U = value less than the limit of detection.

Table 4-4. Water quality data for Starr Ditch (Stray Horse Gulch) (Stations SD-1A and SD3).

Date	*Data Source ID*	*Q (m3/s)*	*TSS (mg/L)*	*DOC (mg/L)*	*TOC (mg/L)*	*pH (su)*	*dissolved Cd (µg/L)*	*total Cd (µg/L)*	*dissolved Cu (µg/L)*	*total Cu (µg/L)*	*dissolved Zn (µg/L)*	*total Zn (µg/L)*
11/16/1984	SW-5, USEPA	1.642E-02				7.6	5	5	25	30	362	599
3/25/1985	SW-5, USEPA	4.531E-03	181		6.16	7.4	5	17	14	147	1620	3170
6/17/1985	SW-5, USEPA	9.911E-03	32		0.8	3.3	285	261	531	482	37100	33400
9/9/1985	SW-5, USEPA	Dry										
11/11/1985	SW-5, USEPA	Dry										
5/2/1991	SD-1, WCC	1.727E-02	1680	4		6.45	136	772	16.8	12900	6140	10600
6/12/1991	SD-1, WCC	2.832E-03	126	8		3.62	410	357	910	838	52400	44600
7/24/1991	SD-1, WCC	5.663E-03	34	14		8.14	4.7	7	2.8	17	177	512
9/17/1991	SD-1, WCC	Dry										
3/24/1992	SD-1, WCC	2.832E-04	586	16								
5/15/2001	SD-1A, RMC	No Flow	4				387	394	553	591	101000	102
5/15/2001	SD-3, RMC	2.718E-02	15				202	232	258	311	26500	30.9
5/23/2001	SD-1A, RMC	No Flow										
5/23/2001	SD-3, RMC	1.133E-03										
4/23/2002	SD-3, RMC	No Flow										
5/22/2003	SD-3, TTRMC	3.398E-03	16			6.51	220	232	77.3	132	29600	30500
5/21/2004	SD-1A, CMC	2.120E-04	46.7	1.5	1.9	1.5	250	220	61	54	91000	78000

Q = flow; TSS = total suspended solids; DOC = dissolved organic carbon; TOC = total organic carbon; U = value less than the limit of detection.

Table 4-5. Water quality data for middle California Gulch (downstream of Oregon Gulch) (Station CG-4).

Date	*Data Source ID*	*Q (m3/s)*	*TSS (mg/L)*	*DOC (mg/L)*	*TOC (mg/L)*	*pH (su)*	*dissolved Cd (µg/L)*	*total Cd (µg/L)*	*dissolved Cu (µg/L)*	*total Cu (µg/L)*	*dissolved Zn (µg/L)*	*total Zn (µg/L)*
11/16/1984	SW-7, USEPA	7.164E-02				6.3	227		42		36100	
3/25/1985	SW-7, USEPA	7.759E-02	614		9.78	5.07	71	130	38	1590	21200	37600
6/17/1985	SW-7, USEPA	1.099E-01	52		0.78	3.2	390	382	3750	3620	79800	76600
9/9/1985	SW-7, USEPA	3.596E-02	24		0.68	4.9	323	282	1730	1340	76100	67100
11/11/1985	SW-7, USEPA	3.030E-02	36		0.77	4.44	250	196	447	774	67400	59000
5/2/1991	CG-4, WCC	6.230E-02	868	2		2.89	146	151	888	2420	42100	52100
6/12/1991	CG-4, WCC	2.549E-02	14	0.5		3.99	313	276	863	722	71900	61200
7/24/1991	CG-4, WCC	1.982E-02	148	10		7.43	78.4	148	4.2	346	9920	17900
9/17/1991	CG-4, WCC	2.832E-03	208	2		5.23	83	77.1	88.3	102	55200	51100
3/24/1992	CG-4, WCC	1.727E-02	12	0.5		7.32	26.8	27.1	8.1	39.7	13400	12400
5/15/2001	CG-4, RMC	1.506E-01	64			3.86	95.5	98.4	491	522	18000	18800
5/23/2001	CG-4, RMC	7.787E-02	9			4.18	80.5	77.5	279	277	17100	16600
4/23/2002	CG-4, RMC	3.851E-02	12			6.97	12.3	13.1	5.9	17.4	4840	4950
5/22/2003	CG-4, TTRMC	5.947E-03	10			4.62	238	240	452	430	35000	37000
5/21/2004	CG-4, CMC	1.133E-03	18	U	U	7.05	29	28	U	28	14000	13000

Q = flow; TSS = total suspended solids; DOC = dissolved organic carbon; TOC = total organic carbon; U = value less than the limit of detection.

Table 4-6. Water quality data for lower California Gulch (confluence with the Arkansas River) (Station CG-6).

Date	*Data Source ID*	*Q (m3/s)*	*TSS (mg/L)*	*DOC (mg/L)*	*TOC (mg/L)*	*pH (su)*	*dissolved Cd (µg/L)*	*total Cd (µg/L)*	*dissolved Cu (µg/L)*	*total Cu (µg/L)*	*dissolved Zn (µg/L)*	*total Zn (µg/L)*
11/16/1984	SW-12, USEPA	4.304E-02				7	47	62	23	26	14710	20170
3/25/1985	SW-12, USEPA	1.422E-01	388		2.47	5.91	61	99	15	1100	19300	28700
6/17/1985	SW-12, USEPA	1.090E-01	58		3.1	4	277	282	2500	2560	55600	57700
9/9/1985	SW-12, USEPA	7.362E-02	11		19	7.5	60	102	52	541	13000	25200
11/11/1985	SW-12, USEPA	5.493E-02	52		4.6	6.63	73	79	25	305	22400	26400
5/1/1991	CG-6, WCC	9.996E-02	446	11		6.9	47.8	57.3	8.7	494	11800	15700
6/12/1991	CG-6, WCC	4.814E-02	10	14		7.45	137	138	20.7	300	33400	32500
7/24/1991	CG-6, WCC	7.759E-02	148	16		8	9.1	186	6.8	16.9	114	9690
9/17/1991	CG-6, WCC	3.115E-02	32	6		8.26	2.9	5.6	10.8	11.4	35	2840
3/24/1992	CG-6, WCC	3.993E-02	1	1.5		7.77	8	11.7	5.2	27.1	3090	4820
5/15/2001	CG-6, RMC	1.158E-01	23			4.94	76.3	83.2	281	302	16000	17000
5/23/2001	CG-6, RMC	7.532E-02	11			4.92	66.6	67.4	456	438	15400	15200
4/23/2002	CG-6, RMC	4.984E-02	30			8.44	3.71	11	5.3	25.1	1030	36000
5/22/2003	CG-6, RMC	4.474E-02	10			7.47	48.7	60.8	15.1	83	10600	12400
5/23/2003	CG-6, TTRMC	5.324E-02	52			7.95	52.7	68	21.1	156	10600	14200
5/21/2004	CG-6, CMC	1.303E-02	22	5	6.9	7.9	1.9	5	7.4	16	740	1100

Q = flow; TSS = total suspended solids; DOC = dissolved organic carbon; TOC = total organic carbon; U = value less than the limit of detection.

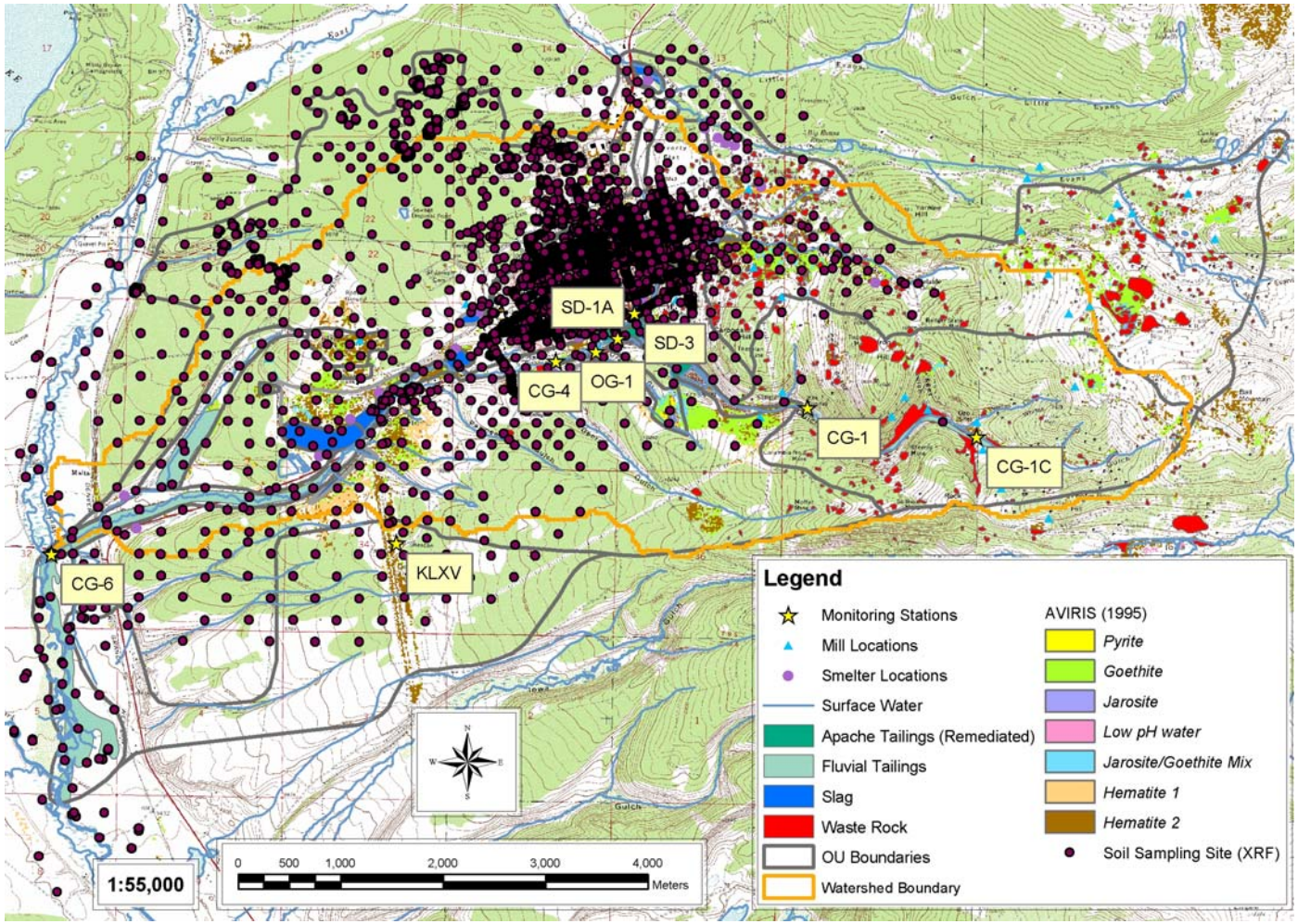

Figure 4-6. Soil contaminant sampling locations and mine waste distributions including AVIRIS imagery.

4.3.4 Database Usability and Limitations

The California Gulch database was compiled in order to support development of a fully distributed, watershed scale chemical transport and fate model for the site. The majority of the data comprising the database were derived from Superfund project reports. Data from those reports were subject to the quality assurance and quality control (QA/QC) procedures that were applicable to Superfund projects at the time those data were collected. All QA/QC approved data from the project reports were considered usable for model development purposes without further QA/QC review. Similarly, data from NRCS and USGS constitute official, publicly distributed products of those agencies and were considered usable for model development without further QA/QC review.

Some limitations of the California Gulch database are worth noting. The database largely focused on upland areas, particularly the physical characteristics and chemicals content of mine wastes and surface soils. Although many samples have been collected over time, most synoptic surface water quality samples were collected during periods of snowmelt-driven flow and all water quality samples in the database were collected at flows of 0.14 m^3/s (5 cfs) or less. No data have been collected at flows that would be representative of extreme flow conditions (1 to 10 m^3/s or more). Further, times series water quality data for any individual storm event (i.e. numerous samples over time for a single event) do not exist for any monitoring site. Also, the watershed is an active USEPA Superfund project area. Several remediation efforts have been conducted to address site contamination. As a result, changing conditions on the land surface may have altered the relationships between concentration and discharge over time.

It is also worth noting that spatial and temporal distributions of rainfall intensities for any storm event are uncertain to an extent because areal rainfall estimates for the watershed must be interpolated based on observations at distant point gages. The watershed covers an area of over 30 km^2 (11.8 mi^2). For interpolation over the entire area of the watershed, point rainfall values must be projected a distance of up to 3.8 km (2.3 miles). Because the correlation between the rainfall time series at different gages decreases significantly as distance between gages increases, the uncertainty of rainfall estimates for distant regions

of the watershed increases. However, it should be recognized that this limitation is common to many sites and is not unique to California Gulch.

5.0 MODEL CALIBRATION AND VALIDATION

5.1 MODEL ORGANIZATION AND PARAMETERIZATION

The California Gulch watershed was simulated using the TREX watershed model. To resolve surface topography as well as the spatial distribution of mine wastes, the watershed was simulated at a 30-meter by 30-meter grid scale. Digital elevation model (DEM) data for the site obtained from the USGS were used to delineate the watershed area.[3] The resultant rectangular raster grid has 147 rows and 372 columns. Within this raster grid, the watershed area is defined by 34,002 cells that comprise the active model domain for the overland plane. The DEM was also used to delineate the channel network with the watershed. The delineated channel network is comprised of 25 links (reaches). The watershed outlet is defined at the location of the California Gulch confluence with the East Fork of the Arkansas River. The rectangular model grid, the active model domain (delineated watershed area), and channel network are presented in Figure 5-1. Watershed elevations, 17 soil types, and 13 land uses were simulated based on USGS and NRCS data as presented in Figures 4-3 to 4-5.

Soil survey data and field samples indicate that the grain size distributions of particles comprising the soils and sediments of the gulch are extremely variable. Particles range in size from clays to boulders. To represent this range of particle types, solids were simulated as six state variables (classes). The characteristics of these six solids classes are presented in Table 5-1.

The physical characteristics of soils were defined from values reported for each soils type in the NRCS SSURGO database and also based on texture using the methods described by Rawls et al. (1983) and Rawls et al. (1993). Properties assigned include the grain size

[3] Watershed delineation for this grid was performed by Rosalia Rojas-Sanchez.

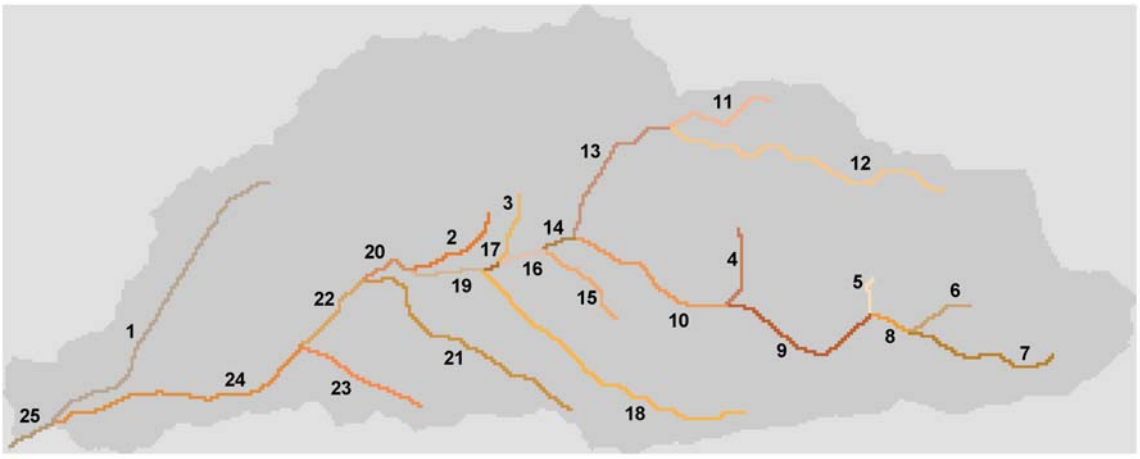

Figure 5-1. California Gulch model domain for overland plane and channels.

Table 5-1. Model state variables for solids.

Solids Type	Mean Diameter, d_p (mm)	Settling Speed, ω_0 (mm/s)	Erosion Threshold, V_{cb} (mm/s)
Boulder	256	1919	3930
Cobble	128	1357	2780
Gravel	16	479	982
Sand	0.50	36	74
Silt	0.031	0.88	1.8
Clay	0.002	0.0034	0.009

distribution, porosity, erodibility (K), effective hydraulic conductivity (K_h), and capillary suction head (H_c). Soil properties for California Gulch are summarized in Table 5-2. In the overland plane, the soil column was defined as two layers with a total thickness of 15 cm (6 inches). The total soil layer thickness was selected based on review of NRCS soils data that indicates the uppermost soil horizons can be underlain by a layer of coarser material at a depth of 12 to 23 cm (5 to 9 inches) and further underlain by even coarser layers that contain a significant fraction of cobble and larger-sized material. This total soil thickness is also reasonable because a single event is not expected to completely denude the land surface of erodible, unconsolidated soils. Given the typically large slopes within the watershed, this is even reasonable for large events that potentially have the power to mobilize more soil because it is unlikely that highly erodible soils exist along steep hillslopes subject to the most erosive action. Note that soils underlying ponded areas were assumed to be Leadville sandy loam. Also note that soils in urban areas are Leadville sandy loam. For urban soil types, differences in erodibilities (K) and effective hydraulic conductivities (K_h) represent differences in land use, particularly the extent of impermeable cover.

The physical characteristics of the channel network and sediment bed were defined from Superfund project data and samples collected during field surveys conducted in 2004. Properties assigned include geometry, grain size distribution, porosity, effective hydraulic conductivity (K_h), and capillary suction head (H_c). These channel and sediment properties are summarized in Table 5-3. In the channel network, the sediment bed was defined as two layers with a total thickness of 10 cm (4 inches). This total sediment bed thickness was selected to permit at least some description of the limited extent of sediment availability from the streambed. Bed samples collected from the gulch indicate that in some locations the channel bed has a relatively thin layer of finer sediment (sand and gravel) that overlie layers of much coarser material that includes large rock fragments or bed rock (hardpan). Description of the bed as two thin layers over hardpan is reasonable because it is possible that a large storm event could cause channel incision sufficient to erode all unconsolidated material from the bed given the large channel bed slopes. Use of two bed layers also allows description of a finer surface layer over a coarser subsurface.

Table 5-2. California Gulch watershed model soils properties.

Soil	*Slope (%)*	*Erodibility K (tons/acre)*	*$V_{critical}$ (m/s)*	*Effective K_h (m/s)*	*H_c (m)*	*Porosity*	*Boulder (%)*	*Cobble (%)*	*Gravel (%)*	*Sand (%)*	*Silt (%)*	*Clay (%)*
Wet Alluvial Land	1-5	0.200	0.089	1.50E-06	2.32E-02	0.429	0.0	5.0	35.0	50.0	5.0	5.0
Gravel Pit	3-35	0.020	0.020	1.50E-06	2.32E-02	0.429	10.0	10.0	20.0	50.0	5.0	5.0
Rosane loam	1-5	0.200	0.089	1.50E-06	9.06E-03	0.431	0.0	0.0	0.0	35.0	32.5	32.5
Troutville gravelly sandy loam	3-35	0.150	0.020	1.70E-06	3.45E-03	0.429	5.0	10.0	25.0	35.0	12.5	12.5
Perian Soils	20-45	0.050	0.007	1.50E-06	1.50E-02	0.430	10.0	5.0	10.0	45.0	15.0	15.0
Water (Ponds)	3-35	0.280	0.020	1.50E-06	5.09E-02	0.430	2.0	3.0	10.0	55.0	15.0	15.0
Newfork gravelly sandy loam	1-3	0.100	0.115	2.00E-06	7.10E-03	0.429	0.0	10.0	25.0	40.0	12.5	12.5
Perian gravelly sandy loam	3-9	0.050	0.038	2.00E-06	7.10E-03	0.429	2.0	8.0	35.0	35.0	10.0	10.0
Leadville sandy loam	3-35	0.280	0.020	1.50E-06	5.09E-02	0.430	2.0	3.0	10.0	55.0	15.0	15.0
Mine Pits and Dumps	3-35	0.020	0.020	2.80E-06	8.70E-05	0.428	5.0	65.0	20.0	10.0	0.0	0.0
Slickens (mill tailings)	3-35	0.640	0.020	1.50E-06	8.24E-04	0.430	0.0	0.0	0.0	20.0	40.0	40.0
Placer diggings and tailings	3-35	0.020	0.020	1.00E-06	8.70E-05	0.428	0.0	70.0	20.0	10.0	0.0	0.0
Bross gravelly sandy loam	9-45	0.050	0.010	1.50E-06	1.63E-03	0.429	5.0	10.0	40.0	30.0	7.5	7.5
Tomichi sandy loam	5-25	0.240	0.018	1.50E-06	2.84E-02	0.430	5.0	5.0	10.0	50.0	15.0	15.0
Urban21 (low density urban)	3-35	0.140	0.020	1.25E-07	5.09E-02	0.430	0.5	1.0	10.0	58.5	15.0	15.0
Urban22 (high density urban)	3-35	0.028	0.020	8.50E-08	5.09E-02	0.430	0.5	1.0	10.0	58.5	15.0	15.0
Urban23 (commercial area)	3-35	0.240	0.020	1.25E-06	5.09E-02	0.430	0.5	1.0	10.0	58.5	15.0	15.0

Note: soils at high elevations can influenced by snow or ice in late spring or early fall. Effective K_h values presented are for snow-free conditions.

Table 5-3. California Gulch watershed model channel and sediment properties.

Channel Link(s)	*Bottom Width (m)*	*Bank Height (m)*	*Sideslope (m/m)*	*Sinuosity (dimensionless)*	*Effective K_h (m/s)*	*Manning n*	*Porosity*	*Boulder (%)*	*Cobble (%)*	*Gravel (%)*	*Sand (%)*	*Silt (%)*	*Clay (%)*
1-2	2	1	0	1	0	0.180	0.400	45.0	50.0	3.0	2.0	0.0	0.0
3-12	2	1	0	1	0	0.080	0.400	45.0	50.0	3.0	2.0	0.0	0.0
13	2	1	0	1	5.00E-07	0.120	0.400	45.0	50.0	3.0	2.0	0.0	0.0
14	2	1	0	1	0	0.080	0.400	45.0	50.0	3.0	2.0	0.0	0.0
15	2	1	0	1	0	0.095	0.400	45.0	50.0	3.0	2.0	0.0	0.0
16	2	1	0	1	0	0.080	0.400	45.0	50.0	3.0	2.0	0.0	0.0
17 (Nodes 1-4)	2	1	0	1	0	0.080	0.400	45.0	50.0	3.0	2.0	0.0	0.0
17 (Nodes 5-7)	2	1	0	1	5.00E-07	0.080	0.400	45.0	50.0	3.0	2.0	0.0	0.0
18	2	1	0	1	0	0.095	0.400	45.0	50.0	3.0	2.0	0.0	0.0
19-20	2	1	0	1	5.00E-07	0.080	0.400	45.0	50.0	3.0	2.0	0.0	0.0
21	2	1	0	1	0	0.095	0.400	45.0	50.0	3.0	2.0	0.0	0.0
22	1	0.35	0	1	5.00E-07	0.080	0.400	45.0	50.0	3.0	2.0	0.0	0.0
23	2	1	0	1	0	0.095	0.400	45.0	50.0	3.0	2.0	0.0	0.0
24	1	0.35	0	1	0	0.080	0.400	45.0	50.0	3.0	2.0	0.0	0.0
25	1	0.35	0	1	0	0.080	0.400	45.0	50.0	3.0	2.0	0.0	0.0

Critical erosion velocity (v_c) thresholds for each soil type were estimated from unit stream power considerations based on the relationship of Moore and Burch (1986):

$$v_c = \frac{0.002}{S_0} \tag{5.1}$$

where: v_c = critical velocity for soil erosion (m/s) [L/T]

S_0 = ground surface slope [dimensionless]

For simplicity, the ground surface slope was computed as the geometric mean of the range slopes on which the soil type occurs as reported by the NRCS. For example, the Leadville soil type occurs on ground slopes that range from 0.03 to 0.35 (3% to 35%) corresponding to an S_0 value of 0.102.

Stream bed sediments across the site are non-cohesive and erosion is assumed to occur independently for each solids size class within the bed. Critical erosion thresholds for grain erosion in the sediment bed were estimated from unit stream power considerations based on the relationships of Yang (1996):

$$v_c = \begin{cases} \left(\dfrac{2.5}{log\left(u_* d_p / \nu\right) - 0.06} + 0.66 \right) \omega_0 & for \quad 1.2 < \dfrac{u_* d_p}{\nu} \le 70 \\ 2.05 \omega_0 & for \quad 70 \le \dfrac{u_* d_p}{\nu} \end{cases} \tag{5.2}$$

where: v_c = critical velocity for sediment bed grain erosion [L/T]

u_* = shear velocity [L/T]

d_p = particle diameter [L]

ν = kinematic viscosity [L^2/T]

ω_0 = settling velocity [L/T]

Land use characteristics were defined from values in the USGS National Land Cover Database (NCLD). Characteristics assigned include the surface roughness (Manning n), rainfall interception depth, land cover factor (C), and land management factor (P). Surface roughness values were selected from tabulated values presented by Woolhiser et al. (1990) and USACE (1998). Interception depths were based on tabulated values presented by Linsley et al. (1982), Woolhiser et al. (1990), and Bras (1990). Land cover and management practice factors were selected based on the values presented by Wischmeier and Smith (1978) as summarized by Julien (1998). Land use characteristics for California Gulch are summarized in Table 5-4. Note that several land use types for the site are not accurately identified in the NLCD. The open water land use represents tailing ponds. Since the time the NLCD data were captured, tailing ponds have been dewatered so the open water land use was treated as bare rock (NCLD Class 31). The row crop land use is misclassified and was treated as grassland (NLCD Class 71).

Table 5-4. California Gulch watershed model land use characteristics.

Land Use/Cover	*NLCD Class*	*Manning n*	*Interception (mm)*	*C*	*P*
Open Water	11	0.150	0	0.20	
Perennial Ice/Snow	12	0.150	0.25	0.005	
Low Intensity Residential	21	0.075	0.1	0.01	
High Intensity Residential	22	0.050	0	0.001	
Commercial/Industrial/Transportation	23	0.150	0.1	0.10	
Bare Rock/Sand/Clay	31	0.150	0	0.20	
Deciduous Forest	41	0.450	0.5	0.04	1.0
Evergreen Forest	42	0.450	2	0.04	
Mixed Forest	43	0.450	2	0.06	
Shrubland	51	0.400	2	0.08	
Grasslands/Herbaceous	71	0.300	1	0.042	
Pasture/Hay	81	0.300	1	0.042	
Row Crops	82	0.300	1	0.042	

Three chemical state variables were simulated: cadmium (Cd), copper (Cu), and zinc (Zn). Chemical concentrations and distributions in soil and sediment were estimated from Superfund project data and AVIRIS imagery. Average chemical concentrations by media for each operable unit were presented in Table 4-3. AVIRIS data were collected in 1995 and calibrated to ground conditions (Swayze et al. 2000). Initial chemical concentrations for each cell in the model domain were assigned using waste rock, tailings, and slag distributions, the AVIRIS mineral map, and the concentration matrix from Table 4-3. Two-phase partitioning was simulated where the total concentration is the sum of the dissolved and particulate phases. Partition (distribution) coefficients for Cd, Cu, and Zn were selected based on the data of Sauvé et al. (2000, 2003) and Lu and Allen (2001). The partition coefficient is sensitive to numerous environmental factors, the most significant of which is pH. As functions of pH, partition coefficients (log K_d) for Cd, Cu, and Zn are (Sauvé et al. 2000):

$$log\, K_{d,Cd} = (0.49 \pm 0.02)pH - (0.60 \pm 0.49) \tag{5.3}$$

$$log\, K_{d,Cu} = (0.27 \pm 0.02)pH + (1.49 \pm 0.13) \tag{5.4}$$

$$log\, K_{d,Zn} = (0.62 \pm 0.03)pH - (0.97 \pm 0.21) \tag{5.5}$$

where: $log\, K_{d,\,Me}$ = partition (distribution) coefficient for a metal (Cd, Cu, or Zn)

pH = $-log[H^+]$

$[H^+]$ = hydronium ion concentration (activity)

As summarized in Tables 4-3 to 4-6, the pH of California Gulch surface water is highly variable and has been observed to range from less than 3 to more than 8. Over this range of pH variation, partition coefficients (log K_d) for Cd, Cu, and Zn can vary be more than a factor of three (in log space). Direct simulation of pH as a model state variable was not feasible. To nonetheless account for the pH dependence of the partition coefficient, a representative surface water pH of 6.0 was selected. The distribution coefficients used for Cd, Cu, and Zn are: log $K_{d,\,Cd}$ = 2.34, log $K_{d,\,Cu}$ = 3.24, log $K_{d,\,Zn}$ = 2.54.

5.2 HYDROLOGIC CALIBRATION AND VALIDATION

The June 12-13, 2003 storm was used to calibrate the model. The simulation period was 24 hours. There was no precipitation for several days preceding this event. The hydrologic parameters subject to calibration were effective hydraulic conductivity (K_h) and flow resistance (Manning n). Calibrated hydrologic model parameter values for soil and sediment were presented in Tables 5-2 and 5-3. Graphs of rainfall, observed flow, and simulated flow for the June storm at Stations CG-1, SD-3, CG-4, and CG-6 are presented in Figures 5-2 to 5-5.

The September 5-8, 2003 storm was used to validate the model. The simulation period was 72 hours. Again, there was no precipitation for several days preceding this event. With one exception, model parameters values for the validation simulation were identical to the values for the calibration simulation. Graphs of rainfall, observed flow, and simulated flow for the September storm at Stations CG-1, SD-3, CG-4, and CG-6 are presented in Figures 5-6 to 5-9.

As noted, model parameters values for the validation simulation were identical to the values for the calibration simulation with one exception. The exception was that effective hydraulic conductivities for the June event were 50% less than the September event value for the Mine Pits and Dumps (MP), Troutville (TrE), and Bross (BrF) soil types. This change in parameterization was necessary to account for partially frozen soil conditions that existed for soils at the highest elevations in the watershed during the June storm. Data for the Fremont Pass SNOTEL site (Site Number: 485, Station ID: 06k08s) were obtained from the NRCS National Water and Climate Center. The Fremont Pass SNOTEL instrument cluster is located approximately 12 km (8 miles) from the California Gulch watershed at an elevation of 3,475 m (11,400 feet) and is expected to be representative of higher elevation conditions in the gulch. These data indicate that significant snowpack existed and that air temperatures were below freezing during the June 12-13, 2003 storm, with snow-water equivalent depths ranging from 6.3 to 7.3 cm (2.5 to 2.9 inches) during the June storm. No snow was on the ground and air temperatures were well above freezing during the September 2003 event. The effective hydraulic conductivity values in Table 5-2 and 5-3 represent snow-free conditions.

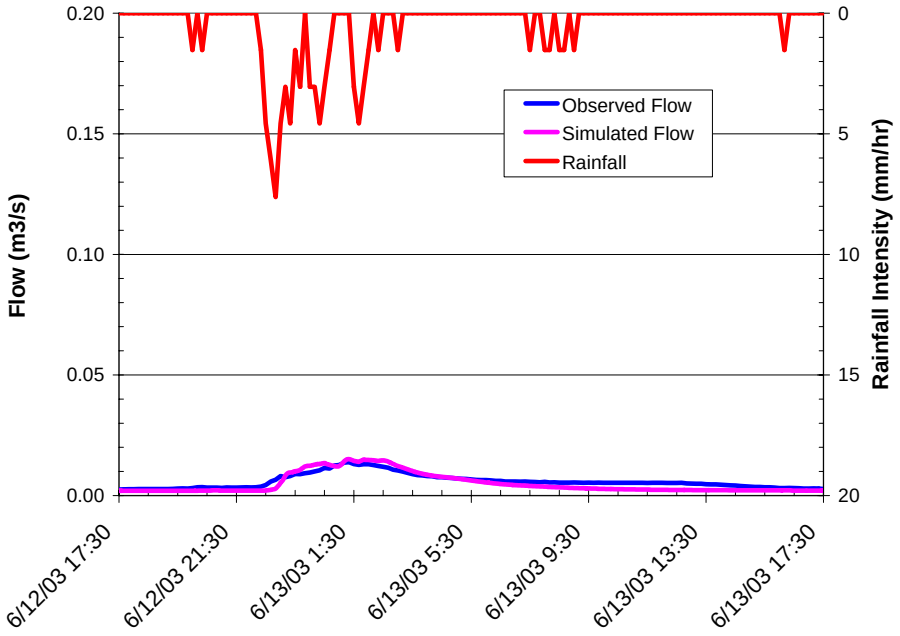

Figure 5-2. Hydrologic calibration at Station CG-1 (June 12-13, 2003).

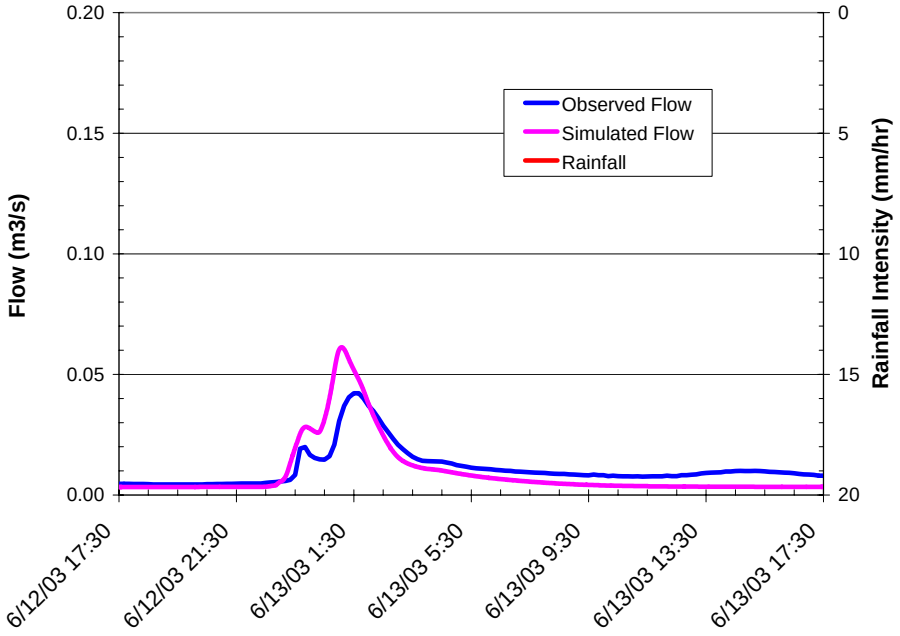

Figure 5-3. Hydrologic calibration at Station SD-3 (June 12-13, 2003).

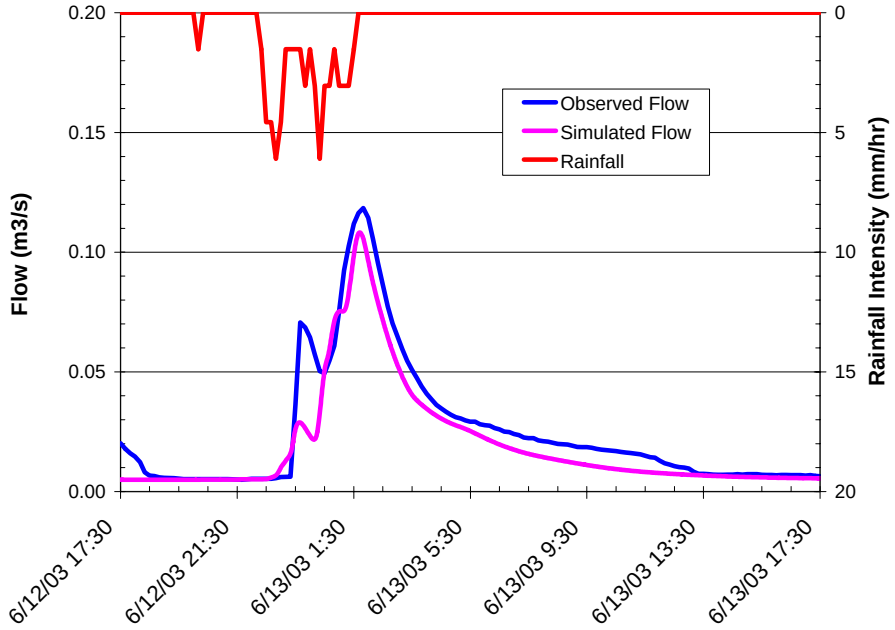

Figure 5-4. Hydrologic calibration at Station CG-4 (June 12-13, 2003).

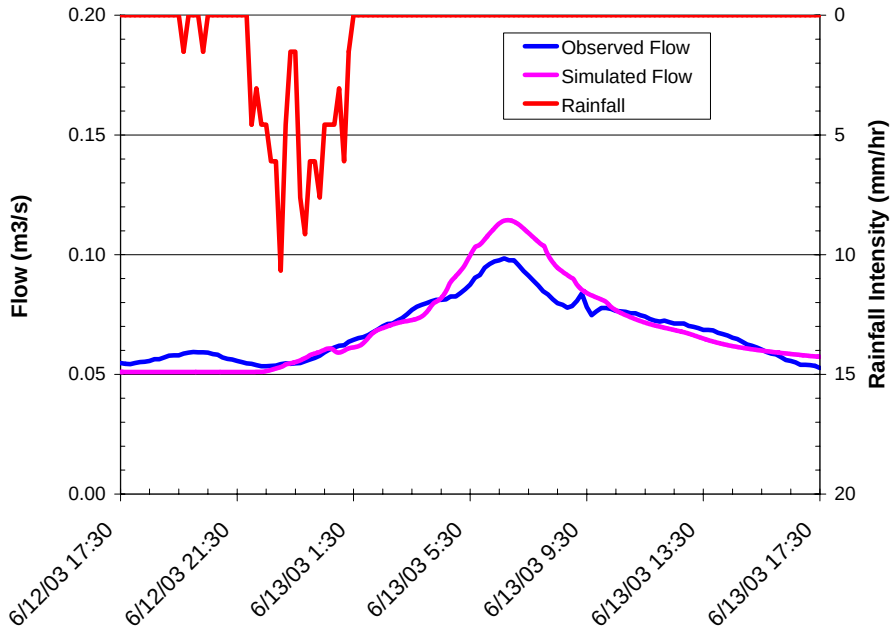

Figure 5-5. Hydrologic calibration at Station CG-6 (June 12-13, 2003).

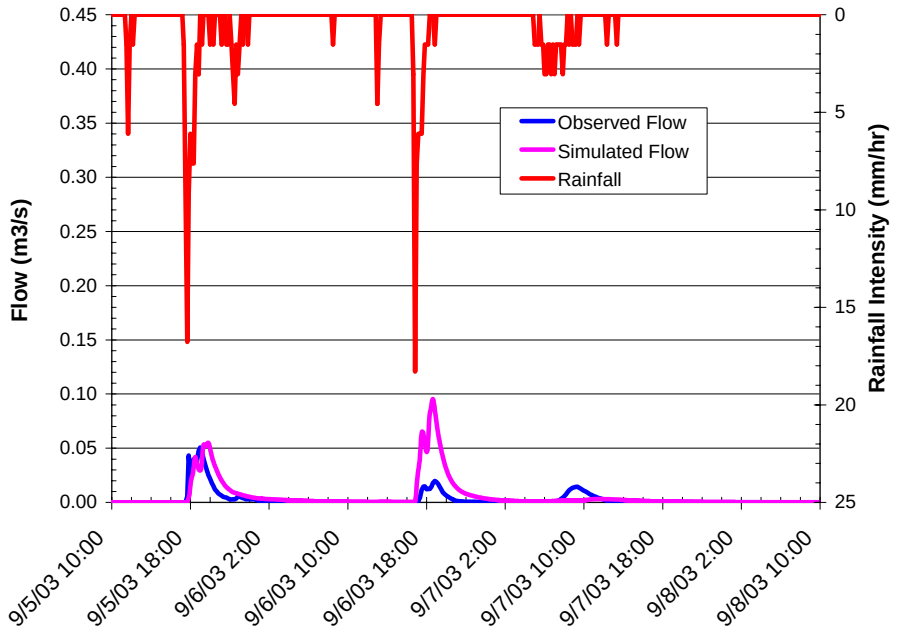

Figure 5-6. Hydrologic validation at Station CG-1 (September 5-8, 2003).

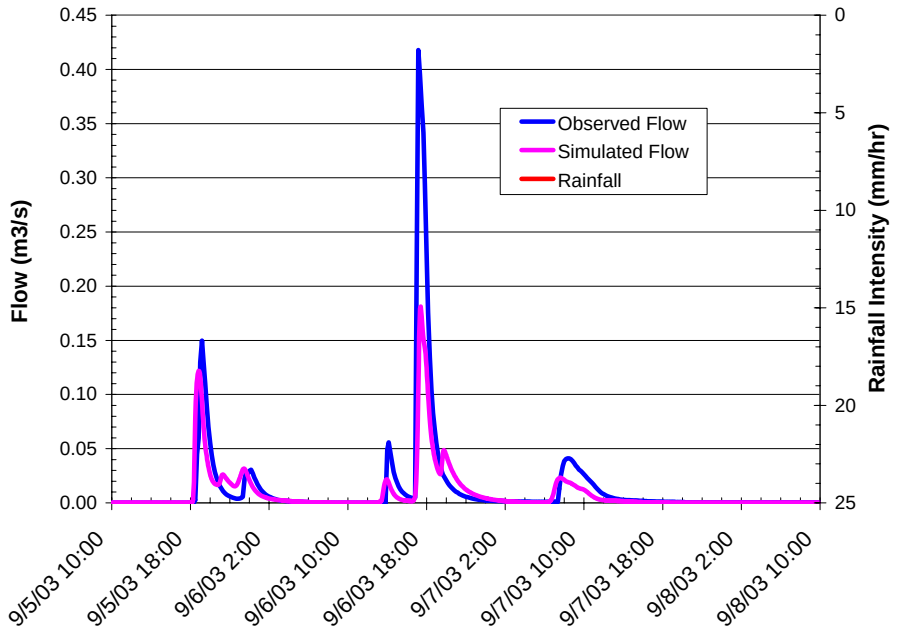

Figure 5-7. Hydrologic validation at Station SD-3 (September 5-8, 2003).

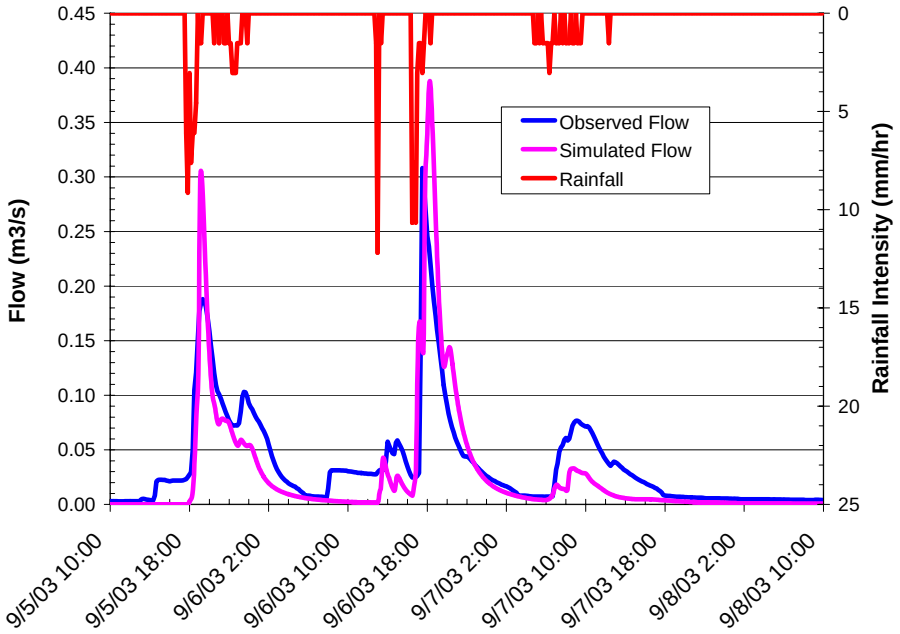

Figure 5-8. Hydrologic validation at Station CG-4 (September 5-8, 2003).

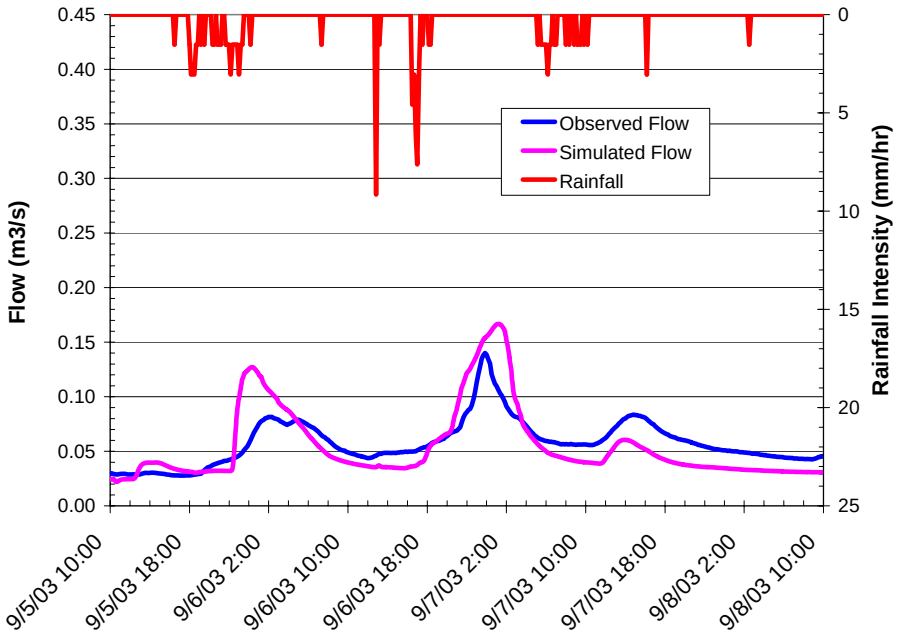

Figure 5-9. Hydrologic validation at Station CG-6 (September 5-8, 2003).

Model performance was evaluated by comparing the relative percent difference (RPD) between model results and observations for three metrics: (1) total flow volume; (2) peak flow; and (3) time to peak flow. Summaries of the performance evaluation for the June calibration and September validation simulations are presented in Table 5-5.

Overall performance for the calibration simulation was quite good. The flow volume, peak flow, and time to peak are all accurately simulated. The total flow volume RPD was -8.6%, the peak flow RPD was +15.6%, and the time to peak RPD was -1.5%. Although less strong than the calibration, the overall model performance for the validation simulation was also good. In particular, the total flow volume RPD across all stations for the September event was +11.3%. Note that RPD values for all stations are arithmetic averages of the individual station values. If computed on a flow volume weighted average basis, RPD values for all stations would generally be less than those summarized in Table 5-5 because relative errors at stations with larger flows (CG-4 and CG-6) tend to be lower than at stations with smaller flows.

5.3 SEDIMENT TRANSPORT CALIBRATION AND VALIDATION

The sediment transport parameters subject to calibration were: (1) soil erodibility (K); (2) the land cover factor (C); and (3) the land management practice factor (P). Calibrated model parameter values for soil and sediment were presented in Tables 5-2 and 5-3. Lands in the watershed are not managed for agriculture or as rangelands, management practice factors were set to 1.0. Graphs of observed and simulated total suspended solids (TSS) concentrations vs. flow for the June and September storms at Stations CG-1, SD-3, CG-4, and CG-6 are presented in Figures 5-10 to 5-13.

Note that observed TSS concentration data were collected over the period 1984 to 2004 and are not paired in time with the events simulated. In the absence of comparable time series data, model performance was evaluated by comparing the range of model results to the range of observations as a function of flow. Summaries of the performance evaluation for the June calibration and September validation simulations are presented in Table 5-6.

Table 5-5. Hydrologic model performance evaluation summary.

Event	*Station*	*Metric*								
		Total Volume (m3)			*Peak Flow (m3/s)*			*Time to Peak (hrs)*		
		Observed	*Simulated*	*RPD*	*Observed*	*Simulated*	*RPD*	*Observed*	*Simulated*	*RPD*
June	CG-1	491	430	-12.4	0.014	0.015	+9.4	7.83	7.82	-0.2
	SD-3	906	824	-9.1	0.042	0.061	+45.4	8.00	7.58	-5.2
	CG-4	2136	1701	-20.4	0.118	0.108	-8.6	8.33	8.20	-1.6
	CG-6	5606	6031	+7.6	0.098	0.114	+16.2	13.17	13.30	+1.0
	All Stations			-8.6			+15.6			-1.5
September	CG-1: 1st Peak 2nd Peak 3rd Peak	737	1541	+109	0.051 0.020 0.014	0.055 0.095 0.003	+8.9 +382 -78.3	9.00 8.83 3.33	9.80 8.65 5.45	+8.9 -2.1 +63.5
	SD-3: 1st Peak 2nd Peak 3rd Peak	3570	2371	-33.6	0.150 0.412 0.041	0.122 0.181 0.023	-18.7 -56.6 -43.3	9.17 7.16 2.33	8.85 7.40 1.60	-3.4 +3.3 -31.4
	CG-4: 1st Peak 2nd Peak 3rd Peak	9571	7138	-25.4	0.188 0.308 0.077	0.306 0.388 0.033	+62.5 +25.8 -56.9	9.33 7.50 3.00	9.15 8.25 2.75	-2.0 +10.0 -8.3
	CG-6: 1st Peak 2nd Peak 3rd Peak	14997	14276	-4.8	0.082 0.140 0.084	0.127 0.167 0.060	+55.9 +19.0 -27.6	16.00 13.83 8.83	14.35 15.20 7.95	-10.3 -9.9 -10.0
	All Stations: 1st Peak 2nd Peak 3rd Peak			+11.3			+27.1 +92.5 -51.5			-1.7 +5.3 +3.4

Note: values for "All Stations" are the arithmetic average of the four individual station values.

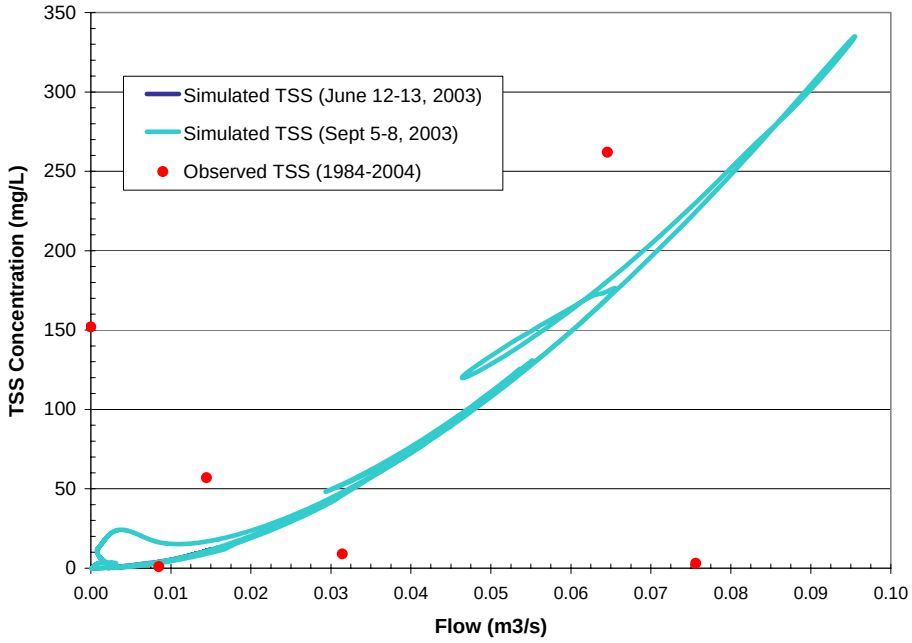

Figure 5-10. Sediment transport calibration and validation at Station CG-1.

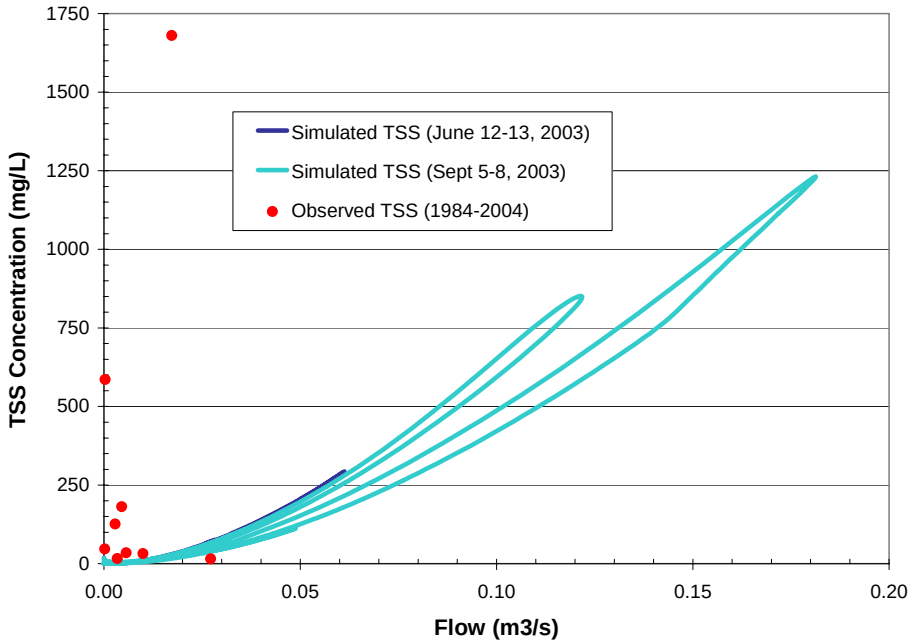

Figure 5-11. Sediment transport calibration and validation at Stations SD-3.

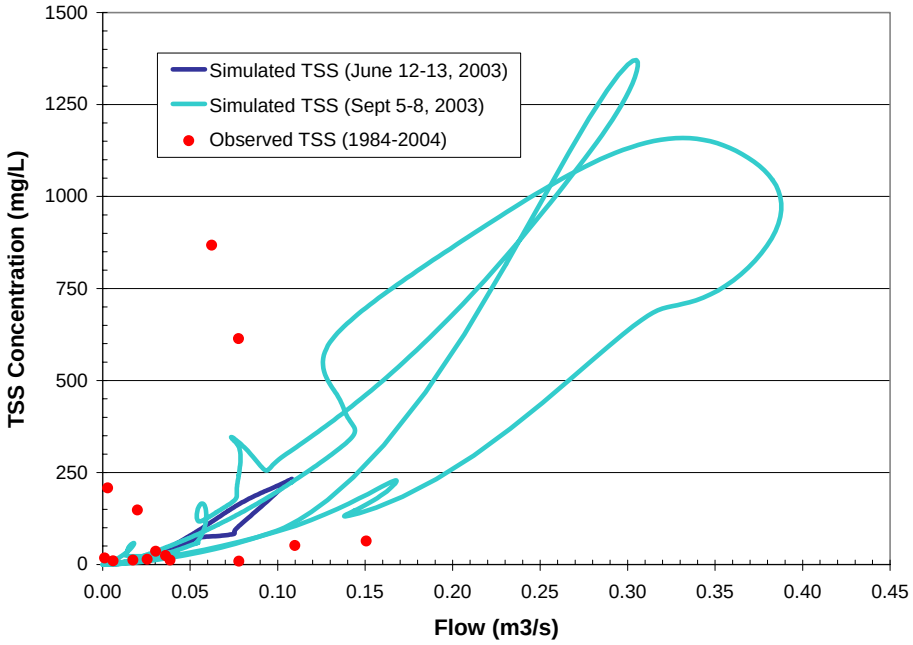

Figure 5-12. Sediment transport calibration and validation at Station CG-4.

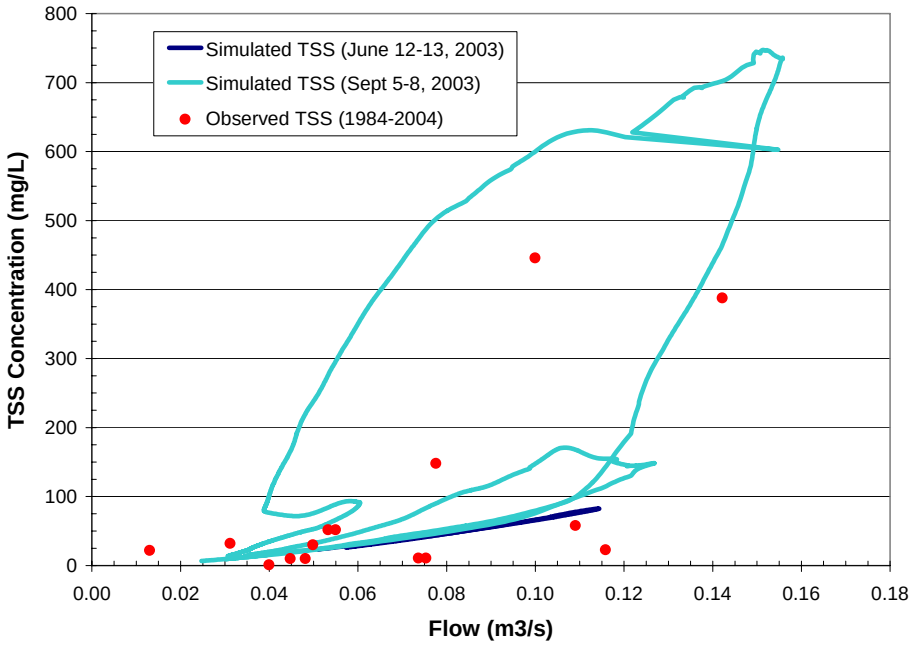

Figure 5-13. Sediment transport calibration and validation at Station CG-6.

Table 5-6. Sediment transport model performance evaluation summary.

Station	Observed TSS (mg/L)			Simulated TSS (mg/L)			Modeled Period
	low	median	high	low	median	high	
CG-1	1.0	37.3	386	3.77	8.42	11.9	June 03
				3.52	49.3	335	Sept 03
SD-3	4.0	40.4	1680	6.92	47.1	293	June 03
				4.01	30.1	1231	Sept 03
CG-4	9.0	30.0	868	1.87	13.6	233	June 03
				1.62	26.9	1370	Sept 03
CG-6	1.0	30.0	446	11.7	31.7	82.6	June 03
				4.47	27.2	747	Sept 03

Overall performance for both the calibration and validation simulations was well within the range of observations and considered to be satisfactory. In general, the minimum, median, and maximum values observed were reproduced. However, in some instances the model has a low bias where simulated TSS is less than observed. Given the extent of infiltration in upland areas (98% of all rainfall infiltrates), only a small mass of solids is delivered from upland areas to the channel network. Most solids transported through the stream channel during the simulation originate from the sediment bed. This low bias may be attributable to uncertainty in the initial grain size distribution of solids in the sediment bed or the erosion (incipient motion) threshold for each solids type.

5.4 CHEMICAL TRANSPORT CALIBRATION AND VALIDATION

The chemical transport parameter subject to calibration was the partition (distribution) coefficient (log K_d). The calibrated distribution coefficient (log K_d) values for Cd, Cu, and Zn were: log $K_{d,\,Cd}$ = 2.34, log $K_{d,\,Cu}$ = 3.24, log $K_{d,\,Zn}$ = 2.54. Graphs of observed total metals concentrations and simulated total metals concentrations vs. flow for both the June and September storms at Stations CG-1, SD-3, CG-4, and CG-6 are presented in Figures 5-14 to 5-17. The total metals concentration is the sum of the dissolved and particulate phases.

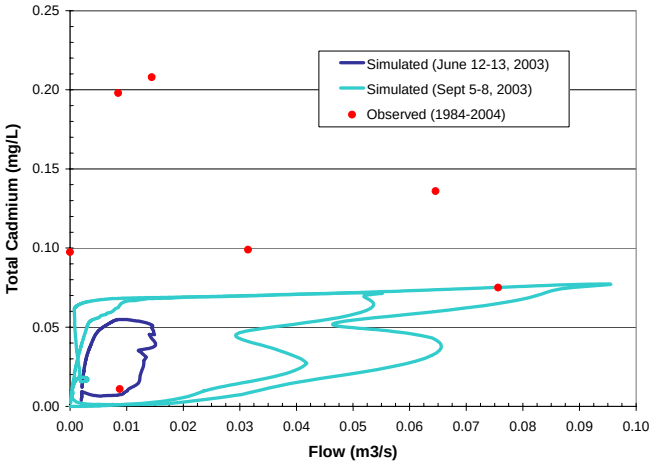

a) Total cadmium

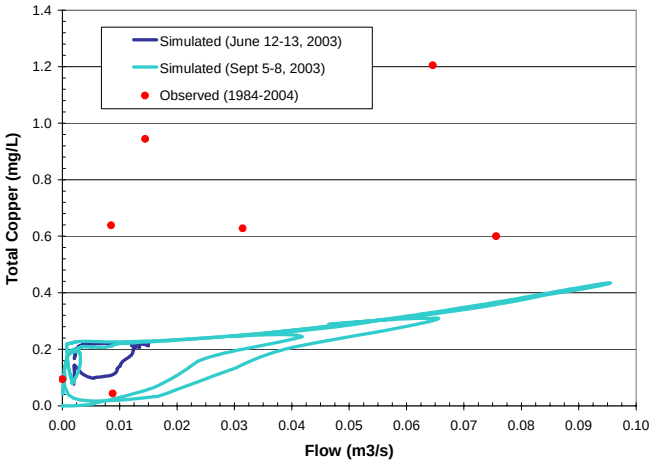

b) Total copper

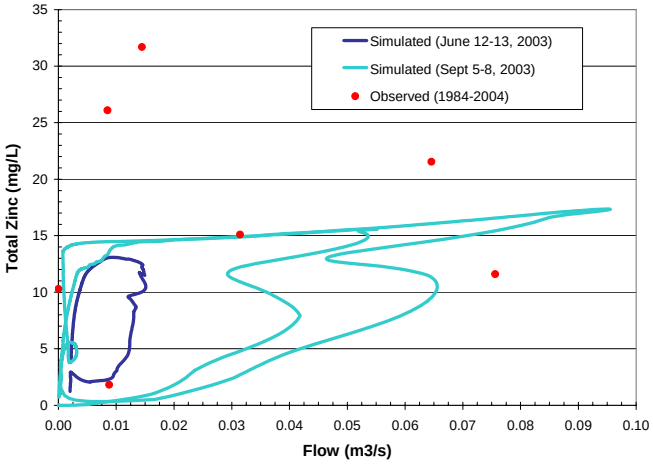

c) Total zinc

Figure 5-14. Chemical transport calibration and validation at Station CG-1.

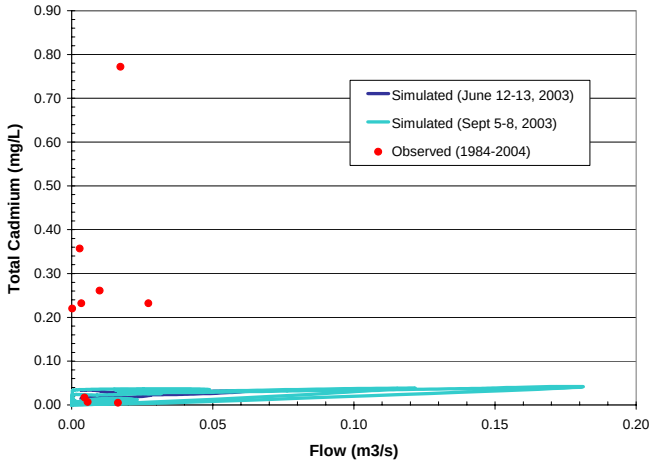

a) Total cadmium

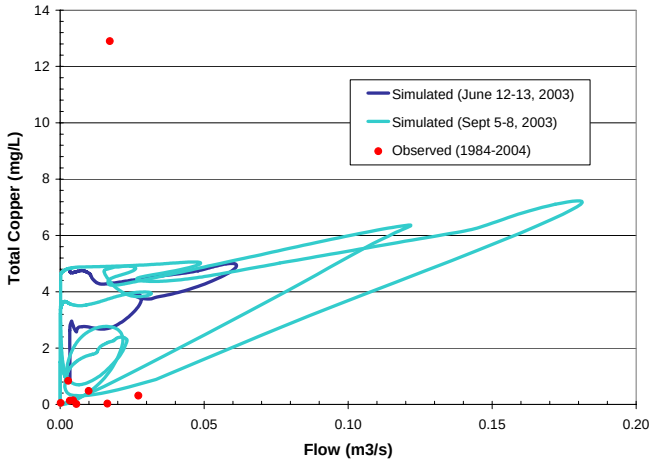

b) Total copper

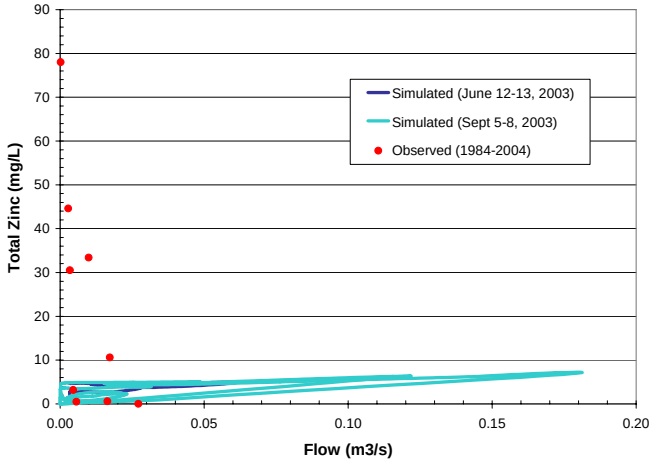

c) Total zinc

Figure 5-15. Chemical transport calibration and validation at Station SD-3.

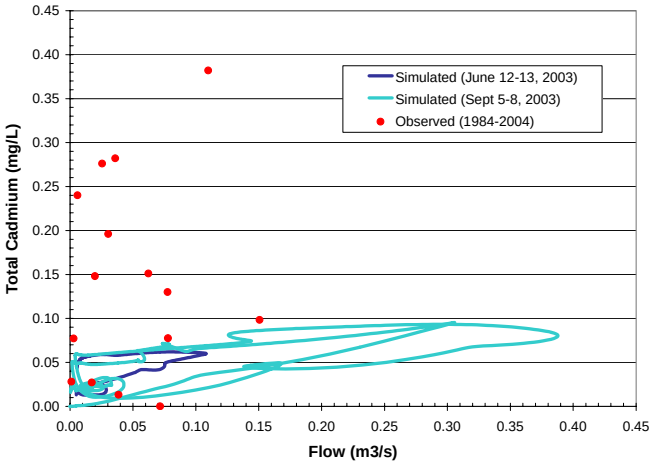

a) Total cadmium

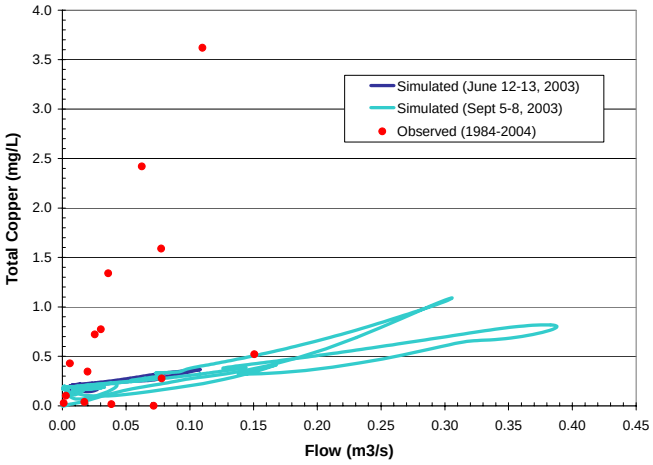

b) Total copper

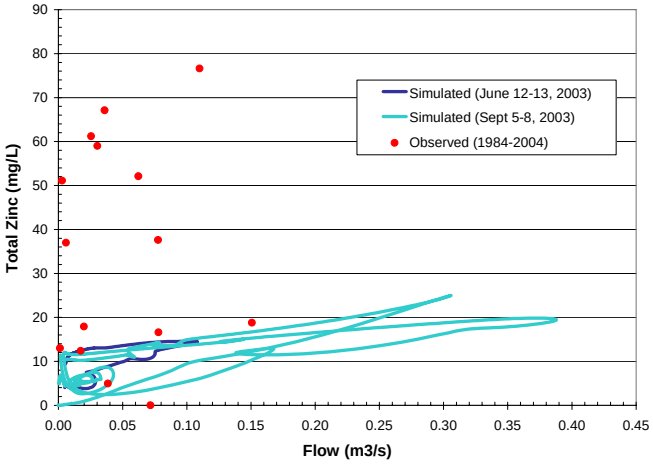

c) Total zinc

Figure 5-16. Chemical transport calibration and validation at Station CG-4.

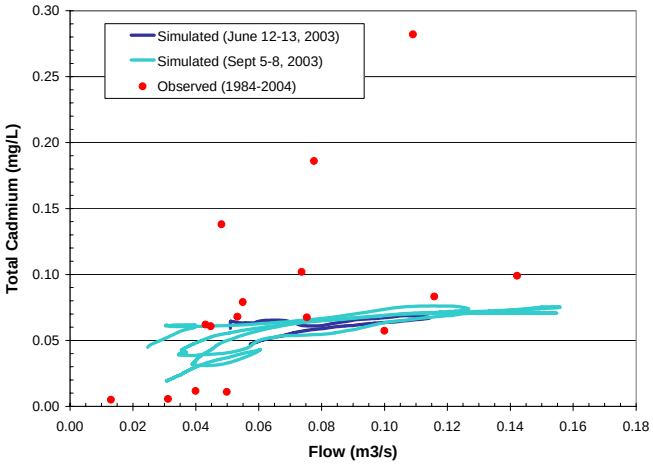

a) Total cadmium

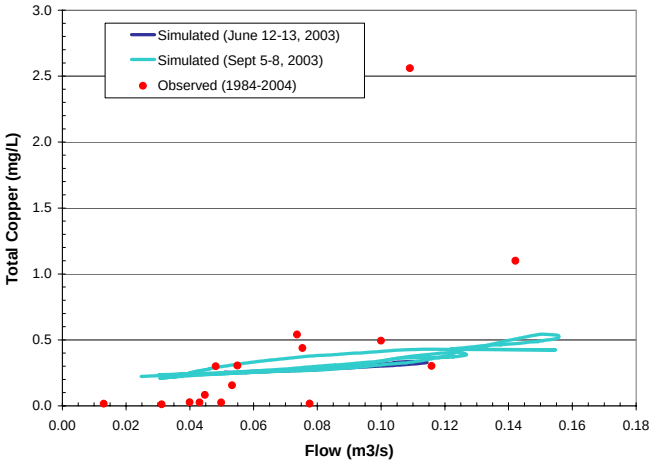

b) Total copper

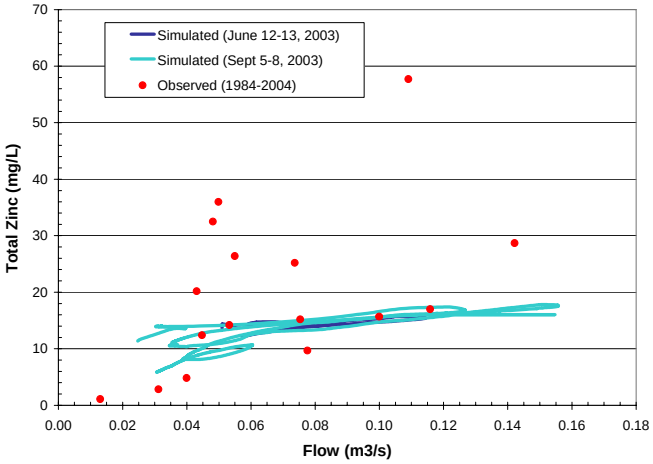

c) Total zinc

Figure 5-17. Chemical transport calibration and validation at Station CG-6.

Like suspended solids, note that observed metals concentration data were collected over the period 1984 to 2004 and are not paired in time with the events simulated. In the absence of comparable time series data, model performance was evaluated by comparing the range of model results to the range of observations as a function of flow. Summaries of the performance evaluation for the June calibration and September validation simulations are presented in Table 5-7.

Overall performance for both the calibration and validation simulations was within the range of observations and considered to be satisfactory. In general, the minimum and median values observed were reproduced. However, with respect to maximum values the model has a low bias as simulated metals concentrations are typically much less than observed values. As was noted for suspended solids, only small masses of metals are delivered from upland areas to the channel network, given the extent of infiltration. Consequently, most metals transported through the stream channel during the simulation originate from the sediment bed. This low bias may be attributable to uncertainty in the initial grain size distribution of solids in the sediment bed and is compounded by uncertainty in the initial bed sediment metals concentrations. It is also worth noting that concentration boundary conditions for metals in stream base flow were assumed to be zero.

Model performance for dissolved metals is similar to performance for total metals. Graphs of observed dissolved metals concentrations and simulated dissolved metals concentrations vs. flow for both the June and September storms at Stations CG-1, SD-3, CG-4, and CG-6 are presented in Appendix C. Simulated metals phase distributions for both storms at Station CG-6 are also presented in Appendix C.

Note that there is an added degree of uncertainty for dissolved metals concentration observations. In many instances the reported dissolved phase concentration exceeds total metals concentrations. Although the differences are generally small, the dissolved fraction should never exceed the total. Despite this anomaly, the dissolved and total concentration data met quality assurance criteria and are considered valid data.

Table 5-7. Chemical transport and fate model performance evaluation summary.

Station	Metal	Observed Total Metals (mg/L)			Simulated Total Metals (mg/L)			Modeled Period
		low	median	high	low	median	High	
CG-1	Cd	0.011	0.044	1.82	0.007	0.045	0.055	June 03
					0.001	0.068	0.077	Sept 03
	Cu	0.098	0.600	15.1	0.111	0.219	0.225	June 03
					0.019	0.245	0.435	Sept 03
	Zn	0.208	1.39	31.7	2.33	11.5	13.1	June 03
					0.343	14.5	17.4	Sept 03
SD-3	Cd	0.005	0.232	0.772	0.016	0.030	0.033	June 03
					0.002	0.028	0.042	Sept 03
	Cu	0.017	0.229	12.9	0.042	0.059	0.095	June 03
					0.014	0.056	0.235	Sept 03
	Zn	0.031	6.88	78.0	2.67	4.45	5.00	June 03
					0.324	4.38	7.23	Sept 03
CG-4	Cd	0.013	0.139	0.382	0013	0.057	0.062	June 03
					0.002	0.050	0.095	Sept 03
	Cu	0.017	0.476	3.62	0.137	0.225	0.367	June 03
					0.026	0.209	1.09	Sept 03
	Zn	4.95	37.3	76.6	3.73	12.3	14.6	June 03
					0.380	11.2	25.0	Sept 03
CG-6	Cd	0.005	0.068	0.282	< 0.001	0.061	0.069	June 03
					< 0.001	0.044	0.076	Sept 03
	Cu	0.011	0.228	2.56	0006	0.261	0.336	June 03
					0.002	0.240	0.542	Sept 03
	Zn	1.10	16.4	57.7	0.074	13.9	15.3	June 03
					0.034	11.2	17.8	Sept 03

5.5 MODEL SENSITIVITY AND UNCERTAINTY ANALYSIS

Model sensitivity was explored by parameter perturbation as part of calibration efforts. During calibration, model parameters were varied within accepted ranges of values representing the inherent uncertainty of each parameter. Sensitive parameters were identified based on the extent to which model results varied in response to perturbation. For the hydrologic model, the most sensitive parameters were the effective hydraulic conductivity (K_h) and flow resistance (Manning n). For the sediment transport model, the most sensitive parameters are typically the soil erodibility (K) and land cover factor (C). The land management practice factor (P) was not considered to be uncertain because lands in the watershed are not managed for agriculture or as rangelands. For the chemical transport and fate model, the most sensitive parameter was the chemical partition coefficient (K_d). For each uncertain (sensitive) parameter upper and lower limits were established as presented in Tables 5-8 through 5-10. Model uncertainty was then assessed using the logic tree approach described by Mishra (2001).

Effective hydraulic conductivities vary widely between soil types and even within a single soil association. As presented in the NRCS SSURGO database, the estimated K_h value for any given soil type typically varies by a factor of three. Upper K_h values were assumed to be two times larger and lower bound values 33% smaller than the calibrated value. Within this range, the effective K_h values for each soil type overlap the bounds of the next larger or smaller class of hydraulic conductivities as estimated from soil texture.

Flow resistance (Manning n) also varies widely. This variation depends on the type and condition of vegetative cover as well as the flow state (laminar or turbulent) and relative submergence of roughness elements. As presented by Woolhiser et al. (1990) and USACE (1998), Manning n values for overland flow range from 0.01 for asphalt to 0.48 for dense sod or forest litter. Similarly, Manning n values for open channel flow range from 0.025 to 0.080 for mountain streams or more for floodplain areas as presented by Chow (1959). To simplify the analysis, only the variation of overland roughness was explored. Upper bound overland Manning n values were assumed to be 50% larger and lower bound values 50% smaller than the calibrated value.

Table 5-8. Soil parameter bounds for uncertainty analysis: effective hydraulic conductivity and soil erodibility.

Soil Type	*Symbol*	*Effective K_h (m/s)*			*Soil Erodibility (K) (tons/acre)*		
		lower	*calibrated*	*upper*	*lower*	*calibrated*	*upper*
Wet Alluvial Land	Wa	1.00E-06	1.50E-06	3.00E-06	0.100	0.200	0.400
Gravel Pit	GP	1.00E-06	1.50E-06	3.00E-06	0.010	0.020	0.040
Rosane loam	RtC	1.00E-06	1.50E-06	3.00E-06	0.100	0.200	0.400
Troutville gravelly sandy loam	TrE	1.13E-06	1.70E-06	3.40E-06	0.075	0.150	0.300
Perian Soils	PIF	1.00E-06	1.50E-06	3.00E-06	0.025	0.050	0.100
Water (Ponds) (treated as LeE)	W	1.00E-06	1.50E-06	3.00E-06	0.140	0.280	0.560
Newfork gravelly sandy loam	NfB	1.00E-06	2.00E-06	4.00E-06	0.050	0.100	0.200
Perian gravelly sandy loam	PgD	1.00E-06	2.00E-06	4.00E-06	0.025	0.050	0.100
Leadville sandy loam	LeE	1.00E-06	1.50E-06	3.00E-06	0.140	0.280	0.560
Mine Pits and Dumps	MP	1.87E-06	2.80E-06	5.60E-06	0.010	0.020	0.040
Slickens (mill tailings)	Sw	1.00E-06	1.50E-06	3.00E-06	0.320	0.640	1.280
Placer diggings and tailings	Pn	6.67E-07	1.00E-06	2.00E-06	0.010	0.020	0.040
Bross gravelly sandy loam	BrF	1.00E-06	1.50E-06	3.00E-06	0.025	0.050	0.100
Tomichi sandy loam	ToE	1.00E-06	1.50E-06	3.00E-06	0.120	0.240	0.480
Urban21 (low density urban)	(LeE)	8.33E-08	1.25E-07	2.50E-07	0.070	0.140	0.280
Urban22 (high density urban)	(LeE)	5.67E-08	8.50E-08	1.70E-07	0.014	0.028	0.056
Urban23 (commercial area)	(LeE)	8.33E-07	1.25E-06	2.50E-06	0.120	0.240	0.480

Table 5-9. Land use parameter bounds for uncertainty analysis: overland Manning n and soil cover factor.

Land Use	*NLCD Class*	*Manning n*			*Soil Cover Factor (C) (dimensionless)*		
		lower	*calibrated*	*upper*	*lower*	*calibrated*	*upper*
Open Water (treated as barren)	11	0.075	0.150	0.225	0.10	0.20	0.40
Perennial Ice/Snow	12	0.075	0.150	0.225	0.003	0.005	0.010
Low Intensity Residential	21	0.038	0.075	0.112	0.005	0.01	0.02
High Intensity Residential	22	0.025	0.050	0.075	0.0005	0.001	0.002
Commercial/Industrial/Transportation	23	0.075	0.150	0.225	0.05	0.10	0.20
Bare Rock/Sand/Clay	31	0.075	0.150	0.225	0.10	0.20	0.40
Deciduous Forest	41	0.225	0.450	0.675	0.02	0.04	0.08
Evergreen Forest	42	0.225	0.450	0.675	0.02	0.04	0.08
Mixed Forest	43	0.225	0.450	0.675	0.03	0.06	0.12
Shrubland	51	0.200	0.400	0.600	0.04	0.08	0.12
Grasslands/Herbaceous	71	0.150	0.300	0.450	0.021	0.042	0.084
Pasture/Hay	81	0.150	0.300	0.450	0.021	0.042	0.084
Row Crops (treated as grasslands)	82	0.150	0.300	0.450	0.021	0.042	0.084

Table 5-10. Chemical distribution coefficient bounds for uncertainty analysis.

Chemical	*Distribution Coefficient (Log K_d) (L/kg)*		
	lower (pH=5)	*calibrated (pH=6)*	*upper (pH=7)*
Cd	1.85	2.34	2.83
Cu	2.97	3.24	3.51
Zn	1.92	2.54	3.16

Soil erodibility and land cover factors typically vary as functions of both soil type and land use. As presented in the NRCS SSURGO database, the K value for many soils can vary a factor or two or more. As summarized by Julien (1998), the C value for any given land use depends on the vegetative cover and can also vary by a factor or two or more. Upper and lower bounds for both soil erodibility and land cover factors were assumed to be two times more and two times less than calibrated values, respectively.

Chemical distribution coefficients vary widely as a function of pH and the characteristics of the sorbent. As presented by Sauvé et al. (2000, 2003) and Lu and Allen (2001), distribution coefficients for Cd, Cu, and Zn can vary by more than 50%. Upper and lower bound log K_d values were computed as described by Equations 5.3 through 5.5 and assuming that the upper and lower pH limits are 5.0 and 7.0, respectively.

Overall model uncertainty envelope bounds were estimated from the combination of individual parameter values that cause the largest increase (upper bound) or decrease (lower bound) in model response. The upper bound occurs for conditions of maximum surface runoff, maximum soil erosion, and minimum chemical partitioning. The lower bound occurs for conditions of minimum runoff, minimum erosion, and maximum partitioning. Graphs showing the model uncertainty envelopes for flow for the calibration and validation simulations at Stations CG-1, SD-3, CG-4, and CG-6 are presented in Figures 5-18 to 5-21. Graph showing representative model uncertainty envelopes for clay at Station CG-6 are presented Figure 5-22. Graphs showing representative model uncertainty envelopes for total metals concentrations at Station CG-6 are presented in Figure 5-23. Additional model uncertainty results are summarized in Appendix D.

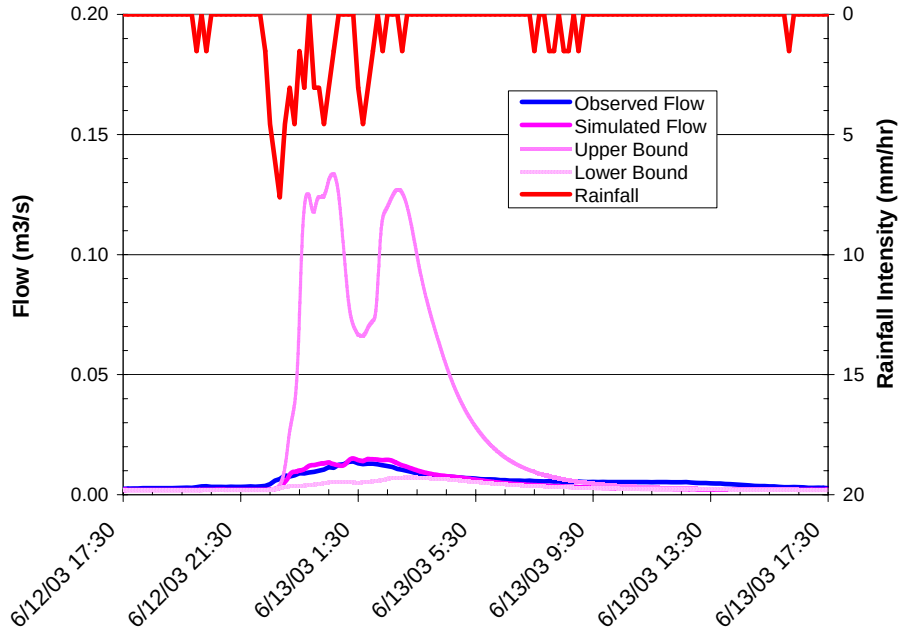

a) Calibration: June 12-13, 2003.

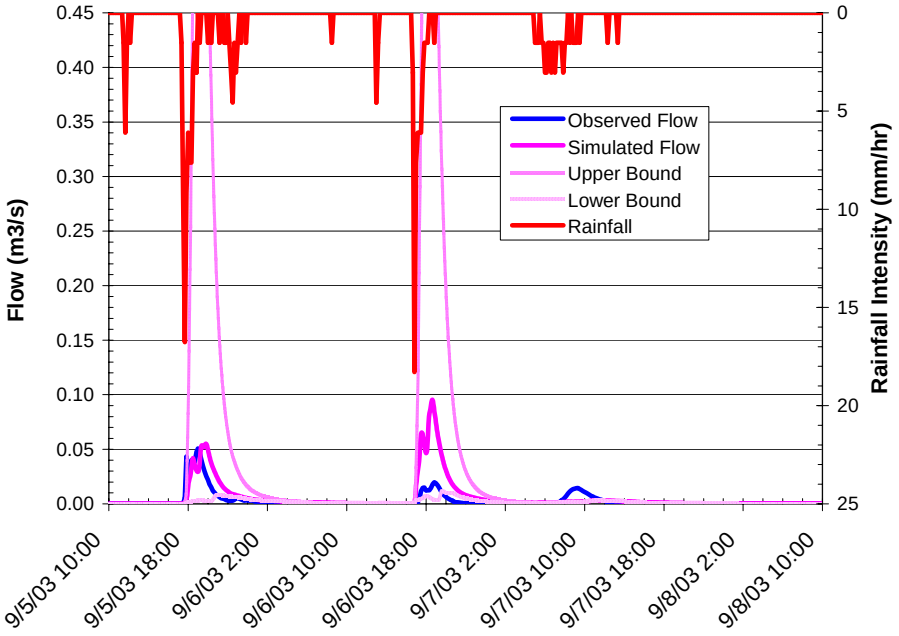

b) Validation: September 5-8, 2003.

Figure 5-18. Hydrologic uncertainty envelopes at Station CG-1.

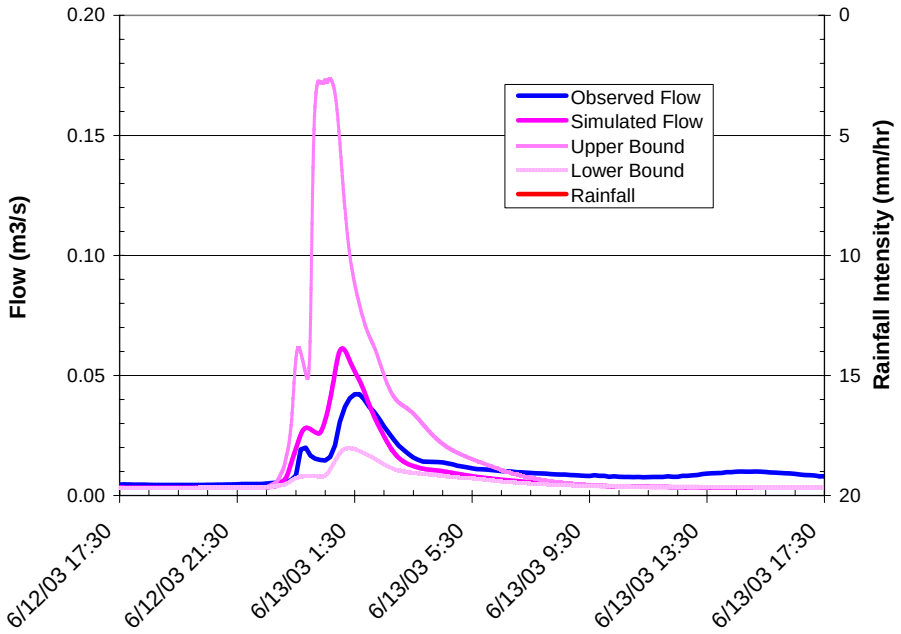

a) Calibration: June 12-13, 2003.

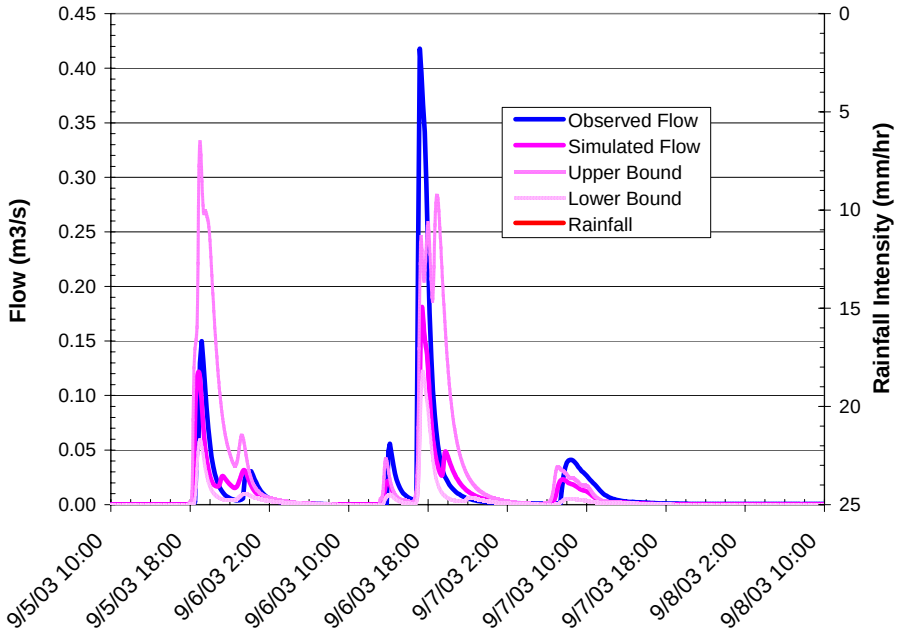

b) Validation: September 5-8, 2003.

Figure 5-19. Hydrologic uncertainty envelopes at Station SD-3.

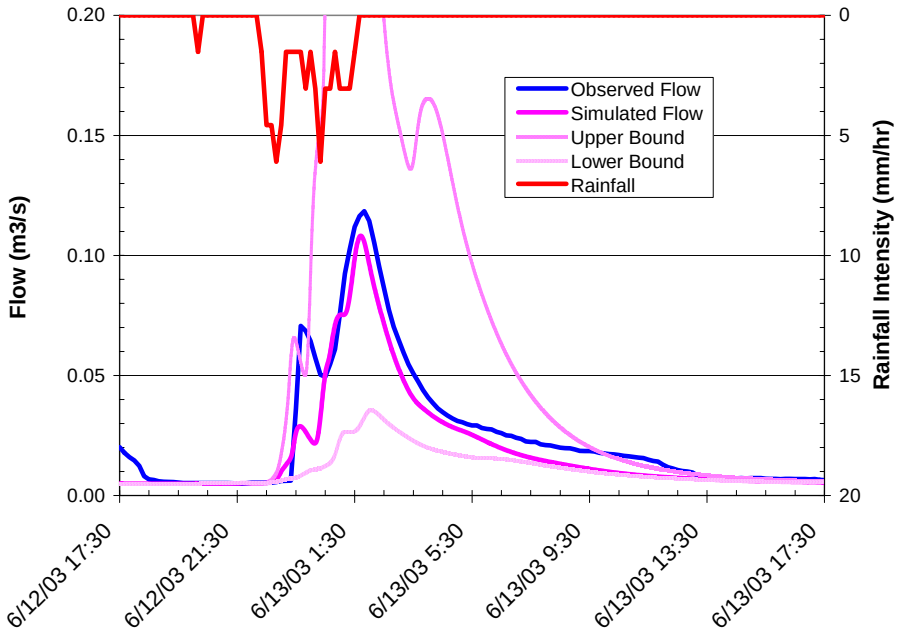

a) Calibration: June 12-13, 2003.

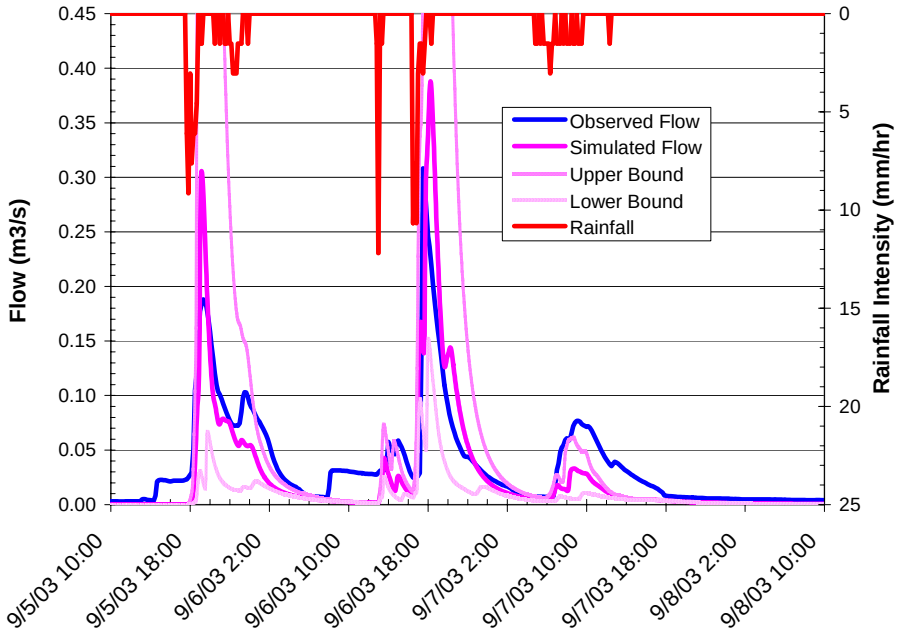

b) Validation: September 5-8, 2003.

Figure 5-20. Hydrologic uncertainty envelopes at Station CG-4.

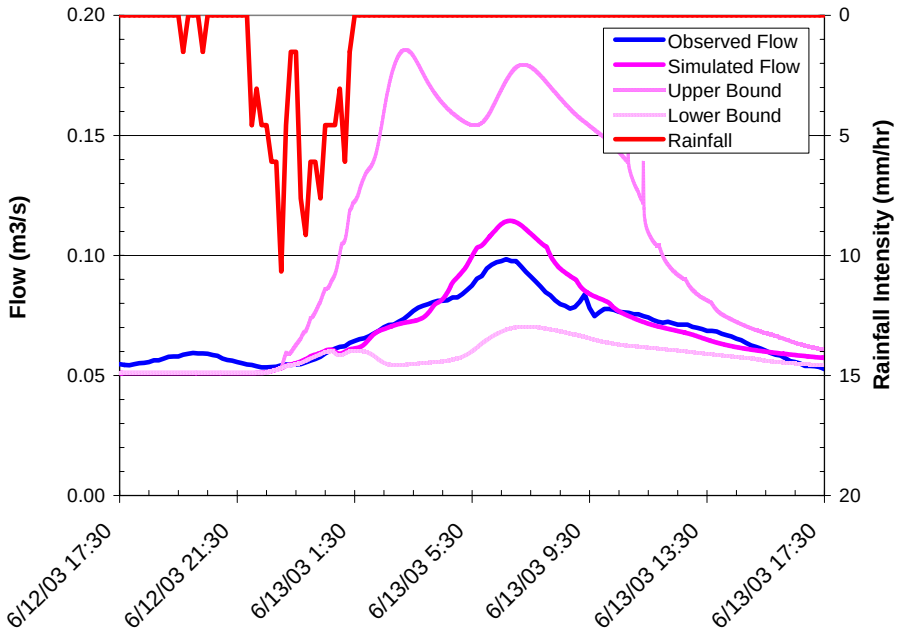

a) Calibration: June 12-13, 2003.

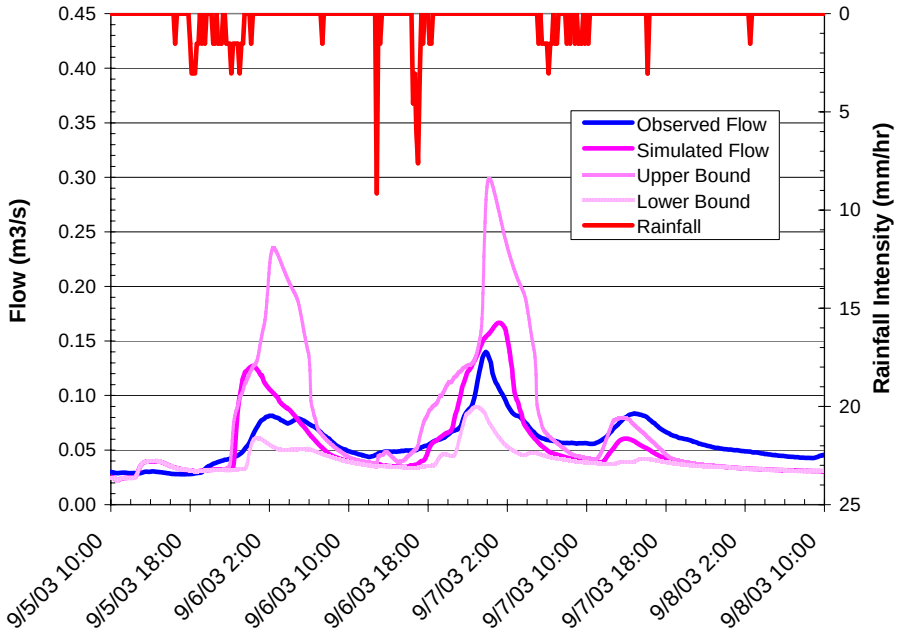

b) Validation: September 5-8, 2003.

Figure 5-21. Hydrologic uncertainty envelopes at Station CG-6.

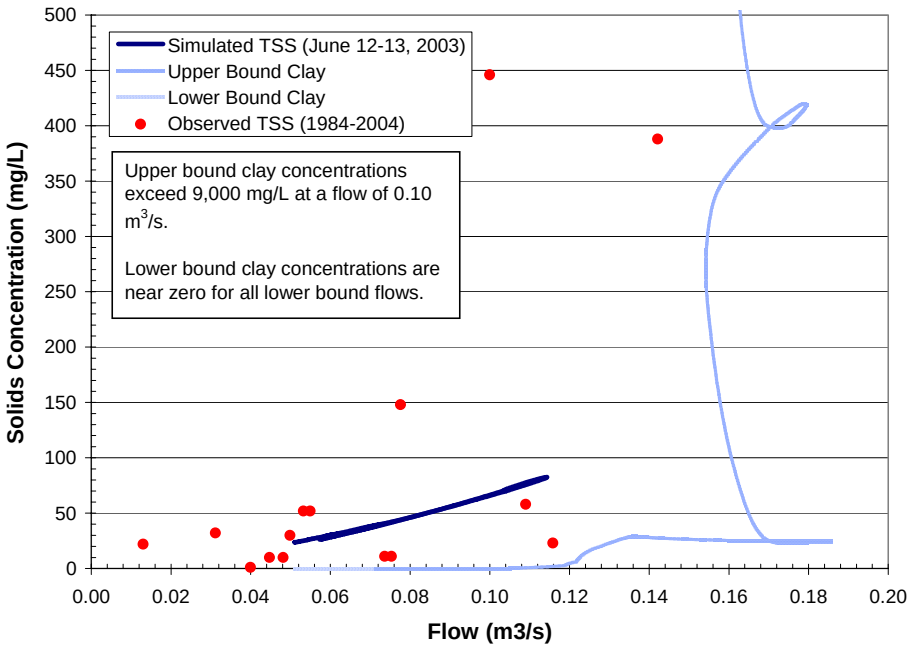

a) Calibration: June 12-13, 2003

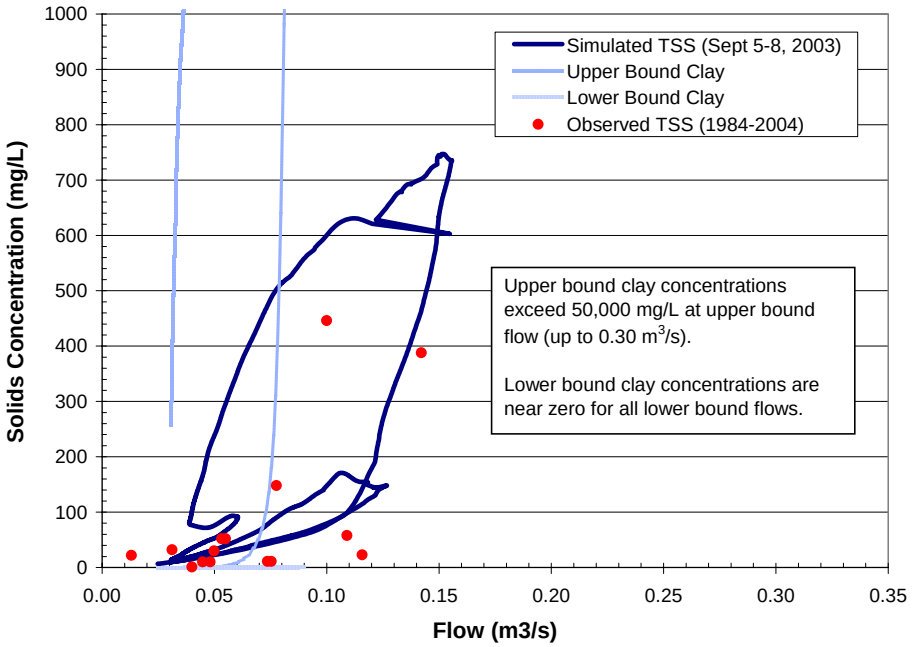

b) Validations: September 5-8, 2003

Figure 5-22. Sediment transport uncertainty envelope at Station CG-6.

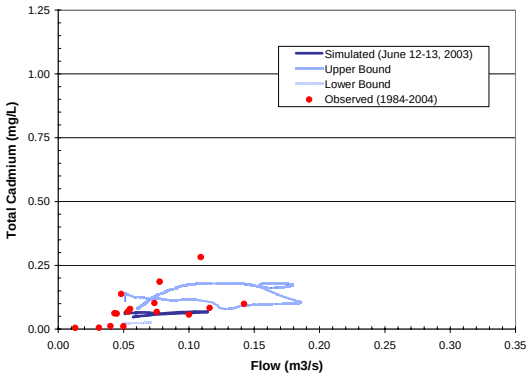

a) Total cadmium: June 12-13, 2003

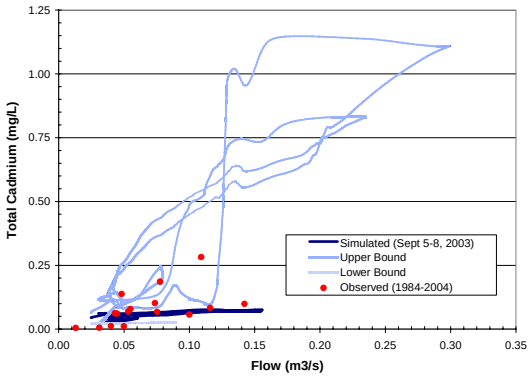

b) Total cadmium: September 5-8, 2003

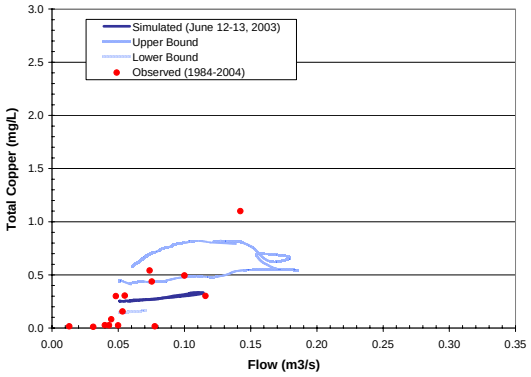

c) Total copper: June 12-13, 2003

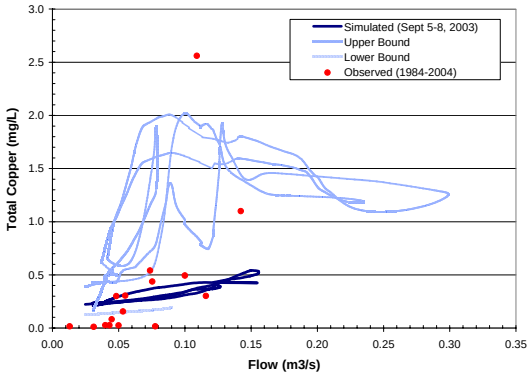

d) Total copper: September 5-8, 2003

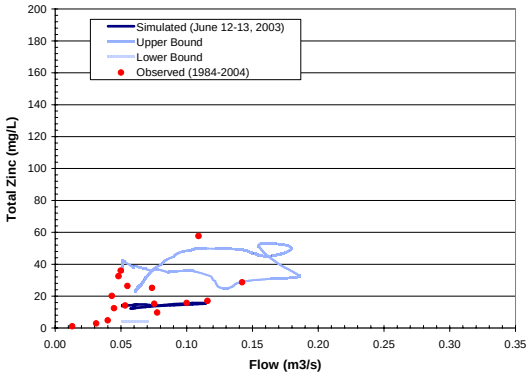

e) Total zinc: June 12-13, 2003

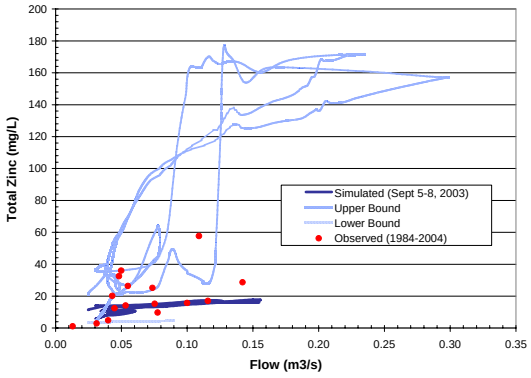

f) Total zinc: September 5-8, 2003

Figure 5-23. Chemical transport uncertainty envelope at Station CG-6.

5.6 DISCUSSION

Overall model performance was judged to be quite reasonable. High quality data were available to construct and evaluate the hydrologic components of the California Gulch application. Other than the need to account for snow and ice conditions during the calibration event, model parameterization for the June and September 2003 storms was identical. In terms of flow volumes, the average relative percent difference between simulated and observed values was -8.6% for the calibration (June) and +11.3% for the validation (September) events. Average model performance for the peak flow and time to peak metrics was also quite good as was summarized in Table 5.5. Data to evaluate the sediment and chemical transport components of the California Gulch application were less strong. Observed total suspended solids (TSS) and total metals concentration observations were collected over a small range of flows across a 20-year period. No time series concentration data are available for direct comparison to model results for the events simulated or any other period of record. Given this limitation of the database, only the range of observed and simulated concentrations could be meaningfully compared. Nonetheless, in terms of these broad ranges, model performance was again considered to be quite reasonable as the model properly reproduces the rage of observed values.

Soils within the watershed have very high infiltration capacities. As calibrated, roughly 98% of all rainfall infiltrates and relatively little overland flow is generated. Although the model calibration simulates channel flows well for both events, it is worth noting that calibrated K_h values are less than values that would be estimated based on soil texture and grain size considerations alone. Calibrated K_h values range from 1.5×10^{-6} to 2.8×10^{-6} m/s (0.54 to 1.01 cm/hr). Based solely on texture, these values are in the range of sandy loam to silt loam soils (Rawls et al. 1983; Rawls et al. 1993). While generally applicable to the Leadville sandy loam soil type, values for mined areas could be greater due to the presence of larger particle sizes and rock fragments, which are often associated with increased pore volume and pore size in soils. However, as demonstrated in Figures 5-18 to 5-21 use of larger effective K_h values resulted in simulated flows that were significantly less than observed values.

Several possible explanations for this exist. One possibility is that over time finer soil particles weathered from larger rock fragments have filled the void spaces in the soil matrix such that the infiltration characteristics of the overall soil aggregate are controlled by the finer soil particles. Another possibility is that water infiltrated on steep hillslopes travels through the soil as interflow and returns to the surface at some down gradient point. Considering the very steep slopes in parts of the watershed, this seems very reasonable. A third possibility is that water infiltrated on very porous, mined areas eventually reaches less porous, undisturbed soil layers that force the water to move laterally until it returns to the surface at the toe of a waste pile. Given the extent of disturbed soils and mined wastes, this possibility also seems quite reasonable.

Relationships between observed TSS and metals concentration and flow in surface water are complex. Observed TSS values show some structure with flow and generally increase as flow increases. However, observed metals concentrations show less structure. At least in the case of TSS, high concentrations at the lowest flows may indicate the presence of precipitated flocs of metal oxide or hydroxide compounds, depending on pH, metals concentrations, and the concentrations of other ions. Precipitated flocs in suspension would be retained on the filters used to separate solids from whole water samples. In contrast, high metals concentrations could reflect the influx from of metals groundwater. Given that many metals samples were collected during spring snowmelt periods when groundwater inputs to the gulch tend to be largest, this seems reasonable. The possibility of significant groundwater inputs of metals is further supported by the observation that reported dissolved phase metals concentrations often equal total metals concentrations.

Despite the connection between surface water and groundwater and the likely input of metals from groundwater, the metals concentration boundary conditions for base flow were assigned zero concentrations. Because of the complexity of site hydrogeology, it is difficult to determine realistic, *a priori* metals base flow boundary concentrations because observations do not exist for the events simulated. Monitoring well data could be used to assign boundary concentrations. However, the uncertainty of the boundary values would be large since metals readily sorb to soils and sediment. As a result of sorption and retardation during subsurface flow, concentrations at points of influx to the surface water

system can be very different than observed at distant monitoring wells. While use of zero boundary concentrations contributes to the model's low bias for metals transport, this was judged to be preferable to use of alternative, potentially arbitrary, non-zero values.

When considering overall model performance, it is important to recall that the goal of the California Gulch application was to demonstrate that the TREX modeling framework can be used to successfully simulate chemical transport at the watershed scale. Independent of specific detail regarding the degree of calibration optimality, the goal of the model application effort was achieved. The model was able to accurately reproduce observed conditions across the site. Where high quality data exist, model performance is excellent. Even where less detailed information exists, the model was nonetheless able to reproduce the range and basic trends of observations for this complex site. The success of the model application indicates that TREX is a viable tool for simulating chemical transport at the watershed scale.

More complete discussion of model results is presented in Appendix E. Potential model limitations are also described and discussed. Recommendations for future studies are also described.

6.0 MODEL APPLICATION: EXTREME STORM FORECAST

6.1 MODEL SET-UP AND PARAMETERIZATION

The 1-in-100 year recurrence interval, 2-hour duration rainfall event was selected as an extreme storm for simulation to further demonstrate model applicability. Simons and Associates, Inc. (SAI) performed an extensive review of precipitation records for Leadville and the surrounding region to estimate rainfall intensities for a range of storm recurrence intervals and durations (SAI, 1997a). From that analysis, the 1-in-100-year recurrence interval, 2-hour duration rainfall event was estimated to have an intensity of 22 mm/hour (0.87 inches/hr) and was assumed to have a uniform distribution over the entire watershed (SAI, 1997a). SAI (1997a) further found that the probability of very intense rainfall events is greatest during July or August, when average (unsaturated and snow-free) soil conditions are most common.

TREX was used to simulate the hydrology, sediment transport, and chemical transport and fate for the California Gulch 1-in-100-year, 2-hour duration event. For all parameters other than rainfall intensity, model set-up and initialization for the 1-in-100-year event simulation was identical to the September 2003 storm simulation. Uncertainty envelope parameterizations were also identical to the values used for the September 2003 storm.

It is worth noting that flow conditions during large events may be much different than exist during the small events typical of the watershed. More overland flow will be generated because rainfall rates exceed infiltration rates. Flow volume and depth in the channel network will be also much greater. The capacity of the small rills and low flow conveyance channels that control flow during typical storms will be exceeded and flow conveyance will be controlled by conditions within the high flow channels. As flow depths and volumes increase, boundary roughness can decrease as vegetation is bent down by the force of the flow. Where local water depths exceed back heights, flooding

will occur as water and any transported solids and chemicals will move out on to the floodplain (overland plane). This is significant because flows during a 1-in-100-year event are expected to be more than two orders of magnitude larger than model calibration conditions. Despite these possible differences, channel geometry and roughness values used for the 1-in-100-year event simulation were identical to model calibration values.

6.2 SIMULATION RESULTS

Water depths across the watershed at different times during the 1-in-100-year event are presented in Figure 6-1. Estimated event flows at Stations CG-1, SD-3, CG-4, and CG-6 are presented in Figures 6-2 to 6-5. The peak flow at the watershed outlet was estimated to be 22 m^3/s. Uncertainty envelopes for Stations CG-1 and SD-3 are relatively small. However, because of the extent of porous mine wastes with high infiltration capacities, lower bound flow values are roughly 50% less than upper bound values. The uncertainty envelope at Station CG-6 varies by a factor of 10 and is strongly influenced by overland infiltration conditions. Given the large contributing area, even relatively small changes to effective hydraulic conductivities can substantially influence flow at CG-6.

In the absence of field measurements for comparison, the hydrographs for this simulation were compared to the results of California Gulch watershed flows as summarized by SAI (1997a). The results of this study are within the range of values reported by others as presented in Table 6-1. It is worth noting that most prior modeling efforts for California Gulch used a curve number approach to estimate runoff. The differences in the results of earlier studies are attributable to differences in assumed precipitation depths, curve numbers for runoff, and surface roughness. In contrast to curve number approaches, the TREX application is based on the Green and Ampt (1911) physically-based infiltration model. The TREX application also used the 1-in-100 year, 2-hour duration rainfall intensity as estimated by SAI (1997a). Unfortunately, SAI only includes results for their 24-hour duration event. However, the estimated rainfall intensity for the 24-hour event is 2.54 mm/hr (0.1 inches/hr) and it is interesting to note that the intensity of that storm is less than the lower bound of effective hydraulic conductivity of the soils in watershed. Under such conditions, virtually no runoff would be generated except in imperious areas.

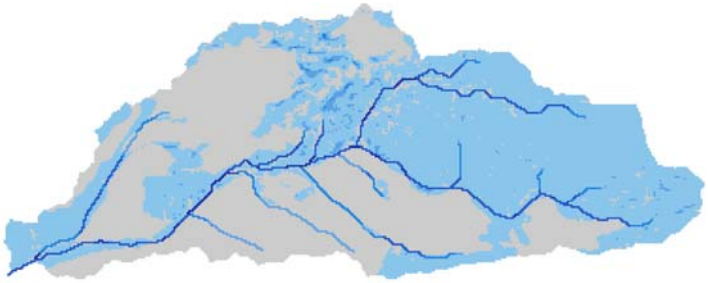

a) Water depth at 30 minutes (m)

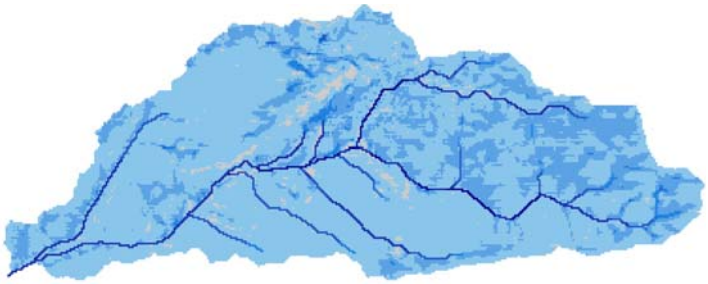

b) Water depth at 60 minutes (m)

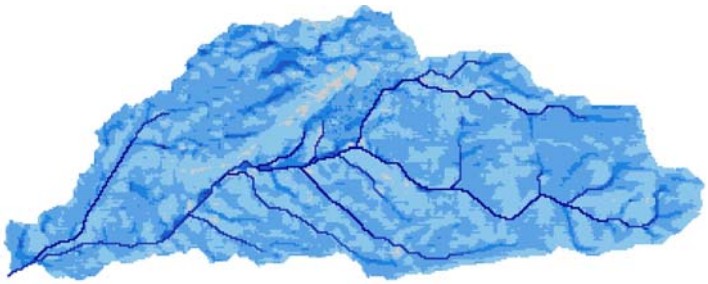

c) Water depth at 120 minutes (m) (rain ends after 120 minutes)

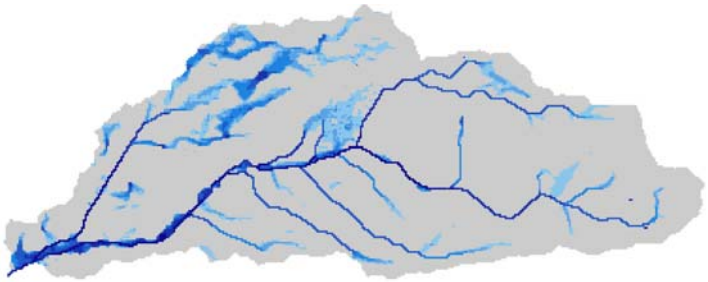

d) Water depth at 240 minutes (m)

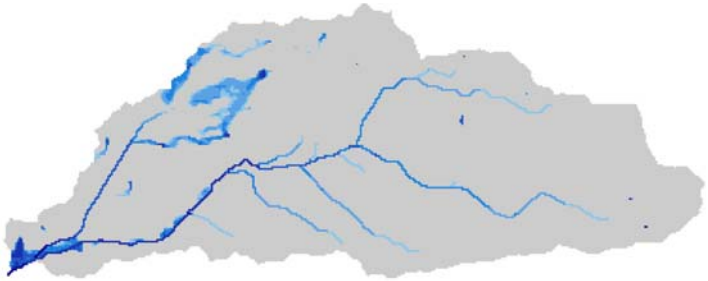

e) Water depth at 480 minutes (m)

Figure 6-1. Estimated 1-in-100-year event water depths.

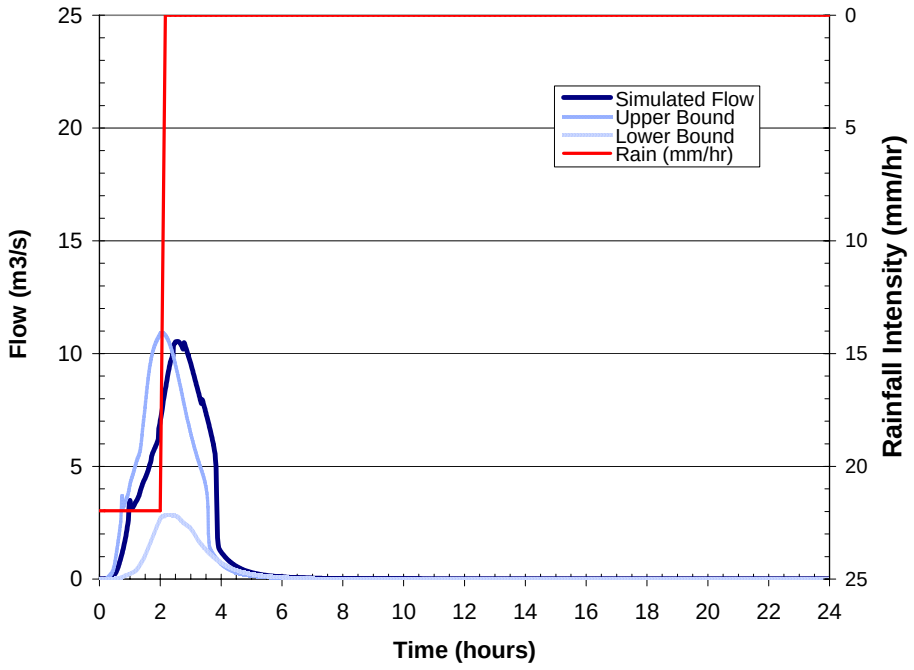

Figure 6-2. Estimated 1-in-100-year event flows at Station CG-1.

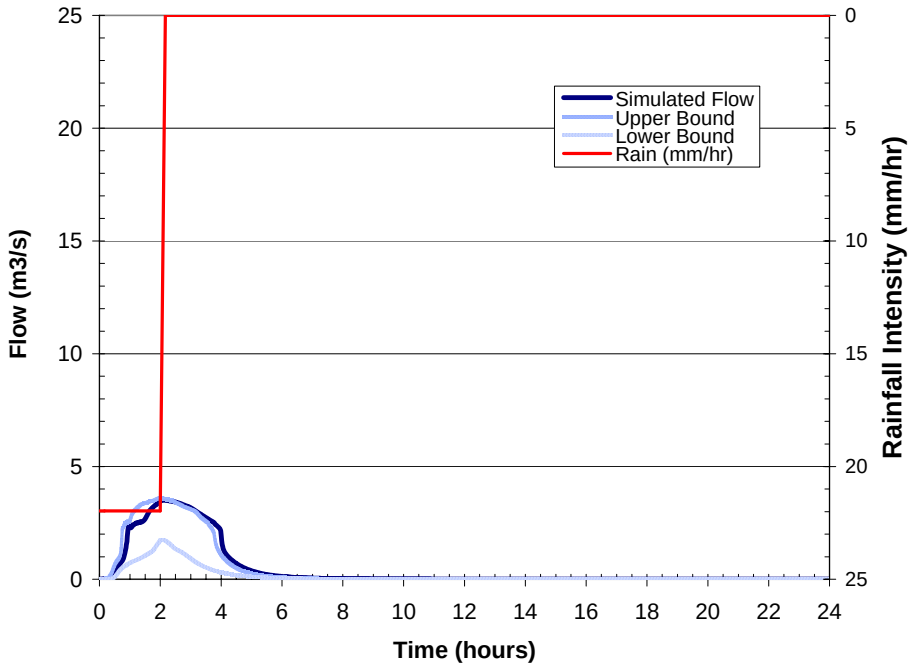

Figure 6-3. Estimated 1-in-100-year event flows at Station SD-3.

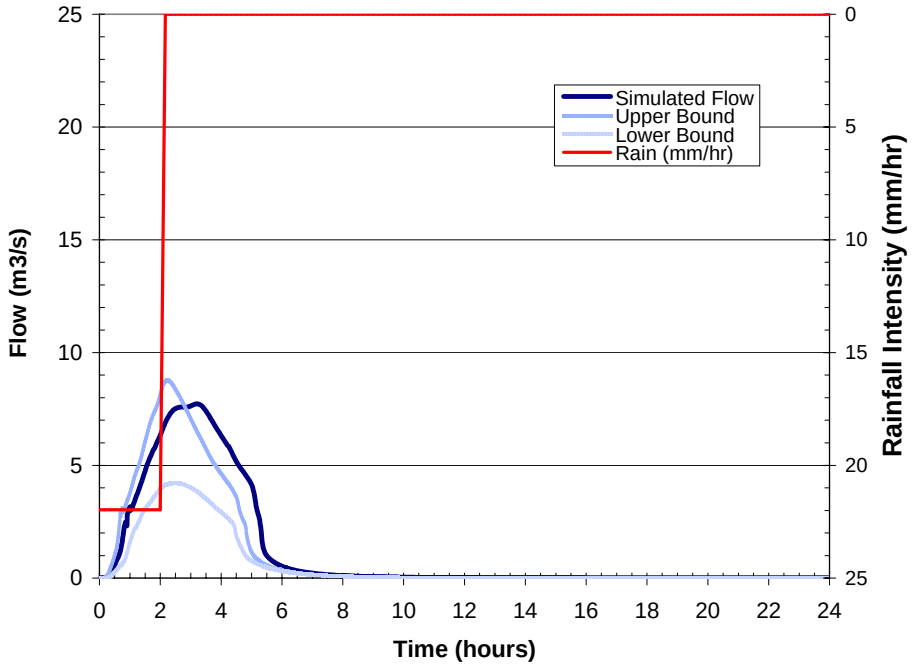

Figure 6-4. Estimated 1-in-100-year event flows at Station CG-4.

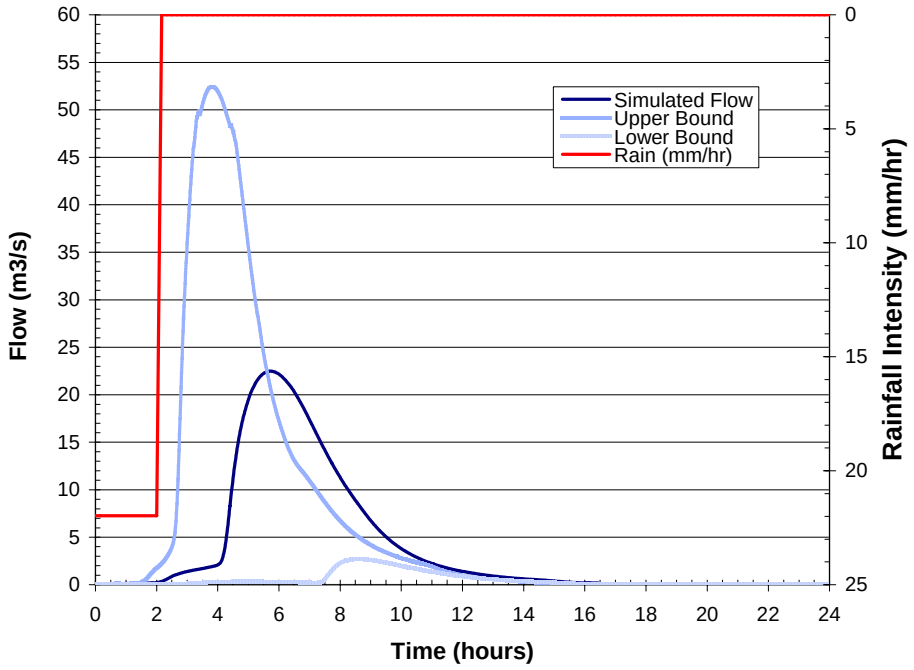

Figure 6-5. Estimated 1-in-100-year event flows at Station CG-6.

Table 6-1 Comparison of California Gulch extreme storm peak flow estimates.

Investigation	*Recurrence Interval*	*Duration*	*Peak Flow (m^3/s) at Location*		
			Upper California Gulch	*Stray Horse Gulch/Starr Ditch*	*Lower California Gulch*
USACE (1983)	1-in-100-year		2.6		7.6
Dames and Moore (1989)	1-in-500-year		11		
WWC (1993c) Golder (1996)	1-in-100-year 1-in-50-year				26 17
USBR (1996)	1-in-500-year 1-in-100-year			23 12	
SAI (1997a,b)	1-in-500-year 1-in-100-year 1-in-50-year	24 hour	10 3.8 2.6	5.7 2.0 1.4	11 4.8 3.5
TREX (this study)	1-in-100-year	2 hour	8.0	3.2	22

Abbreviations: Golder = Golder Associates, Inc.; SAI = Simons and Associates, Inc.; USACE = U.S. Army Corps of Engineers; USBR = U.S. Bureau of Reclamation; WCC = Woodward-Clyde Consultants.

Solids and zinc concentrations across the watershed at different times during the 1-in-100-year event are presented in Figure 6-6 and 6-7. Cumulative solids and chemical export (loads) for Stations CG-1, SD-3, CG-4, and CG-6 are presented in Figures 6-8 to 6-11. Export at CG-1 exceeds the Export at SD-3 for solids and all metals. With the exception of copper, cumulative export of solids, cadmium, and zinc at CG-4 is only slightly larger than the sum of export at CG-1 and SD-3. Driven by the large flows generated by the intense rainfall of the event and the corresponding erosion of soils and sediment, export at CG-6 is very large. For solids, export at CG-6 is estimated to be more than 10,000 metric tons while export for cadmium, copper, and zinc is 215 kg (475 lbs), 520 kg (1150 lbs), and 15,300 kg (33,700 lbs), respectively.

Beyond estimating export, TREX also tracks and reports the net accumulation of mass across the model domain during a simulation. Net accumulation is computed from the difference between the gross erosion and gross deposition flux of material for each cell in

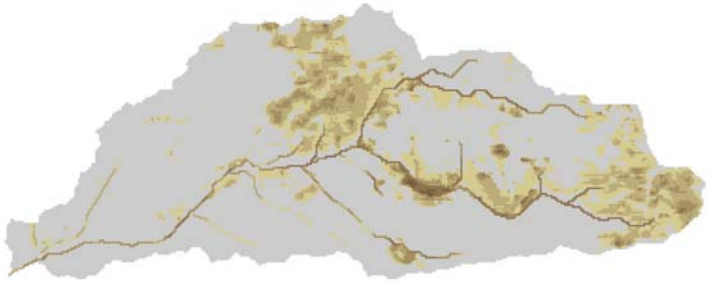

a) TSS concentration at 30 minutes (mg/L)

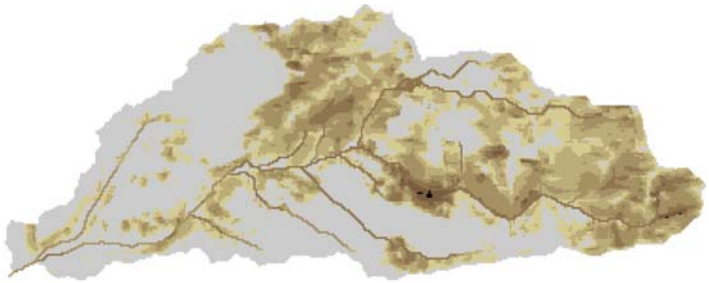

b) TSS concentration at 60 minutes (mg/L)

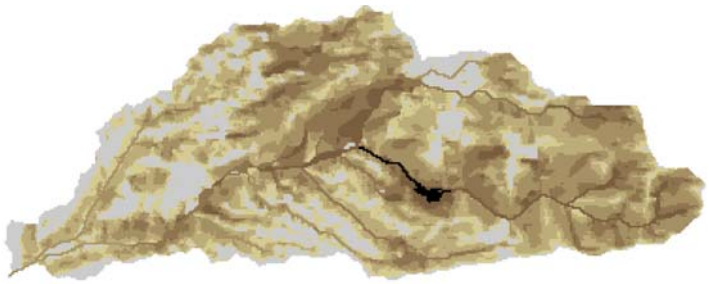

c) TSS concentration at 120 minutes (mg/L) (rain ends after 120 minutes)

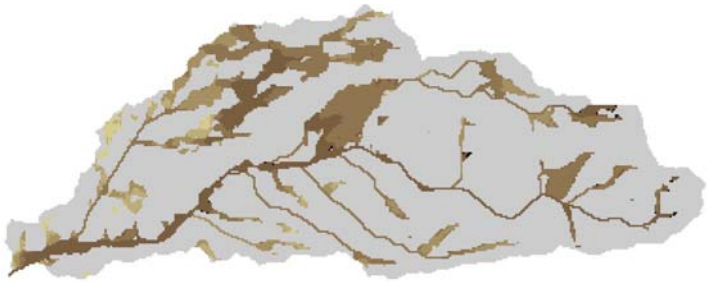

d) TSS concentration at 240 minutes (mg/L)

e) TSS concentration at 480 minutes (mg/L)

Figure 6-6. Estimated 1-in-100-year event total suspended solids concentrations.

a) Total zinc at 30 minutes (mg/L)

b) Total zinc at 60 minutes (mg/L)

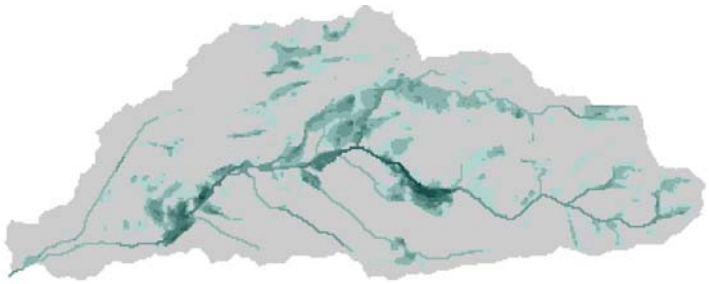

c) Total zinc at 120 minutes (mg/L) (rain ends after 120 minutes)

d) Total zinc at 240 minutes (mg/L)

e) Total zinc at 480 minutes (mg/L)

Figure 6-7. Estimated 1-in-100-year event total zinc concentrations.

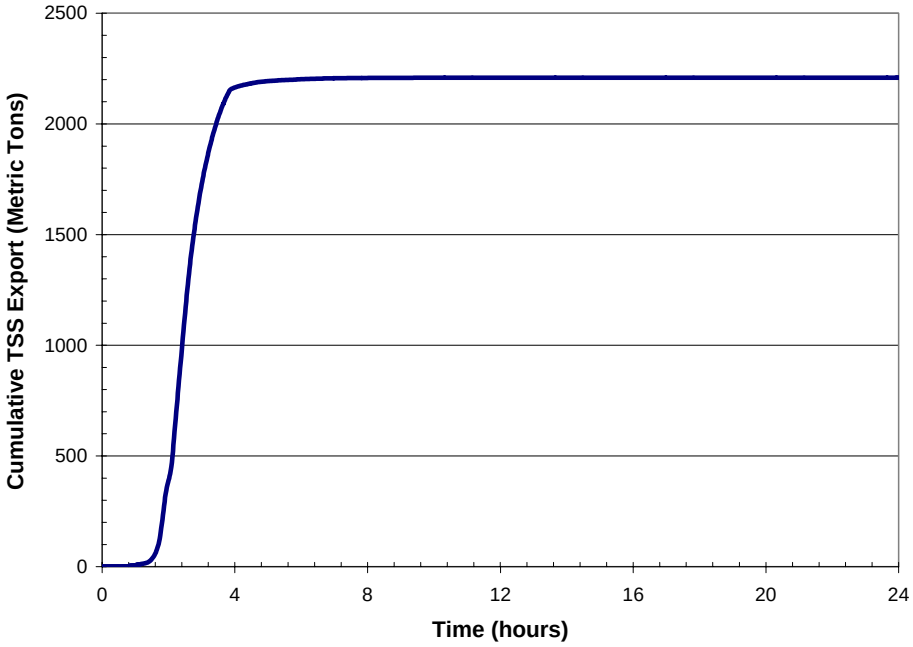

a) Cumulative solids export (kg)

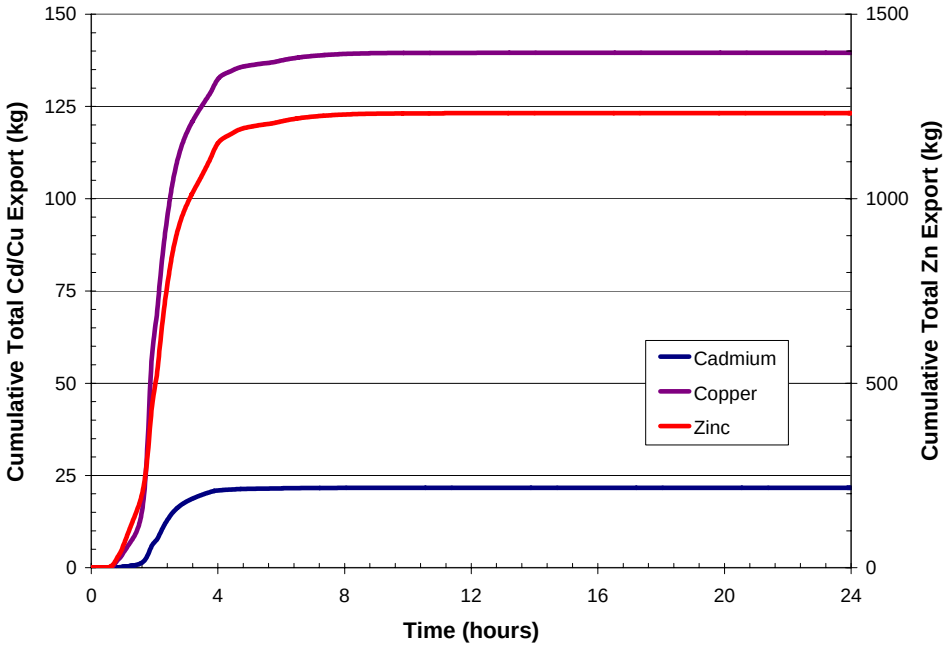

b) Cumulative metals export (kg): cadmium, copper, zinc

Figure 6-8. Estimated 1-in-100year event solids and metals export at Station CG-1.

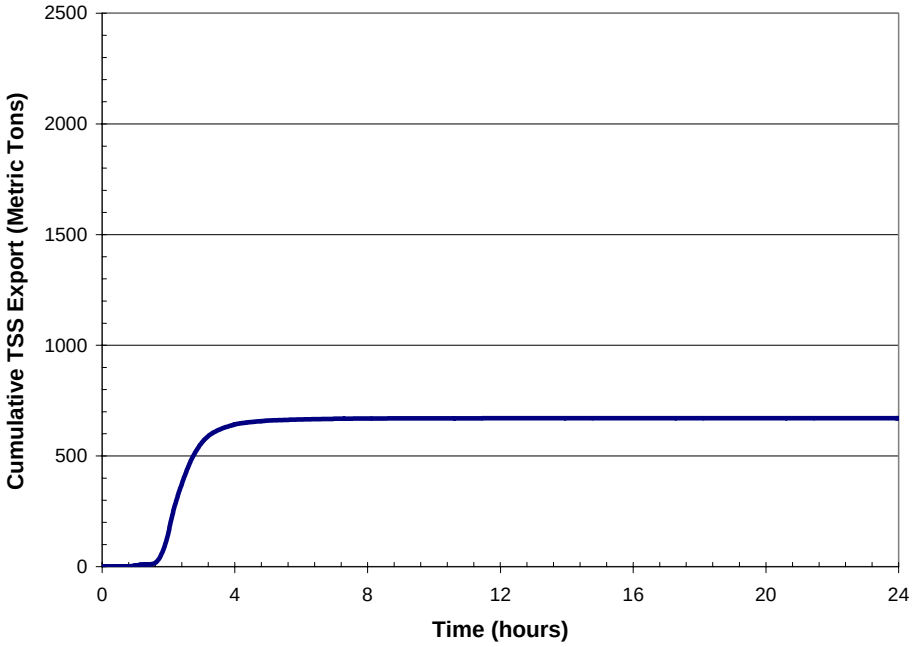

a) Cumulative solids export (kg)

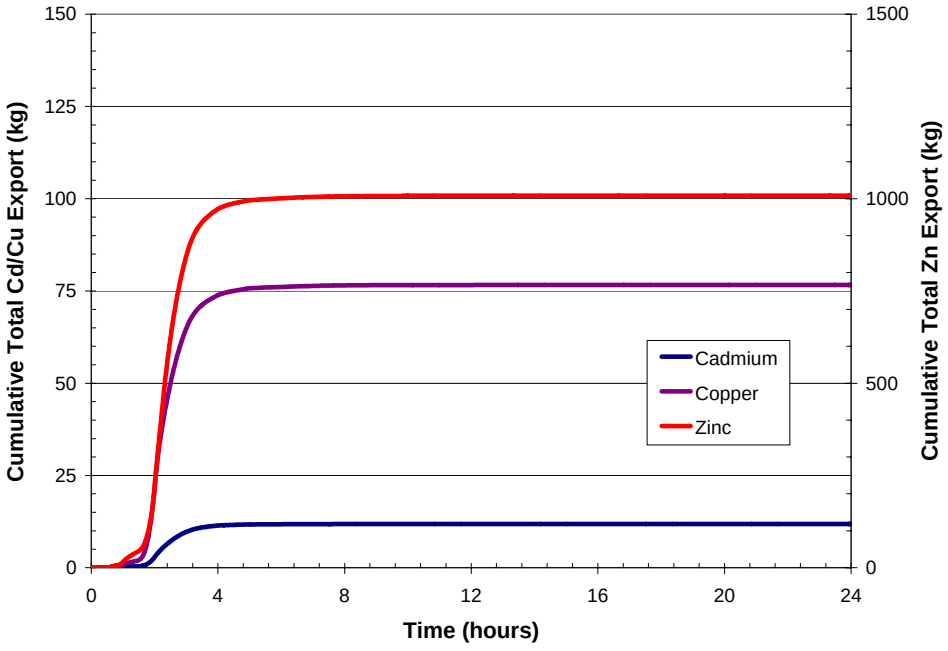

b) Cumulative metals export (kg): cadmium, copper, zinc

Figure 6-9. Estimated 1-in-100year event solids and metals export at Station SD-3.

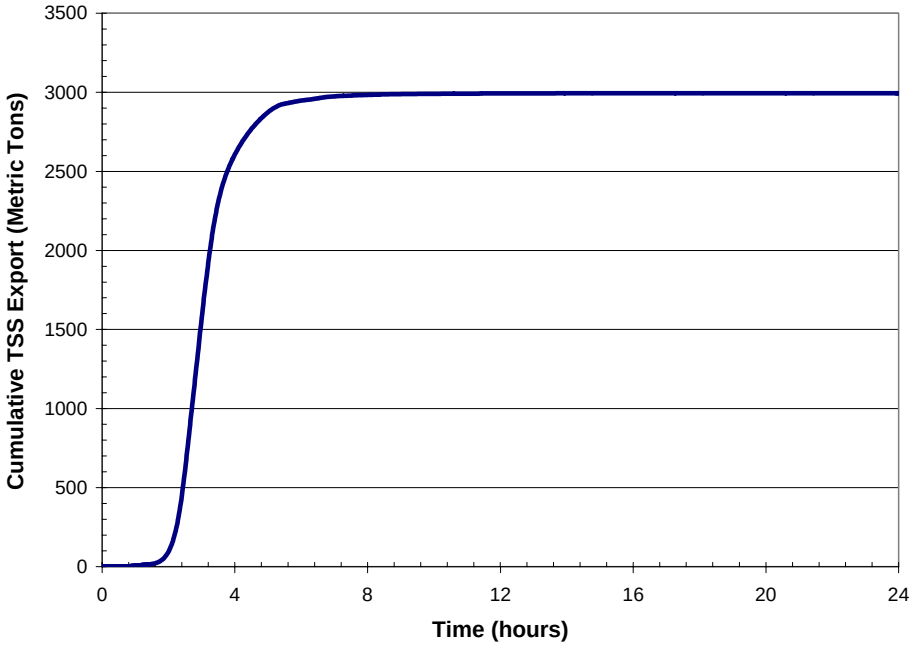

a) Cumulative solids export (kg)

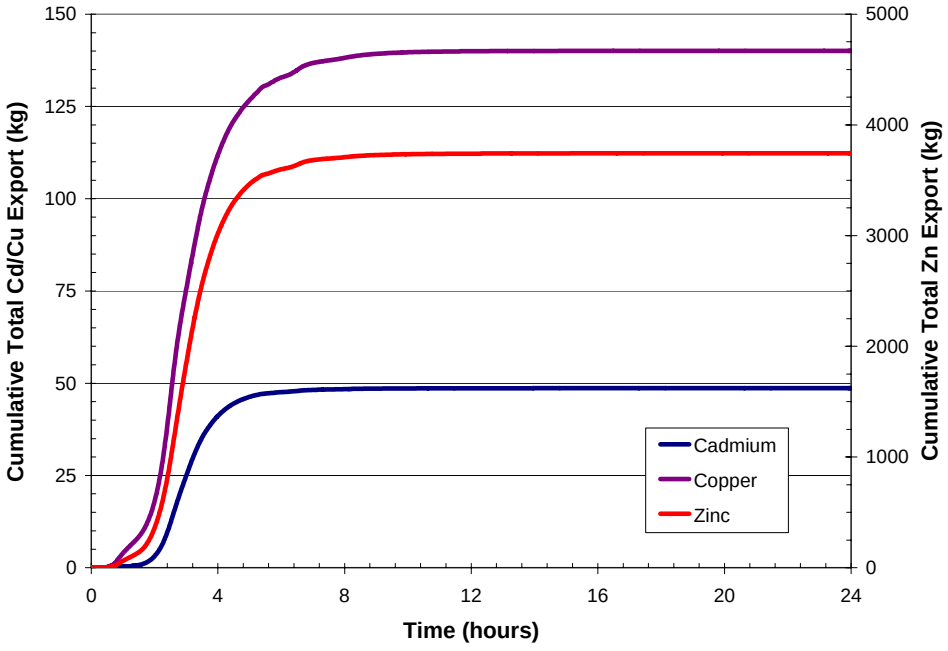

b) Cumulative metals export (kg): cadmium, copper, zinc

Figure 6-10. Estimated 1-in-100year event solids and metals export at Station CG-4.

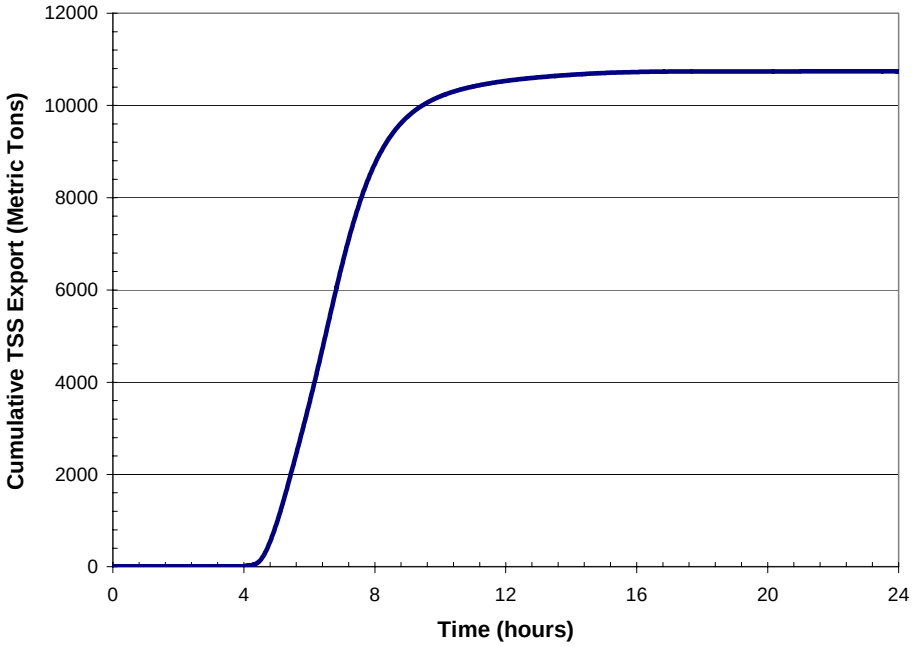

a) Cumulative solids export (kg)

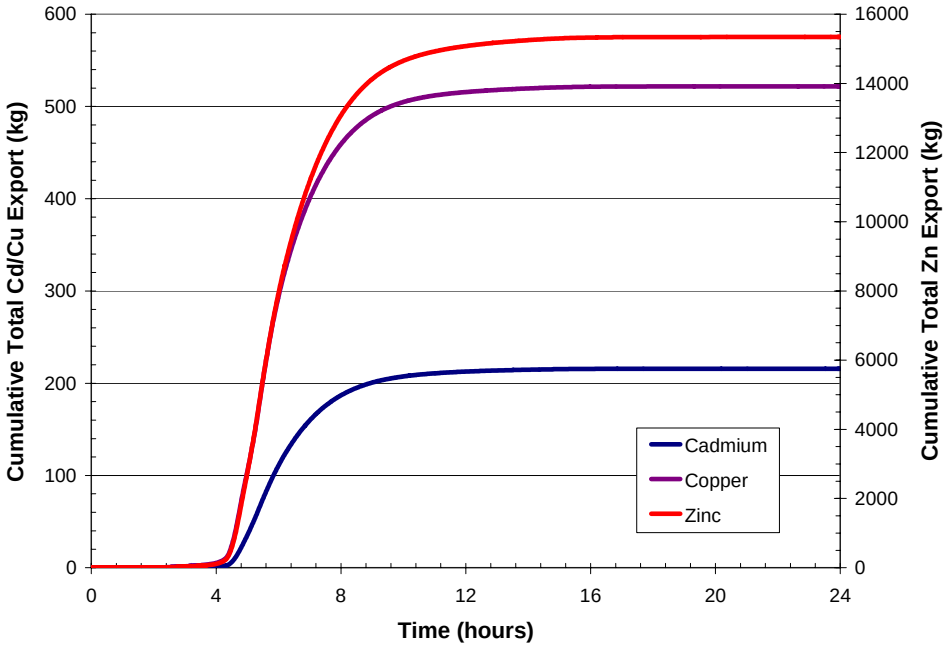

b) Cumulative metals export (kg): cadmium, copper, zinc

Figure 6-11. Estimated 1-in-100year event solids and metals export at Station CG-6.

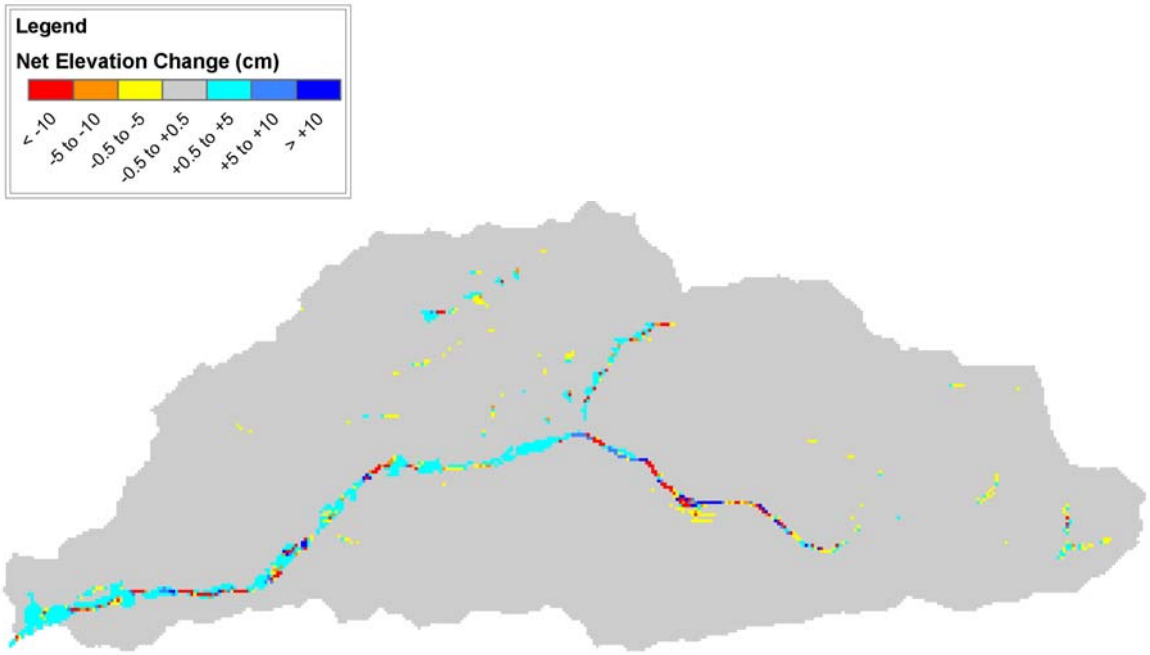

Figure 6-12. Estimated 1-in-100-year event net elevation change.

the model domain. The estimated net elevation change for the overland plane (excluding elevation changes within the stream channel network) over the 1-in-100-year event simulation period is presented in Figure 6-12. Estimated gross erosion, gross deposition, and net accumulation of cadmium, copper, and zinc for the overland plane for the 1-in-100-year event simulation are presented in Figures 6-13 to 6-15.

Although no direct measurements of concentrations or loads exist for flows as large as the 1-in-100-year event, a rough check on model performance can be made by comparing loads at lower flows and extrapolating to high flow conditions. During Spring 2003 the dissolved zinc load (export) at Station CG-6 was estimated to average approximately 45 kg/day (100 lbs/day) and ranged from 22 to 110 kg/day (50 to 250 lbs/day) (TTRMC, 2003). Flows during this period were typically 0.07 m^3/s (2.5 cfs) and ranged from 0.03 to 0.15 m^3/s (1 to 5 cfs) (TTRMC, 2003). This corresponds to a typical dissolved zinc concentration of 7.5 g/m^3 during low flow conditions. Assuming that this concentration stays constant as flow increases, load scales directly with flow. At CG-6, the average

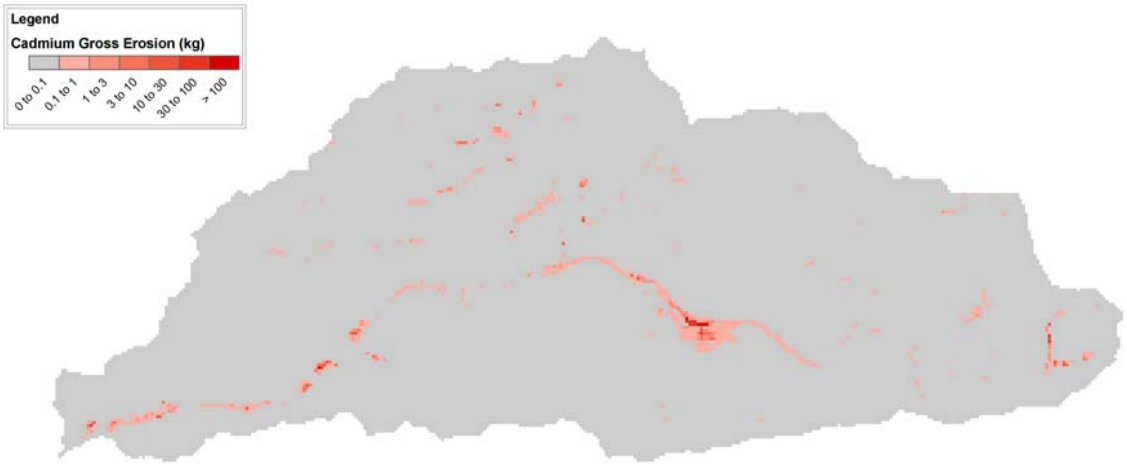

a) Gross erosion (kg)

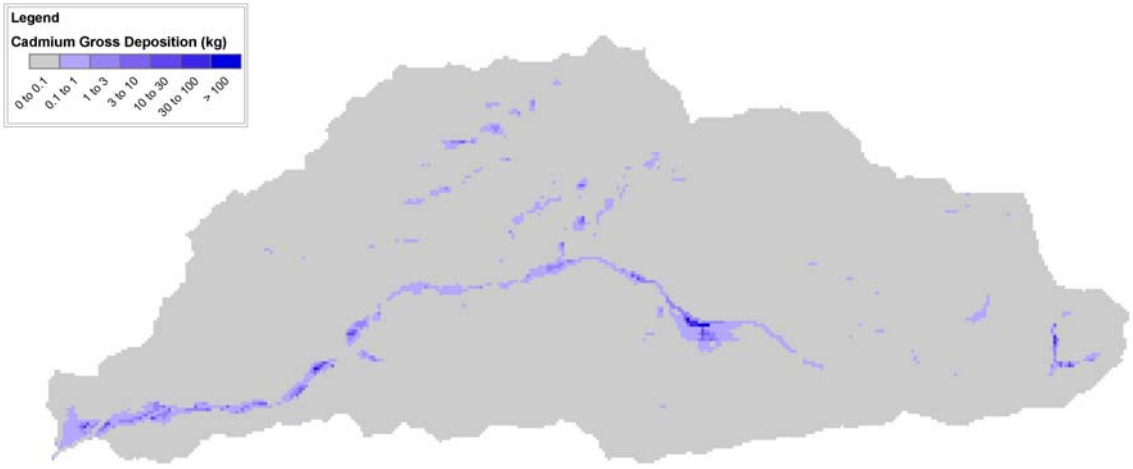

b) Gross deposition (kg)

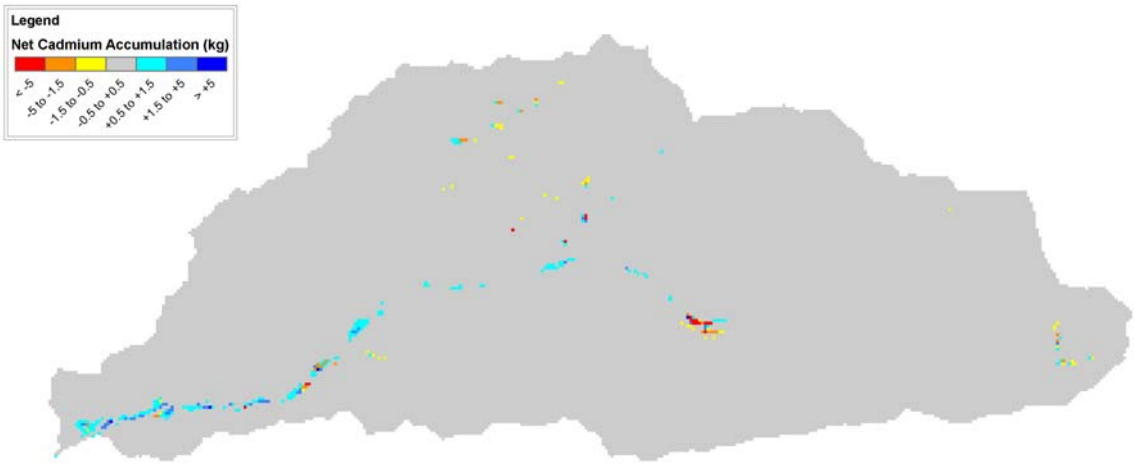

c) Net accumulation (kg)

Figure 6-13. Estimated 1-in-100 year event cumulative cadmium transport.

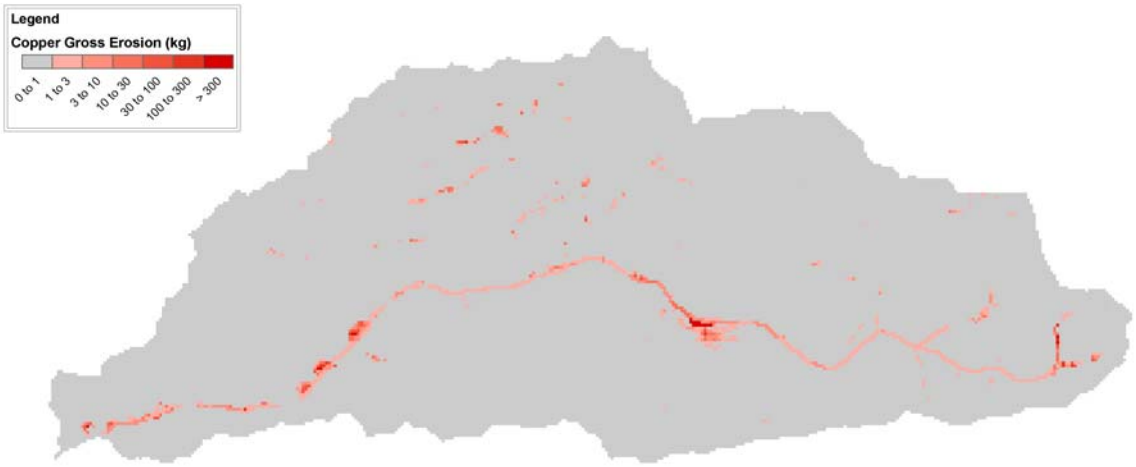

a) Gross erosion (kg)

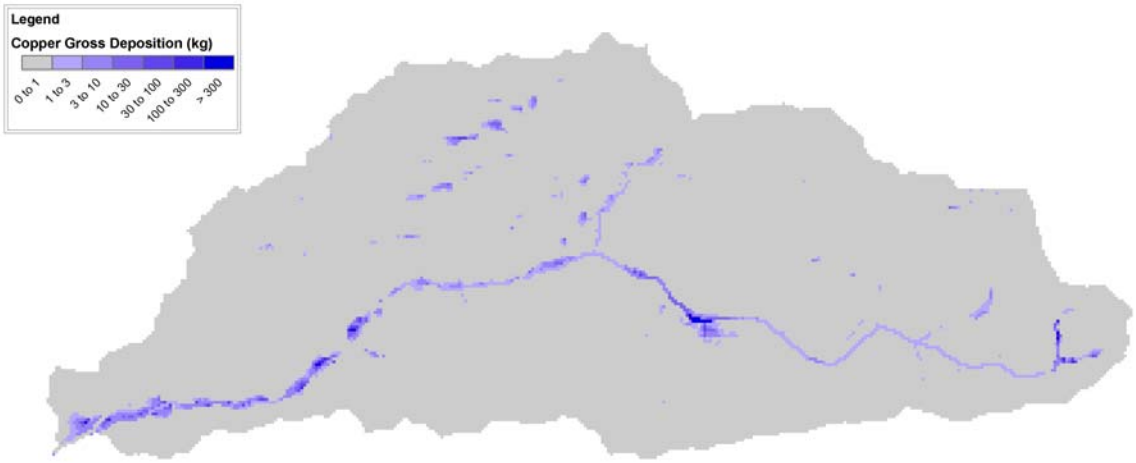

b) Gross deposition (kg)

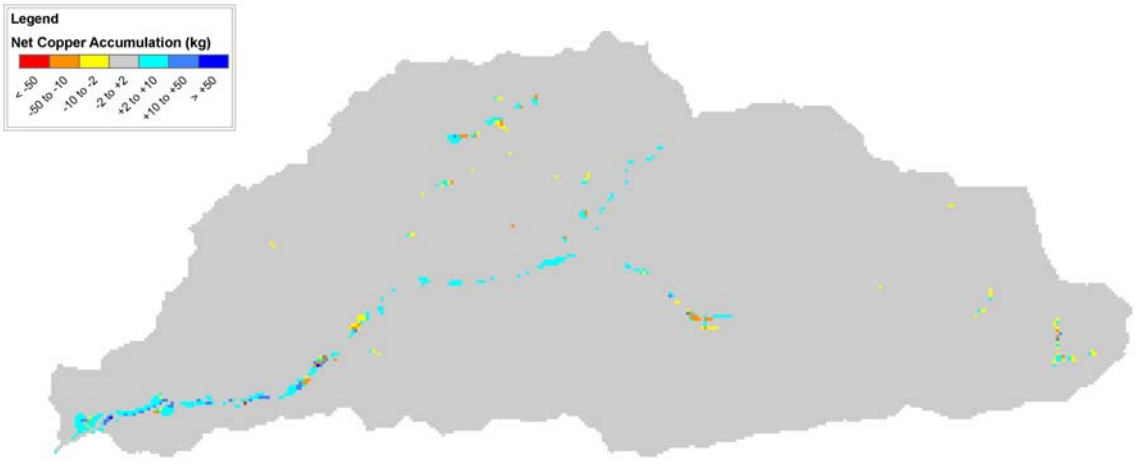

c) Net accumulation (kg)

Figure 6-14. Estimated 1-in-100 year event cumulative copper transport.

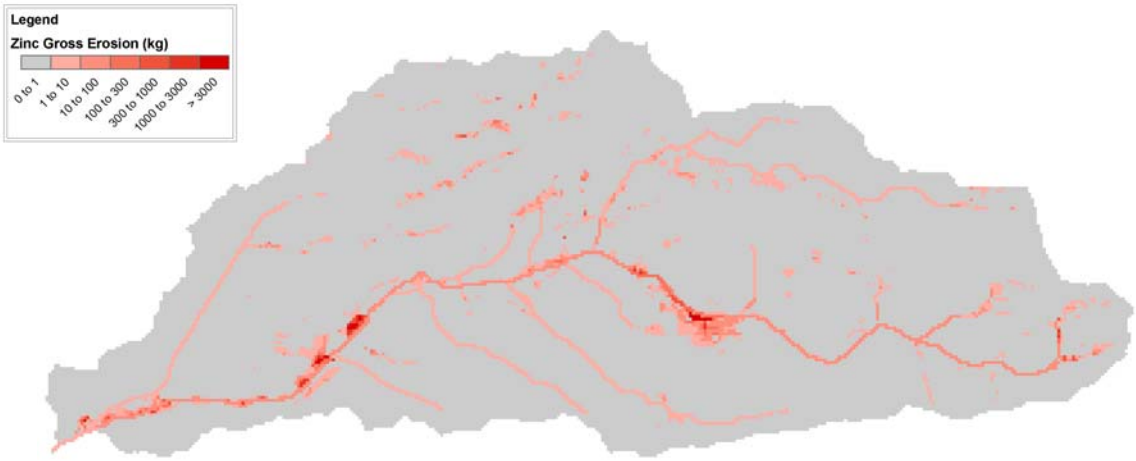

a) Gross erosion (kg)

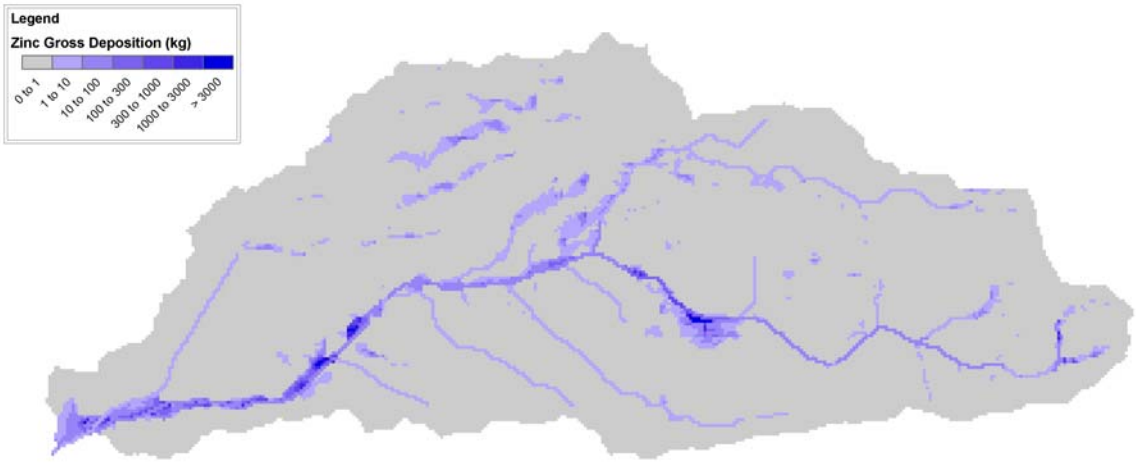

b) Gross deposition (kg)

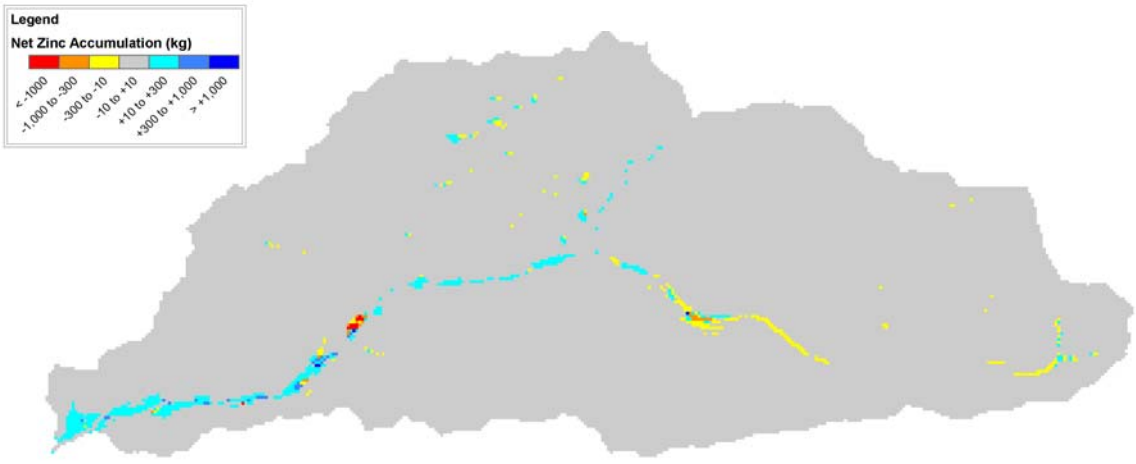

c) Net accumulation (kg)

Figure 6-15. Estimated 1-in-100 year event cumulative zinc transport.

flow for the 1-in-100-year event is 4 m^3/s and the peak flow is 22 m^3/s. Extrapolating the observed load using 7.5 g/m^3 as a representative concentration, the inferred dissolved zinc load is 2,600 kg/day (5,700 lbs/day) at the average event flow rate and 14,250 kg/day (31,000 lbs/day) at the peak event flow. This compares well with a simulated dissolved zinc load of 9,500 kg/day for the 1-in-100-year event.

The 1-in-100-year event generates significant overland flow and mobilizes large masses of solids and associated chemicals from the land surface. During transport, particulate phase chemicals can enter the dissolved phase. However, nearly 75% of the water on the overland plane infiltrates before reaching the watershed outlet during this event. As water infiltrates, dissolved chemicals in transport will also infiltrate. Representative dissolved phase chemical infiltration fluxes for zinc at different times during the 1-in-100-year event are presented in Figure 6-16. During the simulation, the zinc mass returned to the soil as water infiltrates is approximately 1400 kg and equals nearly 10% of the zinc mass exported from the watershed. This suggests that dissolved phase transport and infiltration may significantly influence the long term redistribution of metals across the site.

The model can be used to address questions of management interest to guide mine waste impact mitigation efforts for California Gulch. Examining the export estimates presented in Figures 6-8 to 6-11, loads of solids and metals passing Station CG-1 are roughly twice the size of loads passing Station SD-3. This suggests upper California Gulch is a more significant contributor of material to downstream areas than the Stray Horse Gulch and Starr Ditch contributing areas. However, model results also indicate that the solids and metals masses exported from the lower gulch are larger than the loads imported from the upstream channel network. This suggests that during high flow events flood waters have the potential to erode tailings present along channel margins throughout the lower gulch.

More detailed information can be obtained by using the model to track chemical export from different source areas. An example for zinc transport during the 1-in-100-year event is presented. The site was divided into four source areas as presented in Figure 6-17. The source areas are: (1) Stray Horse Gulch; (2) upper California Gulch; (3) lower California Gulch (excluding channel floodplain areas); and (4) lower California Gulch floodplain.

a) Flux at 30 minutes (g/s)

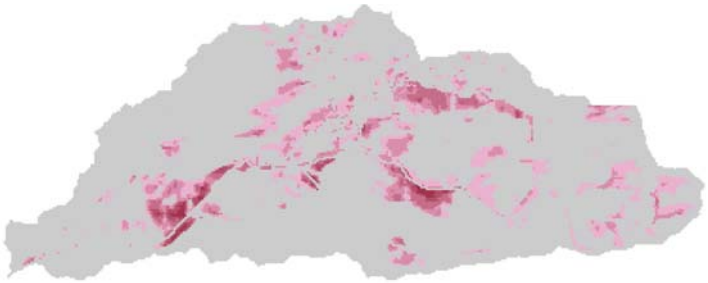

b) Flux at 60 minutes (g/s)

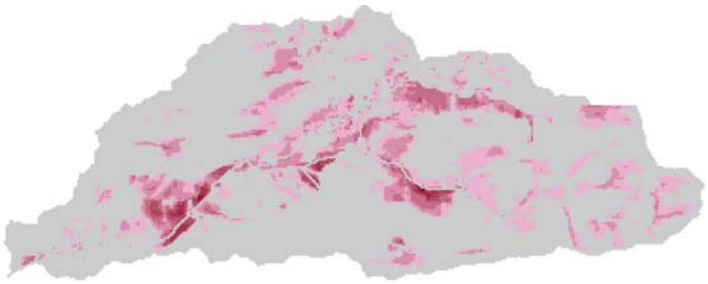

c) Flux at 120 minutes (g/s) (rain ends after 120 minutes)

d) Flux at 240 minutes (g/s)

e) Flux at 480 minutes (g/s)

Figure 6-16. Estimated 1-in-100-year event dissolved zinc infiltration fluxes.

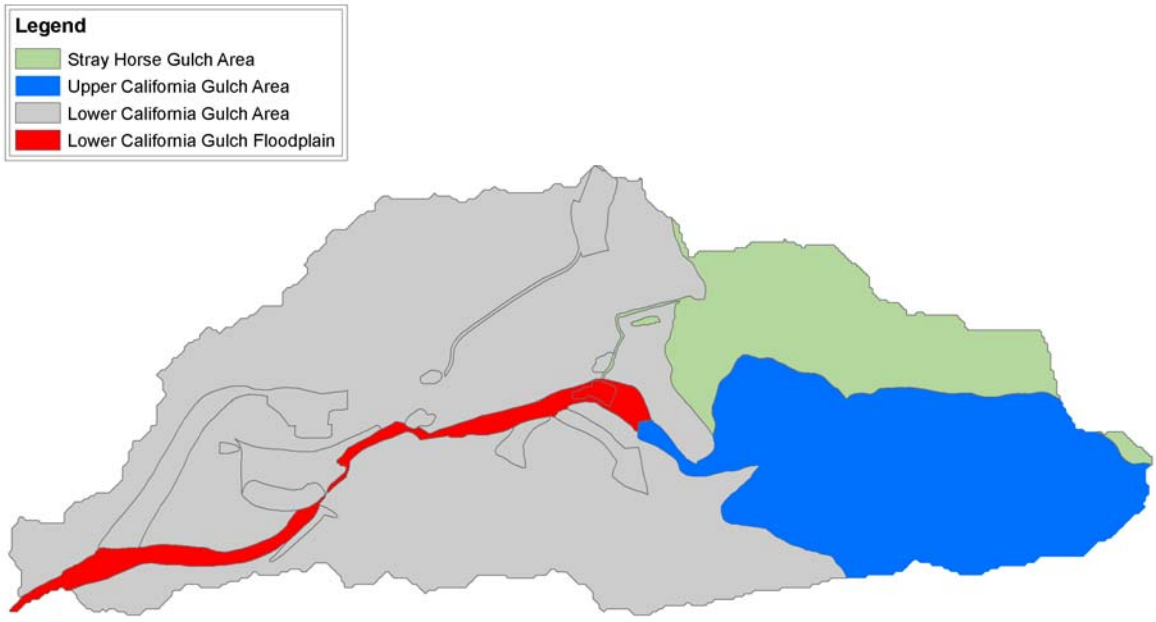

Figure 6-17. California Gulch source areas for chemical tracking example.

Table 6-2. Estimated zinc import and export for chemical source tracking example.

Source Area	*Import (kg)*		*Export (kg)*	
	Overland	*Channels*	*Overland*	*Channels*
1	52	44	1	2
2	6,320	1,210	23	34
3	21,600	3,570	970	470
4	N/A		10,800	3000

Source Areas: 1 = Stray Horse Gulch; 2 = Upper California Gulch; 3 = Lower California Gulch; 4 = Lower California Gulch Floodplain.

Import = net accumulation of mass within Source Area 4; Export = net transport of mass through Source Area 4 and delivered to the Arkansas River; Overland = mass imported to and deposited on the overland plane or mass transported and exported by overland flow; Channels = mass imported to and deposited in the channel network or mass transported and exported by channel flow.

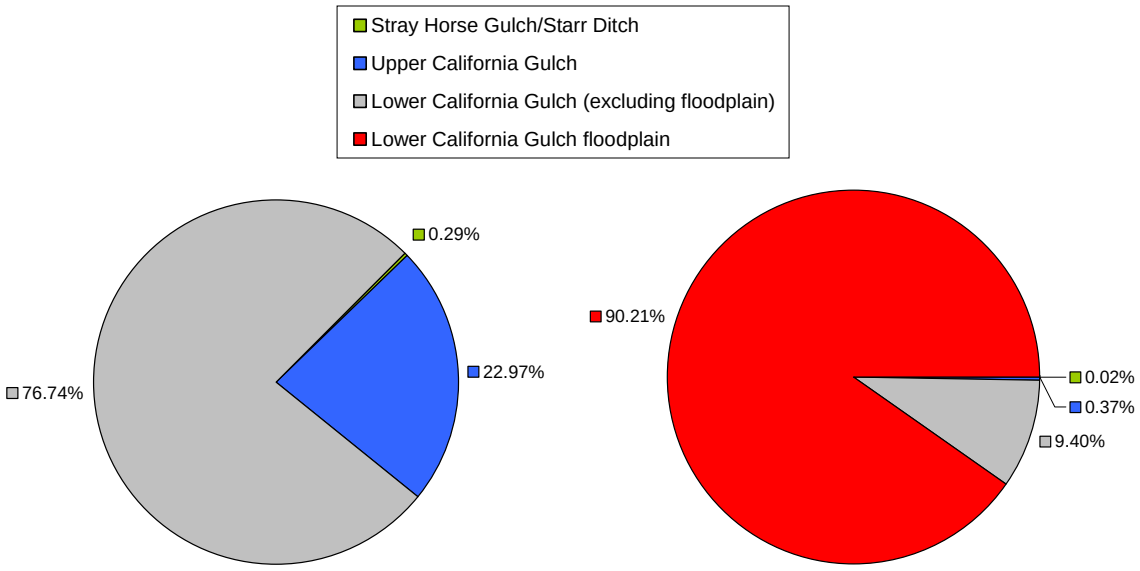

a) Estimated zinc import (%)

b) Estimated zinc export (%)

Figure 6-18. Relative import and export contributions by source area.

Zinc within each source area was treated as an independent chemical state variable. Zinc import and export for Source Area 4 are summarized in Table 6-2. To better visualize the source area relationships, the relative contribution of each area to import and export are presented in Figure 6.18.

With respect to export, approximately 90% of the total zinc export is estimated to originate from Source Area 4 (lower gulch floodplain). Zinc export from more distant source areas is more limited because flows are smaller (less erosion) and the potential for deposition is larger since transport distances are longer and slopes decrease in floodplain areas. Nonetheless, under extreme storm conditions all areas contribute mass to total zinc export. However, since mining and ore processing activities did not occur directly in this area, the mass exported from Source Area 4 must have originated from other source areas over time. This is more clearly demonstrated by considering mass import. For the 1-in-100-year event, the estimated overall zinc mass import (32,800 kg) exceeds the overall mass export (15,300 kg) and the zinc mass inventory within Source Area 4 is estimated to increase by approximately 15,500 kg. More than 76% of the total mass entering the area originates from Source Area 3. Contributions from Source Areas 2 and 1 are estimated to

be approximately 23% and less than 1%, respectively. Note that much of the zinc mass transported from Source Area 3 originates from slag piles that sit immediately adjacent to the boundary with Source Area 4.

6.3 DISCUSSION

The results of the 1-in-100-year event simulation compare favorably to the results of other flow studies. The estimated zinc export from the watershed also compares very favorably to the dissolved zinc load inferred by extrapolation of field data. However, it should be recognized that the TREX application to California Gulch was calibrated to flow conditions much lower than this extreme event. Flows within California Gulch are typically small and are conveyed in small rills or low flow conveyance channels (LFCCs) incised within larger channels. During typical flow conditions, stream flow is controlled by the geometry and roughness of the LFCC. Increasing channel width and bank height and decreasing roughness to better represent high flow channel conditions increases peak flow at CG-6 from 22 m^3/s to 28 m^3/s. Flood wave attenuation is also reduced. Although this change in peak flow is relatively small, a more significant difference is that flooding would be reduced since the high flow channel network has greater conveyance than the low flow network. As the extent of flooding decreases, corresponding floodplain sediment transport would also decrease. Further discussion regarding the representation of channel geometry and roughness is presented in Appendix E. Despite the uncertainty that may be introduced by differences in channel conditions, model application efforts for the 1-in-100-year event were successful.

The zinc source tracking example clearly illustrates how the model can be used to assess the relative impacts that different source areas have on downstream conditions. In this case, the model results demonstrate the extent to which upstream sources contribute to export. From the perspective of chemical delivery to the Arkansas River, areas closest to the watershed outlet contribute the most to export. However, model results indicate that more distant sources contribute to the buildup of chemicals in the lower gulch floodplain area. Such imported mass would then be available for export during future events, suggesting that a series of events can transport chemicals from even very distance sources

over time. With respect to managing site remediation efforts, these model results further suggest that there is a significant risk for recontamination of downstream sites over time due to the potential for transport from upstream areas.

It should be noted that the zinc mass tracking example could be further refined to provide more resolved results. Additional source areas could be defined to further delineate significant chemical inputs to the lower gulch floodplain. For example, the slag piles associated with the former smelter sites adjacent to the floodplain could be treated as a separate source area. Recognizing that ore processed at former smelter sites was likely mined in Stray Horse Gulch (Source Area 1) or upper California Gulch (Source Area 2), it may be appropriate to conclude that a considerable portion of the zinc mass imported from the lower California Gulch watershed outside of the floodplain (Source Area 3) actually originates from Stray Horse Gulch or upper California gulch.

When interpreting the mass fate of solids and metals, note that the TREX application to California Gulch does not account for the impacts of mine waste remediation efforts or the effect that the detention pond at the Yak Tunnel treatment plant has on flow or sediment and contaminant transport. Located just downstream of Station CG-1, construction of the Yak Tunnel facilities was completed in 1992. Other remediation actions have also occurred across the site over the past ten years. Nonetheless, the results presented may still be representative of historical conditions that existed for many years prior to the construction of the Yak Tunnel facilities and the initiation of significant remediation efforts.

7.0 CONCLUSIONS AND RECOMMENDATIONS

7.1 CONCLUSIONS

Efforts to develop TREX, a fully distributed numerical model to assess the watershed transport and fate of contaminants, were successful. Model functionality and performance were successfully demonstrated by a site-specific application to the California Gulch watershed. Specific conclusions regarding the numerical model development and application efforts are summarized below:

1. TREX is a powerful, new model to simulate contaminant transport and fate at the watershed scale. This model provides capabilities to represent event hydrology, sediment transport, and chemical transport and fate processes including: (1) chemical erosion, advection, and deposition; (2) chemical partitioning and phase distribution; and (3) chemical infiltration and redistribution. TREX is fully-distributed and is designed to be compatible with data from raster GIS sources. In particular, data describing elevation, soil types, land use, and contaminant distributions can be processed in a GIS and used as model inputs. Model outputs are also designed to be compatible for use with a GIS to facilitate visualization of chemical transport and fate simulation results.

2. Model performance was successfully demonstrated by site-specific application to the California Gulch watershed. Using a database of observations for the period 1984-2004, site hydrology, sediment transport, and chemical transport and fate were simulated for two events. A June 12-13, 2003 event was used for calibration. A September 5-8, 2003 event was used for validation. The model accurately reproduced the observed volumes, peak flows, and times to peak for these events. Average relative percent differences for flow volume estimates was -8.6% for the calibration event and +11.3% for the validation event. The model also reproduced the observed range of total suspended solids concentrations. In addition, the

model was also able to reasonably reproduce total metals concentrations. Within California Gulch, a significant fraction of the total metals in surface water exists in the dissolved phase. However, in soils and sediment nearly all the metals mass is a particulate form. This indicates California Gulch metals transport simulations should account for partitioning and phase distribution in order to better describe interactions between surface water, soils, and sediment.

3. Model results suggest that flood waters during high flow events have the potential to erode layers of tailings present along channel margins throughout the lower gulch. More detailed zinc source tracking results indicate that 90% of the zinc exported from the watershed during the 1-in-100 year event simulation originates from the lower gulch floodplain (source Area 4). The results further indicate that 76% of zinc mass imported to the lower gulch floodplain originates from elsewhere in the lower gulch watershed (Source Area 3) and 23% originates from upper California Gulch (Source Area 2).

7.2 RECOMMENDATIONS FOR FUTURE STUDIES

Recommendations for future TREX model framework development are:

1. TREX should be extended to permit simulation of irregular, compound channel geometries with variable roughness. If modified to better handle discontinuities in channel geometry, the Γ parameter set described by Buhman et al. (2002) could be readily implemented.

2. Thresholds for use of the modified Kilinc-Richardson overland sediment transport capacity relationship should be examined. During high flow conditions sediment transport may be limited to the rate at which rainfall or flow can detach individual grains from the bulk soil matrix. Under supply limited conditions, transport capacity relationships may not be applicable. Supply limited conditions may occur along floodplain margins of channel networks during large floods. Vegetative cover in the floodway may act to limit grain detachment and soil erosion. Further assessment of limiting conditions or thresholds is recommended to better determine the range of applicability for this relationship

3. Tools such as PEST (Doherty, 2001a,b) should be adapted for use with TREX to automate the model calibration and parameter uncertainty assessment process.

REFERENCES

Abbott, M.B., Bathurst, J.C., Cunge, J.A., O'Connell, P.E., and Rasmussen, J. 1986a. An introduction to the European Hydrological System—Système Hydrologique Europèen, SHE. 1: History and philosophy of a physically-based, distributed modelling system. Journal of Hydrology, 87(1-2):45-59.

Abbott, M.B., Bathurst, J.C., Cunge, J.A., O'Connell, P.E., and Rasmussen, J. 1986b. An introduction to the European Hydrological System—Système Hydrologique Europèen, SHE. 2: Structure of a physically-based, distributed modelling system. Journal of Hydrology, 87(1-2):61-77.

Abramowitz, M. and Stegun, I.A. 1972. Handbook of Mathematical Functions. Applied Mathematics Series 55. National Bureau of Standards, Washington, D.C.

Ackers, P., and White, W.R. 1973. Sediment transport: new approach and analysis. Journal of the Hydraulics Division, American Society of Civil Engineers, 99(HY11):2041-2060.

Ambrose, R.B., Martin, J.L. and Wool, T.A. 1993. WASP5, A hydrodynamic and water quality model — Model theory, user's manual, and programmer's guide. U.S. Environmental Protection Agency, Office of Research and Development, Environmental Research Laboratory, Athens, Georgia.

Arnold, J.G., Allen, P.M., and Bernhardt, G.. 1993. A comprehensive surface groundwater flow model. Journal of Hydrology, 142(1-4):47-69.

Bagnold, R.A. 1977. Bedload transport by natural rivers. Water Resources Research 13(2):303-311.

Bathurst, J.C., Ewen, J., Parkin G., O'Connell, P.E., and Cooper, J.D. 2004. Validation of catchment models for predicting land-use and climate change impacts: 3. Blind validation for internal and outlet responses. Journal of Hydrology, 287(1-4):74-94.

Beuselinck, L., Govers, G., Steegen, A., and Quine, T.A. 1999. Sediment transport by overland flow over an area of net deposition. Hydrological Processes, 13(17):2769-2782.

Bian, L., Sun, H., Blodgett, C.F., Egbert, S.L., Li, W., Ran, L., and Koussis, A.D. 1996. An integrated interface system to couple the SWAT model and ARC/INFO. Proceedings of the Third International Conference on Integrating GIS and Environmental Modeling, Santa Fe, New Mexico. January 21-25, 1996.

Bicknell, B.R., Imhoff, J.C., Kittle, J.L., Jr., Donigian, A.S., Jr., and Johanson, R.C. 1997. Hydrological Simulation Program—Fortran: User's manual for version 11. U.S. Environmental Protection Agency, National Exposure Research Laboratory, Athens, Georgia. EPA/600/R-97/080. 755 p.

Bicknell, B.R., Imhoff, J. C., Kittle, J.L., Jr., Jobes, T.H., and Donigian, A.S., Jr. 2001. Hydrological Simulation Program—Fortran: User's manual for version 12. U.S. Environmental Protection Agency, National Exposure Research Laboratory, Athens, Georgia. 873 p.

Buhman, D.L., Gates, T.K., and Watson, C.C. 2002. Stochastic variability of fluvial hydraulic geometry: Mississippi and Red Rivers. Journal of Hydraulic Engineering, 128(4): 426-437.

Bras, R.L. 1990. Hydrology: An Introduction to Hydrologic Science. Addison-Wesley Publishing Company, Reading, Massachusetts. 643 p.

Brown, L.C. and Barnwell, T.O. 1987. The enhanced stream water quality models QUAL2E and QUAL2E-UNCAS: documentation and user manual. U.S. Environmental Protection Agency, Environmental Research Laboratory, Athens, Georgia. EPA /600/3-87/007. 189 p.

Burban, P.Y., Xu, Y., McNeil, J., and W. Lick. 1990. Settling speeds of flocs in fresh and sea waters. Journal of Geophysical Research (C) Oceans, 95(C10):18213-18220.

Capel, P. and S. Eisenriech, S. 1990. Relationship between chlorinated hydrocarbons and organic carbon in sediment and porewater. Journal of Great Lakes Research, 16(2):245-257.

CDM. 1994. Final Soils Investigation Data Report California Gulch CERCLA site Leadville, Colorado (Four Volumes). Camp, Dresser, and McKee, Inc., Denver, Colorado. Prepared for: Resurrection Mining Company Denver, Colorado. Dated: July 15, 1994.

Chapra, S.C. 1997. Surface Water-Quality Modeling. McGraw-Hill Companies, Inc. New York, New York. 844 pp.

Chapra, S.C., and Canale, R.P. 1985. Numerical Methods for Engineers with Personal Computer Applications (First Edition). McGraw-Hill, Inc., New York, New York. 570 pp.

Cheng, N.S. 1997. Simplified settling velocity formula for sediment particle. Journal of Hydraulic Engineering, 123(2):149-152.

Clements, W., Carlisle, D., Lazorchak, J., and Johnson, P. 2000. Heavy metals structure benthic communities in Colorado mountain streams. Ecological Applications, 10(2):626-638.

Clements, W., Carlisle, D., Courtney, L., and Harrahy, E. 2002. Integrating observational and experimental approaches to demonstrate causation in stream biomonitoring studies. Environmental Toxicology and Chemistry, 21(6):1138-1146.

CMC. 2004. Final Site Wide Water Quality Summary for the Sampling Events Conducted the year of 2003. Colorado Mountain College/Natural Resource Management Institute. Leadville, Colorado. Prepared for: USEPA. Denver, Colorado. Dated: January 2004.

Crawford, N.H., and Linsley, R.K.. 1966. Digital Simulation in Hydrology: Stanford Watershed Model IV. Department of Civil Engineering, Stanford University, Stanford, California. Technical Report 39. 210 p. (Dated: July, 1966.)

Dames and Moore. 1989. Design of California Gulch Channel for 500-year Peak Flows. Dames and Moore, Golden, Colorado.

Day, T.J. 1980. A study of the transport of graded sediments. Hydraulics Research Station, Wallingford, UK. Report IT 190.

DiToro, D.M. 1985. A particle interaction model of reversible organic chemical sorption. Chemosphere, 14(9-10):1503-1538.

DiToro, D.M. 2001. Sediment Flux Modeling. John Wiley and Sons, Inc., New York, New York. 624 pp.

Doherty, J. 2001a. PEST-ASP User's Manual. Watermark Numerical Computing, Brisbane, Australia.

Doherty, J. 2001b. PEST Surface Water Utilities User's Manual. Watermark Numerical Computing, Brisbane, Australia, and University of Idaho, Idaho Falls, Idaho.

Doherty, J., and Johnston, J.M. 2003. Methodologies for calibration and predictive analysis of a watershed model. Journal of the American Water Resources Association, 39(2):251-256.

Donigian, A.S., Jr., and Crawford, N.H. 1976a. Modeling Pesticides and Nutrients on Agricultural Lands, Environmental Research Laboratory, Athens, Georgia. EPA 600/2-7-76-043. 317 p.

Donigian, A.S., Jr., and Crawford, N.H 1976b. Modeling Nonpoint Pollution From the Land Surface, Environmental Research Laboratory, Athens, Georgia. EPA 600/3-76-083. 280p.

Donigian, A.S, Jr., Beyerlein, D.C., Davis, H.H., Jr., and Crawford, N.H. 1977. Agricultural Runoff Management (ARM) Model Version II: Refinement and Testing, Environmental Research Laboratory, Athens, Georgia. EPA 600/3-77-098. 294 p.

Donigian, A.S., Jr., Imhoff, J.C., Bicknell, Brian, Kittle, J.L., Jr. 1984. Application guide for Hydrological Simulation Program—Fortran (HSPF). U.S. Environmental Protection Agency, Environmental Research Laboratory, Athens, Georgia. EPA-600/3-84-065. 177 p.

Downer, C.W., and Ogden, F.L. 2004. GSSHA: model to simulate diverse stream flow producing processes. Journal of Hydrologic Engineering, 9(3):161-174.

Eadie, B., N. Morehead, and P. Landrum. 1990. Three-phase partitioning of hydrophobic organic compounds in Great Lakes waters. Chemosphere, 20(1-2):161-178.

Eadie, B., N. Morehead, V. Klump, and P. Landrum. 1992. Distribution of hydrophobic organic compounds between dissolved and particulate organic matter in Green Bay waters. Journal of Great Lakes Research, 18(1):91-97.

Eagleson, P.S. 1970. Dynamic Hydrology. McGraw-Hill Book Company, New York, New York. 462 pp.

Engelund, F., and Hansen, E. 1967. A monograph on sediment transport in alluvial streams. Teknisk Vorlag, Copenhagen, Denmark. 62 pp.

Ewen, J., Parkin, G., and O'Connell, P.E. 2000. SHETRAN: distributed river basin flow and transport modeling system. Journal of Hydrologic Engineering, 5(3):250-258.

Ewen, J., Bathurst, J.C., Parkin, G., O'Connell, E., Birkinshaw, S., Adams, R., Hiley, R., Kilsby, C., and Burton, A. 2002. SHETRAN: physically-based distributed river basin modeling system. In: Mathematical Modeling of Small Watershed Hydrology, V.P. Singh, D.K. Frevert and S.P. Meyer, eds. Water Resources Publications, Englewood, Colorado. pp. 43-68.

Exner, F. M. 1925, Über die wechselwirkung zwischen wasser und geschiebe in flüssen, Sitzungber. Acad. Wissenscaften Wien Math. Naturwiss. Abt. 2a, 134:165–180.

Fetter, C.W. 2001. Applied Hydrogeology, Fourth Edition. Prentice-Hall, Inc. Upper Saddle River, New Jersey. 598 p.

Fiorucci, P., La Barbera, P., Lanza, L.G., and Minciardi, R. 2001. A geostatistical approach to multisensor rain field reconstruction and downscaling. Hydrology and Earth System Sciences, 5(2):201-213.

Foster, G.R., Lane, L.J., Nowlin, J.D., Laflen, J.M., and Young, R.A. 1980. "A model to estimate sediment from field sized areas." In: CREAMS: a field scale model for chemicals, runoff and erosion from agricultural management systems, W. G. Knisel, ed. U.S. Department of Agriculture, Washington, D.C. Conservation Report Number 26. pp. 36-64.

Gessler, J. 1965. The Beginning of Bedload Movement of Mixtures Investigated as Natural Armouring in Channels. Technical report No. 69, The Laboratory of

Hydraulic Research and Soil Mechanics, Swiss Federal Institute of Technology, Zurich (translation by W. M. Keck Laboratory of Hydraulics and Water Resources, California Institute of Technology, Pasadena, California).

Gessler, J. 1967. The beginning of bedload movement of mixtures investigated as natural armoring in channels. California Institute of Technology, Pasadena, California. 89pp.

Gessler, J. 1971. Beginning and ceasing of sediment motion. In: River Mechanics, Shen, H.W., ed. H.W. Shen, Fort Collins, Colorado. pp. 7:1–7:22.

Golder. 1996. Surface Water Remedial Investigation Report California Gulch Site Leadville, Colorado (Two Volumes). Golder Associates, Inc., Lakewood, Colorado. Prepared for: ASARCO, Inc., Denver, Colorado. Dated: May 1996.

Golder. 1997. Field Investigation Data Report for the Apache Tailings Supplemental Remedial Investigation. Golder Associates Inc., Lakewood, Colorado. Prepared for: ASARCO, Inc., Denver, Colorado. Dated: April 7, 1997.

Green, W.H. and Ampt, G.A. 1911. Studies on soil physics, 1: the flow of air and water through soils. Journal of Agricultural Sciences 4(1):11-24.

Haralampides, K., McCourquodale, J.A., Krishnappan, B.G. 2003. Deposition properties of fine sediment. Journal of Hydraulic Engineering, 129(3):230-234.

Harbaugh, A.W., Banta, E.R., Hill, M.C., and McDonald, M.G. 2000. MODFLOW-2000, the U.S. Geological Survey modular ground-water model -- User guide to modularization concepts and the Ground-Water Flow Process. U.S. Geological survey, Denver, Colorado. Open-File Report 00-92. 121 p.

HDR. 2002. Final focused feasibility study for Operable Unit 6, California Gulch NPL site, Leadville, Colorado. 2002. Report prepared for U.S. Environmental Protection Agency Region 8. HDR Engineering, Inc., Omaha, Nebraska. Dated: September 11, 2002.

Holley, E.R. 1969. Unified view of diffusion and dispersion. Journal of the Hydraulics Division, American Society of Civil Engineers, 95(2):621-631.

Holm, P.E., Rootzén, H., Borggaard, O.K., Møberg, J.P., and Christensen, T.H. 2003. Correlation of cadmium distribution coefficients to soil characteristics. Journal of Environmental Quality, 32(1):138-145.

HSI. 1986. Water-Quality Modeling Study Yak Drainage Tunnel Leadville District. Hydro-Search, Inc., Golden, Colorado. Prepared for: Leadville Corporation. Leadville, Colorado. Dated: December 1, 1986

IMCC. 1992. Inactive and abandoned non-coal mines: A scoping study. Interstate Mining Compact Commission, Herndon, Virginia. Report prepared by Resource Management Associates, Clancy, Montana. Cooperative Agreement X-81 7900-01-O (July).

Imhoff, J.C., Stoddard, A., Buchak, E.M., and Hayter, E. 2003. Evaluation of Contaminated Sediment Fate and Transport Models: Final Report. U.S. Environmental Protection Agency, Office of Research and Development, National Exposure Research Laboratory, Athens, Georgia. Contract Number 68-C-01-037, Work Assignment No. 1-10. 153 p.

Johanson, R.C., Imhoff, J.D., and Davis, H.H., Jr. 1980. Users manual for hydrological simulation program—Fortran (HSPF). Environmental Research Laboratory, Athens, Georgia. EPA-600/9-80-015.

Johnson, B.E., Julien, P.Y., Molnar, D.K., and Watson, C.C. 2000. The two-dimensional upland erosion model CASC2D-SED. Journal of the American Water Resources Association, 36(1):31-42.

Julien, P.Y. 1998. Erosion and Sedimentation (First Paperback Edition). Cambridge University Press, Cambridge, UK. 280 p.

Julien, P.Y. 2002. River Mechanics. Cambridge University Press, Cambridge, UK. 434 p.

Julien, P.Y. and Saghafian, B. 1991. CASC2D User's Manual - A Two Dimensional Watershed Rainfall-Runoff Model. Department of Civil Engineering, Colorado State University, Fort Collins, Colorado. Report CER90-91PYJ-BS-12. 66 p.

Julien, P.Y., Saghafian, B., and Ogden, F.L. 1995. Raster-Based hydrologic modeling of spatially-varied surface runoff. Water Resources Bulletin, AWRA, 31(3):523-536.

Julien, P.Y. and Rojas, R. 2002. Upland erosion modeling with CASC2D-SED. International Journal of Sediment Research, 17(4):265-274.

Julien, P.Y., and Frenette, M. 1985. Modeling of rainfall erosion. Journal of Hydraulic Engineering, 11(10):1344-1359.

Julien, P.Y., and Simons, D.B. 1985. Sediment transport capacity of overland flow. Transactions of the American Society of Agricultural Engineers, 28(3):755-762.

Kandel, D.D., Westerm A.W., and Grayson, R.B. 2005. Scaling from process timescales to daily time steps: a distribution function approach. Water Resources Research, 41(2):W02003.

Karickhoff, S.W., Brown, D.S., and Scott, T.A. 1979. Sorption of hydrophobic pollutants on natural sediments. Water Research, 13(3):241-248.

Kashian, D.R., Prusha, B., and Clements, W.H. 2004. Influence of total organic carbon and UV-B radiation on zinc toxicity and bioaccumulation in aquatic communities. Environmental Science and Technology, 38(23):6371-6376.

Kilinc, M.Y., and Richardson, E.V. 1973. Mechanics of soil erosion from overland flow generated by simulated rainfall. Hydrology Papers, Number 63. Colorado State University, Fort Collins, Colorado.

Kipp, K.L, Jr. 1997. Guide to the Revised Heat and Solute Transport Simulator: HST3D Version 2. U.S. Geological Survey, Denver, Colorado. Water Resources Investigations Report 97-4157. 149 p.

Krishnappan, B.G. 2000. In situ distribution of suspended particles in the Frasier River. Journal of Hydraulic Engineering, 126(8):561-569.

Krone, R.B. 1962. Flume studies of the transport of sediments in estuarial shoaling processes. Final Report. Hydraulic Engineering Laboratory and Sanitary Engineering Research Laboratory, University of California, Berkeley, California.

Landrum, P., M. Rheinhold, S. Nihart, and B. Eadie. 1985. Predicting bioavailability of xenobiotics to Pontoporeia Hoya in the presence of humic and fulvic materials and natural dissolved organic matter. Environmental Toxicology and Chemistry, 4(4):459-467.

Landrum, P., Nihart, S. Eadie, B. and Herche L. 1987. Reduction in bioavailability of organic contaminants to the amphipod Pontoporeia Hoya by dissolved organic matter of sediment interstitial waters. Environmental Toxicology and Chemistry, 6(1):11-20.

Lanza, L.G., Ramirez, J.A., and Todini, E. 2001. Stochastic rainfall interpolation and downscaling. Hydrology and Earth System Sciences, 5(2):139-143.

Li, R.M., Stevens, M.A., and Simons, D.B. 1976. Solutions to Green-Ampt infiltration equations. Journal of Irrigation and Drainage Division, ASCE, 102(IR2):239-248.

Linsley, R.K., Kohler, M.A., and Paulhus, J.L.H. 1982. Hydrology for Engineers (Third Edition). McGraw-Hill Book Company, New York, New York. 508 p.

Loehle, C. 1997. A hypothesis testing framework for evaluating ecosystem model performance. Ecological Modeling, 97(3):153-165.

Loehle, C., and Ice, G. 2002. Criteria for evaluating watershed models. Hydrological Science and Technology, 19(1-4). Proceedings of the 2002 American Institute of Hydrology Annual Meeting and International Conference, Portland, Oregon, October 13-17.

Lu, Y., and Allen, H. 2001. Partitioning of copper onto suspended particulate matter in river waters. Science of the Total Environment 277(1-3):119-132.

Mackay, N.G., Chandler, R.E., Onof, C., and Wheater, H.S. 2001. Dissagregation of spatial rainfall fields for hydrological modeling. Hydrology and Earth System Sciences, 5(2):165-173.

Mehta, A., McAnally, W., Hayter, J., Teeter, A., Heltzel, S., and Carey, W. 1989. Cohesive sediment transport. II: application. Journal of Hydraulic Engineering, 115(8):1094-1112.

Meyer, L.D., and Weischmeier, W.H. 1969. Mathematical simulation of the process of soil erosion by water. Transactions of the American Society of Agricultural Engineers, 12(6):754-762.

Mishra, S. 2001. Dealing with uncertainty in environmental model predictions. EOS, Transactions, American Geophysical Union, 82(47):565 (November).

MKC. 1992. Report for Zinc Slag Pile Remedial Investigation at the California Gulch Site Leadville, Colorado. Morrison Knudsen Corporation, Environmental Services Division. Prepared for: Denver and Rio Grande Western Railroad Company. (Administrative Order on Consent: CERCLA-VIII-92-06) Dated: December 11, 1992.

Molnár, D.K. and Julien, P.Y. 2000. Grid size effects on surface runoff modeling. Journal of Hydrologic Engineering, 5(1):8-16.

Moore, C., and Doherty, J. 2005. Role of the calibration process in reducing model predictive error. Water Resources Research, 41(5):W05020.

Moore, I.D., and Burch, G.J. 1986. Sediment transport capacity of sheet and rill flow: application of unit stream power theory. Water Resources Research, 22(8):1350-1360.

Neitsch, S.L., Arnold, J.G., Kiniry, J.R., Williams, J.R., and King, K.W. 2002. Soil and Water Assessment Tool Theoretical Documentation, Version 2000. U.S. Department of Agriculture, Agricultural Research Service, Temple Texas. 506 p.

Ogden, F.L., 1997. CASC2D Reference Manual (Version 1.17). Department of Civil and Environmental Engineering, University of Connecticut, Storrs, Connecticut. U-37, 106 p.

Ogden, F.L. and Julien, P.Y. 2002. CASC2D: A Two-Dimensional, Physically-Based, Hortonian Hydrologic Model. In: Mathematical Models of Small Watershed Hydrology and Applications, Singh, V.P. and Frevert, D., eds., Water Resources Publications, Littleton, Colorado. pp. 69-112.

Onishi, Y. and Wise, S.E. 1979. Mathematical Model, SERATRA, for Sediment-Contaminant Transport in Rivers and its Application to Pesticide Transport in Four Mile and Wolf Creeks in Iowa. Battelle, Pacific Northwest Laboratories, Richland, Washington.

Partheniades, E. 1992. Estuarine sediment dynamics and shoaling processes. In: Handbook of Coastal and Ocean Engineering, Volume 3: Harbours, Navigation Channels, Estuaries, and Environmental Effects, pp. 985-1071. Herbich, J. B., Ed. Gulf Publishing Company, Houston, Texas.

Phillip, J.R. 1957a. The theory of infiltration: 1. The infiltration equation and its solution. Soil Science, 83:345-357.

QEA. 1999. PCBs in the Upper Hudson River, Volume 2: A model of PCB Fate, Transport, and Bioaccumulation. Prepared for General Electric, Albany, New York. Prepared by Quantitative Environmental Analysis, LLC, Montvale, New Jersey. Job Number GENhud:131. May.

Rawls, W.J., Brakensiek, D.L., and Miller, N. 1983. Green-Ampt infiltration parameters from soils data. Journal of Hydraulic Engineering, 109(1):62-69.

Rawls, W.J, Ahuja, L.R., Brakensiek, D.L., and Shirmohammadi, A. 1993. "Infiltration and Soil Movement." In: Handbook of Hydrology, Maidment, D.R., ed. McGraw-Hill, Inc., New York, New York. pp 5.1-5.51.

Richards L.A. 1931. Capillary conduction of liquids in porous mediums. Physics, 1:318-333.

RMC. 2001. Synoptic Sampling of Stray Horse Gulch/Starr Ditch and California Gulch, Spring 2001. Rocky Mountain Consultants, Inc., Longmont, Colorado. Prepared for Colorado Department of Public Health and Environment, Hazardous Materials and Waste Division, Denver, Colorado. Dated: November, 2001. RMC Job No. 19-0424.002.01.

RMC. 2002. Synoptic Sampling of California Gulch and Arkansas River, Spring 2002. Rocky Mountain Consultants, Inc., Longmont, Colorado. Prepared for Colorado Department of Public Health and Environment, Hazardous Materials and Waste Division, Denver, Colorado. Dated: November, 2001. RMC Job No. 19-0424.002.01.

Rojas, R. 2002. GIS-based Upland Erosion Modeling, Geovisualization and Grid Size Effects on Erosion Simulations with CASC2D-SED. Ph.D. dissertation, Department of Civil Engineering, Colorado State University, Fort Collins, Colorado.

SAI. 1997a. Hydrologic Analysis of the California Gulch Watershed. Simons and Associates, Inc., Fort Collins, Colorado. Prepared for Resurrection Mining Company. Dated: February 25, 1997.

SAI. 1997b. Hydrologic Analysis of the 500-Year Flood, California Gulch. Simons and Associates, Inc., Fort Collins, Colorado. Prepared for Resurrection Mining Company. Dated: February 25, 1997.

Schwarzenbach, R.P., Geschwend, P.M., and Imboden, D.M. 1993. Environmental Organic Chemistry. Wiley-Interscience, New York.

Simons, D.B., and Sentürk, F. 1992. Sediment Transport Technology – Water and Sediment Dynamics (Revised Edition). Water Resources Publications, Littleton, Colorado.

Singh, V.P. 1995. Computer Models of Small Watershed Hydrology. Water Resources Publications, Highlands Ranch, Colorado.1144 pp.

Smith, R.E., and Parlange, J.-Y. 1978. A parameter efficient hydrologic infiltrations model. Water Resources Research, 14(3):533-538.

Sauvé, S.F., Hendershot, W., and Allen, H.E. 2000. Solid-solution partitioning of metals in contaminated soils: dependence on pH, total metal burden, and organic matter. Environmental Science and Technology 34(7):1125-1131.

Sauvé, S.F., Manna, S., Turmel, M.C., Roy, A.G., and Courchesne, F. 2003. Solid-solution partitioning of Cd, Cu, Ni, Pb, and Zn in the organic horizons of a forest soil. Environmental Science and Technology 37(22):5191-5196.

Swayze, G., Smith, K., Clark, R., Sutley, S., Pearson, R., Vance, J., Hageman, P., Briggs, P., Meier, A., Singleton, M., and Roth, S. 2000. Environmental Science and Technology, 34(1):47-54.

TechLaw. 2001. Second Five-Year Review Report for California Gulch. TechLaw, Inc., Lakewood, Colorado. Prepared for: Region VIII USEPA Denver, Colorado. Dated: September 28, 2001.

Thomann, R.V. and J.A. Meuller. 1987. Principles of Surface Water Quality Modeling and Control. Harper and Row Publishers, Inc., New York, New York. 644 pp.

TTRMC. 2003. Synoptic Sampling of Stray Horse Gulch/Starr Ditch, California Gulch, and the Arkansas River, May 2003. Tetra Tech RMC, Longmont, Colorado. Prepared for Colorado Department of Public Health and Environment, Hazardous Materials and Waste Division, Denver, Colorado. Dated: November, 2001. Tetra Tech RMC Job No. 19-0424.002.01.

USACE. 1990. Combined-Population Frequency Analysis Utilizing a Rainfall Runoff Model in the Rocky Mountains. U.S. Army Corps of Engineers, Omaha Engineering District, Omaha, Nebraska.

USACE. 1998. HEC-1 Flood Hydrograph Package User's Manual. U.S. Army Corps of Engineers, Hydraulic Engineering Center, Davis, CA. (Report: CPD-1A, June 1998.)

USBR. 1996. Stray Horse Gulch and Little Stray Horse Gulch, near Leadville, Colorado. 500-, 100-, 50-, 25-, and 10-year HEC-1 Model Study. Prepared by: Bullard, K.L. U.S. Bureau of Reclamation, Technical Service Center, Denver, Colorado

USDA. 1975. Soil Survey of Chaffee-Lake Area, Colorado. U.S. Department of Agriculture, Soil Conservation Service, Washington, D.C.

USDA. 1986. Urban Hydrology for Small Watersheds: Technical Release 55 (TR-55). U.S. Department of Agriculture, Natural Resources Conservation Service,

Conservation Engineering Division, Washington, D.C. (210-VI-TR-55, Second Ed., June 1986)

USDA. 1991. State soil geographic (STATSGO) data base: data use information. U.S. Department of Agriculture, National Resource Conservation Service, National Soil Survey Center, Washington, D.C. Miscellaneous Publication Number 1492. 110 p. (Revised: July 1994)

USDA, 1995. Soil survey geographic (SSURGO) data base: data use information. U.S. Department of Agriculture, National Resource Conservation Service, National Soil Survey Center, Washington, D.C. Miscellaneous Publication Number 1527. 110 p.

USEPA. 1987a. California Gulch Superfund Site Phase I Remedial Investigation Report. U.S. Environmental Protection Agency, Region VIII, Denver, Colorado. Dated: May 1987. (No report author or organization was listed. USEPA was the sponsor and assumed author. However, review of other documents suggests that this report may have been prepared for USEPA by CH2M-Hill.)

USEPA. 1987b. Appendices: California Gulch Superfund Site Remedial Investigation Report (Two Volumes). U.S. Environmental Protection Agency, Region VIII, Denver, Colorado. Dated: May 1987.

USEPA. 1987c. Interpretive Addenda: California Gulch Superfund Site Remedial Investigation Report. U.S. Environmental Protection Agency, Region VIII, Denver, Colorado. Dated: December 1987.

USEPA. 1996. Managing Environmental Problems at Inactive and Abondoned Metals Mine Sites. U.S. Environmental Protection Agency, Office of Research and Development, Washington, D.C. EPA/625/R-95/007 (October).

USEPA. 2003. Megasites: Presentation for the NACEPT Superfund Subcommittee. Prepared by: E. Southerland. U.S. Environmental Protection Agency, Washington, D.C. Obtained from: http://www.epa.gov/swerrims/docs/naceptdocs/megasites.pdf. Dated: November 5, 2003. Accessed: October 25, 2004.

van Rijn, L.C. 1984a. Sediment transport, part I: bed load transport. Journal of Hydraulic Engineering, 110(10):1431-1456.

van Rijn, L.C. 1984b. Sediment transport, part I: suspended load transport. Journal of Hydraulic Engineering, 110(11):1612-1638.

Velleux, M., Westenbroek, S., Ruppel, J., Settles, M., and Endicott, D. 2001. A User's Guide to IPX, the In-Place Pollutant Export Water Quality Modeling Framework, Version 2.7.4. U.S. Environmental Protection Agency, Office of Research and Development, National Health and Environmental Effects Research Laboratory, Mid-Continent Ecology Division, Large Lakes Research Station, Grosse Ile, Michigan. 179 pp. EPA/600/R-01/079.

Walsh. 1992. Soil Inventory and Map California Gulch Study Area Leadville, Colorado. Walsh and Associates, Inc., Boulder, Colorado. Prepared for: Glenn L. Anderson, ASARCO, Inc., Golden, Colorado. Dated: May 6, 1992.

Walsh. 1993. Final Smelter Remedial Investigation Report California Gulch Site Leadville, Colorado (Two Volumes). Walsh and Associates, Inc., Boulder, Colorado. Prepared for: Glenn Anderson, Environmental Manager ASARCO, Inc., Golden, Colorado. Dated: April 28, 1993.

WCC 1993a. Mine Waste Piles Remedial Investigation Report (Draft, Three Volumes). Woodward-Clyde Consultants, Denver, Colorado. Prepared for: ASARCO, Inc., Golden, Colorado. Dated: February 1993.

WCC. 1993b. Tailings Disposal Area Remedial Investigation Report (Draft, Four Volumes). Woodward-Clyde Consultants, Denver, Colorado. Prepared for: ASARCO, Inc., Golden, Colorado. Dated: February 1993.

WCC. 1993c. Surface Water Remedial Investigation Report (Draft, Three Volumes). Woodward-Clyde Consultants, Denver, Colorado. Prepared for: ASARCO, Inc., Golden, Colorado. Dated: February 1993.

WCC. 1993d. Aquatic Ecosystem Characterization Report (Draft). Woodward-Clyde Consultants, Denver, Colorado. Prepared for: ASARCO, Inc., Golden, Colorado. Dated: February 1993.

Wicks, J.M., and Bathurst, J.C. 1996. SHESED: a physically based, distributed erosion and sediment yield component for the SHE hydrological modeling system. Journal of Hydrology, 175(1-4):213-238.

Williams, J.R. 1975. Sediment routing for agricultural watersheds. Water Resources Bulletin, 11(5):965-974.

Woolhiser, D.A., Smith, R.E., and Goodrich, D.C. 1990. KINEROS, A Kinematic Runoff and Erosion Model: Documentation and User Manual. U.S. Department of Agriculture, Agriculture Research Service. ARS-77 (March, 1990).

Yang, C. T. 1973. Incipient motion and sediment transport. Journal of the Hydraulics Division, American Society of Civil Engineers, 99(HY10):1679-1704.

Yang, C. T. 1996. Sediment Transport: Practice and Theory. McGraw-Hill, Inc. New York, New York. 480 pp.

Zheng, C. and Wang, P.P. 1999. MT3DMS, A modular three-dimensional multi-species transport model for simulation of advection, dispersion and chemical reactions of contaminants in groundwater systems; documentation and user's guide. U.S. Army Engineer Research and Development Center Contract Report SERDP-99-1, Vicksburg, Mississippi. 202 p.

APPENDIX A: IMPLEMENTATION OF EROSION THRESHOLDS

OVERVIEW

One objective of this research is to apply a watershed-scale chemical transport model to a high mountain watershed. Conditions within such watersheds are highly variable and sediment transport relationships must be applied to a wide range of situations. Using the California Gulch watershed as an example, flows during runoff events are expected to range from near zero to more than 20 m^3/s. Surface and channel slopes are also highly variable and range from near zero to more than 60% (0.60 m/m). Sediment transport is expected to vary even more widely as particle sizes can range from boulders to clays. Unfortunately, no existing sediment transport relationships are applicable to this range of conditions without modification. As an outgrowth, overland and channel sediment transport relationships were reviewed to develop simple modifications that allow robust simulation of sediment transport across an extended range of flows, slopes, and particles sizes.

OVERLAND SEDIMENT TRANSPORT CAPACITY

As part of the development of the CASC2D (CASC2D-SED) watershed model (Johnson et al. 2000; Julien and Rojas, 2002), the Kilinc and Richardson (KR) (1973) relationship was used to simulate sediment transport for the overland plane. The KR relationship, as modified to include Universal Soil Loss Equation (USLE) soil, cover, and management factors, has been successfully used to describe the sediment transport capacity for sheet and rill flow erosion for soils with particles that range from sands to clays:

$$q_s = 1.542 \times 10^8 \, q^{2.035} S_f^{\,1.66} \hat{K} \hat{C} \hat{P} \qquad \text{(A.1)}$$

where:

q_s	=	total sediment transport capacity (kg/m s) [M/LT]
q	=	unit flow rate of water = $v_a \, h$ [L^2/T]
v_a	=	advective (flow) velocity of water [L/T]
h	=	surface water depth [L]
S_f	=	friction slope [dimensionless]

$\hat{K}$ = USLE soil erodibility factor [dimensionless]

$\hat{C}$ = USLE soil cover factor [dimensionless]

$\hat{P}$ = USLE soil management practice factor [dimensionless]

For situations where soils are fine-grained (and overland flows are relatively large), the KR relationship is a reasonable estimator of sediment transport rates as demonstrated by Johnson et al. (2000) and Julien and Rojas (2002). However, when extrapolating to a wider range of flows and particles sizes, the KR relationship requires modification.

Since it is applied to the aggregate soil matrix and is independent of grain size, the most significant limitation of the KR relationship is that the implicit threshold for incipient motion is zero. This means that the transport capacity of any particle within the matrix will always be greater than zero regardless of particle size or exerted shear stress as long as the unit flow and friction slope are non-zero. Although sediment transport by sheet flow is very efficient, an explicit erosion threshold is needed to account for situations where flow conditions are well below the incipient motion threshold of the aggregate soil or large particles within the soil matrix. As modified to include an explicit erosion threshold, the KR relationship becomes:

$$q_s = \begin{cases} 1.542 \times 10^{8} \left(q - q_c\right)^{2.035} S_f^{\,1.66} \hat{K}\hat{C}\hat{P} & for \quad q > q_c \\ 0 & for \quad q \le q_c \end{cases} \tag{A.2}$$

where: $(q - q_c)$ = excess unit flow [L^2/T]

q_c = critical unit flow for erosion (for aggregate the soil matrix) = $v_c h$ [L^2/T]

v_c = critical velocity for erosion [L/T]

Note that in their original analysis, Kilinc and Richardson (1973) present a number of alternative relationships where sediment transport capacities were expressed as functions of excess shear stress or excess stream power. Inclusion of an explicit erosion threshold

based on unit flow is not conceptually different than thresholds based on shear stress or stream power.

It is also worth noting that during the Kilinc and Richardson (1973) experiments with bare sand soils, applied shear stresses exceeded critical shear stresses for erosion in all cases. In some test cases applied shear stresses up to 20 times larger than critical shear stresses. Under these conditions, the excess unit flow would approximately equal the total unit flow, $(q - q_c) \approx q$, and inclusion of an explicit erosion threshold would not alter the KR relationship for it's original range of application. In other test cases the applied shear stress exceeded the critical threshold by only a small margin. Under those conditions excess unit flows could differ significantly from the total unit flow, $(q - q_c) << q$. Although the value of leading coefficient might differ, the form of the KR relationship would not change even when excess flows are less than total flows. When larger particles are present in the soil matrix, critical shear stresses would be larger and excess unit flows could also differ significantly from the total unit flow. For these conditions, an erosion threshold is needed to account for decreasing sediment transport capacity in order to permit extension of the KR relationship to larger particle sizes.

To illustrate the influence of the erosion threshold, transport capacities for soils with different particle diameters were computed from the KR relationship with and without a threshold and compared in Table A-1. In this analysis, unit flows vary from 0.003 to 0.018 m^2/s and slopes vary from 0.10 to 0.30 m/m. This range of unit flows and slopes is within the range of the original experimental conditions used by Kilinc and Richardson (1973). The particle sizes examined are 0.125 mm (fine sand), 2 mm (very fine gravel), and 16 mm (coarse gravel). Critical velocities for each case were computed from critical shear stress (τ_c) and Darcy-Weisbach fraction factor (f) values as reported by Kilinc and Richardson (1973). When the erosion threshold is neglected, non-zero sediment transport capacities are computed for each case. When the erosion threshold is included, sediment transport capacities are zero when flow conditions are below incipient motion thresholds for the particles. For particles in the range Kilinc and Richardson (1973) considered, inclusion of the erosion threshold reduces the transport capacities when the excess unit flow is close to the critical value. This introduces an underprediction bias into the results.

Table A-1. Comparison of overland sediment transport capacities.

d_p (mm)	q (m2/s)	S_0 (m/m)	h (m)	τ_c (Pa)	q_c (m2/s)	q_s No Threshold (kg/m/s)	q_s With Threshold (kg/m/s)
0.125	2.94E-05	0.1	4.83E-04	0.145	1.80E-05	0.0020	0.0003
	6.75E-05	0.1	7.33E-04		4.14E-05	0.0109	0.0016
	1.20E-04	0.1	9.25E-04		7.23E-05	0.0349	0.0053
	1.54E-04	0.1	9.87E-04		8.80E-05	0.0582	0.0103
	3.24E-05	0.2	3.32E-04		1.42E-05	0.0078	0.0024
	6.88E-05	0.2	4.79E-04		2.18E-05	0.0359	0.0165
	1.21E-04	0.2	5.54E-04		3.64E-05	0.1137	0.0550
	1.58E-04	0.2	6.25E-04		4.34E-05	0.1936	0.1004
	3.33E-05	0.3	3.00E-04		1.30E-05	0.0161	0.0059
	6.92E-05	0.3	4.02E-04		2.13E-05	0.0713	0.0338
	1.23E-04	0.3	4.81E-04		3.15E-05	0.2314	0.1272
	1.58E-04	0.3	5.49E-04		3.78E-05	0.3819	0.2188
2	2.94E-05	0.1	4.83E-04	1.26	5.31E-05	0.0020	0
	6.75E-05	0.1	7.33E-04		1.22E-04	0.0109	0
	1.20E-04	0.1	9.25E-04		2.13E-04	0.0349	0
	1.54E-04	0.1	9.87E-04		2.60E-04	0.0582	0
	3.24E-05	0.2	3.32E-04		4.18E-05	0.0078	0
	6.88E-05	0.2	4.79E-04		6.42E-05	0.0359	0.0001
	1.21E-04	0.2	5.54E-04		1.07E-04	0.1137	0.0014
	1.58E-04	0.2	6.25E-04		1.28E-04	0.1936	0.0064
	3.33E-05	0.3	3.00E-04		3.84E-05	0.0161	0
	6.92E-05	0.3	4.02E-04		6.27E-05	0.0713	0.0006
	1.23E-04	0.3	4.81E-04		9.27E-05	0.2314	0.0137
	1.58E-04	0.3	5.49E-04		1.11E-04	0.3819	0.0317
16	2.94E-05	0.1	4.83E-04	12	1.64E-04	0.0020	0
	6.75E-05	0.1	7.33E-04		3.77E-04	0.0109	0
	1.20E-04	0.1	9.25E-04		6.57E-04	0.0349	0
	1.54E-04	0.1	9.87E-04		8.01E-04	0.0582	0
	3.24E-05	0.2	3.32E-04		1.29E-04	0.0078	0
	6.88E-05	0.2	4.79E-04		1.98E-04	0.0359	0
	1.21E-04	0.2	5.54E-04		3.31E-04	0.1137	0
	1.58E-04	0.2	6.25E-04		3.95E-04	0.1936	0
	3.33E-05	0.3	3.00E-04		1.19E-04	0.0161	0
	6.92E-05	0.3	4.02E-04		1.93E-04	0.0713	0
	1.23E-04	0.3	4.81E-04		2.86E-04	0.2314	0
	1.58E-04	0.3	5.49E-04		3.44E-04	0.3819	0

However, this condition generally occurs when overland flow and sediment transport are at a minimum for all practical purposes. Where flow conditions increase beyond the erosion threshold, this bias becomes negligible. Further, this bias could be eliminated by adjusting (increasing) the leading coefficient of the KR relationship as previously noted.

CHANNEL SEDIMENT TRANSPORT CAPACITY

As part of the development of the CASC2D (CASC2D-SED) watershed model (Johnson et al. 2000; Rojas, 2002), the Engelund and Hansen (EH) (1967) relationship was used to simulate sediment transport for channel networks. The EH equation, originally developed for non-cohesive, sand bed channels with dunes, has been successfully applied to sediments with particles that range from sands to clays:

$$C_w = 0.05\left(\frac{G}{G-1}\right)\frac{v_a S_f}{\left[(G-1)g d_p\right]^{0.5}}\left[\frac{R_h S_f}{(G-1)d_p}\right]^{0.5} \qquad \text{(A.3)}$$

where: C_w = concentration of entrained sediment particles by weight at the transport capacity [dimensionless]

G = particle specific gravity [dimensionless]

v_a = advective (flow) velocity (in the down-gradient direction) [L/T]

S_f = friction slope [dimensionless]

R_h = hydraulic radius of flow [L]

g = gravitation acceleration [L/T^2]

d_p = particle diameter [L]

For situations where sediments are fine-grained (and non-cohesive), the EH relationship is a reasonable estimator of sediment transport rates as demonstrated by Julien (1998), Johnson et al. (2000) and Julien and Rojas (2002). However, when extrapolating to a wider range of particle sizes, the EH relationship requires modification.

Although grain size is a parameter and sediment transport capacities for larger particles decrease as particle size increases, the most significant limitation of the EH relationship is that the implicit threshold for incipient motion is zero. This means that the transport capacity of any particle will always be greater than zero regardless of particle size or exerted unit stream power as long as the flow velocity, friction slope, and hydraulic radius are non-zero. An explicit erosion threshold is needed to account for situations where flow conditions are well below the incipient motion threshold of the particles in the bed. Since the EH relationship is based on unit stream power considerations, a critical unit stream power erosion threshold is appropriate. As modified to include an explicit erosion threshold, the EH relationship becomes:

$$C_w = \begin{cases} 0.05\left(\frac{G}{G-1}\right)\frac{(v_a - v_c)S_f}{\left[(G-1)gd_p\right]^{0.5}}\left[\frac{R_h S_f}{(G-1)d_p}\right]^{0.5} & for \quad v_a > v_c \\ 0 & for \quad v_a \le v_c \end{cases} \tag{A.4}$$

where: v_c = critical velocity for erosion [L/T]

Note that many other channel sediment transport capacity relationships include explicit erosion thresholds. The sand and gravel sediment transport relationships described by Yang (1996) are of particular note because they include an identical erosion threshold.

To illustrate the influence of the erosion threshold, transport capacities for sediment with different particle diameters were computed from the EH relationship with and without a threshold and compared in Table A-2. In this analysis, flow velocities vary from 0.15 to 2.0 m/s and slopes vary from 0.001 to 0.30 m/m. This range of velocities and slopes is within the range found in high mountain watersheds such as California Gulch. The particle sizes examined are 2 mm (very fine gravel), 16 mm (coarse gravel) and 256 mm (large cobble, small boulder). Critical velocities for each case were computed from critical shear stress (τ_c), assuming a Manning n roughness factor value of 0.050. These flow and slope conditions are below the incipent motion threshold for many cases. When

Table A-2. Comparison of channel sediment transport capacities.

d_p *(mm)*	v_a *(m/s)*	S_f *(m/m)*	h *(m)*	τ_c *(Pa)*	v_c *(m/s)*	C_w *No Threshold (ppm)*	C_w *With Threshold (ppm)*
2	0.150	0.001	0.125	1.26	0.158	13	0
	0.300	0.010	0.061		0.141	562	298
	1.000	0.010	0.463		0.191	4621	3740
	2.000	0.010	3.000		0.227	15539	13778
	0.150	0.100	0.004		0.089	2236	908
	0.300	0.100	0.010		0.106	7500	4855
	1.000	0.100	0.066		0.143	61647	52834
	2.000	0.100	0.202		0.170	207301	189681
	0.150	0.300	0.002		0.078	7678	3707
	0.300	0.300	0.005		0.092	25818	17879
	1.000	0.300	0.028		0.125	212208	185762
	2.000	0.300	0.082		0.148	713595	660720
16	0.150	0.001	0.125	12	0.488	2	0
	0.300	0.010	0.061		0.435	70	0
	1.000	0.010	0.463		0.588	578	238
	2.000	0.010	3.000		0.699	1942	1263
	0.150	0.100	0.004		0.275	279	0
	0.300	0.100	0.010		0.327	938	0
	1.000	0.100	0.066		0.441	7706	4306
	2.000	0.100	0.202		0.525	25913	19115
	0.150	0.300	0.002		0.239	960	0
	0.300	0.300	0.005		0.285	3227	165
	1.000	0.300	0.028		0.385	26526	16324
	2.000	0.300	0.082		0.457	89199	68802
256	0.150	0.001	0.125	223	2.105	0	0
	0.300	0.010	0.061		1.877	4	0
	1.000	0.010	0.463		2.536	36	0
	2.000	0.010	3.000		3.015	121	0
	0.150	0.100	0.004		1.185	17	0
	0.300	0.100	0.010		1.408	59	0
	1.000	0.100	0.066		1.902	482	0
	2.000	0.100	0.202		2.262	1620	0
	0.150	0.300	0.002		1.032	60	0
	0.300	0.300	0.005		1.227	202	0
	1.000	0.300	0.028		1.658	1658	0
	2.000	0.300	0.082		1.971	5575	79
Note: computed assuming rectangular channel; width = 3m; Manning n = 0.05.							

the erosion threshold is neglected, non-zero sediment transport capacities are computed for each case. When the erosion threshold is included, sediment transport capacities are zero when flow conditions are below incipient motion thresholds for the particles. Further, transport capacities are also reduced for cases where flow conditions only exceed the motion threshold by a small margin.

DISCUSSION

Explicit erosion threshold are necessary when sediment transport rates are computed for materials that include a wide range of particle sizes. In situations where transport conditions are below the applicable incipient motion threshold, transport capacities should be zero. Similarly, when transport conditions are just above motion thresholds, sediment transport capacities should be less than when conditions are well above the thresholds. The erosion thresholds added to the KR and EH relationships address these physically-based considerations and allow convenient extensions of these relationships to a wider range of flow conditions and particle sizes.

No existing sediment transport relationships are designed to address the full spectrum of flow conditions and particle sizes. These extensions described are extrapolations outside the range for which the KR and EH relationships were first developed. Until improved sediment transport relationships specifically designed to address the range of conditions commonly found in many watershed become available, use of the erosion threshold-modified KR and EH relationships is a reasonable and convenient approach for model application.

APPENDIX B: TREX USER'S MANUAL

TREX Watershed Modeling Framework User's Manual:
Model Theory and Description

TABLE OF CONTENTS

LIST OF TABLES

LIST OF FIGURES

1.0 INTRODUCTION

TREX, the Two-dimensional Runoff, Erosion, and Export model, is generalized watershed rainfall-runoff, sediment transport, and contaminant transport modeling framework. This framework is based on the CASC2D watershed model (Julien et al. 1995; Johnson et al. 2000; Julien and Rojas, 2002) with chemical transport and fate processes from the USEPA WASP and IPX series of stream water quality models (Ambrose et al. 1993; Velleux et al. 1996; Velleux et al. 2001). TREX has three main components: 1) hydrology; 2) sediment transport; and 3) chemical transport and fate. Model theory and process descriptions are presented in Section 2.0. The numerical implementation of the process in the TREX model computer code is presented in Section 3.0. Descriptions of model input files are presented in Section 4.0. Descriptions of model output files are presented in Section 5.0.

The code has been subjected to extensive testing to ensure accuracy and error-free performance. However, it should be noted that (like all software) TREX is large and complex and coding errors (bugs) may still exist. It is also important to note that some aspects of the TREX framework and model source code are still under development. Where possible, developmental features and code are noted. Inclusion of these development portions of the framework is intended to demonstrate how the basic framework can be readily expanded to permit model use for an even wider range of conditions than can already be simulated. Nonetheless, users are advised to carefully review the TREX source code before use to ensure it performs correctly for any given application.

2.0 MODEL THEORY AND PROCESS DESCRIPTIONS

2.1 HYDROLOGIC PROCESSES

The main processes in the hydrologic submodel are: 1) rainfall and interception; 2) infiltration and transmission loss; 3) storage; and 4) overland and channel flow.

2.1.1 Rainfall and Interception

The hydrologic cycle begins with precipitation reaching the near surface of the land or water. Precipitation includes both rainfall and snowfall. Since snowfall can be represented as an equivalent depth (or volume) of water, it may be expressed as equivalent precipitation. The gross volume of water reaching the near surface is:

$$\frac{\partial V_g}{\partial t} = i_g A_s \tag{2.1}$$

where: V_g = gross precipitation water volume [L^3]

i_g = gross precipitation rate [L/T]

A_s = surface area over which precipitation occurs [L^3]

t = time [T]

Interception is the reduction in the volume of gross precipitation due to water retention by vegetative cover. As precipitation falls to the surface, a portion of the gross precipitation at the surface may contact vegetative canopy and may be held on foliage by surface tension (Eagleson, 1970). Much of the precipitation falling during the early period of an event may be stored on vegetative surfaces (Linsley et al. 1982). Intercepted water can return to the atmosphere by evaporation. Alternatively, intercepted water may reach the land surface when the force of gravity acting of water drops exceeds the surface tension force holding water to plant surfaces. Conceptually, interception may be represented as a volume. The net rainfall volume equals the gross rainfall volume minus the volume lost to interception (Linsley et al. 1982):

$$V_i = \left(S_i + Et_R\right)A_s \tag{2.2}$$

$$\begin{aligned} V_n &= V_g - V_i \qquad for: V_g > V_i \\ V_n &= 0 \qquad\qquad for: V_g \le V_i \end{aligned} \tag{2.3}$$

where: V_i = interception volume [L^3]

S_i = interception capacity of projected canopy per unit area [L^3/L^2]

E = evaporation rate [L/T]

t_R = precipitation event duration [T]

V_n = net precipitation volume reaching the surface [L^3]

Note that when the cumulative gross rainfall volume that occurs during an event is less than the interception volume, the net rainfall volume (or depth) reaching the land surface is zero. For single storm events, recovery of interception volume by evaporation can be neglected. The net precipitation volume may also be expressed as a net (effective) precipitation rate:

$$i_n = \frac{1}{A_s}\frac{\partial V_n}{\partial t} \tag{2.4}$$

where: i_n = net (effective) rainfall rate at the surface [L/T]

2.1.2 Infiltration and Transmission Loss

Infiltration is the downward transport of water from the surface to the subsurface. The rate at which infiltration occurs may be affected by several factors including hydraulic conductivity, capillary action and gravity (percolation) as the soil matrix reaches saturation. Many relationships have been used to describe infiltration including expressions presented by Green and Ampt (1911), Richards (1931), Philip (1957), and Smith and Parlange (1978). The Green and Ampt relationship is often used because of its ease of application. This relationship assumes a sharp wetting front exists between the infiltration zone and soil at the initial water content (piston flow) and that the length of the wetted zone increases as infiltration progresses. Neglecting the depth of ponding at the surface (i.e. assuming that the pressure head is much smaller than the suction head), the general equation showing the Green and Ampt relationship can be expressed as (Li et al. 1976; Julien, 2002):

$$f = K_h\left(1 + \frac{H_c(1 - S_e)\theta_e}{F}\right) \tag{2.5}$$

where: f = infiltration rate [L/T]

K_h = effective hydraulic conductivity [L/T]

H_c = capillary pressure (suction) head at the wetting front [L]

θ_e = effective soil porosity = (φ-θ_r) [dimensionless]

φ = total soil porosity [dimensionless]

θ_r = residual soil moisture content [dimensionless]

S_e = effective soil saturation [dimensionless]

F = cumulative (total) infiltrated water depth [L]

Similar to infiltration in overland areas, water in stream channels may be lost to the subsurface by transmission loss. The rate at which transmission loss occurs in a channel may be affected by several factors, particularly hydraulic conductivity. For ephemeral streams, capillary suction head may be significant when stream sediments are unsaturated. Relationships to describe the volume of transmission loss are presented by Lane (1983). Abdullrazzak and Morel-Seytoux (1983) and Freyberg (1983) use the Green and Ampt (1911) relationship to assess transmission loss. Following the form of the Green and Ampt relationship and accounting for the depth of (ponded) water in the stream channel (hydrostatic head), the transmission loss rate may be expressed as:

$$t_l = K_h\left(1 + \frac{(H_w + H_c)(1 - S_e)\theta_e}{T}\right) \tag{2.6}$$

where:
- t_l = transmission loss rate [L/T]
- K_h = effective hydraulic conductivity [L/T]
- H_w = hydrostatic pressure head of water (depth of water in channel) [L]
- H_c = capillary pressure (suction) head at the wetting front [L]
- θ_e = effective sediment porosity = (φ-θ_r) [dimensionless]
- φ = total sediment porosity [dimensionless]
- θ_r = residual sediment moisture content [dimensionless]
- S_e = effective sediment saturation [dimensionless]
- T = cumulative (total) depth of water transported by transmission loss [L]

For single storm events, recovery of infiltration capacity by evapotranspiration and percolation can be neglected. Similarly, recovery of transmission loss capacity by evaporation or other processes can also be neglected for single storm events.

2.1.3 Storage

Water may be stored in depressions on the land surface as small, discontinuous surface pools. Precipitation retained in such small surface depressions is depression storage (Linsley et al. 1982). Water in depression storage may be conceptualized as a volume or, when normalized by surface area, a depth. In effect, the depression storage depth represents a threshold limiting the occurrence of overland flow. When the water depth is below the depression storage threshold, overland flow is zero. Note that water in depression storage is still subject to infiltration and evaporation.

Similar to depression storage in overland areas, water in channels may be stored in depressions in the stream bed (as the channel water depth falls below some critical level, flow is zero and the water surface discontinuous but individual pools of water remain).

This mechanism is termed dead storage. Note that water in dead storage is still subject to transmission loss and evaporation.

For single storm events, recovery of depression storage volume by evaporation can be neglected. Similarly, recovery of dead storage volume by evaporation can also be neglected for single storm events.

2.1.4 Overland and Channel Flow

Overland flow can occur when the water depth on the overland plane exceeds the depression storage threshold. Overland flow is governed by conservation of mass (continuity) and conservation of momentum. The two-dimensional (vertically integrated) continuity equation for gradually-varied flow over a plane in rectangular (x, y) coordinates is (Julien et al. 1995; Julien, 2002):

$$\frac{\partial h}{dt} + \frac{\partial q_x}{dx} + \frac{\partial q_y}{dy} = i_n - f + W = i_e \tag{2.7}$$

where: h = surface water depth [L]

q_x , q_y = unit discharge in the x- or y-direction = Q_x/B_x , Q_y/B_y [L^2/T]

Q_x , Q_y = flow in the x- or y-direction [L^3/T]

B_x , B_y = flow width in the x- or y-direction [L]

W = unit discharge from/to a point source/sink [L^2/T]

i_e = excess precipitation rate [L/T]

Momentum equations for the x- and y-directions may be derived by relating the net forces per unit mass to flow acceleration (Julien et al. 1995; Julien, 2002). In full form, with all terms retained, these equations can be expressed in dimensionless form as the friction slope and are known as the Saint Venant equations. The full Saint Venant equations may be simplified by neglecting small terms that describe the local and convective acceleration components of momentum, resulting in the diffusive wave approximation (of the friction slope) for the x- and y-directions:

$$S_{fx} = S_{0x} - \frac{\partial h}{dx} \tag{2.8}$$

$$S_{fy} = S_{0y} - \frac{\partial h}{dy} \tag{2.9}$$

where: S_{fx} , S_{fy} = friction slope (energy grade line) in the x- or y-direction [dimensionless]

S_{0x} , S_{0x} = ground surface slope in the x- or y-direction [dimensionless]

To solve the overland flow equations for continuity and momentum, five hydraulic variables must be defined in terms of a depth-discharge relationship to describe flow resistance. Assuming that flow is turbulent and resistance can be described using the Manning formulation (in S.I. units), the depth-discharge relationships are (Julien et al. 1995; Julien, 2002):

$$q_x = \alpha_x h^{\beta} \tag{2.10}$$

$$q_y = \alpha_y h^{\beta} \tag{2.11}$$

$$\alpha_x = \frac{S_{fx}^{1/2}}{n} \tag{2.12}$$

$$\alpha_y = \frac{S_{fy}^{1/2}}{n} \tag{2.13}$$

where: α_x , α_y = resistance coefficient for flow in the x- or y-direction [$L^{1/3}/T$]

β = resistance exponent = 5/3 [dimensionless]

n = Manning roughness coefficient [$T/L^{1/3}$]

Similarly, channel flow can occur when the water depth in the channel exceeds the dead storage threshold. Channel flow is also governed by conservation of mass (continuity) and conservation of momentum. At the watershed it is convenient to represent channel flows in a watershed as one-dimensional (along the channel in the down-gradient direction). The one-dimensional (laterally and vertically integrated) continuity equation for gradually-varied flow along a channel is (Julien et al. 1995; Julien, 2002):

$$\frac{\partial A_c}{dt} + \frac{\partial Q}{dx} = q_l \tag{2.14}$$

where: A_c = cross sectional area of flow [L^2]

Q = total discharge [L^3/T]

q_l = lateral flow into or out of the channel [L^2/T]

Based on the momentum equation for the down-gradient direction and again neglecting terms for local and convective acceleration, the diffusive wave approximation may be used for the friction slope (see Eq. 2.7). To solve the channel flow equations for continuity and momentum, the Manning relationship may be used to describe flow resistance (Julien et al. 1995; Julien, 2002):

$$Q = \frac{1}{n} A_c R_h^{2/3} S_f^{1/2} \tag{2.15}$$

where: R_h = hydraulic radius of flow = A_c/P [L]

P = wetted perimeter of channel flow [L]

2.2 SEDIMENT TRANSPORT PROCESSES

The movement of water across the overland plane or through a channel network can transport and redistribute soil and sediment throughout a watershed. The main processes in the sediment transport submodel are: 1) advection-diffusion; 2) erosion; 3) deposition; and 4) bed processes (bed elevation dynamics).

2.2.1 Advection-Diffusion

For the overland plane in two-dimensions (vertically integrated), the concentration of particles in a flow is governed by conservation of mass (sediment continuity) (Julien, 1998):

$$\frac{\partial C_s}{dt} + \frac{\partial \hat{q}_{tx}}{dx} + \frac{\partial \hat{q}_{ty}}{dy} = \hat{J}_e - \hat{J}_d + \hat{W}_s = \hat{J}_n \tag{2.16}$$

where: C_s = concentration of sediment particles in the flow [M/L^3]

$\hat{q}_{tx}$, $\hat{q}_{ty}$ = total sediment transport areal flux in the x- or y-direction [M/L^{2}T]

$\hat{J}_e$ = sediment erosion volumetric flux [M/L^{3}T]

$\hat{J}_d$ = sediment deposition volumetric flux [M/L^{3}T]

$\hat{W}_s$ = sediment point source/sink volumetric flux [M/L^{3}T]

$\hat{J}_n$ = net sediment transport volumetric flux [M/L^{3}T]

The total sediment transport flux in any direction has three components, advective, dispersive (mixing), and diffusive, and may be expressed as (Julien, 1998):

$$\hat{q}_{tx} = v_x C_s - (R_x + D)\frac{\partial C_s}{dx} \tag{2.17}$$

$$\hat{q}_{ty} = v_y C_s - (R_y + D)\frac{\partial C_s}{dy} \tag{2.18}$$

where: v_x , v_y = flow (advective) velocity in the x- or y-direction [L/T]

R_x , R_y = dispersion (mixing) coefficient the x- or y-direction [L^2/T]

D = diffusion coefficient [L^2/T]

$v_x C_s$ = advective flux in the x-direction = J_x [M/L^2T]

$v_y C_s$ = advective flux in the y-direction = J_y [M/L^2T]

$R_x \frac{\partial C_s}{dx}$ = dispersive flux the x-direction [M/L^2T]

$R_y \frac{\partial C_s}{dy}$ = dispersive flux the y-direction [M/L^2T]

$D \frac{\partial C_s}{dx}$ = diffusive flux the x-direction [M/L^2T]

$D \frac{\partial C_s}{dy}$ = diffusive flux the y-direction [M/L^2T]

The dispersive and diffusive flux terms in Eqs. (2.16) and (2.17) are negatively signed to indicate that mass is transported in the direction of decreasing concentration gradient. Note that both dispersion and diffusion are represented in forms that follow Fick's Law. However, dispersion represents a relatively rapid turbulent mixing process while diffusion represents a relatively slow a Brownian motion, random walk process (Holley, 1969). In turbulent flow, dispersive fluxes are typically several orders of magnitude larger than diffusive fluxes. Further, flow conditions for intense precipitation events are usually advectively dominated as dispersive fluxes are typically one to two orders smaller than advective fluxes. As a result, both the dispersive and diffusive terms may be neglected.

Similarly, for the channel plane in one-dimension (laterally and vertically integrated), the concentration of particles in a flow is governed by conservation of mass (sediment continuity) (Julien, 1998):

$$\frac{\partial C_s}{dt} + \frac{\partial \hat{q}_{tx}}{dx} = \hat{J}_e - \hat{J}_d + \hat{W}_s = \hat{J}_n \tag{2.19}$$

Individual terms for the channel advection-diffusion equation are identical to those defined for the overland plane. Similarly, the diffusive flux term can be neglected. The dispersive flux is expected to be larger than to the corresponding term for overland flow. However, the channel dispersive flux still may be neglected relative to the channel advective flux during intense runoff events.

2.2.2 Erosion

Erosion is the entrainment (gain) of material from a bottom boundary into a flow by the action of water. The erosion flux may be expressed as a mass rate of particle removal

from the boundary over time and the concentration (bulk density) of particles at the boundary:

$$J_e = v_r C_{sb} \tag{2.20}$$

where: J_e = erosion flux [M/L^{2}T]

v_r = resuspension (erosion) velocity [L/T]

C_{sb} = concentration of sediment at the bottom boundary (in the bed) [M/L^3]

Entrained material may be transported as either bedload or suspended load. However, for overland sheet and rill flows, bedload transport by rolling and sliding may predominate as the occurrence of saltation and full suspension may be limited (Julien and Simons, 1985). Entrainment rates may be estimated from site-specific erosion rate studies or, in general, from the difference between sediment transport capacity and advective fluxes:

$$v_r = \frac{J_c - v_a C_s}{\rho_b} \qquad for: J_c > v_a C_s$$

$$v_r = 0 \qquad for: J_c \le v_a C_s \tag{2.21}$$

where: v_r = resuspension (erosion) velocity [L/T]

J_c = sediment transport capacity areal flux [M/L^{2}T]

v_a = advective (flow) velocity (in the x- or y-direction) [L/T]

C_s = concentration of entrained sediment in the flow [M/L^3]

ρ_b = bulk density of bed sediments [M/L^3]

In the overland plane, particles can be detached from the bulk soil matrix by raindrop (splash) impact and entrained into the flow by hydraulic action when the exerted shear stress exceeds the stress required to initiate particle motion (Julien and Frenette, 1985; Julien and Simons, 1985). The overland erosion process is influenced by many factors including precipitation (rainfall) intensity and duration, runoff length, surface slope, soil characteristics, vegetative cover, exerted shear stress, and particle size. Raindrop impact may generally be neglected when flow depths are greater than three times the average raindrop diameter (Julien, 2002). Julien and Simons (1985) summarize numerous relationships to describe the transport capacity of overland flow. Julien (1998, 2002) recommends a modified form of the Kilinc and Richardson (1973) relationship that includes soil erodibility, cover, and management practice terms from the Universal Soil Loss Equation (USLE) (Meyer and Weischmeier, 1969) to estimate the total overland sediment transport capacity (for both the x- and y-directions):

$$q_s = 1.542 \text{ x} 10^8 \, q^{2.035} S_f^{\,1.66} \hat{K} \hat{C} \hat{P} \tag{2.22}$$

$$J_c = \frac{q_s}{B_e} \tag{2.23}$$

where:
- q_s = total sediment transport capacity (kg/m s) [M/LT]
- q = unit flow rate of water = $v_a \, h$ [L^2/T]
- S_f = friction slope [dimensionless]
- $\hat{K}$ = USLE soil erodibility factor [dimensionless]
- $\hat{C}$ = USLE soil cover factor [dimensionless]
- $\hat{P}$ = USLE soil management practice factor [dimensionless]
- B_e = width of eroding surface in flow direction [L]

In channels, sediment particles can be entrained into the flow when the exerted shear stress exceeds the stress required to initiate particle motion. For non-cohesive particles, the channel erosion process is influenced by factors such as particle size, particle density and bed forms. For cohesive particles, the erosion process is significantly influenced by inter-particle forces (such as surface charges that hold grains together and form cohesive bonds) and consolidation. Total (bed material) load transport capacity relationships account for the both bedload and suspended load components of sediment transport. Yang (1996) and Julien (1998) provide summaries of numerous total load transport relationships. The Engelund and Hansen (1967) relationship is considered a reasonable estimator of the total load:

$$C_w = 0.05 \left(\frac{G}{G-1} \right) \frac{v_a S_f}{\left[(G-1) g d_p \right]^{0.5}} \left[\frac{R_h S_f}{(G-1) d_p} \right]^{0.5} \tag{2.24}$$

$$J_c = \frac{v_a C_t}{A_c} \tag{2.25}$$

where:
- C_w = concentration of entrained sediment particles by weight at the transport capacity [dimensionless]
- G = particle specific gravity [dimensionless]
- v_a = advective (flow) velocity (in the down-gradient direction) [L/T]
- S_f = friction slope [dimensionless]
- R_h = hydraulic radius [L]
- g = gravitation acceleration [L/T^2]

d_p = particle diameter [L]

A_c = cross sectional area of flow [L^2]

C_t = concentration of entrained sediment particles at the transport capacity

= $\frac{10^6 G C_w}{G + (1 - G) C_w}$ (g/m^3) [M/L^3]

It is worth noting that one feature common to both the Kilinc and Richardson (1973) and Engelund and Hansen (1967) relationships is that the implicit threshold for incipient motion is zero. This means that the transport capacity of any particle will always be greater than zero, regardless of particle size or the exerted shear stress, as long as the unit flow or flow velocity and friction slope are non-zero. This can lead to inconsistent results when erosion rates are computed from sediment transport capacities. The inferred erosion rate will almost always be greater than zero because the difference between the transport capacity and advective flux will nearly always be greater than zero. Consequently, a non-zero erosion rate can be computed even when the exerted shear stress is far less than the incipient motion threshold for the material. To address this limitation, an incipient motion threshold can be added to the modified Kilinc and Richardson (1973) and Engelund and Hansen (1967) relationships.

$$q_s = 1.542 \times 10^8 (q - q_c)^{2.035} S_f^{1.66} \hat{K} \hat{C} \hat{P} \tag{2.26}$$

$$C_w = 0.05 \left(\frac{G}{G-1} \right) \frac{(v_a - v_c) S_f}{\left[(G-1) g d_p \right]^{0.5}} \left[\frac{R_h S_f}{(G-1) d_p} \right]^{0.5} \tag{2.27}$$

where: q_c = critical unit flow for erosion (for the aggregate soil matrix) [L^2/T]

= $v_c h$

v_c = critical velocity for erosion [L/T]

h = surface water depth [L]

2.2.3 Deposition

Deposition is the sedimentation (loss) of material entrained in a flow to a bottom boundary by gravity. The deposition process is influenced by many factors including particle density, diameter, and shape, and fluid turbulence. The deposition flux may be expressed as a mass rate of particle removal from the water column over time and the concentration of sediment particles that are entrained in the flow:

$$J_d = v_{se} C_s \tag{2.25}$$

where: J_d = deposition flux [M/L^2/T]

v_{se} = effective settling (deposition) velocity [L/T]

C_s = concentration of sediment particles in the flow [M/L^3]

Coarse particles (>62 μm) are typically inorganic and non-cohesive and generally have large settling velocities under quiescent conditions. Numerous empirical relationships to describe the non-cohesive particle settling velocities are available. Summaries of relationships and settling velocities are presented by Yang (1996) and Julien (1998). For non-cohesive (fine sand) particles with diameters from 62 μm to 500 μm, the settling velocity can be computed as (Cheng, 1997):

$$v_s = \frac{\nu}{d_p}\left[\left(25 + 1.2{d_*}^2\right)^{0.5} - 5\right]^{1.5} \tag{2.26}$$

$$d_* = d_p\left[\frac{(G-1)g}{\nu^2}\right]^{1/3} \tag{2.27}$$

where: v_{sq} = quiescent settling velocity [L/T]

ν = kinematic viscosity of water [L^2/T]

d_p = particle diameter [L]

d_* = dimensionless particle diameter [dimensionless]

G = specific gravity [dimensionless]

g = gravitational acceleration [L/T^2]

Medium particles (10 μm < d_p <62 μm) can vary in character. Inorganic particles may behave in a non-cohesive manner. In contrast, organic particles (potentially including particles with organic coatings) may behave in a cohesive manner. Fine particles (<10 μm) often behave in a cohesive manner. If behavior is largely non-cohesive, settling velocities may be estimated as described by Julien (1998). If the behavior is cohesive, flocculation may occur. Floc size and settling velocity depend on the conditions under which the floc was formed (Burban et al. 1990; Krishnappan, 2000; Haralampides et al. 2003). When flocculation occurs, settling velocities of cohesive particles can be approximated by relationship of the form (Burban et al. 1990):

$$v_s = a{d_f}^m \tag{2.28}$$

where: v_s = floc settling velocity (cm/s) [L/T]

a = experimentally determined constant = 8.4 x 10^{-3}

d_f = median floc diameter (μm) [L]

m = experimentally determined constant = 0.024

However, depending on fluid shear, particle surface charge, and other conditions, fine particles may not flocculate. Under conditions which limit floc formation, fine particles can have very small, near zero settling velocities.

As a result of turbulence and other factors, not all particles settling through a column of flowing water will necessarily reach the sediment-water interface or be incorporated into the sediment bed (Krone, 1962). Beuselinck et al. (1999) suggest this process also occurs for the overland plane. As a result, effective settling velocities in flowing water can be much less than quiescent settling velocities. The effective settling velocity of a particle can be described as a reduction in the quiescent settling velocity by the probability of deposition (Krone 1962; Mehta et al. 1989):

$$v_{se} = P_{dep} v_s \tag{2.29}$$

where: v_{se} = effective settling velocity [L/T]

v_s = "quiescent" settling velocity [L/T]

P_{dep} = Probability of deposition [dimensionless]

The probability of deposition varies with shear stress near the sediment bed and particle size. As particle size decreases or shear stress increases, the probability of deposition decreases. For non-cohesive particles, the probability of deposition has been described as a function of bottom shear stress (Gessler, 1965; Gessler 1967; Gessler, 1971):

$$P_{dep} = P = \frac{1}{\sqrt{2\pi}} \int_{-\infty}^{Y} e^{-0.5x^2} dx \tag{2.30}$$

$$Y = \frac{1}{\sigma}\left(\frac{\tau_{cd,n}}{\tau} - 1\right) \tag{2.31}$$

where: P = probability integral for the Gaussian distribution

σ = experimentally determined constant = 0.57

τ_0 = bottom shear stress (M/LT^2)

$\tau_{cd,n}$ = critical shear stress for deposition of non-cohesive particles, defined as the shear stress at which 50% of particles deposit (M/LT^2)

For coarse particles, the critical shear stress for deposition can be computed from a force balance following the method of van Rijn (1984a,b) as summarized by QEA (1999), with

the particle diameter equal to the mean diameter for a range of particle size in a class (i.e. $d_p = d_{50}$).

For cohesive particles, the probability of deposition has also been described as a function of bottom shear stress (Partheniades, 1992):

$$P_{dep} = 1 - P = 1 - \frac{1}{\sqrt{2\pi}} \int_{-\infty}^{Y} e^{-0.5x^2} dx \tag{2.32}$$

$$Y = \frac{1}{\sigma} \ln \left[0.25 \left(\frac{\tau_{cd,c}}{\tau} - 1 \right) e^{1.27 \tau_{cd}} \right] \tag{2.33}$$

where: σ = experimentally determined constant = 0.49

τ_0 = bottom shear stress (M/LT^2)

$\tau_{cd,c}$ = critical shear stress for deposition of cohesive particles, defined as the shear stress at which 100% of the particles deposit (M/LT^2)

The probability integrals in Equations 3.11 and 3.13 can be approximated as (Abramowitz and Stegun, 1972):

$$\begin{aligned} P &= 1 - F(Y)\left(0.4362X - 0.1202X^2 + 0.9373X^3\right) \quad \text{for } Y > 0 \\ P &= 1 - P(|Y|) \quad \text{for } Y < 0 \end{aligned} \tag{2.34}$$

$$F(Y) = \frac{1}{\sqrt{2\pi}} e^{-0.5Y^2} \tag{2.35}$$

$$X = (1 + 0.3327Y)^{-1} \tag{2.36}$$

2.2.4 Soil and Sediment Bed Processes

In response to the difference between bedform transport, erosion, and deposition fluxes, the net addition (burial) or net loss (scour) of particles from the bed causes the bed surface elevation to increase or decrease. The rise or fall of the bed surface is governed by the sediment continuity (conservation of mass) equation, various forms of which are attributed to Exner (1925) (see Simons and Sentürk, 1992). Julien (1998) presents a derivation of the bed elevation continuity equation for an elemental control volume that includes vertical and lateral (x- and y-direction) transport terms. Neglecting bed consolidation and compaction processes, and assuming that only vertical mass transport processes (erosion and deposition) occur, the sediment continuity equation for the change in elevation of the soil or sediment bed surface may be expressed as:

$$\rho_b \frac{\partial z}{dt} + v_{se} C_s - v_r C_{sb} = 0 \qquad (2.37)$$

where: z = elevation of the soil surface or sediment bed [L]

ρ_b = bulk density of soil or bed sediments [M/L^3]

v_{se} = effective setting (deposition) velocity [L/T]

C_s = concentration of sediment particles in the water column [M/L^3]

v_{se} = resuspension (erosion) velocity [L/T]

C_{sb} = concentration of sediment particles in the soil or sediment bed [M/L^3]

2.3 CHEMICAL TRANSPORT AND FATE PROCESSES

The movement of water and sediment across the overland plane or through a channel network can also transport and redistribute chemicals throughout a watershed. On the land surface and in channel environments, chemical typically exist in three phases: 1) dissolved in water, 2) bound with dissolved organic compounds (DOC) or other binding ligands or complexation agents; and 3) particle-associated. The pathways that affect chemical movements and interactions in the environment depend on the phase in which the chemicals are present. The main processes in the chemical transport and fate submodel are: 1) chemical partitioning and phase distribution; 2) advection-diffusion; 3) erosion; 4) deposition; 5) infiltration; and 6) mass transfer and transformation processes (chemical reactions).

2.3.1 Chemical Partitioning and Phase Distribution

Many chemicals are hydrophobic and readily partition between dissolved, bound, and particle-associated (particulate) phases. Partitioning to bound and particulate phases is a function of chemical affinity for surfaces and ion exchange (ionic chemicals) or organic carbon (neutral chemicals) (Karichoff et al. 1979; Schwarzenbach et al. 1993; Chapra, 1997). The equilibrium distribution of chemicals between phases is described by the partition (distribution) coefficient, concentration and binding effectiveness of binding agents, and the concentration of particles or organic carbon. Mechanistically, partitioning is a function of the equilibrium rate at which chemicals sorb (move out of the dissolved phase) and desorb (move back into the dissolved phase). If the rates at which chemicals partition are much faster than the rates of other mass transfer processes, local equilibrium is assumed to exist and the dissolved, bound and particulate phase chemical concentrations can be expressed in terms of the total chemical concentration (sum of phases) (Thomann and Mueller, 1987; Chapra, 1997).

Chemicals may partition to all particle types (sorbents) present in a solution. The equilibrium partition (distribution) coefficient to any particle is defined as (Thomann and Mueller, 1987):

$$\P_{p_n} = K_{p_n} = f_{oc\,n} K_{oc} \tag{2.38}$$

where: $\P_{p_n}$ = equilibrium partition (distribution) coefficient for particle "*n*" [L^3/M]

K_{p_n} = equilibrium partition (distribution) coefficient for particle "*n*" [L^3/M]

f_{oc_n} = fraction organic carbon of particle "*n*" [dimensionless]

K_{oc} = organic carbon normalized partition coefficient [L^3/M]

For particulate phases in the water column, equilibrium partition coefficients vary with the concentration of suspended solids as a result of particle interactions. Particle-dependent partition coefficients are described as (DiToro, 1985):

$$\P_{px_n} = \frac{\P_{p\,n}}{1 + \sum_{n=1}^{N} m_n \P_{p\,n} / \nu_x} = \frac{f_{oc} K_{oc}}{1 + \sum_{n=1}^{N} f_{oc\,n} m_n K_{oc} / \nu_x} \tag{2.39}$$

where: $\P_{px_n}$ = particle-dependent partition coefficient [L^3/M]

n = particle index = 1, 2, 3, etc.

m_n = concentration of particle "*n*" [M/L^3]

ν_x = particle interaction parameter [dimensionless]

For the bound phase, the equilibrium binding coefficient is defined as:

$$\P_b = D_e f_{oc\,D} K_{oc} \tag{2.40}$$

where: $\P_b$ = equilibrium binding coefficient [L^3/M]

f_{oc_D} = fraction organic carbon of DOC [dimensionless]

D_e = DOC-binding effectiveness coefficient [dimensionless]

Conceptually, dissolved organic compounds are composed entirely of organic carbon (f_{oc_D} = 1). Under those conditions, the equilibrium binding coefficient would equal the organic carbon partition coefficient. However, at least for neutral organic chemical binding in some surface waters (the Great Lakes), observed binding coefficients were up to 100 times smaller than K_{oc} (Eadie et al. 1990; Eadie et al. 1992). Also, in sediment observed binding coefficients were up to 10 times smaller than K_{oc} (Landrum et al. 1985; Landrum et al. 1987; Capel and Eisenreich, 1990). One explanation for decreased binding efficiency is photobleaching of DOC by ultraviolet (UV-B) radiation (Kashian et al. 2004).

The equilibrium partition coefficient can be used to describe the fraction of the total chemical that is associated with each phase as follows (Thomann and Mueller, 1987; Chapra, 1997):

$$f_d = \frac{1}{1 + D_{oc} \P_b + \sum_{n=1}^{N} m_n \P_{px_n}} \tag{2.41}$$

$$f_b = \frac{D_{oc} \P_b}{1 + D_{oc} \P_b + \sum_{n=1}^{N} m_n \P_{px_n}} \tag{2.42}$$

$$f_{p_n} = \frac{m_n \P_{px_n}}{1 + D_{oc} \P_b + \sum_{n=1}^{N} m_n \P_{px_n}} \tag{2.43}$$

$$f_d + f_b + \sum_{n=1}^{N} f_{p_n} = 1 \tag{2.44}$$

where: f_d = fraction of the total chemical in the dissolved phase [dimensionless]

f_b = fraction of the total chemical in the DOC-bound phase [dimensionless]

n = particle index = 1, 2, 3, etc.

f_{p_n} = fraction of the total chemical in the particulate phase associated with particle "n" [dimensionless]

Equations 2.41-2.43 are presented for the water column. For the sediment bed, $\P_{p_n}$ is used in place of $\P_{px_n}$.

Lu and Allen (2001) present extensive assessments of copper partitioning onto suspended particulate matter in river water. They performed a series of adsorption experiments and found that many factors may influence the partition coefficient including pH, total suspended solids concentration, total copper concentration, dissolved organic matter, particulate organic matter, hardness, and ionic strength. Their results suggest that adsorption to organic matter binding sites in aqueous and solid phases plays the biggest role in controlling the extent of copper partitioning. However, Lu and Allen (2001) found that the most significant environmental factors affecting the value of the partition coefficient were the total suspended solids (TSS) concentration and pH. Graphs showing variation of the copper partition coefficient as a function of key environmental conditions are presented in Figure 2-1. Holm et al. (2003) found that cadmium partitioning, like copper, was highly correlated with soil cation exchange capacity, which is largely determined by organic carbon and clay content. Also, cadmium partition coefficients

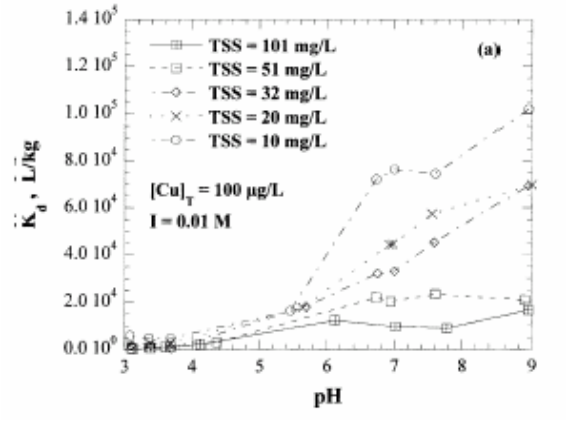

a) K_d as a function of pH and TSS concentration

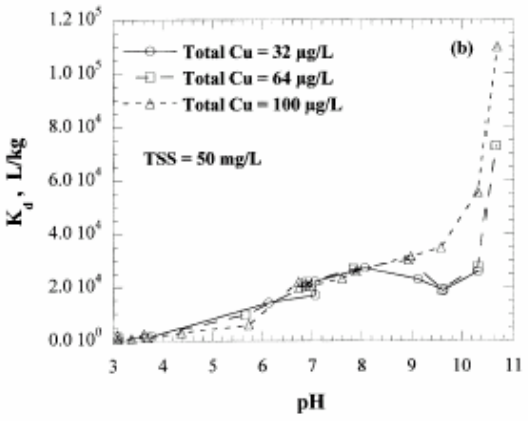

b) K_d as a function of pH and copper concentration

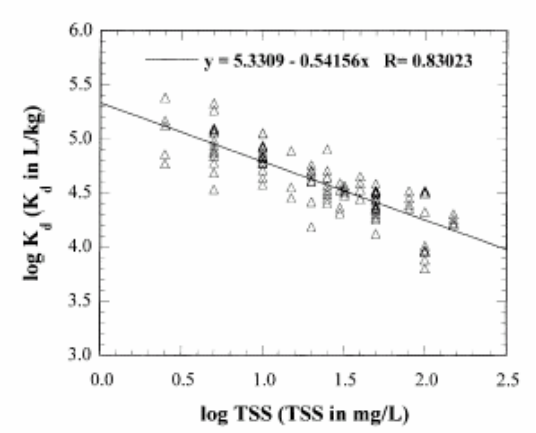

c) K_d as a function of TSS concentration

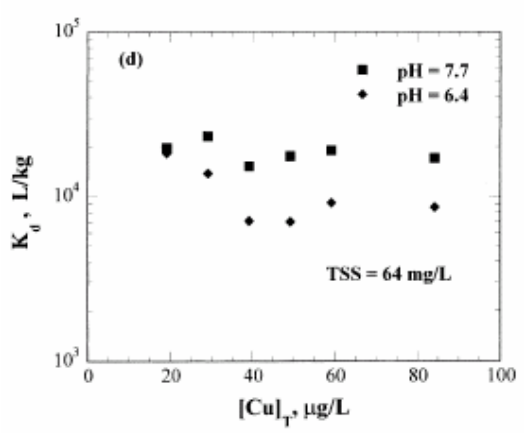

d) K_d as a function of copper concentration and pH

Figure 2-1. Copper partitioning vs. environmental conditions (Lu and Allen, 2001).

were found to decrease by an order of magnitude as soil pH decreased from 6.7 to 5.3. Similar behavior is also expected for zinc because, like copper and cadmium, it is divalent. Sauvé et al. (2000, 2003) noted that distribution coefficients for cadmium, copper, and zinc and other divalent metals are sensitive to pH. Sauvé et al. (2003) reported distribution coefficients (log K_d) values for acidic (pH 4.4) soils were low: Cd log K_d = 3.05; Cu log K_d = 2.98; and Zn log K_d = 2.75. While pH may be the most important variable for partitioning, Sauvé et al. (2000, 2003) also noted the importance of organic matter as, after being normalized for pH, sorptive capacities for organic soils were reported to be up to 30 times larger than those observed for mineral soils.

2.3.2 Chemical Advection

Advection transports all chemical phases. For two-dimensional flow in the overland plane, a chemical continuity (conservation of mass) equation analogous the sediment continuity equation can be written as:

$$J_{xc} = v_x \left(f_d + f_b + \sum_{n=1}^{N} f_{p_n} \right) C_c = v_x C_c \tag{2.45}$$

$$J_{yc} = v_y \left(f_d + f_b + \sum_{n=1}^{N} f_{p_n} \right) C_c = v_y C_c \tag{2.46}$$

where: J_{xc} , J_{yc} = chemical advective flux in the x- or y-direction [M/L^{2}T]

v_x , v_y = advective velocity in the x- or y-direction [L/T]

n = particle index = 1, 2, 3, etc.

v_{r_n} = resuspension (erosion) velocity of particle "n" [L/T]

f_d = fraction of the total chemical in dissolved phase in the water column [dimensionless]

f_b = fraction of the total chemical in the bound phase in the water column [dimensionless]

f_{pn} = fraction of the total chemical in particulate phase associated with particle "n" in the sediment column [dimensionless]

C_c = total chemical concentration in the water column [M/L^3]

Similarly, for one-dimensional flow in channels a chemical continuity (conservation of mass) equation analogous the sediment continuity equation is identical to Equation 2.45.

2.3.3 Erosion and Deposition of Particulate Phase Chemicals

Chemicals associated with particles in the water column will enter the sediment bed if those particles settle. Similarly, chemicals associated with particles in the sediment bed will return to the water column if those particles are entrained (resuspend). The factors that control particle transport between the water column and sediment bed were described in Section 2.2.2. Since particle phase chemicals move with the particles transported, the erosion and deposition fluxes of chemicals are described as (Thomann and Mueller, 1987):

$$J_{ec} = \sum_{n=1}^{N} v_{rn} f_{p2_n} C_{c2} \tag{2.47}$$

$$J_{dc} = \sum_{n=1}^{N} v_{sen} f_{p1_n} C_{c1} \tag{2.48}$$

where: J_{ec} = chemical erosion flux [M/L^{2}T]

J_{dc} = chemical deposition flux [M/L^{2}T]

n = particle index = 1, 2, 3, etc.

v_{r_n} = resuspension (erosion) velocity of particle "n" [L/T]

v_{se_n} = effective settling velocity of particle "n" [L/T]

f_{p1_n} = fraction of the total chemical in particulate phase associated with particle "n" in the water column [dimensionless]

f_{p2_n} = fraction of the total chemical in particulate phase associated with particle "n" in the sediment column [dimensionless]

C_{c1} = total chemical concentration in the water column [M/L^3]

C_{c2} = total chemical concentration in the soil/sediment column [M/L^3]

2.3.4 Chemical Infiltration and Subsurface Transport

Chemicals associated with the dissolved and bound phase in the water column will enter the soil or sediment bed if the water transporting those chemicals infiltrates. When chemical partition coefficients are low and a significant fraction of the total chemical mass is in a mobile form, chemical infiltration may be significant. To account for this process, the chemical infiltration flux can be computed from the water infiltration flux as:

$$J_{ic} = v_i \left(f_{d1} + f_{b1} \right) C_{c1} = v_i f_{m1} C_{c1} \tag{2.49}$$

where: J_{ic} = chemical infiltration flux [M/L^{2}T]

v_i = infiltration rate or transmission loss of water [L/T], previously defined as f in Eq. (2.5) or t_l in Eq. (2.6)

f_{d1} = fraction of the total chemical in dissolved phase in the water column [dimensionless]

f_{b1} = fraction of the total chemical in bound phase in the water column [dimensionless]

f_{m1} = fraction of the total chemical in the mobile phase in the water column [dimensionless] = $f_{d1} + f_{b1}$

C_{c1} = total chemical concentration in the water column [M/L^3]

Once in the subsurface, infiltrated chemicals would be subject to repartitioning with the chemical mass associated with porewater and particles in the soil column and transport via groundwater. The flow of groundwater through the soil also has the potential to leach chemicals from the soil column. Due to adsorption and the comparatively high bulk density of particles in the soil, subsurface chemical transport is subject to retardation (Fetter, 2001). Chemicals subject to retardation travel trough the subsurface at rates less than the average linear velocity of water. The retardation factor for a chemical in the subsurface is computed as (Fetter, 2001):

$$R = 1 + \frac{\rho_b}{\theta_e} K_p \tag{2.50}$$

where: R = Retardation factor [dimensionless]

ρ_b = soil bulk density [M/L^3]

θ_e = effective soil porosity (void volume/total volume) [dimensionless]

K_p = chemical equilibrium partition (distribution) coefficient [L^3/M]

2.3.5 Other Chemical Mass Transfer and Transformation Processes

Beyond partitioning and mass transport processes, the fate of chemicals is potentially influenced by a number of other processes such as biodegradation, hydrolysis, oxidation, photolysis, and volatilization, and dissolution. However, for general simulation of elemental metals such as cadmium, copper, and zinc, volatilization, biodegradation, and photolysis do not occur. Hydrolysis and oxidation can affect the ionic speciation and phase distribution of metallic chemicals but do not affect the total chemical concentration. The effect that possible hydrolysis or oxidation reactions have on phase distributions of metals can be represented in terms of the chemical distribution (partitioning) coefficient.

3.0 TREX WATERSHED MODELING FRAMEWORK IMPLEMENTATION

3.1 GENERALIZED CONCEPTUAL MODEL FRAMEWORK

A generalized conceptual framework for the TREX watershed chemical transport and fate model is presented in Figure 3-1. At present, this framework research focuses on the event transport of metals in surface waters. Consequently, several possible processes in the general conceptual framework can be neglected because storm events are short-lived, lasting no more than a few hours. In particular, mass transfer and reactions processes such as volatilization, biodegradation, hydrolysis, and photodegradation can be neglected because of the short time scale for simulations or because these processes do not occur for metals. Other processes, such as dispersion and diffusion can also be neglected because at the time scale of event simulations transport processes are reasonable expected to be dominated by advection. At the event time scale, subsurface transport is also neglected. As a result, the transport and fate processes most important for the event simulation of metals are:

- Advective water column transport;
- chemical partitioning between water (truly dissolved), dissolved organic compounds (DOC) (or other binding agents) (bound), and solid (particulate) phases;
- Transport (erosion, deposition, net burial/unburial) of solids and particulate chemicals;
- Infiltration of dissolved and bound (mobile) phase chemicals;
- External sources and sinks of water, solids and chemicals.

Dynamic mass balance equations were developed based on the process descriptions presented in Section 2.0. In their most general form, these mass balance equations form a system of coupled partial differential equations that are functions of time and space. These equations describe the relationship between material inputs (precipitation or loads) and mass (water depth or constituent concentrations). To solve these equations, three simplifying assumptions were made and the equations expressed in finite difference form (Thomann and Mueller, 1987; Chapra, 1997):

1. Water column volumes are constant with respect to time during any interval ($\partial V/\partial t = 0$);
2. Surficial sediments do not move horizontally within the sediment bed; and
3. Chemical partitioning to solids and binding is rapid relative to other processes (local equilibrium).

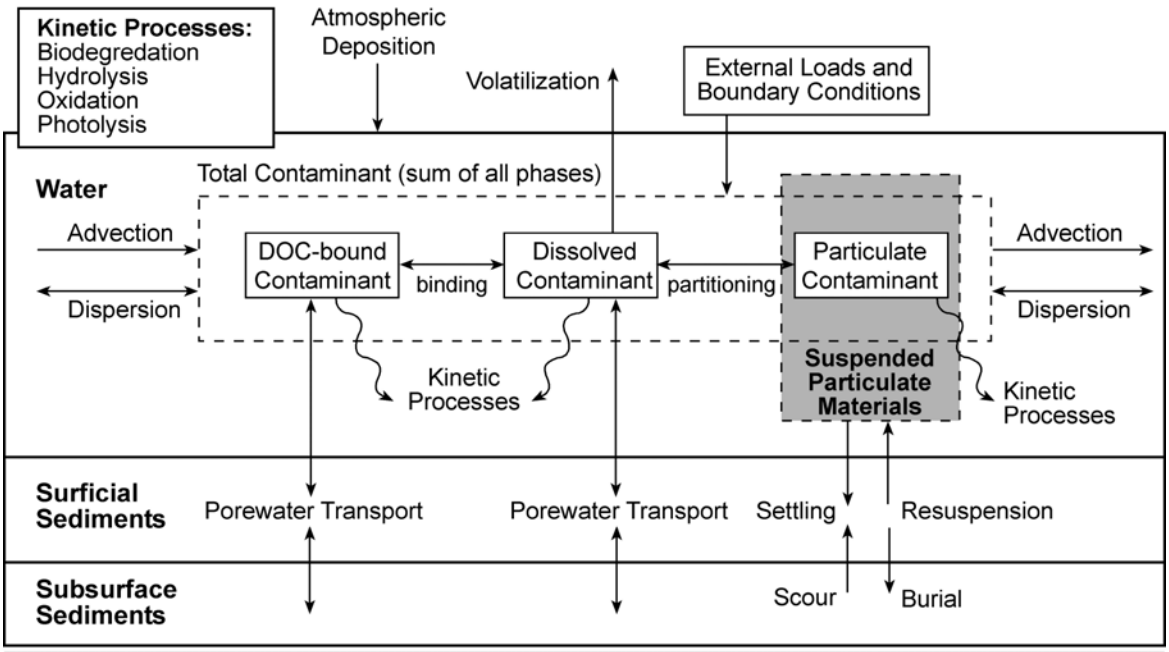

Figure 3-1. Generalized conceptual model framework.

The state variables in the model framework for the overland plane (denoted with the subscript "ov") and channel network (denoted with the subscript "ch") are: water depth (h), solids concentration (C_s), and chemical concentration (C_c). The corresponding equations for the water column and bed are:

Water Depth in the Overland Plane and Channel Network

$$\frac{\partial h_{ov}}{\partial t} = i_e - \frac{1}{B_x}\frac{\partial Q_{ovx}}{\partial x} - \frac{1}{B_y}\frac{\partial Q_{ovy}}{\partial y} - \frac{q_l}{L_c} + \frac{W_w}{A_c} \tag{3.1}$$

$$\frac{\partial (h_{ch} B_c)}{\partial t} = q_l - \frac{\partial Q_{ch}}{\partial x} + \frac{W_w}{L_c} \tag{3.2}$$

Solids in the Water Column of the Overland Plane and Channel Network

$$\frac{\partial C_{s,ov}}{\partial t} = v_r C_{sb,ov}\frac{A_s}{V_w} - v_{se} C_{s,ov}\frac{A_s}{V_w} - v_x C_{s,ov}\frac{A_c}{V_w} - v_y C_{s,ov}\frac{A_c}{V_w} - v_f C_{s,ov}\frac{A_c}{V_w} + \frac{W_s}{V_w} \tag{3.3}$$

$$\frac{\partial C_{s,ch}}{\partial t} = v_r C_{sb,ch} \frac{A_s}{V_w} - v_{se} C_{s,ch} \frac{A_s}{V_w} - v_x C_{s,ch} \frac{A_c}{V_w} + v_f C_{s,ov} \frac{A_c}{V_w} + \frac{W_s}{V_w} \tag{3.4}$$

Solids in the Soil and Sediment Bed

$$\frac{\partial C_{sb,ov}}{\partial t} = v_{se} C_{s,ov} \frac{A_s}{V_s} - v_r C_{sb,ov} \frac{A_s}{V_s} \tag{3.5}$$

$$\frac{\partial C_{sb,ch}}{\partial t} = v_{se} C_{s,ch} \frac{A_s}{V_s} - v_r C_{sb,ch} \frac{A_s}{V_s} \tag{3.6}$$

Total Chemical in the Water Column of the Overland Plane and Channel Network

$$\begin{aligned} \frac{\partial C_{c,ov}}{\partial t} = {} & v_r C_{cb,ov} f_{pb} \frac{A_s}{V_w} - v_{se} C_{c,ov} f_p \frac{A_s}{V_w} - v_x C_{c,ov} \frac{A_c}{V_w} - v_y C_{c,ov} \frac{A_c}{V_w} - v_f C_{c,ov} \frac{A_c}{V_w} \\ & - v_{i,ov} C_{c,ov} \left(f_d + f_b\right) \frac{A_s}{V_w} + \frac{W_c}{V_w} \end{aligned} \tag{3.7}$$

$$\begin{aligned} \frac{\partial C_{c,ch}}{\partial t} = {} & v_r C_{cb,ch} f_{pb} \frac{A_s}{V_w} - v_{se} C_{c,ch} f_p \frac{A_s}{V_w} - v_x C_{c,ch} \frac{A_c}{V_w} + v_f C_{c,ov} \frac{A_c}{V_w} \\ & - v_{i,ch} C_{c,ch} \left(f_d + f_b\right) \frac{A_s}{V_w} + \frac{W_c}{V_w} \end{aligned} \tag{3.8}$$

Total Chemical in the Soil and Sediment Bed

$$\frac{\partial C_{cb,ov}}{\partial t} = v_{se} C_{c,ov} f_p \frac{A_s}{V_s} - v_r C_{cb,ov} f_{pb} \frac{A_s}{V_s} \tag{3.9}$$

$$\frac{\partial C_{cb,ch}}{\partial t} = v_{se} C_{c,ch} f_p \frac{A_s}{V_s} - v_r C_{cb,ch} f_{pb} \frac{A_s}{V_s} \tag{3.10}$$

where:

h	=	flow depth of water column [L]
C_s , C_{sb}	=	solids concentration in water column and bed [M/L^3]
C_c , C_{cb}	=	total chemical concentration in water column and bed [M/L^3]
Q_x , Q_y	=	flow in the x- or y-direction [L^3/T]
q_l	=	lateral unit flow from overland plane to channel (floodplain) [L^2/T]
L_c	=	length of channel in flow direction [L]

A_c , A_s = cross sectional area in flow direction, bed surface area [L^2]

V_w , V_s = volume of water and sediments [L^3]

v_x , v_y , v_f = flow velocity in the x- or y-direction and between overland plane and channel (floodplain) [L/T]

v_r , v_{es} , v_i = resuspension (erosion), effective settling (deposition), and infiltration (or transmission loss) velocities [L/T]

f_d , f_b , f_p = dissolved, bound, and particulate chemical fractions [dimensionless]

$W_{w,s,c}$ = material point source/sink: water [L^3/T], solids, or chemical [M/T]

Each term in the mass balance equations represents a process in the conceptual framework. The variables in each term represent model parameters. Thomann and Mueller (1987) and Chapra (1997) provide more detailed presentations of mass balance equations for chemical transport.

3.2 GENERAL DESCRIPTION OF THE NUMERICAL FRAMEWORK

To simulate hydrologic, sediment, and chemical transport, values must be assigned to each model parameter and the mass balance equations defined by the conceptual model framework must be solved. Numerical integration techniques are needed to solve the model equations. TREX uses a finite difference control volume implementation of the generalized mass balance equation. To generate solutions, the framework computes dynamic mass balances for each state variable and accounts for all material that enters, accumulates within, or leaves a control volume through precipitation excess, external loads, advection, erosion, and deposition. TREX also features a "semi-Lagrangian" soil/sediment bed layer submodel to account for the vertical distribution of the physical and chemical properties of the overland soil and channel sediment columns (see Section 3.3). These equations are solved using Euler's method for numerical integration (Chapra and Canale, 1985):

$$s\big|_{t+dt} = s\big|_t + \frac{\partial s}{\partial t}\bigg|_t dt \tag{3.11}$$

where: $s\big|_{t+dt}$ = value of model state variable at time $t+dt$ [L] or [M/L^3]

$s\big|_t$ = value of model state variable at time t [L] or [M/L^3]

$\frac{\partial s}{\partial t}\Big|_t$ = value of model state variable derivative at time t [L/T] or [M/L^3T]

dt = time step for numerical integration [T]

3.3 TREX FRAMEWORK FEATURES

The initial basis for development of TREX was CASC2D. As part of the model development process, CASC2D's underlying hydrologic and sediment transport submodels were significantly enhanced before chemical transport and fate components were added to create the TREX framework. An overview of TREX features is presented in Table 3-1. As part of the overall development effort, the entire body of TREX source code is organized to significantly improve code structure and modularity and to provide complete, line-by-line documentation. Beyond allowing development of chemical transport and fate features to proceed, the TREX code is structured so that future categories of model features can be added to the framework without having to reconstruct the basic code. As presented in Figure 3-2, the code is designed so that the calculations for each process at any time level are independent and information is carried forward from hydrology to sediment transport to chemical transport in order to generate a solution. At any time level, flow is assumed to be unaffected by sediment and chemical transport and sediment transport is affected by chemical transport, so calculations for these three components have a natural hierarchy.

Within TREX, many features of the original CASC2D code were significantly enhanced and many new features were added. In particular, the TREX code is designed to simulate multiple watershed outlets and to also allow channel network branching in the upstream and downstream directions. This permits simulation of braided tributaries and distributary flows that might occur around alluvial fans or where a river system meets a large

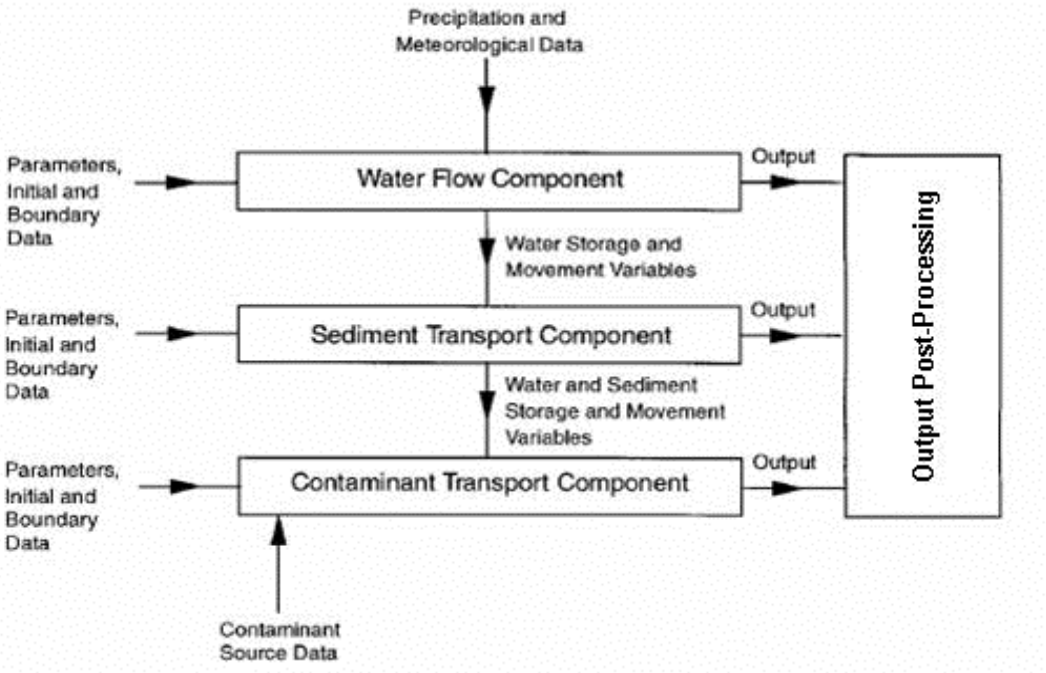

Figure 3-2. TREX Hierarchy and information flow (after Ewen et al 2000).

Table 3-1. Comparative overview of TREX features.

Model Component	*Prior CASC2D Code*	*TREX Code*	*Status*
General Model Controls			
Numerical integration time step	One time step limited to critical value regardless of flow	Series of time step values that can be optimized based on flow	Tested
Hydrologic Submodel			
Water depth initial condition	Assumed to be zero but recent code allowed a non-zero flow depth in channels (dry start)	User can specify any value for depth overland, in channels, or infiltrated (wet or dry start)	Tested
Flow outlets and downstream boundary conditions	Limited to one outlet, assumed normal depth	Any number of outlets possible, downstream control or normal depth can be specified	Partially tested
Floodplain interaction	Present in initial code (Julien et al. 1995) but not in recent code (Rojas, 2002).	Restored feature and enhanced to compute flooding from water surface elevations	Tested
Channel topology: orientation	Channel connections limited to four (N-S or E-W) directions	Channel connections in all eight raster grid directions	Tested
Channel topology: branching	Converging branches, limited to two branches upstream	Converging and diverging branches with 2-7 branches	Tested
Flow point sources and sinks	None	Point sources for overland plane and channel network	Partially tested
Sediment Transport Submodel			
Number of particle types	Limited to three: sand, silt, clay	Unlimited number of types	Tested
Floodplain sediment transport	None: solids passing through overland part of a floodplain cell instantly move to channel	Occurs whenever water depth in overland part of floodplain cell exceeds zero	Tested
Channel erosion	Limited: only solids deposited during simulation erode; net bed elevation change never < 0	Not restricted; channels can incise and net change in bed elevation can be < 0	Tested
Solids point sources and sinks	None	Point sources for overland plane and channel network	Partially tested
Chemical Transport Submodel			
Number of chemical types	None	Unlimited	Tested
Chemical transport and fate	None	Three-phase partitioning with advection, erosion, deposition	Tested
Chemical point sources and sinks	None	Point sources for overland plane and channel network	Partially tested

receiving waterbody on a low slope. Another significant enhancement is the addition of flow point sources and sinks. Note that TREX does not consider groundwater flow processes other than water loss at the surface by infiltration or channel transmission loss. However, to account for other water losses or gains, groundwater interactions could be represented as a series of time-variable point sources and sinks. In effect, this feature allows TREX to be externally coupled with groundwater flow and transport modeling tools such as MODFLOW (Harbaugh et al. 2000), HST3D (Kipp, 1997), and MT3DMS (Zheng and Wang, 1999).

Another key feature of the enhanced TREX framework is the representation of the bed and bed processes. The bed itself is presented as a vertical stack (layers). Typical water quality modeling approaches use an Eulerian (fixed) frame of reference for all compartments. In contrast, TREX uses what is termed a "semi-Lagrangian" (floating) frame of reference (Velleux et al. 2001). In the Eulerian approach, the control volume for mass balance calculations is fixed in space and material is advected through the control volume. With respect to the bed, the deposition or erosion of material causes the entire frame of reference (all layers in the stack) to advect (upward or downward). As control volumes relocate, material is advected between adjacent layers. This advection can affect contaminant distributions in the bed. In the semi-Lagrangian approach, the control volume of the surface bed layer is allowed to expand or contract in response to erosion or deposition. Because the entire frame of reference for all bed layers is not relocated, the mixing that occurs with the Eulerian approach is eliminated. Velleux et al. (2001) and Imhoff et al. (2003) present further descriptions of the semi-Lagrangian approach and its details.

3.4 COMPUTATIONAL CONSIDERATIONS

The TREX source code is written in C and conforms to ANSI C99 conventions. The code was compiled and simulations executed on several computing systems to ensure a degree of portability. The computers, operating systems, and compilers used for code development are presented in Table 3-2. It is worth noting that TREX is a computationally intensive application. Simulations with hydrology, six solids types, and three chemical types on a domain with 34,000 elements required approximately 18.5 CPU hours on a system with a 1.3 GHz Intel Itanium2 (64-bit) processor.

Table 3-2. Computers, operating systems, and compiler used for code development.

Processor	***Operating System***	***Development Environment/Compiler***
Intel Itanium2 (64-bit)	Windows XP 64-bit Edition	Intel C++ 8.1
AMD Athlon	Windows 2000 Redhat Enterprise Linux	Visual Studio .Net GCC
Intel Pentium4	Windows XP	Visual Studio .Net
Intel Pentium3	Windows XP	Visual C++ 6.0

3.5 PROGRAM OPERATION

TREX is operated from a command line interface (the command prompt under the Windows operating system). TREX requires that the user specify one argument. This argument is the path and file name of the TREX main input file. The main input file provides the basic model input parameters that control a simulation. The main input file also contains the names of ancillary model input files that delineate specific characteristics of the simulation such as the watershed boundary mask, elevations, soil classes, and land use, etc. Descriptions of the main and ancillary input files are presented in Section 4.0. When run from the command prompt under the Windows operating system, the command stream to begin execution of a TREX simulation is of the form:

C:\trex.exe *inputfilename.inp*

During execution, TREX generates a series of output files. Depending on the number of cells in the spatial domain and number of state variables simulated and the frequency of reporting, the size of model output can be quite large (>5 GB). Descriptions of TREX output file types are presented in Section 5.0.

4.0 DESCRIPTION AND ORGANIZATION OF MODEL INPUT FILES

4.1 INPUT FILE STRUCTURE OVERVIEW

TREX has a main input file that controls most aspects a simulation. Within this main input file, the inputs are divided into six groupings of related parameters (Data Groups A-F). The main input file also specifies a number of ancillary input files that are required to operate the model. The ancillary model input files are used to delineate specific characteristics of the simulation such as the watershed boundary mask, elevations, soil classes, and land use, etc. Ancillary files are each organized into Data Groups.

The organization and content of each Data Group is described in a series of tables presented in the following sections of this manual. Each Data Group is itself divided into records and fields. In general, the name of each variable, its type, and expected units is described. Variables names starting with "n" describe the number of elements associated with a parameter (i.e. nsolids = number of solids types, nchems = number of chemicals, ndt = number of time steps, etc.) Variables ending with "opt" are switches that toggle operation of model processes. Variables containing "ic", "bc", and "w" are associated with initial conditions (ic), boundary conditions (bc), and loads/forcing functions (w). Variable types include int (integer), float (floating point), char (an unbroken sequence of characters without a space or tab), and string (a sequence of characters that can include spaces and tabs). Inputs are typically specified in metric units (m, m/s, g/m^3, etc.).

Model controls for time steps (dt), printout, initial conditions (ICs), boundary conditions (BCs), and loads/forcing functions are input as paired values in a time series (i.e. pairs of {function value at time t, time t}). Time steps and print intervals are step functions (i.e. the input value is used until time t, after which the next value is used). ICs, BCs, and loads are piecewise linear functions (i.e. values are linearly interpolated between times specified).

4.2 MAIN MODEL INPUT FILE

Within this main input file, the inputs are divided into six groupings (Data Groups) of related parameters. Data Group A is used to specify general controls for the simulation such as the simulation type and the series of times steps to be used for numerical integration. Data Group B is used to specify parameters for hydrologic simulations. Data Group C is used to specify parameters for sediment transport simulations. Data Group D is used to specify parameters for chemical transport simulations. Data Group E is used to specify parameters for environmental conditions such as air temperature and wind speed. Data Group F is used to specify parameters for model output control. However, users should note that not all possible combinations of model inputs are fully implemented in the model at this time. Users are advised to review the TREX source code.

4.2.1 Data Group A: General Controls

Data Group A: General Controls

Record	Description
1	Header1 (string)
2	Header2 (string)
3	"KSIM" (char), ksim (int) {1 = hydrology, 2 = sediment, 3 = chemical}, "NROWS" (char), nrows (int), "NCOLS" (char), ncols (int), "DX" (char), dx (float) (m), "DY" (char), dy (float) (m), "TSTART" (char), tstart (float) (hrs)
4	"NDT" (char), ndt (int) {number of time step values}
	for idt = 1, ndt
5	dt[idt] (float) (s), dttime[idt] (float) (hrs)
Note	Record 5 is repeated for idt = 1, ndt
6	"NPRINTOUT" (char), nprintout (int) {number of print intervals for tabular output}
	for iprntout = 1, nprintout
7	printout[iprntout] (float) (hrs), printouttime[iprntout] (float) (hrs)
Note	Record 7 is repeated for iprntout = 1, nprintout
8	"NPRINTGRID" (char), nprintgrid (int) {number of print intervals for grids output}
	for iprntgrid = 1, nprintgrid
9	printgrid[iprntgrid] (float) (hrs), printgridtime[iprntgrid] (float) (hrs)
Note	Record 9 is repeated for iprntgrid = 1, nprintgrid
10	"ECHO" (char), echofile (string)

4.2.2 Data Group B: Hydrologic Simulation Parameters

Data Group B: Hydrologic Simulation Parameters

Record	*Description*
1	Header (string)
2	"MASK" (char), maskfile (string)
	call ReadMaskFile
3	"ELEVATION" (char), elevationfile (string) (m)
	call ReadElevationFile

Data Group B: Hydrologic Simulation Parameters (continued)

4	“INFOPT” (char), infopt (int) (0 = no infiltration, 1 = infiltration)
	if ksim = 1 {for ksim > 1, see Data Group C}
	if infopt = 1 {there is infiltration but no sediment transport}
5	“NSOILS” (char), nsoils (int) (number of soil types)
	for isoil = 1, nsoils
6	kh[isoil] (float) (m/s), capsh[isoil] (float) (m), soilmd[isoil] (float) (dimensionless), soilname[isoil] (string)
Note	Record 6 is repeated for isoil = 1, nsoils
7	“SOIL_TYPES” (char), soilfile (string)
	call ReadSoilFile
	endif infiltopt
8	“NLANDS” (char), nlands (int) (number of land use types)
	for iland = 1, nlands
9	nmanningov[iland] (float) (n units), interceptionclass[iland] (float) (mm), landname[iland] (string)
Note	Record 9 is repeated for iland = 1, nlands
10	“LAND_USE” (char), landusefile (string)
	call ReadLandUseFile
	endif ksim = 1
11	“STORAGE_DEPTHS” (char), storagedepthfile (string) (m)
	call ReadStorageDepthFile
12	“CHNOPT” (char), chnopt (int) (0 = no channels, 1 = channels)
	if chnopt = 1
13	“TPLGYOPT” (char), tplgyopt (int) {0 = compute topology from channel property file and link, and node masks, 1 = topology read from topology file}, “CTLOPT” (char), ctlopt (int) (0 = no transmission loss, 1 = transmission loss) {channel transmission loss option}, “FLDOPT” (char), fldopt (int) {0 = floodplain water transfer is from overland to channel only, 1= floodplain water transfer can be in either direction depending on water surface elevations}, “OUTOPT” (char), outopt (int) {0 = pour water from overland to channel portion of cell before routing overland at outlets, 1 = route water overland before pouring into channel at outlets}
	if tplgyopt = 0 then
14	“LINK” (char), linkfile (string)

Data Group B: Hydrologic Simulation Parameters (continued)

	call ReadLinkFile
15	“NODE” (char), nodefile (string)
	call ReadNodeFile
16	“CHANNEL” (char), chanfile (string) {includes channel “dead” storage}
	call ReadChannelFile
	call ComputeTopology
Note	Records 14, 15, and 16 are only input if tplgyopt = 0.
	elseif tplgyopt = 1
17	“TOPOLOGY” (char), topofile (string) {combines the channel property, and the link and node masks} {also includes channel “dead” storage}
	call ReadTopologyFile {for future use...}
Note	Record 17 is only input if tplgyopt = 1.
Warning	Option not fully implemented
	endif tplgyopt
	if ksim = 1 {for ksim > 1, see Data Group C}
	if ctlopt = 1 {there is channel transmission loss but no sediment transport}
18	“TRANSMISSION_LOSS_PROPERTIES” (char), channeltlossfile (string)
	call ReadTransmissionLossProperties {read none-by-node transmission loss parameter values}
	endif ctlopt = 1
	endif ksim = 1
	endif chnopt
19 (ICov)	“INITIAL_WATER_OVERLAND” (char), initialwaterovfile (string) (m)
	call ReadInitialWaterOverlandFile
	if infopt = 1
20 (ICsoil)	“INITIAL_INFILTRATION” (char), initialinfiltrationfile (string) (m)
	call ReadInitialInfiltrationFile
	endif infopt = 1
	if (chnopt = 1) then
21 (ICch)	“INITIAL_WATER_IN_CHANNELS” (char), initialwaterchfile (string) (m)

Data Group B: Hydrologic Simulation Parameters (continued)

	call ReadInitialWaterChannelFile
22 (ICsed)	“INITIAL_TRANSMISSION_LOSS” (char), initialtranslossfile (string) (m)
	call ReadInitalTransmissionLossFile
	endif chnopt
23 (Wov)	rainopt (int) {e.g. 0 = uniform in space, 1 = IDW spatial interpolation, 2 = time series grid read} {other options such as space-time rainfall model output, PRISM, Kriging can be added here} {Only options 0 and 1 are implemented.}
	if rainopt = 1
24	“IDWradius” (char), idwradius (float) (m), “IDWexponent” (char), idwexponent (float) (dimensionless)
	else if rainopt > 1
Warning	Warn user option(s) not implemented. Once implemented, a record like Record 22 will need to be inserted...
	endif rainopt (=1)
Note	We do not need to check for rainopt = 0 because there are no parameters to enter for this case...
	if rainopt <= 1
25	“NRAINGAGES” (char), nrg (int) {by default rain is uniform if only one rain gage is specified and distributed if there is more than one gage}
Check	if rainopt = 0 and nrg > 1, warn and abort...
	if nrg > 0
26	“CONV1” (char), convunits (float), “CONV2” (char), convtime (float), “SCALE” (char), scale (float)
	for irg = 1, nrg
27	“GAGE” (char), rgid[irg] (int), rgx[irg] (float) (m), rgy[irg] (float) (m), nrpairs[irg] (int)
	for irpairs = 1, nrpairs[irg]
28	rfintensity[irg][ipairs] (float) (m/s), rftime[irg][ipairs] (float) (hrs)
Note	Records 27 and 28 are repeated as a group for irg = 1, nrg. Record 26 is repeated for ipairs = 1, npairs[irg].
Also Note	Records 25-28 apply for rainopt involving spatial interpolation of point data (IDW, Kriging, etc...). This control structure may need revision for spatial interpolation of grid data...
	endif nrg > 0

Data Group B: Hydrologic Simulation Parameters (continued)

	endif rainopt <= 1
29 (Wov)	"NUMBER_OF_OVERLAND_FLOW_SOURCES" (char) (Flows point sources that enter or leave the overland plane by means other than rainfall or runoff, i.e. a well, a spring, irrigation diversion, etc.), nqwov (int)
	if nqwov > 0
30	"CONV1" (char), convunits (float), "CONV2" (char), convtime (float), "SCALE" (char), scale (float)
	for i = 1, nqovw
31	qwovrow[i] (int), qwovcol[i], nqwovpairs[i] (int), qwovdescription[i] (string) {qwovdescription is read to end of line as character}
	for ipairs = 1, nqovwpairs[i]
32	qwov[i][ipairs] (float) (m3/s), qwovtime[i][ipairs] (float) (hrs)
Note	Records 31 and 32 are repeated as a group for i = 1, nqwov. Record 32 is repeated for ipairs = 1, nqwovpairs[i]. qwov units: m^3/s.
	endif nqwov > 0
	if chnopt = 1
33 (Wch)	"NUMBER_OF_CHANNEL_FLOW_SOURCES" (char) (Flows that enter or leave the model domain by means other than rainfall, i.e. a mine adit, a spring, irrigation diversion, etc.), nqwch (int)
	if nqchw > 0
34	"CONV1" (char), convunits (float), "CONV2" (char), convtime (float), "SCALE" (char), scale (float)
	for i = 1, nqwch
35	qwchlink[i] (int), qwchnode[i], nqwchpairs[i] (int), qwchdescription[i] (string) {qdescription is read to end of line as character}
	for ipairs = 1, nqwchpairs[i]
36	qwch[i][ipairs] (float) (m3/s), qwchtime[i][ipairs] (float) (hrs)
Note	Records 35 and 36 are repeated as a group for i = 1, nqwch. Record 36 is repeated for ipairs = 1, nqwchpairs[i]. qwch units: m^3/s.
	endif nqwch > 0
	endif chnopt = 1
37 (BC)	"NUMBER_OF_WATERSHED_OUTLETS/BOUNDARIES" (char) (Locations where flows leave the model domain via the overland plane and channel network), noutlets (int)
	for i = 1, noutlets

Data Group B: Hydrologic Simulation Parameters (continued)

38	"OUTLET_CELL" (char), iout[i] (int) (m), jout[i] (int) (m), sovout[i] (float) (dimensionless), dbcopt[i] (int) {0 = normal depth ($s_f = s_o$), 1 = specified water depth time series}
	if dbcopt[i] > 0
39	"CONV1" (char), convunits (float), "CONV2" (char), convtime (float), "SCALE" (char), scale (float)
40	nqbcpairs[i] (int), qbcdescription[i] (string) {qbcdescription is read to end of line as character}
	for ipairs = 1, nqbcpairs[i]
41	qbc[i][ipairs] (float) (m), qbctime[i][ipairs] (float) (hrs)
Note	Records 38-41 are repeated as a group for i = 1, noutlets. Records 39-41 are only input if dbcopt > 0. If dbcopt > 0, Records 39 and 40 are input once and Record 41 is repeated for ipairs = 1, nqbcpairs[i]. qbc units: m.
42	"NQREPORTS" (char), nqreports (int)
	for iqreport = 1, nqreports
43	qreprow[iqreport] (int), qrepcol[iqreport] (int), qarea[iqreport] (float) (km2), qunitsopt[iqreport] (int) (1 = m3/s, 2= mm/hr), stationid (char)
Note	Record 43 is repeated for iqreport = 1, nqreports

4.2.3 Data Group C: Sediment Transport Simulation Parameters

Data Group C: Sediment Transport Simulation Parameters

Record	*Description*
	if ksim >= 2 then (if ksim >= 2, then sediment transport is simulated)
1	Header (string)
2	"NSOLIDS" (char), nsolids (int), "NSGROUPS" (char), nsgroups (int)
Note	nsolids = number of particle types, nsgroups = number of reporting groups for solids, particles in a reported group are summed for a group total
3	"ADVOVOPT" (char), advovopt (int), "ADVOVSCALE", advovscale (float), "DSPOVOPT" (char), dspovopt (int), "DSPOVSCALE", dspovscale (float), "DEPOVOPT" (char), depovopt (int), "DEPOVSCALE", depovscale (float), "ERSOVOPT" (char), ersovopt (int), "ERSOVSCALE", ersovscale (float), "TNSOVOPT" (char), tnsovopt (int), "TNSOVSCALE", tnsovscale (float), "ELEVOVOPT" (char), elevovopt (int)

Data Group C: Sediment Transport Simulation Parameters (continued)

Note	advovopt: 0 = advection bypassed, 1 = advection; dspovopt: 0 = dispersion bypassed, 1 = dispersion; depovopt: 0 = deposition bypassed, 1 = deposition using the fall velocity, 2 = deposition using the fall velocity and the probability of deposition); ersovopt: 0 = erosion bypassed, 1 = transport capacity limited erosion (Kilinc-Richardson), 2 = erosion from excess shear stress (untested); tnsovopt: 0 = no transformations bypassed, 1 = transformations occur; elevovopt: 0 = overland elevation update calculations bypassed, 1 = overland elevations updated
	if chnopt > 0
4	“ADVCHOPT” (char), advchopt (int), “ADVCHSCALE”, advchscale (float), “DSPCHOPT” (char), dspchopt (int), “DSPCHSCALE”, dspchscale (float), “DEPCHOPT” (char), depchopt (int), “DEPCHSCALE”, depchscale (float), “ERSCHOPT” (char), erschopt (int), “ERSCHSCALE”, erschscale (float), “TNSCHOPT” (char), tnschopt (int), “TNSCHSCALE”, tnschscale (float), “ELEVCHOPT” (char), elevchopt (int)
Note	advchopt: 0 = advection bypassed, 1 = advection; dspchopt: 0 = dispersion bypassed, 1 = dispersion; depchopt: 0 = deposition bypassed, 1 = deposition using the fall velocity, 2 = deposition using the fall velocity and the probability of deposition; erschopt: 0 = erosion bypassed, 1 = transport capacity limited erosion (Engelund and Hansen), 2 = erosion from excess shear stress (untested) {other options such as Ackers and White, Yang, etc. can be added here}; tnschopt: 0 = no transformations bypassed, 1 = transformations occur; elevchopt: 0 = channel bed elevation update calculations bypassed, 1 = channel bed elevations updated
	endif chnopt > 0
Also Note	The process options for Records 3 and 4 toggle use (on or off) of the different process routines (for sediment transport). However, when zero is selected for a process option, the process is bypassed but the user must still enter process parameters (as if the option = 1) as required in later records.
5	Header (string): “PARTICLE GROUP NAMES FOR REPORTING”
	for igroup = 1, nsgroups
6	“GROUPNUMBER” (char), particlegroupname[igroup] (string)
Note	Record 6 is repeated for igroup = 1, nsgroups.
7	Header (string): “PARTICLE CHARACTERISTICS: ds, G, ws,” {depending on process options add:} “cncopt, tcdov, tcdch,” ... “groupnumber, particlename”
PARTICLE	for isolid = 1, nsolids
8a (general)	ds[isolid] (float), spgravity[isolid] (float), ws[isolid] (float)
	if depovopt > 1 or depchopt > 1 or ersovopt > 1 or erschopt > 1
8b (type)	cncopt[isolid] (int) (cohesive/non-cohesive transport option) {0 = non-cohesive (Gessler), 1 = cohesive (Partheniades)}

Data Group C: Sediment Transport Simulation Parameters (continued)

	if depovopt > 1
8c (dep ov)	tcdov[isolid] (float) (N/m2 = Pa)
	endif depovopt > 1
	if ersovopt > 1
8d (ers ov)	tceov[isolid] (float) (N/m2 = Pa), zageov[isolid] (float) (dimensionless)
	endif ersovopt > 1
	if chnopt > 0
	if depchopt > 1
8e (dep ch)	tcdch[isolid] (float) (N/m2 = Pa)
	endif depchopt > 1
	if erschopt = 1 {modified Engelund and Hansen}
8f (ers ch = 1)	vcch[isolid] (float) (m/s) {critical velocity motion threshold}
	elseif erschopt > 1
8g (ers ch > 1)	tcech[isolid] (float) (N/m2 = Pa), zagech[isolid] (float) (dimensionless)
	endif ersovopt = 1
	endif chnopt > 0
	endif depovopt > 1 or depch > 1 or ersovopt > 1 or erschopt > 1
8h	sgroupnumber[isolid] (int), particlename[isolid] (string)
Note	Record 8 (a-g) is repeated for isolid = 1, nsolids.
	if tnsovopt > 0 or tnschopt > 0
9	Header (string): “PARTICLE REACTIONS: abrasion, flocculation, dissolution, etc.”
REACTIONS	for i = 1, nsolids
10	“SOLID” (char), isolid (int), “NFIELDS” (char), nfields (int)
	for ifields = 1, nfields[ichem]
11	ncns (int), fieldname (string)
	for icns = 1, ncns
12	sname (char), sid (int), svalue (float)

Data Group C: Sediment Transport Simulation Parameters (continued)

13	“NSYIELDS” (char), ncyields (int)
	for iyield = 1, nsyields
14	syldfrom[iyield] (int), syldto[iyield] (int), syldprocess[iyield] (int), syield[iyield] (float) (g/g)
Note	Records 10, 11, 12, and 13 are repeated as a group for i = 1, nsolids. Record 10 is input once. Records 11 and 12 are repeated as a group for iflds = 1, nflds[i]. Within this group, Record 12 is repeated for icns = 1, ncns. Record 13 is input once. Record 14 is repeated for iyield = 1, nyields.
15 (ICov)	Header (string): “SOIL CHARACTERISTICS: erosion parameters, grain size distribution etc.”
16	“NSOILS” (char), nsoils (int) {number of soil types}
PED...	for isoil = 1, nsoils
	if infiltopt = 0 {no infiltration, but there still is sediment transport}
	if ersovopt <= 1
17	kusle[isoil] (float) (dimensionless), vcov[isoil] (float) (m/s), porosityov[isoil] (float), soilname[isoil] (string) {for ksim >1, infopt = 0, and ersovopt = 1, kusle is the only soil parameter specified; cusle and pusle are land use parameters...}
	else (ersovopt > 1)
18	mexpov[isoil] (float) (dimensionless), porosityov[isoil] (float), soilname[isoil] (string)
	endif ersovopt <= 1
	elseif infopt > 0 {both infiltration and sediment transport}
	if ersovopt <= 1
19	kusle[isoil] (float) (dimensionless), vcov[isoil] (float) (m/s), porosityov[isoil] (float) (dimensionless), kh[isoil] (float) (m/s), capsh[isoil] (float) (m), soilmd[isoil] (float) (dimensionless), soilname[isoil] (string)
	else (ersovopt > 1)
20	mexpov[isolid] (float) (dimensionless), porosityov[isoil] (float) (dimensionless), kh[isoil] (float) (m/s), capsh[isoil] (float) (m), soilmd[isoil] (float) (dimensionless), soilname[isoil] (string)
	endif ersovopt <= 1
21a (label)	“SoilGSD:” (char)
	for isoil=1, nsolids
21b (gsd)	gsdov[isoil][isolid] (float)
Check	Compute gsdovtot += gsdov[isoil][isolid]. If gsdovtot != 1.0 then abort.

Data Group C: Sediment Transport Simulation Parameters (continued)

Note	Record 17/18/19/20 and 21 are repeated as a group. Only one Record (17 or 18 or 19 or 20) is entered. The record that is entered depends on the values of infopt and ersovopt. The group is repeated for isoil = 1, nsoils.
	endif infopt = 0
22	Header (string): “LAND USE CHARACTERISTICS: Cusle, grain size distribution”
23	“NLANDS” (char), nlands (int) {number of land use types}
	if ersovopt <= 1
	for iland = 1, nlands
24	nmanningov[iland] (float) (n units), interceptionclass[iland] (float) (mm), cusle[iland] (float) (dimensionless), pusle[iland] (float) (dimensionless), landname[iland] (string)
	else (ersovopt > 1)
	for iland = 1, nlands
25	nmanningov[iland] (float) (n units), interceptionclass[iland] (float) (mm), ayov[iland] (float) (g/cm2), landname[iland] (string)
	endif ersovopt <= 1
Note	Only one Record (24 or 25) is entered. The record that is entered depends on the value of ersovopt and is repeated for iland = 1, nlands.
26	“LAND_USE” (char), landusefile (string)
	call ReadLandUseFile
27	Header (string): “SOIL STACK AND LAYER PROPERTIES: thickness, grain size distribution”
28	“MAXSTACKOV” (char), maxstackov (int), “MINVOLOV” (char), minvolov (float) (dimensionless), “MAXVOLOV” (char), maxvolov (float) (dimensionless), “STKOVOPT” (char), stkovopt (int)
29	“SOIL_STACK” (char), soilstackfile (string)
	call ReadSoilStackFile
	for i = maxstackov to 1 (reverse order)
30	“THICKNESS_LAYERn” (char), thicknessgrid (string)
	Read SoilLayerThicknessFile
31	“SOIL_TYPES_LAYERn” (char), soilfile (string)
	call ReadSoilTypeFile
Note	The information for Records 30 and 31 is read in reverse order (layer 1 is last).

Data Group C: Sediment Transport Simulation Parameters (continued)

32	Header (string): “INITIAL SUSPENDED SOLIDS CONCENTRATIONS IN THE OVERLAND PLANE: one grid file for each solids type”
	for isolid=1, nsolids
33	“GRIDFILE_FOR_SOLIDn” (char), initialssovfile (string)
	call ReadInitialSolidsOverland
Note	Record 32 is input once. Record 33 is repeated for isolid
	if chnopt > 0
34 (ICch)	Header (string): “SEDIMENT STACK CHARACTERISTICS AND LAYER PROPERTIES: number of layers, thickness, grain size distribution”
35	“MAXSTACKCH” (char), maxstackch (int), “MINVOLCH” (char), minvolch (float) (dimensionless), “MAXVOLCH” (char), maxvolch (float) (dimensionless), “STKCHOPT” (char), stkchopt (int)
36	“SEDIMENT_PROPERTIES_FILE” (char), sedimentpropertiesfile (string) this may need to include nstackch0 and erosion properties if erschopt > 1
	call ReadSedimentPropertiesFile
37	“INITIAL_SUSP_SOLIDS_CHANNELS” (char), initialsschfile (string)
	call ReadInitialSolidsChannelFile
	endif chnopt > 0
	for isolid = 1, nsolids
38 (Wov)	“NUMBER_OF_OVERLAND_LOADS_FOR_SOLIDSn” (char), nswov[isolid] (int)
	if nswov[isolid] > 0
39	“CONV1” (char), convunits (float), “CONV2” (char), convtime (float), “SCALE” (char), scale (float)
	for isw = 1, nswov[isolid]
40	swovrow[isolid][isw] (int), swovcol[isolid][isw] (int), nswovpairs[isolid][isw] (int), swovopt[isolid][isw] (int), loadname (string) {read to end of line}
	for iswpair = 1, nswovpairs[isolid][isw]
41	swov[isolid][isw][iswpair] (float) (kg/day), swovtime[isolid][isw][iswpair] (float) (hrs)
	endif nswch[isolid] > 0
Note	Records 38, 39, 40, and 41 are repeated as a group for isolid = 1, nsolids. Record 38 is input once. Record 39 is input once. Records 40 and 41 are repeated as a group for isw = 1, nswov[isolid]. Record 41 is repeated for iswpair = 1, nswovpairs[isolid][isw]
	if chnopt > 0

Data Group C: Sediment Transport Simulation Parameters (continued)

42 (Wch)	“NUMBER_OF_CHANNEL_LOADS_FOR_SOLIDSn” (char), nswch[isolid] (int)
	if nswch[isolid] > 0
43	“CONV1” (char), convunits (float), “CONV2” (char), convtime (float), “SCALE” (char), scale (float)
	for isw = 1, nswch[isolid]
44	swchlink[isolid][isw] (int), swchnode[isolid][isw] (int), nswchpairs[isolid][isw] (int), loadname (string) {read to end of line}
	for iswpair = 1, nswchpairs[isolid][isw]
45	swch[isolid][isw][iswpair] (float) (kg/day), swchtime[isolid][isw][iswpair] (float) (hrs)
Note	Records 42, 43, 44, and 44 are repeated as a group for isolid = 1, nsolids. Record 42 is input once. Record 43 is input once. Records 44 and 45 are repeated as a group for isw = 1, nswch[isolid]. Record 45 is repeated for iswpair = 1, nswchpairs[isolid][isw]
	endif nswch[isolid] > 0
	endif chnopt > 0
	for ioutlet = 1, noutlets
	if dbcopt[ioutlet] > 0
46 (BC)	Header (string) {read to end of line} {Example: “SOLIDS BOUNDARY CONDITIONS FOR OUTLET ioutlet”}
47	“CONV1” (char), convunits (float), “CONV2” (char), convtime (float), “SCALE” (char), scale (float)
	for isolid = 1, nsolids
48	nsbcpairs[ioutlet][isolid] (int), bcname (string) {read to end of line} {Example: “BOUNDARY CONDITIONS FOR SOLID TYPE isolid”}
	for isbcpair = 1, nsbcpairs[ioutlet]
49	sbc[ioutlet][isolid][isbcpair] (float) (g/m3), sbctime[ioutlet][isolid][isbcpair] (float) (hrs)
Note	Records 46, 47, 48, and 49 are repeated as a group for ioutlet = 1, noutlets. Record 46 is input once. Records 47, 48, and 49 are only input if dbcopt[ioutlet] > 0. Record 47 is input once. Records 48 and 49 are repeated as a group for isolid = 1, nsolids. Within this group, Record 49 is repeated for isbcpairs = 1, nsbcpairs[ioutlet].
	endif dbcopt[ioutlet] > 0
50	“NSEDREPORTS” (char), nsedreports (int)
	for isedreport = 1, nsedreports

Data Group C: Sediment Transport Simulation Parameters (continued)

51	sedreprow[isedreport] (int), sedrepcol[isedreport] (int), sedarea[isedreport] (float) (km2), sedunitsopt[isedreport] (int) {1 = g/m3, 2 = kg (mass transported over the reporting interval)}, stationid (char)
Note	Record 51 is repeated for isedreport = 1, nsedreports. Reports are for all solids types simulated
	endif ksim >= 2

4.2.4 Data Group D: Contaminant Transport Simulation Parameters

Data Group D: Contaminant Transport Simulation Parameters

Record	*Description*
	if ksim >= 3 then (if ksim >= 3, then chemical transport is simulated)
1	Header (string)
2	"NCHEMICALS" (char), nchems (int), "NCGROUPS" (char), ncgroups (int)
Note	nchems = number of chemical types, ncgroups = number of reporting groups for chemicals, chemicals in a reported group are summed for a group total
3	Header (string): "CHEMICAL GROUP NAMES FOR REPORTING"
	for igroup = 1, ncgroups
4	chemgroupname[igroup] (char)
Note	Record 4 is repeated for igroup = 1, ncgroups.
5	Header (string): "PROPERTIES FOR CHEMICALS"
	for ichem = 1, nchems
6	"CHEMICAL n" (char), ichem (int) (dummy), "NFIELDS" (char), nflds[ichem] (int), "GROUPNUMBER" (char), cgroupnumber[ichem] (int), chemname[ichem] (string)
	for ifields = 1, nfields[ichem]
7	ncns (int), fieldname (string)
	for icns = 1, ncns
8	cname (char), cid (int), cvalue (float)
9	"NCYIELDS" (char), ncyields[ichem] (int)
	for iyield = 1, ncyields
10	cyldfrom[iyield] (int), cyldto[iyield] (int), cyidprocess[iyield] (int), cyield[iyield] (float) (g/g)

Data Group D: Contaminant Transport Simulation Parameters (continued)

Note	Records 5, 6, 7, 8, and 9 are repeated as a group for ichem = 1, nchems. Record 5 is input once. Records 6, 7, and 8 are repeated as a group for iflds = 1, nflds[ichem]. Within this group, Record 8 is repeated for icns = 1, ncns. Record 9 is input once. Record 10 is repeated for iyield = 1, ncyields.
11 (ICov)	Header (string): “INITIAL CHEMICAL CONCENTRATIONS IN SOIL”
	for ilayer = maxlayersov, 1, -1 (reverse order, all possible layers even if null)
	for ichem = 1, nchems
12	“SOIL_ICs_LAYER_ilayer_CHEMICAL_n” (char), soilchemfile (string) (mg/kg)
	call ReadSoilLayerChemicalFile()
Note	Record 12 is repeated for for ilayer = maxlayersov, 1, -1 (reverse order) and ichem = 1, nchems. One grid file for each chemical repeated for each layer.
	for ichem = 1, nchems
13	Header (string): “INITIAL CHEMICAL CONCENTRATIONS IN THE OVERLAND PLANE WATER COLUMN: one grid file for each chemical type”
	for ichem=1, nchems
14	“GRIDFILE_FOR_CHEMICALn” (char), initialchemovfile (string)
	call ReadInitialChemicalOverland
Note	Record 13 is input once. Record 14 is repeated for ichem = 1, nchems
	if chnopt > 0
15 (ICch)	Header (string): “INITIAL CHEMICAL CONCENTRATIONS IN SEDIMENT”
16	“CHEMICAL_SEDIMENT_CONCENTRATION_FILE” (char), sedimentchemfile (string) (mg/kg)
	call ReadSedimentChemicalFile
17	“INITIAL_CHEMICAL_CHANNELS” (char), initialchemchfile (string)
	call ReadInitialChemicalChannelFile
	endif chnopt = 1
	for ichem = 1, nchems
18 (Wov)	“NUMBER OF OVERLAND LOADS FOR CHEMICAL n” (char), ncwov[ichem] (int)
	if ncwov[ichem] > 0
19	“CONV1” (char), conunit (float), “CONV2” (char), contime (float), “SCALE” (char), scale (float)
	for icw = 1, ncwov[ichem]

Data Group D: Contaminant Transport Simulation Parameters (continued)

20	cwovlink[ichem][icw] (int), cwovnode[ichem][icw] (int), ncwovpairs[ichem][icw] (int), loadname (string)
	for icwpair = 1, ncwovpairs[icw]
21	cwov[ichem][icw][icwpair] (float) (kg/day), cwovtime[ichem][icw][icwpair] (float) (hrs)
Note	Records 18, 19, 20, and 21 are repeated as a group for ichem = 1, nchems. Record 18 and 19 are each input once. Records 20 and 21 are repeated for icw = 1, ncwov[ichem]. Record 21 is repeated for icwpair = 1, ncwovpairs[ichem][icw]. Loads for channels only, input as kg/day.
	endif ncwov[ichem] > 0
	if chnopt > 0
	for ichem = 1, nchems
22 (Wch)	"NUMBER OF CHANNEL LOADS FOR CHEMICAL n" (char), ncwch[ichem] (int)
	if ncwch[ichem] > 0
23	"CONV1" (char), conunit (float), "CONV2" (char), contime (float), "SCALE" (char), scale (float)
	for icw = 1, ncwch[ichem]
24	cwchlink[ichem][icw] (int), cwchnode[ichem][icw] (int), ncwchpairs[ichem][icw] (int), loadname (string)
	for icwpair = 1, ncwovpairs[icw]
25	cwch[ichem][icw][icwpair] (float) (kg/day), cwchtime[ichem][icw][icwpair] (float) (hrs)
Note	Records 22, 23, 24, and 25 are repeated as a group for ichem = 1, nchems. Record 22 and 23 are each input once. Records 24 and 25 are repeated for icw = 1, ncwch[ichem]. Record 25 is repeated for icwpair = 1, ncwchpairs[ichem][icw]. Loads for channels only, input as kg/day.
	endif ncwch[ichem] > 0
	endif chnopt > 0
	for ioutlet = 1, noutlets
	if dbcopt[ioutlet] > 0
26 (BC)	Header (string) {read to end of line} {Example: "CHEMICAL BOUNDARY CONDITIONS FOR OUTLET ioutlet"}
27	"CONV1" (char), convunits (float), "CONV2" (char), convtime (float), "SCALE" (char), scale (float)
	for ichem = 1, nchems

Data Group D: Contaminant Transport Simulation Parameters (continued)

28	nsbcpairs[ioutlet][isolid] (int), bcname (string) {read to end of line} {Example: "BOUNDARY CONDITIONS FOR CHEMICAL TYPE ichem"}
	for icbcpair = 1, ncbcpairs[ioutlet]
29	cbc[ioutlet][ichem][icbcpair] (float) (g/m3), cbctime[ioutlet][ichem][icbcpair] (float) (hrs)
Note	Records 26, 27, 28, and 29 are repeated as a group for ioutlet = 1, noutlets. Record 26 is input once. Records 27, 28, and 29 are only input if dbcopt[ioutlet] > 0. Record 27 is input once. Records 28 and 29 are repeated as a group for ichem = 1, nchems. Within this group, Record 29 is repeated for icbcpairs = 1, ncbcpairs[ioutlet].
	endif dbcopt[ioutlet] > 0
30	"NCHEMREPORTS" (char), nchemreports (int)
	for ichemreport = 1, nchemreports
31	chemreprow[ichemreport] (int), chemrepcol[ichemreport] (int), chemarea[ichemreport] (float) (km2), chemunitsopt[ichemreport] (int) {1 = g/m3, 2 = kg (mass transported over the reporting interval)}, stationid (char)
Note	Record 31 is repeated for: ichemreport = 1, nchemreports. Reports are for all chemical types simulated.
	endif ksim >= 3

4.2.5 Data Group E: Environmental Properties

Note that environmental properties are developmental features that are not fully implemented at this time. For chemical transport simulations (ksim =3), Records 1, 2, 10, and 27 are entered. If channels are simulated (chnopt > 0), Record 20 and 37 are also entered. For each of these records, the required input value should each be set to zero until the features of Data Group E are fully implemented.

Data Group E: Environmental Properties (ph, water temp, air temp, etc)

Record	*Description*
1	Header (string) "Data Group E: Environmental Properties"
2	"General_Environmental_Properties_NPROPG" (char), npropg (int)
	for iprop=1, npropov
3	pname (char), pid (int), "CONV1" (char), convunits (float), "SCALE" (char), scale (float), "NFUNCTIONS" (char) (dummy), nenvgtf (int)
4	"Cell_Value_Grid" (char), parameterfile (string)
	call ReadGeneralEnvironmentFile(pid, ilayer, conv1, scale)

Data Group E: Environmental Properties (continued)

	if nenvgtf[iprop] > 0
5	“TimeFunction_Pointer_Grid” (char), tfpointerfile (string)
	call ReadGeneralFunctionPointerFile(iprop)
	for itf=1, nenvgtf[iprop]
6	“TimeFunctionID” (char), tfid (int), tfname (string)
7	“CONV1” (char), convunits (float), “CONV2” (char), convtime (float), “SCALE” (char), scale (float)
8	“NTFGPAIRS”(char), nenvgtfpairs[iprop][itf] (int)
	for itfpair = 1, nenvgtfpairs[iprop][itf]
9	envgtf[iprop][itf][itfpair] (float) (units vary), envgtftime[iprop][itf][itfpair] (float) (hrs)
Note	Units for time function values vary.
	endif nenvgtf[iprop] > 0
Note	Records 3 through 9 are repeated as a group for iprop = 1, npropg. Records 3 and 4 are input once. If nenvgtf[iprop] > 0, Records 5 through 9 are input. Record 5 is input once. Records 6, 7, 8, and 9 are repeated as a group for itf = 1, nenvovtf[iprop]. Within this group, Records 6, 7, and 8 are each input once and Record 9 is repeated for itfpairs = 1, nenvgtfpairs[iprop][itf].
	if ksim > 2
10	“Overland_Environmental_Properties_NPROPOV” (char), npropov (int)
	for iprop=1, npropov
11	pname (char), pidov (int), “CONV1” (char), convunits (float), “SCALE” (char), scale (float), “NFUNCTIONS” (char) (dummy), nenvovtf (int)
12	“Cell_Value_Grid_Layer_n” (char), parameterfile (string)
	call ReadOverlandEnvironmentFile(pid, 0, conv1, scale)
	if nenvovtf[iprop] > 0
13	“TimeFunction_Pointer_Grid” (char), tfpointerfile (string)
	call ReadOverlandFunctionPointerFile(pid, ilayer, conv1, scale)
	endif nenvovtf[iprop] > 0
	for ilayer = maxstackov, 1, -1 {Reverse Order!!}
14	“Cell_Value_Grid_Layer_n” (char), parameterfile (string)
	call ReadOverlandEnvironmentFile
	if nenvovtf[iprop] > 0

Data Group E: Environmental Properties (continued)

15	“TimeFunction_Pointer_Grid” (char), tfpointerfile (string)
	call ReadOverlandFunctionPointerFile
	endif nenvovtf[iprop] > 0
	if nenvovtf[iprop] > 0
	for itf=1, nenvovtf[iprop]
16	“TimeFunctionID” (char), tfid (int), tfname (string)
17	“CONV1” (char), convunits (float), “CONV2” (char), convtime (float), “SCALE” (char), scale (float)
18	“NTFOVPAIRS”(char), nenvovtfpairs[iprop][itf] (int)
	for itfpair = 1, nenvovtfpairs[iprop][itf]
19	envovtf[iprop][itf][itfpair] (float) (units vary), envovtftime[iprop][itf][itfpair] (float) (hrs)
Note	Units for time function values vary.
Note	Records 11 through 19 are repeated as a group for iprop = 1, npropov. Records 11 and 12 are input once. If nenvovtf[iprop] > 0, Record 13 is input once. Records 14 and 15 are input only if ksim > 1 and are repeated as a group for ilayer = maxstackov, 1, -1 (in reverse order). Within this group, Record 16 is only input if nenvovtf[iprop] > 0. Records 16, 17, 18 and 19 are repeated as a group for itf = 1, nenvovtf[iprop]. Within this group, Records 16, 17, and 18 are each input once and Record 19 is repeated for itfpairs = 1, nenvovtfpairs[iprop][itf].
	end if nenvovtf[iprop] > 0
	if chnopt > 0
20	“Channel_Environmental_Properties_NPROPCH” (char), npropch (int)
	for iprop=1, npropch
21	pname (char), pidch (int), fname (char), “CONV1” (char), convunits (float), “SCALE” (char), scale (float), “NFUNCTIONS” (char) (dummy), nenvchtf (int)
22	“ENV_PROPERTY_FILE_FOR_CHANNEL” (char), parameterfile (string) {water column and sediment stack}
	call ReadChannelEnvironmentFile(pid, 0, conv1, scale)
	if nenvchtf[iprop] > 0
	for itf=1, nenvchtf[iprop]
23	“TimeFunctionID” (char), tfid (int), tfname (string)
24	“CONV1” (char), convunits (float), “CONV2” (char), convtime (float), “SCALE” (char), scale (float)

Data Group E: Environmental Properties (continued)

25	“NTFCHPAIRS”(char), nenvchtfpairs[iprop][itf] (int)
	for itfpair = 1, nenvchtfpairs[iprop][itf]
26	envchtf[iprop][itf][itfpair] (float) (units vary), envchtftime[iprop][itf][itfpair] (float) (hrs)
Note	Units for time function values vary.
Note	Records 21, through 26 are repeated as a group for iprop = 1, npropch. Records 21 and 22 are input once. Records 23, 24, 25, and 26 are repeated as a group for itf = nenvchtf[iprop]. Within this group, Records 23, 24, 25 are input once and Record 29 is repeated for itfpair = 1, nenvchtfpairs[itf].
	end if nenvchtf > 0
27	“Overland_Particle_Organic_Carbon_FPOCOVOPT” (char), fpocovopt (int)
Note	fpocovopt is the option for specification of particle organic carbon content: 0 = fpoc for the overland plane not specified (the default value is 1.0, i.e. fpocov[isolid][row][col][layer] = 1.0 and is contant in space and time) 1 = a grid of values for each particle type with associated time functions and pointers is entered for the overland plane (water column and soil stack) and a channel environmental property file with associated time functions and pointers is entered for the channel network
	if focopt > 0
	for isolid=1, nsolids
28	“SOLIDTYPE” (char), pid (int), “SCALE” (char), scale (float), “NFUNCTIONS” (char), nfpocovtf (int)
29	“Cell_Value_Grid_Layer_n” (char), parameterfile (string)
	call ReadOverlandFpocFile(isolid, 0, conv1, scale)
	if nfpocovtf[isolid] > 0
30	“TimeFunction_Pointer_Grid” (char), tfpointerfile (string)
	call ReadOverlandFpocTFPointerFile(pid, ilayer, conv1, scale)
	endif nfpocovtf[isolid] > 0
	if ksim > 1 {ksim must be > 1}
	for ilayer = maxstackov, 1, -1 {Reverse Order!!}
31	“Cell_Value_Grid_Layer_n” (char), parameterfile (string)
	call ReadOverlandFpocFile
	if nfpocovtf[isolid] > 0
32	“TimeFunction_Pointer_Grid” (char), tfpointerfile (string)

Data Group E: Environmental Properties (continued)

	call ReadOverlandFpocTFPointerFile(isolid)
	endif nfpocovtf[isolid] > 0
Note	Records 31 and 32 are repeated as a block for ilayer=maxstackov, 1, -1 (reverse order).
	if nfpocovtf[isolid] > 0
	for itf=1, nfpovovtf[isolid]
33	"TimeFunctionID" (char), tfid (int), tfname (string)
34	"CONV1" (char), convunits (float), "CONV2" (char), convtime (float), "SCALE" (char), scale (float)
35	"NTFOVPAIRS"(char), nfpocovtfpairs[isolid][itf] (int)
	for itfpair = 1, nfpocovtfpairs[isolid][itf]
36	fpocovtf[isolid][itf][itfpair] (float) (units vary), fpocovtftime[isolid][itf][itfpair] (float) (hrs)
Note	Units for time function values vary.
	end if nfpocovtf[isolid] > 0
Note	Records 11 through 19 are repeated as a group for isolid = 1, npropov. Records 11 and 12 are input once. If nfpocovtf[isolid] > 0, Record 13 is input once. Records 14 and 15 are input only if ksim > 1 and are repeated as a group for ilayer = maxstackov, 1, -1 (in reverse order). Within this group, Record 16 is only input if nfpocovtf[isolid] > 0. Records 16, 17, 18 and 19 are repeated as a group for itf = 1, nfpocovtf[isolid]. Within this group, Records 16, 17, and 18 are each input once and Record 19 is repeated for itfpairs = 1, nfpocovtfpairs[isolid][itf].
	endif fpocovopt > 0
	if chnopt > 0
37	"Channel_Particle_Organic_Carbon_FPOCCHOPT" (char), fpocchopt (int)
Note	fpocchopt is the option for specification of particle organic carbon content: 0 = fpoc for the channel is not specified (the default value is 1.0, i.e. fpocch[isolid][link][node][layer] = 1.0 and is contant in space and time) 1 = a channel environmental property file with associated time functions and pointers is entered for the channel network
	if fpocchopt > 0
38	pname (char), pid (int), "SCALE" (char), scale (float), "NFUNCTIONS" (char) (dummy), nfpocchtf (int)

Data Group E: Environmental Properties (continued)

39	"Fpoc_PROPERTY_FILE_FOR_CHANNEL" (char), parameterfile (string) {water column and sediment stack}
	call ReadChannelFpocFile(pid, 0, conv1, scale)
	if nfpocchtf[iprop] > 0
	for itf=1, nfpocchtf[iprop]
40	"TimeFunctionID" (char), tfid (int), tfname (string)
41	"CONV1" (char), convunits (float), "CONV2" (char), convtime (float), "SCALE" (char), scale (float)
42	"NTFCHPAIRS"(char), nfpocchtfpairs[iprop][itf] (int)
	for itfpair = 1, nfpocchtfpairs[iprop][itf]
43	fpocchtf[iprop][itf][itfpair] (float) (units vary), fpocchtftime[iprop][itf][itfpair] (float) (hrs)
Note	Units for time function values vary.
	endif fpocchopt > 0
	endif ksim > 2

4.2.6 Data Group F: Ouput Specification Controls

Data Group F: Ouput Specification Controls

Record	*Description*
1	Header (string)
	if nqreports > 0
2	Header (string) such as "EXPORT TIME SERIES OUPUTS"
3	"WATER_EXPORT" (char), waterexpfile (string)
	if ksim > 1 and nsedreports > 0
4	"SEDIMENT_EXPORT_ROOT" (char), sedexprootfile (string)
5	"SEDIMENT_EXPORT_EXT" (char), sedextension (string)
	if ksim > 2 and nchemreports > 0
6	"CHEMICAL_EXPORT_ROOT" (char), chemexpfile (string)
7	"CHEMICAL_EXPORT_EXT" (char), chemextention (string)
	endif ksim > 2

Data Group F: Ouput Specification Controls (continued)

	endif ksim > 1
8	Header (string) such as “POINT-IN-TIME GRID OUPUTS”
9	“RAINFALL_RATES” (char), rainrategrid (string) (Path and file name)
10	“RAINFALL_DEPTH” (char), raindepthgrid (string) (Path and file name)
11	“INFILTRATION_RATE” (char), infrategrid (string) (Path and file name)
12	“INFILTRATION_DEPTH” (char), infdepthgrid (string) (Path and file name)
13	“WATER_DISCHARGE” (char), qgrid (string) (Path and file name)
14	“WATER_DEPTH” (char), waterdepthgrid (string) (Path and file name)
Note	if other water related grids are desired (i.e. snowmelt), add them here...
	if ksim > 1
15	“SOLID_CONC_WATER_ROOT” (char), solidsconcwatergridroot (string) (report for total and groups) (Path...\root)
16	“SOLID_CONC_SURFACE_LAYER_ROOT” (char), solidsconcsurfgridroot (string) (report for total and groups) (Path...\root)
	if ksim > 2
17	“TOTCHEM_CONC_WATER_ROOT” (char), totchemconcwatergridroot (string) (report for total and groups) (Path...\root)
18	“DISCHEM_CONC_WATER_ROOT” (char), dischemconcwatergridroot (string) (report for groups) (Path...\root)
19	“BNDCHEM_CONC_WATER_ROOT” (char), bndchemconcwatergridroot (string) (report for groups) (Path...\root)
20	“PRTCHEM_CONC_WATER_ROOT” (char), prtchemconcwatergridroot (string) (report for groups) (Path...\root)
21	“TOTCHEM_CONC_SURFACE_LAYER_ROOT” (char), totchemconcsurfgridroot (string) (report for total and groups) (Path...\root)
22	“DISCHEM_CONC_SURFACE_LAYER_ROOT” (char), dischemconcsurfgridroot (string) (report for groups) (Path...\root)
23	“BNDCHEM_CONC_SURFACE_LAYER_ROOT” (char), bndchemconcsurfgridroot (string) (report for groups) (Path...\root)
24	“PRTCHEM_CONC_SURFACE_LAYER_ROOT” (char), prtchemconcsurfgridroot (string) (report for groups) (Path...\root)
25	“DISCHEM_FRAC_WATER_ROOT” (char), dischemfracwatergridroot (string) (report for total and groups) (Path...\root)

Data Group F: Ouput Specification Controls (continued)

26	“BNDCHEM_FRAC_WATER_ROOT” (char), bndchemfracwatergridroot (string) (report for groups) (Path...\root)
27	“MOBCHEM_FRAC_WATER_ROOT” (char), mobchemfracwatergridroot (string) (report for groups) (Path...\root)
28	“PRTCHEM_FRAC_WATER_ROOT” (char), prtchemfracwatergridroot (string) (report for groups) (Path...\root)
29	“DISCHEM_FRAC_SURFACE_LAYER_ROOT” (char), dischemfracsurfgridroot (string) (report for total and groups) (Path...\root)
30	“BNDCHEM_FRAC_SURFACE_LAYER_ROOT” (char), bndchemfracsurfgridroot (string) (report for groups) (Path...\root)
31	“MOBCHEM_FRAC_SURFACE_LAYER_ROOT” (char), mobchemfracsurfgridroot (string) (report for groups) (Path...\root)
32	“PRTCHEM_FRAC_SURFACE_LAYER_ROOT” (char), prtchemfracsurfgridroot (string) (report for groups) (Path...\root)
33	“CHEMICAL_INFILTRATION_GRID_ROOT” (char), infchemfluxgridroot (string) (report for groups) (Path...\root)
	endif ksim > 2
34	Header (string) such as “CUMULATIVE TIME GRID OUTPUTS”
35	“NET_ELEVATION_CHANGE” (char), netelevationgrid (string) (Path and filename)
36	“SOLIDS_GROSS_EROSION” (char), solidserosiongridroot (string) (report for groups) (Path...\root)
37	“SOLIDS_GROSS_DEPOSITION” (char), solidsdepositiongridroot (string) (report for groups) (Path...\root)
38	“SOLIDS_NET_ACCUMULATION” (char), solidsnetaccumgridroot (string) (report for groups) (Path...\root)
	“SOLIDS_GROSS_EROSION” (char), solidserosiongridroot (string) (report for groups) (Path...\root)
	if ksim > 2
39	“CHEMICAL_GROSS_EROSION” (char), chemerosiongridroot (string) (report for groups) (Path...\root)
40	“CHEMICAL_GROSS_DEPOSITION” (char), chemdepositiongridroot (string) (report for groups) (Path...\root)
41	“CHEMICAL_NET_ACCUMULATION” (char), chemnetaccumgridroot (string) (report for groups) (Path...\root)
	endif ksim > 2
	endif ksim > 1

Data Group F: Ouput Specification Controls (continued)

42	Header (string) such as “SIMULATION SUMMARY OUPUTS”
43	“DUMP_FILE” (char), dmpfile (string) (Path and file name)
44	“MASS_BALANCE” (char), msbfile (string) (Path and file name)
45	“SUMMARY_STATISTICS” (char), statsfile (string) (Path and file name)

4.3 ANCILLARY MODEL INPUT FILES

Ancillary input files are used to describe characteristics of the model domain such as watershed boundary mask, elevations, soil classes, and land uses, etc. Ancillary files for the overland plane are organized as grid files (such as those that can be exported from ESRI’s ArcGIS software) that include a header block and a block of grid values specified by row and column. While the exact grid values specified in the ancillary files for the overland plane differ, the format for each file is the same. Users should note that the header used for grid files differs slightly from the native format exported from ArcGIS software. Ancillary files for the channel network are organized as “channel property files” and “sediment property files”. These files specify conditions for each link of the network on a node by node basis. The exact format of each channel or sediment property files differs slightly according to the type of data input.

4.3.1 General Format for Spatial Domain Characteristics Files (Grid Files)

General Format for Spatial Domain Characteristics Files (Grid Files)

Record	*Description*
1	Header1 (string)
2	“NCOLS” (char), gridcols (int)
3	“NROWS” (char), gridrows (int)
4	“XLLCORNER” (char), xllcorner (float)
5	“YLLCORNER” (char), yllcorner (float)
6	“CELLSIZE” (char), cellsize (float)
7	“NODATAVALUE” (char), nodatavalue (int)
	for i = 1, gridrows
	for j = 1, gridcols
8	girdvalue[i][j] (int or float depending on grid) {gridvalue is a sample name...}
Note	Record 8 is repeated for j = 1, grid cols and then repeated again for i = 1, gridrows.

General Format for Spatial Domain Characteristics Files (Grid Files) (continued)

Also Note	Data input is unformatted. However, a typical file will have gridrows number of lines with gridcols number of entries on each line.
Grid Types	Grid files are input for: the simulation mask (int) (imask[][]), ground elevation (float) (elevation[][]), soil types (int) (soiltype[][]), land use classes (int) (landuse[][]), links (int) (link[][]), nodes (int) (nodes[][]), storage depths in the overland plane (float), initial water depths in the overland plane (float), and soil stack elements (int).

4.3.2 Description and Organization of Channel Property and Topology Files

Channel Property File {input for tplgyopt = 0}

Record	*Description*
1	Header {string}
2	CHANLINKS (char), chanlinks (int)
Note	The number of links in the network (nlinks) is already known from the link file. This information is used to check that the channel properties file is compatible with the link file.
	for ilink = 1, nlinks
3	linknum (int) {dummy}, nnodes[ilink] (int)
	for inode = 1, nnodes[ilink]
4	bwidth[ilink][inode] (float), sideslope[ilink][inode] (float), hbank[ilink][inode] (float), nmanning_ch[ilink][inode] (float), sinuosity[ilink][inode] (float), deadstoragedepth[ilink][inode] (float)
Note	Records 3 and 4 are repeated as a group for ilink = 1, nlinks. Record 4 is repeated for inode = 1, nnodes[ilink].

External Channel Topology File {input for tplgyopt = 1} (Not fully implemented)

Record	*Description*
1	Header {string}
2	nlinks (int) {number of links in network}
	for ilink = 1, nlinks
3	linknum (int) {dummy}, nnodes[ilink] (int), downstreamlink[ilink] (int) {the downstream link always starts with the first element of the downstream link...}
	for inode = 1, nnodes[ilink]

External Channel Topology File {input for tplgyopt = 1} (continued)

4	crow (int), ccol (int), bwidth[ilink][inode] (float), sideslope[ilink][inode] (float), hbank[ilink][inode] (float), nmanningch[ilink][inode] (float), sinuosity[ilink][inode] (float), deadstorage[ilink][inode] (float)
Note	Records 3 and 4 are repeated as a group for ilink = 1, nlinks. Record 4 is repeated for inode = 1, nnodes[ilink].

Channel Initial Water Depth File

Record	*Description*
1	Header {string}
2	CHANLINKS (char), chanlinks (int)
Note	The number of links in the network (nlinks) is already known from the link file. This information is used to check that the initial water file is compatible with the link file.
	for ilink = 1, nlinks
3	linknum (int) {dummy}, nnodes[ilink] (int)
	for inode = 1, nnodes[ilink]
4	hch0[ilink][inode] (float)
Note	Records 3 and 4 are repeated as a group for ilink = 1, nlinks. Record 4 is repeated for inode = 1, nnodes[ilink].

Channel Transmission Loss Property File (used only when ksim = 1 and ctlopt > 0)

Record	*Description*
1	Header {string}
2	CHANLINKS (char), chanlinks (int)
Note	The number of links in the network (nlinks) is already known from the link file. This information is used to check that the transmission loss file is compatible with the link file.
	for ilink = 1, nlinks
3	linknum (int) {dummy}, nnodes[ilink] (int)
	for inode = 1, nnodes[ilink]
4	khsed[ilink][inode] (float), capshsed[ilink][inode] (float), sedmd[ilink][inode] (float)
Note	Records 3 and 4 are repeated as a group for ilink = 1, nlinks. Record 4 is repeated for inode = 1, nnodes[ilink].

Channel Initial Transmission Loss Depth File

Record	*Description*
1	Header {string}
2	CHANLINKS (char), chanlinks (int)
Note	The number of links in the network (nlinks) is already known from the link file. This information is used to check that the initial transmission loss file is compatible with the link file.
	for ilink = 1, nlinks
3	linknum (int) {dummy}, nnodes[ilink] (int)
	for inode = 1, nnodes[ilink]
4	translossdepth0[ilink][inode] (float)
Note	Records 3 and 4 are repeated as a group for ilink = 1, nlinks. Record 4 is repeated for inode = 1, nnodes[ilink].

4.3.3 Description and Organization of Sediment Properties File

Sediment Properties File: Stack Extent, Porosity, Thickness, Grain Size Distribution

Record	*Description*
1	Header {string}
2	“CHANLINKS” (char), chanlinks (int), “CHANSOLIDS” (char), chansolids (int), “CHANERSCHOPT” (char), chanerschopt (int) {dummy}, “CHANCTLOPT” (char), chanctlopt (int) {dummy}
Note	The number of links in the network (nlinks) and number of particle types (nsolids) are already known from the link file and main input file. This information is input to check that the sediment properties file is compatible with the channel network and particle types.
	for ilink = 1, nlinks
3	“LINKNUMBER” (char), linknum (int) {dummy}, “NUMNODES” (char), channodes (int) {dummy}
	for inode = 1, nnodes[ilink]
4a	“NODE” (char), nodenum (int) {dummy), “NSTACK” (char), nstackch0[ilink][inode] (int)
	if erschopt > 1
4b	“YIELD” (char), aych[ilink][inode] (float) (g/cm2), “EXPONENT” (char), mexpch[ilink][inode] (float) (dimensionless)
	endif erschopt > 1

Sediment Properties File: Stack Extent, Porosity, Thickness, Grain Size Distribution (continued)

	if ctlopt > 0
4c	“KHSED” (char), kkhsed[ilink][inode] (float) {dummy), “CAPSHSED” (char), capshsed[ilink][inode] (float), “SEDMD” (char), sedmd[ilink][inode] (float)
	endif ctlopt > 0
Note	Record 4 has up to three components. Record 4a is always input. Record 4b is input only if erschopt > 1. Record 4b is input only if ctlopt > 1.
	for ilayer = nstackch0[ilink][inode], 1; ilayer-- {reverse order}
5	“LAYER” (char), layernum (int) {dummy}, “THICKNESS” (char), hlayerch0[ilink][inode][ilayer] (float) (m) {initial thickness of the layer}, “WIDTH” (char), bwlayerch0[ilink][inode][ilayer] (float) (m) {initial bottom width}, “POROSITY” (char), porositych[ilink][inode][ilayer] (float)
6a	“GSD:” (char)
	for isolid = 1, nsolids
6b	gsdch[isolid][ilink][inode][layer] (float)
Note	Records 3, 4a/b/c, 5, and 6a/b are repeated as a group for ilink = 1, nlinks. Within this outer block, Records 4a/b/c, 5, and 6a/b are repeated for inode=1, nnodes[ilink]. Within this inner block, Records 5 and 6a/b are repeated for ilayer = nstackch0[ilink][inode], 1 (ilayer--). Within this innermost block, Record 6b is repeated for isolid = 1, nsolids.
Check	Compute gsdchtot =+ gsd[ilink][inode][isolid][ilayer] and check that gsdchtot = 1.0. Abort if gsdchtot != 1.0 for each node of each link...

Channel Initial Suspended Solids File: initial solids concentration in the channel water column

Record	*Description*
1	Header {string}
2	“CHANLINKS” (char), chanlinks (int), “CHANSOLIDS” (char), chansolids (int)
Note	The number of links in the network (nlinks) and number of particle types (nsolids) are already known from the link file and main input file. This information is input as a check that the initial solids file is compatible with the channel network and particle types.
	for ilink = 1, nlinks
3	“LINKNUMBER” (char), linknum (int) {dummy}, “NUMNODES” (char), channodes (int) {dummy}

Channel Initial Suspended Solids File: initial solids concentration in the channel water column (continued)

	for inode = 1, nnodes[ilink]
4	“NODE” (char), nodenum (int) {dummy)
	for isolid = 1, nsolids
5	csedch[isolid][ilink][inode][0] (float)
Note	Records 3, 4, and 5 are repeated as a group for ilink = 1, nlinks. Within this block, Record 4 and 5 are repeated as a group for inode = 1, nnodes[ilink]. Within this innermost block, Record 5 is repeated for isolid = 1, nsolids.

4.3.4 Description and Organization of Environmental Properties Files

At this time, ancillary files for environmental properties as specified in Data Group E are not fully implemented.

5.0 DESCRIPTION AND ORGANIZATION OF MODEL OUTPUT FILES

TREX produces six categories of output files that echo model inputs, report simulation erros, and present a variety of simulation results. These six categories of output are:

1. Input data echo report;
2. Simulation error report;
3. Export times series;
4. Point-in-time grids;
5. Cumulative time grids; and
6. Simulation performance summaries.

The names of the specific output files in each category are specified by the user in the main model input file. Descriptions of the output in each category follow.

5.1 INPUT DATA ECHO REPORT

The input data echo report presents a summary (echo) of all model inputs read by TREX for a simulation. The echo file is useful for debugging model inputs. If input data are misaligned or other problems with data specified in the main model input file or any ancillary file are detected, the data summarized in the echo file will differ from the data in the input files.

5.2 SIMULATION ERROR REPORT

The simulation error report presents a summary of numerical integration errors detected during a run. This file provide information that may be helpful for diagnosing model stability errors such as the simulation time at which an error was detected, which model routine detected the error, and the cell in which the error occurred. For a successful simulation, the error file will be empty except for an echo of the main model input file used for the simulation.

5.3 EXPORT TIME SERIES OUTPUTS

Export times series are tabular outputs of values of model state variables at specified points in space (reporting stations) reported over time. Results are output according to the print interval specified in Data Group A of the main model input file. Export outputs can be specified for hydrology (water depth or flow at a station), sediment transport (solids concentration or load at a station), and chemical transport (chemical concentration or load

at a station). Export output files are written in a tab-delimited format to facilitate post-processing and analysis in spreadsheet or statistical software.

5.4 POINT-IN-TIME OUTPUTS

Point-in-time outputs are row-column grid files of model state variables over the entire spatial domain reported at a specific point in time. Results are output according to the grid print interval specified in Data Group A of the main model input file. Point-in-time outputs can be specified for hydrology (water depth or flow), sediment transport (solids concentrations including the sum of all solids types), and chemical transport (chemical concentrations by specific phase and phase distribution fractions). Point-in-time output files are written in a format that can be directly imported into geographic information system (GIS) software (in particular ESRI's ArcGIS or Arc/Info) for individual display and the creation of animations (sequential displays of grids for consecutive points in time).

5.5 CUMULATIVE TIME OUTPUTS

Cumulative time outputs are row-column grid files of model state variables over the entire spatial domain reported at the end of the simulation. Results are output once for the entire time period simulated. Cumulative time outputs can be specified for a number of parameters such as the net elevation change and the gross erosion, gross deposition, and net accumulation of solids or chemicals. Cumulative time output files are written in a format that can be directly imported into geographic information system (GIS) software (in particular ESRI's ArcGIS or Arc/Info).

5.6 SIMULATION SUMMARY OUTPUTS

Simulation summary outputs are divided into three formats: 1) a model dump file; 2) a detailed mass balance file; and 3) a summary statistics file. Each of these formats is described below.

5.6.1 The Model Dump File

Note: this output format is not yet implemented…

Once implemented, the model dump file will be a binary (direct access) file that contains an element-by-element, process-by-process, direction-by-direction report (dump) for each state variable for all points in space and all points in time in the model domain. A post-processing program will need to be created to extract binary output and write it in tabular or grid form for futher post-processing and analysis.

5.6.2 Detailed Mass Balance File

The detailed mass balance file is a file that contains an element-by-element, process-by-process, direction-by-direction cumulative summary of mass (or volume) that passed

through each element (overland cell or channel network node) in the model demain during the simulation period. Mass balance files are written in a tab-delimited format to facilitate post-processing and analysis in spreadsheet or statistical software.

5.6.3 Summary Statistics File

Summary statistics file is a simple text file that contains brief summaries of model performance and output for hydrology, sediment transport for the sum of all solids types and each solids type simulated, and chemical transport for each chemical type simulated. For each output class a simple mass balance is presented along with minimum and maximum values for the overland plane and channel network. The overall simulation runtime (wall clock, not CPU time) is also presented at the end of the file.

6.0 DEVELOPMENTAL FEATURES

The TREX framework is designed to be modular to allow future development and addition of expanded features. Future development plans call for addition of a wide range of chemical and particle transformation processes. In particular, chemical biodegradation, hydrolysis, oxidation, photolysis, radioactive decay, volatilization, and dissolution processes may be added to the basic chemical transport submodel. Further development efforts may also include addition of a nutrient submodel to simulate the nitrogen, phosphorus, and carbon cycles at the watershed scale.

To facilitate future expansion, a number of developmental features are present in TREX. These developmental features include provisions for:

1. Additional mass transfer and transformation processes for chemicals;

2. Mass transformation processes for solids (such as mineralization and abrasion);

3. Soil and sediment erosion rate formulations (erosion rates are presently estimated from transport capacity relationships); and

4. Environmental conditions (such as temperature, wind speed, solar radiation, etc.).

While not fully implemented, code for these features already exists in TREX in order to provide a template and speed full development. Descriptions of a number of these developmental features follow.

6.1 CHEMICAL MASS TRANSFER AND TRANSFORMATION PROCESSES

As previously noted, future development plans call for addition of a wide range of chemical and particle transformation processes. In particular, chemical biodegradation, hydrolysis, oxidation, photolysis, radioactive decay, volatilization, and dissolution processes may be added to the basic chemical transport submodel. Overviews of most of these processes are presented in the WASP5 (Ambrose et al. 1993) and IPX (Velleux et al. 2001) manuals. However, the basic computer code needed to implement all of these processes already exists within the TREX framework. Further, code for chemical dissolution and simple first-order biodegradation is fully developed but is untested. Because of their advanced state of development in TREX, overviews of chemical biodegradation and dissolution follow.

6.1.1 Chemical Biodegradation

Chemicals that can be metabolized or co-metabolized by bacteria or other microbes may be subject to transformation by biodegradation. The chemical biodegradation flux may be expressed as a simple first-order process as (after Ambrose et al. 1993):

$$\hat{J}_{bc} = k_b C_c V \tag{6.1}$$

where: $\hat{J}_{bc}$ = chemical biodegradation flux [M/T]

k_b = first-order chemical biodegradation rate [1/T]

C_c = total chemical concentration in the water column or porewater [M/L^3]

V = bulk volume (water and particles) [L^3]

6.1.2 Chemical Dissolution

Chemicals that exist in a pure solid phase and are not sorbed to particles can enter solution by dissolution. The chemical dissolution flux may be expressed as a mass rate of transfer from the pure solid phase to the dissolved (aqueous) phase as (Cussler, 1997; Lynch et al. 2003):

$$\hat{J}_{sc} = k_d \alpha \left(S - f_d C_c \right) \tag{6.2}$$

where: $\hat{J}_{sc}$ = chemical dissolution mass flux [M/T]

k_d = mass transfer coefficient for chemical dissolution [L/T]

$= \dfrac{D}{\delta}$

D = aqueous phase chemical diffusion coefficient for dissolution [L^2/T]

δ = boundary layer film thickness [L]

α = surface area available for mass transfer between solid and liquid [L^2]

S = aqueous solubility of the chemical [M/L^3]

f_d = fraction of the total chemical in the dissolved phase [dimensionless]

C_c = total chemical concentration in the water column or porewater [M/L^3]

Assuming pure solid phase chemical particles are spherical, the surface area available for mass transfer can be expressed as a function of the pure solid phase chemical concentration, particle diameter, and particle density as (after Lynch et al. 2003):

$$\alpha = \frac{6 C_{cp} V}{d_s \rho_p} \tag{6.3}$$

where: C_{cp} = pure solid phase chemical concentration (in particle form) [M/L^3]

V = bulk volume (water and particles) [L^3]

d_p = particle diameter [L]

ρ_p = particle density of pure solid phase chemical [M/L^3]

Following dissolution from the pure solid phase, dissolved chemicals are available for mass transfer (i.e. sorption) or transformation. Under equilibrium conditions, the maximum dissolved phase concentration a chemical can attain is the solubility limit. The solubility of a chemical is influenced by several factors including temperature and the concentrations (activities) of other ions in solution. The chemical dissolution reaction pathway may be useful for more detailed simulation of metal precipitates or explosive chemical compounds such as TNT or RDX that can be present in a granular, pure solid form.

6.2 ENVIRONMENTAL CONDITIONS

The rates at which chemical mass transfer and transformation processes occur often change as environmental conditions vary. Basic hydrologic processes such as evapotranspiration and soil moisture can change and environmental conditions vary. To facilitate development of more detailed chemical fate process representations or long-term hydrological impacts on chemical transport and fate, provisions to add a series of spatially and temporally varying time functions to represent environmental conditions exist in the TREX framework. While further development is needed to fully activate these features, code exists to represent environmental conditions such as wind speed, air temperature, solar radiation, the concentration of dissolved organic carbon (DOC) or other binding agents, the fraction organic carbon or partitioning effectiveness of both dissolved and particulate sorbents for partitioning, hardness, pH, water temperature, the concentration of oxidants, the concentration (population density) of bacteria, and light extinction properties. The developmental code for environmental conditions is organized to permit representation of any number or type of environmental properties as needed. For example, additional properties such as relative humidity or the atmospheric concentration of a chemical can be readily added within the existing framework structure.

7.0 PROGRAMMING GUIDE

7.1 TREX PROGRAMMING OVERVIEW

TREX has a modular design to support future expansions and enhancements. With a basic degree of familiarity, users can customize most functions of the frameworks to create highly specialized application to address a broad range of watershed hydrological, sediment transport, and chemical transport and fate issues. However, some caution is appropriate. TREX is a complex program. No guarantees are made regarding either the suitability of TREX for constructing a specific watershed model application or the computational performance of the code. Although substantial efforts have been taken to examine all aspects of the code, users are strongly advised to carefully examine the TREX source code and all model outputs to ensure proper operation.

The authors would appreciate receiving notification of any problems encountered with the TREX program. Notification may be sent by standard mail, telephone, or email to:

Mark Velleux	John F. England, Jr.	Dr. Pierre Julien
Department of Civil Engineering	U.S. Bureau of Reclamation	Department of Civil Engineering
Colorado State University	Flood Hydrology Group, D-8530	Colorado State University
A211 Enginring Research Center	Bldg. 67, Denver Federal Center	B205 Enginring Research Center
Fort Collins, CO 80523	Denver, CO 80225	Fort Collins, CO 80523
(970) 491-8563	(303) 445-2541	(970) 491-8450
mvelleux@engr.colostate.edu	jengland@do.usbr.gov	pierre@engr.colostate.edu

7.2 TREX AVAILABILITY AND SUPPORT

The TREX program and this user's manual are presently drafts not yet ready for wide public release. As they are in draft form, the TREX code and manual are only available upon request to the authors. Once the present stage of framework development is complete, the authors anticipate that both the TREX code and user's manual will be available for download via Dr. Julien's web site at Colorado State University. The authors hope to post TREX for general distribution by December 2005.

Please note that TREX was developed for academic and research use. TREX is not officially supported by Colorado State University. This means that users should not expect support beyond receiving the program and user's manual unless special arrangements are made with the authors.

7.3 TREX PROGRAM ORGANIZATION AND DESCRIPTION

TREX is a modular program and is comprised of subprocess groups that are organized into functional units for input, initialization, time function update, transport process, integration, output, and deallocation. The main program (trex) calls processes to:

1. Read inputs;
2. Initialize variables;
3. Compute hydrologic (water) transport, sediment (solids) transport, and chemical transport from the simulation iterative time loop;
4. Write outputs; and
5. Deallocate memory and end execution.

The transport process functional units for hydrologic transport, sediment transport, and chemical transport and fate are the core of TREX. These units appear within the model iterative time loop of TREX. The organization of the transport process functional units is presented in Figure 7-1. Descriptions of the main components of each functional unit within TREX follow. Descriptions of data included in global header files also follows.

7.3.1 Input Functional Unit

The input functional unit reads user-specified data from the main model input file, as organized into Data Groups A-F, as well as any ancillary input files required for a simulation. The major modules within this functional unit are:

- ReadInputFile
- ReadDataGroupA
- ReadDataGroupB
- ReadDataGroupC
- ReadDataGroupD
- ReadDataGroupE
- ReadDataGroupF

At the time TREX is executed, the user must specify the name of the main model input file. The main model input file is specified as an argument to the program as described in Section 3.5. The main input file name is stored in global memory and TREX calls ReadInputFile to initiate data input processing operations. As TREX reads Data Groups A-F, a series of utility and secondary modules are called to read any required ancillary input files. The name assigned to each of these secondary modules provides a shorthand description of the module function and use. For example, ReadMaskFile is called to read the row-column grid format file that defines the spatial domain of a simulation. The model echo file is produced as output by the this unit.

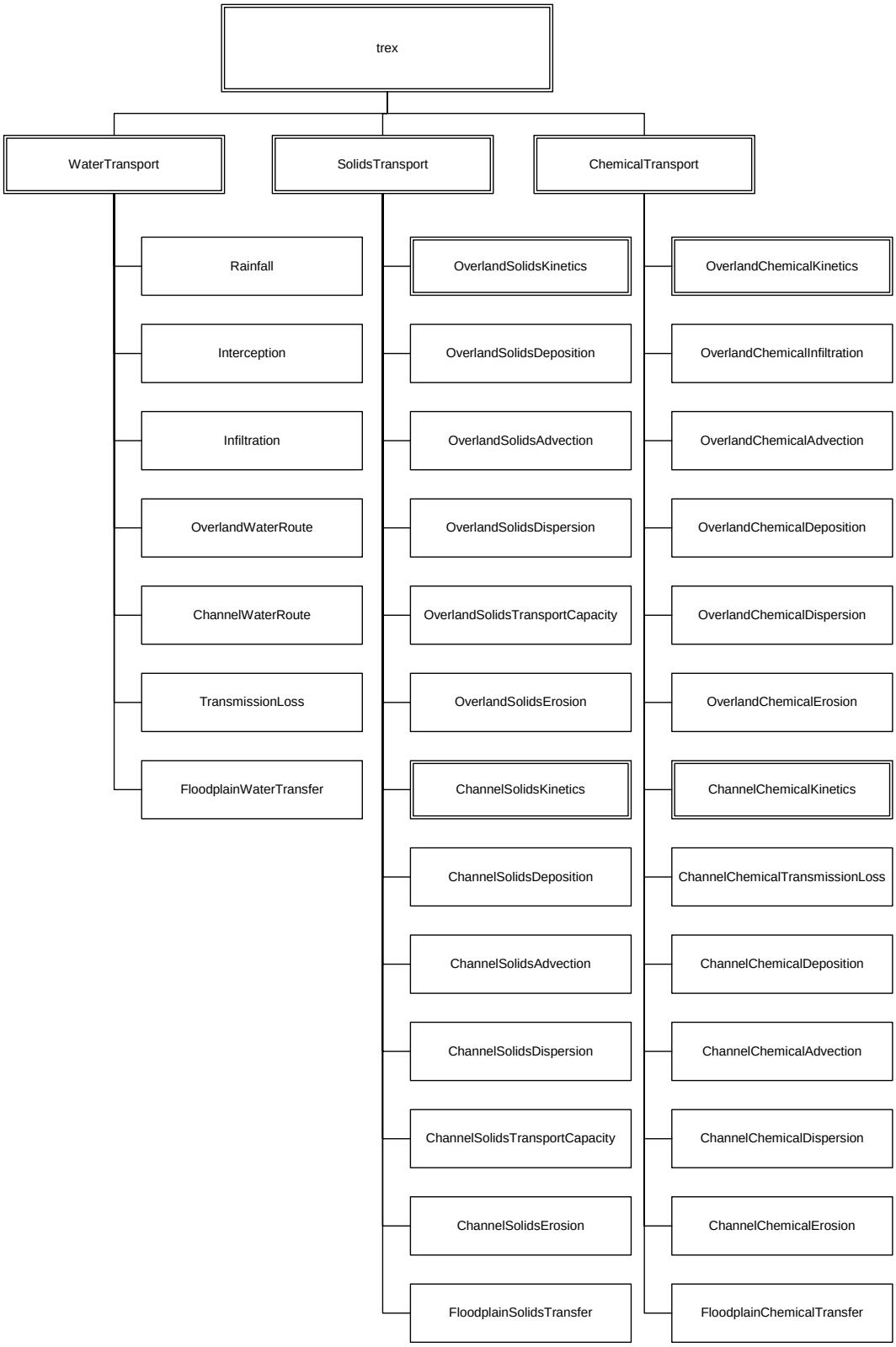

Figure 7-1. Organization of transport process functional units in TREX.

7.3.2 Initialization Functional Unit

The initialization functional unit allocates memory and assigns initial values to variables needed for simulation. The modules within this functional unit, organized by the transport process (water, solids, chemical) for which they initialize variables, are:

- Initialize
- InitializeWater
- InitializeSolids
- InitializeChemical
- InitializeEnvironment
- TimeFunctionInit
- TimeFunctionInitWater
- TimeFunctionInitSolids
- TimeFunctionInitChemical
- TimeFunctionInitEnvironment
- ComputeInitialState
- ComputeInitialStateWater
- ComputeInitialStateSolids
- ComputeInitialStateChemical

Once all model inputs are read, the initialization functional unit initializes all remaining primary and secondary variables that are not defined at the time the main model inputs are read. In addition, this functional unit also creates all basic output file types that will be used during the simulation. For example, the export, detailed mass balance, and summary statistics files are created by this functional unit.

7.3.3 Time Function Update Functional Unit

The time function update functional unit assigns values in time for each time function specified by the user. The modules within this functional unit, organized by transport process (water, solids, chemical), are:

- UpdateTimeFunction
- UpdateTimeFunctionWater
- UpdateTimeFunctionSolids
- UpdateTimeFunctionChemical
- UpdateEnvironment

This functional unit is called from the simulation iterative time loop within TREX. User-specified time functions such as the rainfall intensity (rate) as a gage location, the flow from a point source of water, or the load from a chemical point source are updated for use each time step during the simulation. Values in time are updated between times defined by user input using linear interpolation. Outputs from this functional unit may be subsequently interpolated over space or applied at a point as needed by the modules comprising the transport functional unit.

7.3.4 Transport Process Functional Unit

The transport process functional unit computes rates and fluxes for each hydrological, sediment transport, and chemical transport process specified by the user. The modules within this functional unit, organized by transport process (water, solids, chemical), are:

- WaterTransport
- Rainfall
- Interception
- Infiltration, TransmissionLoss
- OverlandWaterRoute, ChannelWaterRoute
- FloodplainWaterTransfer
- SolidsTransport
- OverlandSolidsKinetics, ChannelSolidsKinetics
- OverlandSolidsDeposition, ChannelSolidsDeposition
- OverlandSolidsAdvection, ChannelSolidsAdvection
- OverlandSolidsDispersion, ChannelSolidsDispersion
- OverlandSolidsTransportCapacity, ChannelSolidsTransportCapacity
- OverlandSolidsErosion, ChannelSolidsErosion
- FloodplainSolidsTransfer
- ChemicalTransport
- OverlandChemicalKinetics, ChannelChemicalKinetics
- OverlandChemicalInfiltration, ChannelChemicalInfiltration
- OverlandChemicalDeposition, ChannelChemicalDeposition
- OverlandChemicalAdvection, ChannelChemicalAdvection
- OverlandChemicalDispersion, ChannelChemicalDispersion
- OverlandChemicalErosion, ChannelChemicalErosion
- FloodplainChemicalTransfer

This functional unit is called from the simulation iterative time loop within TREX. Transport rates and fluxes for each process for each state variable in each overland cell and each channel node are computed for the surface water as well as all layers in the soil and sediment column for each time step during the simulation. Further details regarding the organization of the kinetics (mass transfer and transformation reactions) modules for chemical fate are presented in Figure 7-2. the chemical kinetics subunits include process modules for partitioning, biodegradation, hydrolysis, oxidation, photolysis, radioactive decay, a user-defined reaction, volatilization, dissolution, and transformation yields between chemical state variables.

Figure 7-2. Organization of chemical kinetics process modules within TREX.

7.3.5 Integration Functional Unit

The integration functional unit performs numerical integration to compute values for each state variable over time using the rates and fluxes for each hydrological, sediment transport, and chemical transport process computed by the transport process and time function update functional units. The modules within this functional unit, organized by transport process (water, solids, chemical), are:

- WaterBalance
- OverlandWaterDepth
- ChannelWaterDepth
- SolidsBalance
- OverlandSolidsConcentration
- ChannelSolidsConcentration
- ChemicalBalance
- OverlandChemicalConcentration
- ChannelChemicalConcentration
- NewState
- NewStateWater
- NewStateSolids
- NewStateChemical
- NewStateStack

This functional unit is called from the simulation iterative time loop within TREX. The model state variables are water depth, solids concentration, and chemical concentration. Mass balances are performed by summing the volume and mass fluxes for each state variable to computing new values for depth or concentration. The new state of the domain (water depths, solids concentrations, chemical concentrations, as well as soil or sediment stack volumes) is then stored. At the end of the simulation iterative time loop, utility functions to determine maximum and minimum depths and concentrations are called, the new domain state rest as the current state, and then the simulated time is advanced one time step.

7.3.6 Output Functional Unit

The output functional unit writes program results to a range of user-specified output files. The modules within this functional unit are:

- WriteTimeSeries
- WriteTimeSeriesWater, WriteTimeSeriesSolids, WriteTimeSeriesChemical

- WriteGrids
- WriteGridsWater, WriteGridsSolids, WriteGridsChemical
- WriteDumpFile
- WriteEndGrids
- WriteEndGridsWater, WriteEndGridsSolids, WriteEndGridsChemical
- ComputeFinalState
- ComputeFinalStateWater, ComputeFinalStateSolids, ComputeFinalStateChemical
- WriteMassBalance
- WriteMassBalanceWater, WriteMassBalanceSolids, WriteMassBalanceChemical
- WriteSummary
- WriteSummaryWater, WriteSummarySolids, WriteSummaryChemical

With the exception of the WriteEndGrid series of modules, this functional unit is called from the simulation iterative time loop within TREX. The WriteEndGrids modules are once at the end of the simulation immediately following the simulation iterative time loop. Each time these modules are called, user-specified output is written to file. The WriteTimesSeries modules write to files that hold comma separated values written line by line to form a sequence of model results at specified points in space organized by time. For example, one possible time series output is the water depth or total suspended solids concentrations at a reporting station. The WriteGrid modules write to grid (row-column) output files that hold values for all points in space for a single time in a format. Grid outputs are written in sequence at a user-specified frequency. For example, one possible sequence of grid output is the water depths over the model domain at simulation times of the simulation start (time = 0), 10 minutes, 20 minutes, etc. The WriteEndGrid modules write to files similar to regular grid outputs except that a single grid that holds the difference between start and end conditions over the model domain for the entire simulation is written. The ComputeFinalState modules compute conditions for primary and secondary model variables as needed to prepare detailed mass balance and summary statistics reports. The WriteMassBalance modules write to a single file that holds a detailed mass balance for all state variables. The WriteSummary nodules write to a single file that holds summary detail and simulation statistics for all state variables.

7.3.7 Deallocation Functional Unit

The deallocation functional unit performs end of simulation memory deallocation simulation clean-up tasks. The modules within this functional unit are:

- FreeMemory
- FreeMemoryWater
- FreeMemorySolids
- FreeMemoryChemical

- FreeMemoryEnvironment
- SimulationError
- RunTime

The FreeMemory series of modules of functional unit are called from SimulationError when an trapped error condition occurs or following the simulation iterative time loop within TREX. These modules deallocate memory allocated for primary and secondary variables. At the end of a successful simulation, RunTime is called to determine the wall clock time (not CPU time) elapsed from the start to the end of the simulation.

7.3.8 Global Declaration and Definition Header Files

TREX is designed to operate around large, globally available (common) data blocks. The categories of global data blocks, organized by transport function, are:

- trex_general_declarations, trex_general_definitions
- trex_water_declarations, trex_water_definitions
- trex_solids_declarations, trex_solids_definitions
- trex_chemical_declarations, trex_chemical_definitions
- trex_environmental_declarations, trex_environmental_definitions

Each category of global data is used by a specific layer of the framework. The framework layers are: general model controls, hydrology, sediment transport, and chemical transport. In TREX, information is always (and only) passed forward from one layer to the next.

Declarations files specify included C library files (e.g. stdio.h, math.h, etc.), function prototypes, macros, and external file pointers and variable declarations. Definitions files provide definitions for all externally declared file pointers and variables. General declarations specify information regarding general model controls. Water declarations specify information regarding hydrology. Solids declarations specify information regarding sediment transport. Chemical declarations specify information regarding chemical transport and fate. Environmental declarations specify information regarding environmental conditions.

To make information available to a layer, the global declarations file for that layer must be included in all modules of the layer. The general declarations are common to, and used by, all program layers. The hydrology layer uses the general and water declarations. The sediment transport layer uses the general, water, and solids declarations. The chemical transport layer uses the general, water, solids, chemical, and environmental declarations.

Note that for the present state of development, environmental conditions only affect chemical transport and fate. As environmental condition feature developments continue, the environmental category may be divided into separate groups for hydrology, sediment transport, and chemical transport. For example, wind speed, air temperature, and relative

humidity functions might be used by the hydrology layer to compute evapotranspiration and evaporation of surface water while soil temperature might be used by the sediment transport layer to compute mineralization rates of organic particles.

It is also important to note that information is never passed backwards between layers. For example, the hydrology layer does not and should not have access to global data for sediment or chemical transport. Similarly, sediment transport does not and should not have access to global data for chemical transport and fate. This layered data access and management approach is useful for maintaining framework modularity. Future layers, such as nutrient transport or eutrophication, can be readily added without establishing confusing cross links between layers.

7.4 PROGRAMMING STYLE

To enhance readability, comprehension, and facilitate future development, a consistent programming style has been used for all TREX code development. The authors believe continued use of a consistent programming style is critical for future code maintenance and development. Descriptions of the key conventions of the TREX programming style follow.

7.4.1 Naming Conventions

All variable names in the code are lower case (e.g. nsolids, advsedchoutflux, etc.). All programs module names are a mixture of upper and lower case (e.g. WaterTransport, ChannelChemicalKinetics, etc.). All macros are upper case (e.g. MAXNAMESIZE, TOLERANCE, etc.). Variable names are descriptive. As a short hand, variables for the overland plane include “ov” and those for the channel network include “ch”. Variables for water depth have “h” and flow have “q” in their names. Variables for sediment transport variables include “sed” and those for chemical transport include “chem”. Flux and mass terms include “flux” and “mass”, respectively. Transport process variables also include three character identifiers to denote the specific process with which the variable is associated: “adv” for advection, “dsp” for dispersion, “dep” for deposition, “ers” for erosion, or “dsl” for dissolution, etc. In addition to identifiers such as “ov”, “adv”, and “flux”, transport variables also include “out” or “in” to identify the direction of transport. Each of these name elements are typically concatenated to form the full variable name. For example, the flux of suspended solids transported out of an overland cell by advection would be “advsedovoutflux”. Through use of a consistent naming convention, new state variables and process modules can be added to the framework by using existing modules as templates and using a simple search and replace to include the names of new variables.

7.4.2 Internal Documentation and Comments

The TREX code is extensively documented. Every module includes initial comments that identify the module name, purpose and methods, inputs, outputs, controls, modules called, calling module(s), routine author(s), revision history (if any), and date. Further, virtually every line of code has a comment to explain the line-by-line operation of the

module. Wherever additional information is needed to explain the basis of an operation, a comment block delimited by the string "Note:" occurs and is followed by more in-depth documentation. Comment blocks delimited by the string "Developer's Note:" identify areas that may be the subject of future framework development efforts.

The beginning, interior, and concluding brackets of loop and if structures each have comments to clearly identify the structures. Also, each unit of code within a loop or if structure is indented with tabs to provide further visual cues as to which structure controls the code. The start and end of all loop structures are identified by the strings "loop" and "end loop", respectively. The start and end of all if structures are identified by the strings "if" and "end if", respectively.

7.4.3 Maintaining Consistent Programming Style During Development

In many settings, it is common for a computer program code development team to change over time. This is particularly true in a setting such as a university were computer code is shared among different generations of students and projects. Under such conditions, it is common for code to rapidly mutate until it becomes so unintelligible that sometimes even the immediate code author(s) cannot clearly follow or explain its operation. The experience of the authors is that computer code handled on an informal or ad hoc basis by a changing array of developers quickly becomes unmanageable. To achieve a higher degree of long-term manageability and maintainability over time, the authors strongly recommend that future developers continue to use the programming style conventions employed during initial TREX development.

Continued adherence to naming conventions and use of extensive, line-by-line comments in the code is essential for future maintainability. In addition to providing information regarding program operation, use of consistent comments and variable names also greatly facilitates program testing and debugging. Use of established programming conventions allows newly developed modules to be rapidly screened for the occurrence potential bugs such as incorrect variable name references. For example a common programming error is to reference variables for the channel network in a module for overland plane (or vice versa). Consider a solids transport module where variables csedch and advsedchoutflux have been incorrectly used instead of csedov and advsedovoutflux. By adhering to variable naming conventions, a module can be searched (case sensitive) for the occurrence of the string "sedch" since overland process variables use the string "sedov" and it is very rare for an overland module to ever reference conditions in the channel network. Similarly, the occurrence of the string "sedov" rather than "chemov" would be rare in chemical process modules.

Care should also be taken to prevent "cross-wiring" of program layers. The global data structure needed for any model layer (hydrology, sediment transport, etc.) should contain all variables needed for that layer to operate. In terms of program flow, information should only be passed forward. The global data structure for a later model layer should never be used or available to an earlier model layer.

It is worth reiterating that an important feature of the TREX framework is that all source code for the program is extensively documented. The importance of comprehensive, line-by-line program documentation for future code maintenance and development cannot be overstated. All too often during development efforts, internal code documentation is neglected when programmers add code without adding corresponding, detailed comments for the perceived "speed and ease" of development. This inevitably leads to generation of poorly written, undocumented code. Even if the original authors of undocumented code are available and can still decipher it in the future, it becomes exceedingly difficult for other programmers to manage such code over time. The challenges of managing poorly written and poorly documented code are often difficult to overcome and can be costly in terms of lengthened development time cycles. The consequence of earlier shortcuts taken for "speed and ease" is often that the same body of code ends up being repeatedly redeveloped by subsequent generations of developers. It is the further experience of the authors that code that cannot be fully documented at the time it is first written is in many instances poorly conceived, often poorly structured, and typically leads to effort wasted redeveloping code. For these and many other reasons, the importance of maintaining complete and comprehensive internal documentation of all program code cannot be overemphasized.

8.0 REFERENCES

Abramowitz, M. and Stegun, I.A. 1972. Handbook of Mathematical Functions. Applied Mathematics Series 55. National Bureau of Standards, Washington, D.C.

Ambrose, R.B., Martin, J.L. and Wool, T.A. 1993. WASP5, A hydrodynamic and water quality model -- Model theory, user's manual, and programmer's guide. U.S. Environmental Protection Agency, Office of Research and Development, Environmental Research Laboratory, Athens, Georgia.

Beuselinck, L., Govers, G., Steegen, A., and Quine, T.A. 1999. Sediment transport by overland flow over an area of net deposition. Hydrological Processes, 13(17):2769-2782.

Brown, L.C. and Barnwell, T.O. 1987. The enhanced stream water quality models QUAL2E and QUAL2E-UNCAS: documentation and user manual. U.S. Environmental Protection Agency, Environmental Research Laboratory, Athens, Georgia. EPA /600/3-87/007. 189 p.

Burban, P.Y., Xu, Y., McNeil, J., and W. Lick. 1990. Settling speeds of flocs in fresh and sea waters. Journal of Geophysical Research (C) Oceans, 95(C10):18213-18220.

Capel, P. and S. Eisenriech, S. 1990.Relationship between chlorinated hydrocarbons and organic carbon in sediment and porewater. Journal of Great Lakes Research, 16(2):245-257.

Caruso, B.S. 2003. Water quality simulation for planning restoration of a mined watershed. Water, Air, and Soil Pollution, 150(1-4):359-382.

Chapra, S.C. 1997. Surface Water-Quality Modeling. McGraw-Hill Companies, Inc. New York, New York. 844 pp.

Chapra, S.C., and Canale, R.P. 1985. Numerical Methods for Engineers with Personal Computer Applications (First Edition). McGraw-Hill, Inc., New York, New York. 570 pp.

Cheng, N.S. 1997. Simplified settling velocity formula for sediment particle. Journal of Hydraulic Engineering, 123(2):149-152.

Clements, W., Carlisle, D., Lazorchak, J., and Johnson, P. 2000. Heavy metals structure benthic communities in Colorado mountain streams. Ecological Applications, 10(2):626-638.

Clements, W., Carlisle, D., Courtney, L., and Harrahy, E. 2002. Integrating observational and experimental approaches to demonstrate causation in stream biomonitoring studies. Environmental Toxicology and Chemistry, 21(6):1138-1146.

Clusser, E. L. 1997. Diffusion: mass transfer in fluid systems, 2nd edition. Cambridge University Press, New York, New York. 580 p.

DiToro, D.M. 1985. A particle interaction model of reversible organic chemical sorption. Chemosphere, 14(9-10):1503-1538.

DiToro, D.M. 2001. Sediment Flux Modeling. John Wiley and Sons, Inc., New York, New York. 624 pp.

Eadie, B., N. Morehead, and P. Landrum. 1990. Three-phase partitioning of hydrophobic organic compounds in Great Lakes waters. Chemosphere, 20(1-2):161-178.

Eadie, B., N. Morehead, V. Klump, and P. Landrum. 1992. Distribution of hydrophobic organic compounds between dissolved and particulate organic matter in Green Bay waters. Journal of Great Lakes Research, 18(1):91-97.

Eagleson, P.S. 1970. Dynamic Hydrology. McGraw-Hill Book Company, New York, New York. 462 pp.

Engelund, F., and Hansen, E. 1967. A monograph on sediment transport in alluvial streams. Teknisk Vorlag, Copenhagen, Denmark. 62 pp.

Ewen, J., Parkin, G., and O'Connell, P.E. 2000. SHETRAN: distributed river basin flow and transport modeling system. Journal of Hydrologic Engineering, 5(3):250-258.

Exner, F. M. 1925, Über die wechselwirkung zwischen wasser und geschiebe in flüssen, Sitzungber. Acad. Wissenscaften Wien Math. Naturwiss. Abt. 2a, 134:165–180.

Fetter, C.W. 2001. Applied Hydrogeology, Fourth Edition. Prentice-Hall, Inc. Upper Saddle River, New Jersey. 598 p.

Gessler, J. 1965. The Beginning of Bedload Movement of Mixtures Investigated as Natural Armouring in Channels. Technical report No. 69, The Laboratory of Hydraulic Research and Soil Mechanics, Swiss Federal Institute of Technology, Zurich (translation by W. M. Keck Laboratory of Hydraulics and Water Resources, California Institute of Technology, Pasadena, California).

Gessler, J. 1967. The beginning of bedload movement of mixtures investigated as natural armoring in channels. California Institute of Technology, Pasadena, California. 89pp.

Gessler, J. 1971. Beginning and ceasing of sediment motion. In: River Mechanics, Shen, H.W., ed. H.W. Shen, Fort Collins, Colorado. pp. 7:1–7:22.

Green, W.H. and Ampt, G.A. 1911. Studies on soil physics, 1: the flow of air and water through soils. Journal of Agricultural Sciences 4(1):11-24.

Haralampides, K., McCourquodale, J.A., Krishnappan, B.G. 2003. Deposition properties of fine sediment. Journal of Hydraulic Engineering, 129(3):230-234.

Harbaugh, A.W., Banta, E.R., Hill, M.C., and McDonald, M.G. 2000. MODFLOW-2000, the U.S. Geological Survey modular ground-water model -- User guide to modularization concepts and the Ground-Water Flow Process. U.S. Geological survey, Denver, Colorado. Open-File Report 00-92. 121 p.

Holley, E.R. 1969. Unified view of diffusion and dispersion. Journal of the Hydraulics Division, American Society of Civil Engineers, 95(2):621-631.

Holm, P.E., Rootzén, H., Borggaard, O.K., Møberg, J.P., and Christensen, T.H. 2003. Correlation of cadmium distribution coefficients to soil characteristics. Journal of Environmental Quality, 32(1):138-145.

Imhoff, J.C., Stoddard, A., Buchak, E.M., and Hayter, E. 2003. Evaluation of Contaminated Sediment Fate and Transport Models: Final Report. U.S. Environmental Protection Agency, Office of Research and Development, National Exposure Research Laboratory, Athens, Georgia. Contract Number 68-C-01-037, Work Assignment No. 1-10. 153 p.

Johnson, B.E., Julien, P.Y., Molnár, D.K., and Watson, C.C. 2000. The two-dimensional upland erosion model CASC2D-SED. Journal of the American Water Resources Association, 36(1):31-42.

Julien, P.Y. 1998. Erosion and Sedimentation (First Paperback Edition). Cambridge University Press, Cambridge, UK. 280 p.

Julien, P.Y. 2002. River Mechanics. Cambridge University Press, Cambridge, UK. 434 p.

Julien, P.Y. and Saghafian, B. 1991. CASC2D User's Manual - A Two Dimensional Watershed Rainfall-Runoff Model. Department of Civil Engineering, Colorado State University, Fort Collins, Colorado. Report CER90-91PYJ-BS-12. 66 p.

Julien, P.Y., Saghafian, B., and Ogden, F.L. 1995. Raster-Based hydrologic modeling of spatially-varied surface runoff. Water Resources Bulletin, AWRA, 31(3):523-536.

Julien, P.Y. and Rojas, R. 2002. Upland erosion modeling with CASC2D-SED. International Journal of Sediment Research, 17(4):265-274.

Julien, P.Y., and Frenette, M. 1985. Modeling of rainfall erosion. Journal of Hydraulic Engineering, 11(10):1344-1359.

Julien, P.Y., and Simons, D.B. 1985. Sediment transport capacity of overland flow. Transactions of the American Society of Agricultural Engineers, 28(3):755-762.

Karickhoff, S.W., Brown, D.S., and Scott, T.A. 1979. Sorption of hydrophobic pollutants on natural sediments. Water Research, 13(3):241-248.

Kashian, D.R., Prusha, B., and Clements, W.H. 2004. Influence of total organic carbon and UV-B radiation on zinc toxicity and bioaccumulation in aquatic communities. Environmental Science and Technology, 38(23):6371-6376.

Kilinc, M.Y., and Richardson, E.V. 1973. Mechanics of soil erosion from overland flow generated by simulated rainfall. Hydrology Papers Number 63. Colorado State University, Fort Collins, Colorado.

Kipp, K.L, Jr. 1997. Guide to the Revised Heat and Solute Transport Simulator: HST3D Version 2. U.S. Geological Survey, Denver, Colorado. Water Resources Investigations Report 97-4157. 149 p.

Krishnappan, B.G. 2000. In situ distribution of suspended particles in the Frasier River. Journal of Hydraulic Engineering, 126(8):561-569.

Krone, R.B. 1962. Flume studies of the transport of sediments in estuarial shoaling processes. Final Report. Hydraulic Engineering Laboratory and Sanitary Engineering Research Laboratory, University of California, Berkeley, California.

Landrum, P., M. Rheinhold, S. Nihart, and B. Eadie. 1985. Predicting bioavailability of xenobiotics to Pontoporeia Hoya in the presence of humic and fulvic materials and natural dissolved organic matter. Environmental Toxicology and Chemistry, 4(4):459-467.

Landrum, P., S. Nihart, B. Eadie, and Herche L. 1987. Reduction in bioavailability of organic contaminants to the amphipod Pontoporeia Hoya by dissolved organic matter of sediment interstitial waters. Environmental Toxicology and Chemistry, 6(1):11-20.

Li, R.M., Stevens, M.A., and Simons, D.B. 1976. Solutions to Green-Ampt infiltration equations. Journal of Irrigation and Drainage Division, ASCE, 102(IR2):239-248.

Linsley, R.K., Kohler, M.A., and Paulhus, J.L.H. 1982. Hydrology for Engineers (Third Edition). McGraw-Hill Book Company, New York, New York. 508 p.

Lu, Y., and Allen, H. 2001. Partitioning of copper onto suspended particulate matter in river waters. Science of the Total Environment 277(1-3):119-132.

Lynch, J., Brannon, J., Hatfield, K., and Delfino, J. 2003. An exploratory approach to modeling explosive coumpond persistence and flux using dissolution kinetics. Journal of Contaminant Hydrology, 66(3-4):147-153.

Mehta, A., McAnally, W., Hayter, J., Teeter, A., Heltzel, S., and Carey, W. 1989. Cohesive sediment transport. II: application. Journal of Hydraulic Engineering, 115(8):1094-1112.

Meyer, L.D., and Weischmeier, W.H. 1969. Mathematical simulation of the process of soil erosion by water. Transactions of the American Society of Agricultural Engineers, 12(6):754-762.

Partheniades, E. 1992. Estuarine sediment dynamics and shoaling processes. In: Handbook of Coastal and Ocean Engineering, Volume 3: Harbours, Navigation Channels, Estuaries, and Environmental Effects, pp. 985-1071. Herbich, J. B., Ed. Gulf Publishing Company, Houston, Texas.

Phillip, J.R. 1957a. The theory of infiltration: 1. The infiltration equation and its solution. Soil Science, 83:345-357.

QEA. 1999. PCBs in the Upper Hudson River, Volume 2: A model of PCB Fate, Transport, and Bioaccumulation. Prepared for General Electric, Albany, New York. Prepared by Quantitative Environmental Analysis, LLC, Montvale, New Jersey. Job Number GENhud:131. May.

Rawls, W.J., Brakensiek, D.L., and Miller, N. 1983. Green-Ampt infiltration parameters from soils data. Journal of Hydraulic Engineering, 109(1):62-69.

Richards, L.A. 1931. Capillary conduction of liquids in porous mediums. Physics, 1:318-333.

Richardson, W.L., Smith, V.E., and Wethington, R. 1983. "Dynamic Mass Balance of PCB and Suspended Solids in Saginaw Bay – A Case Study." In: Physical Behavior of PCBs in the Great Lakes, D. Mackay, S. Patterson, and S. J. Eisenreich, eds. Ann Arbor Science Publishers, Ann Arbor, Michigan. pp. 329-366.

Rojas, R. 2002. GIS-based Upland Erosion Modeling, Geovisualization and Grid Size Effects on Erosion Simulations with CASC2D-SED. Ph.D. dissertation, Department of Civil Engineering, Colorado State University, Fort Collins, Colorado.

Schwarzenbach, R.P., Geschwend, P.M., and Imboden, D.M. 1993. Environmental Organic Chemistry. Wiley-Interscience, New York.

Simons, D.B., and Sentürk, F. 1992. Sediment Transport Technology – Water and Sediment Dynamics (Revised Edition). Water Resources Publications, Littleton, Colorado.

Smith, R.E., and Parlange, J.-Y. 1978. A parameter efficient hydrologic infiltrations model. Water Resources Research, 14(3):533-538.

Sauvé, S.F., Hendershot, W., and Allen, H.E. 2000. Solid-solution partitioning of metals in contaminated soils: dependence on pH, total metal burden, and organic matter. Environmental Science and Technology 34(7):1125-1131.

Sauvé, S.F., Manna, S., Turmel, M.C., Roy, A.G., and Courchesne, F. 2003. Solid-solution partitioning of Cd, Cu, Ni, Pb, and Zn in the organic horizons of a forest soil. Environmental Science and Technology 37(22):5191-5196.

Thomann, R.V. and J.A. Meuller. 1987. Principles of Surface Water Quality Modeling and Control. Harper and Row Publishers, Inc., New York, New York. 644 pp.

van Rijn, L.C. 1984a. Sediment transport, part I: bed load transport. Journal of Hydraulic Engineering, 110(10):1431-1456.

van Rijn, L.C. 1984b. Sediment transport, part I: suspended load transport. Journal of Hydraulic Engineering, 110(11):1612-1638.

Velleux, M., Gailani, J., and Endicott, D. 1996. Screening-level approach for estimating contaminant export from tributaries. Journal of Environmental Engineering, 122(6):503-514.

Velleux, M., Westenbroek, S., Ruppel, J., Settles, M., and Endicott, D. 2001. A User's Guide to IPX, the In-Place Pollutant Export Water Quality Modeling Framework, Version 2.7.4. U.S. Environmental Protection Agency, Office of Research and Development, National Health and Environmental Effects Research Laboratory, Mid-Continent Ecology Division, Large Lakes Research Station, Grosse Ile, Michigan. 179 pp. EPA/600/R-01/079.

Yang, C. T. 1996. Sediment Transport: Practice and Theory. McGraw-Hill, Inc. New York, New York. 480 pp.

Zheng, C. and Wang, P.P. 1999. MT3DMS, A modular three-dimensional multi-species transport model for simulation of advection, dispersion and chemical reactions of contaminants in groundwater systems; documentation and user's guide. U.S. Army Engineer Research and Development Center Contract Report SERDP-99-1, Vicksburg, Mississippi. 202 p.

APPENDIX C: MODEL DISSOLVED PHASE RESULTS

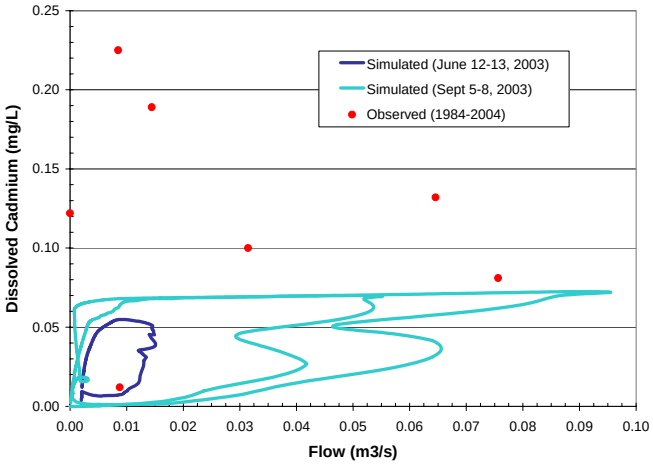

a) Dissolved cadmium

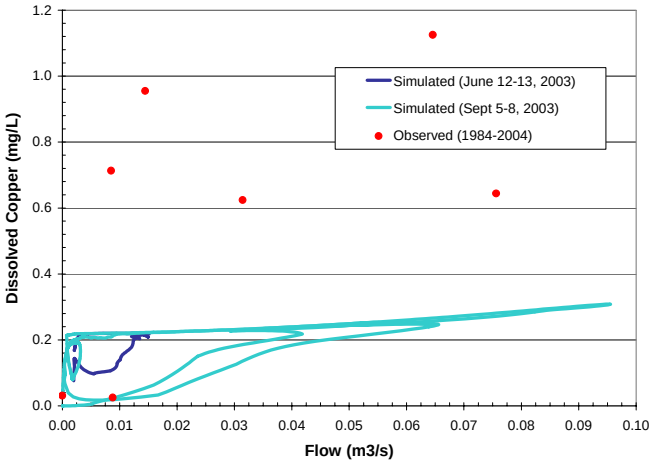

b) Dissolved copper

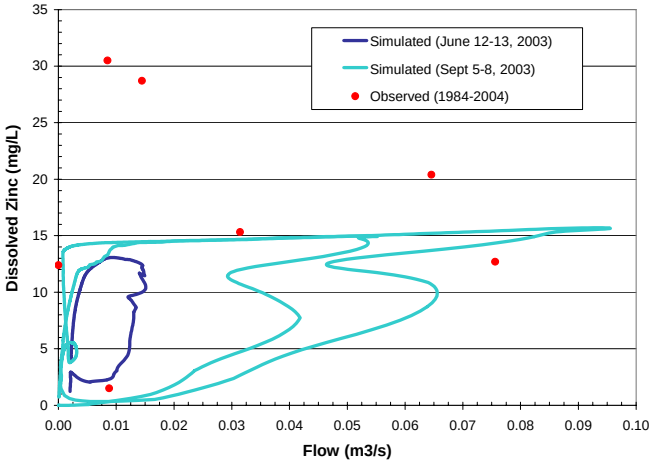

c) Dissolved zinc

Figure C-1. Dissolved chemical calibration and validation at Station CG-1.

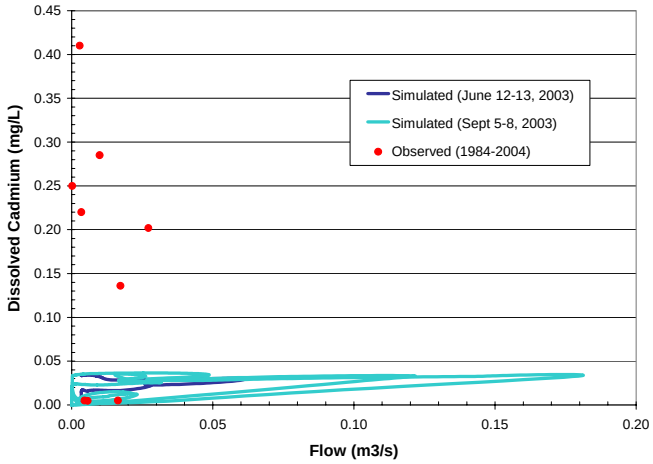

a) Dissolved cadmium

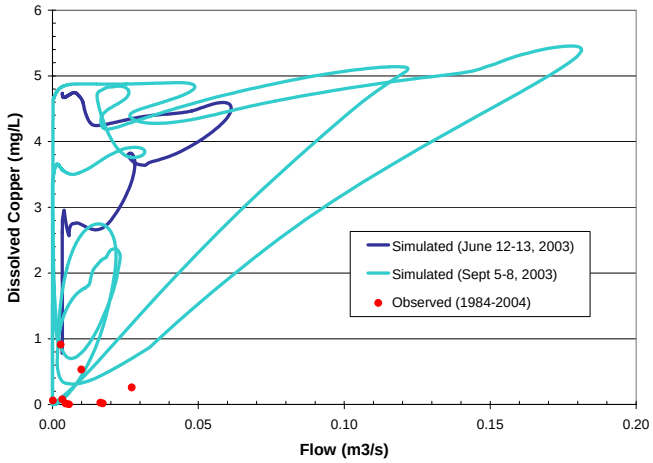

b) Dissolved copper

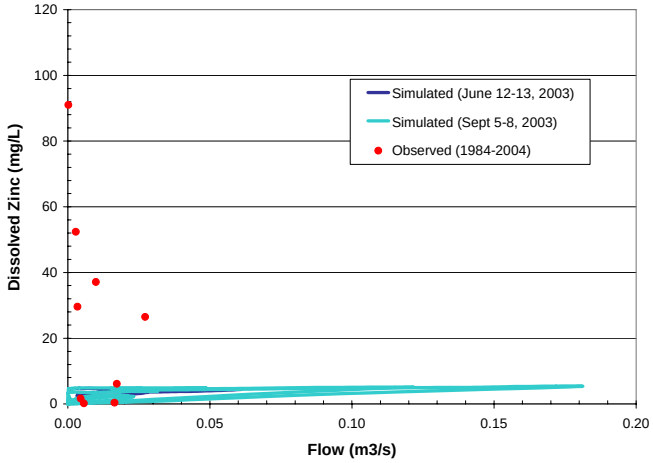

c) Dissolved zinc

Figure C-2. Dissolved chemical calibration and validation at Station SD-3.

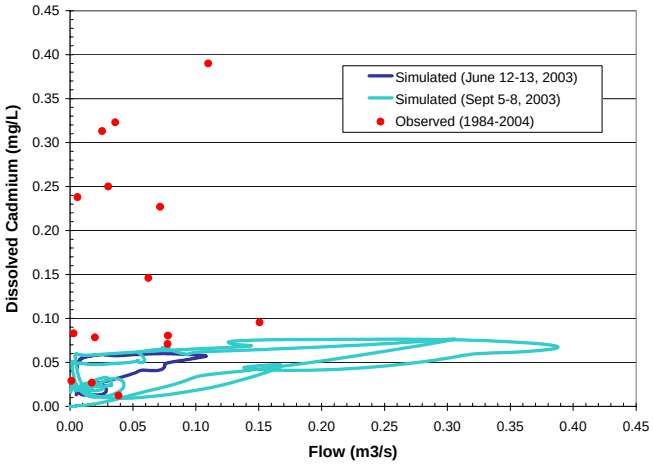

a) Dissolved cadmium

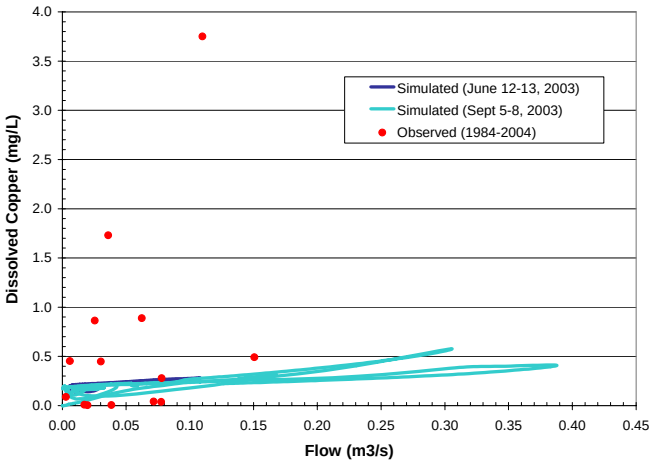

b) Dissolved copper

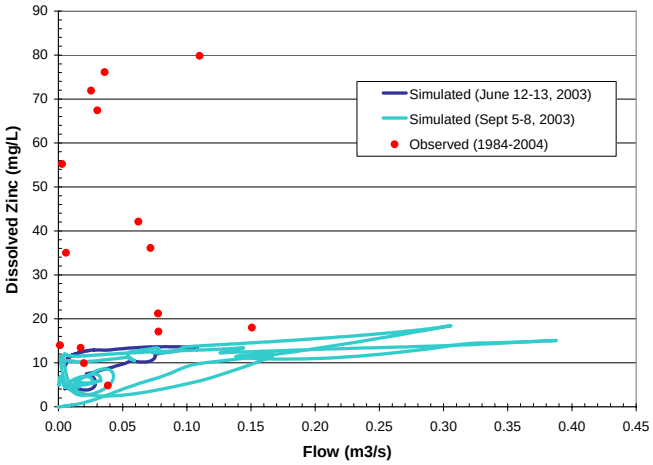

c) Dissolved zinc

Figure C-3. Dissolved chemical calibration and validation at Station CG-4.

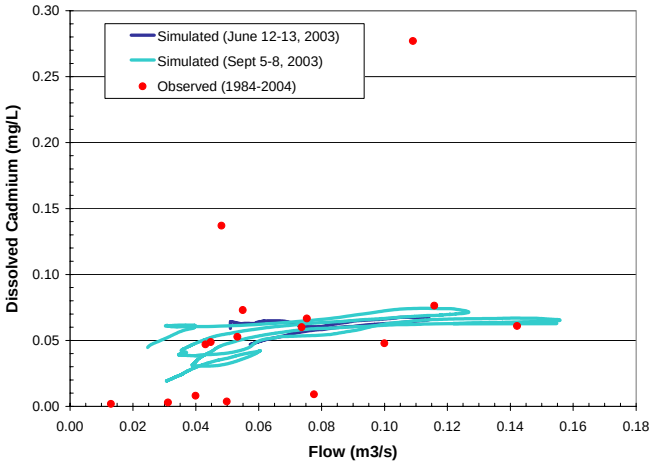

a) Dissolved cadmium

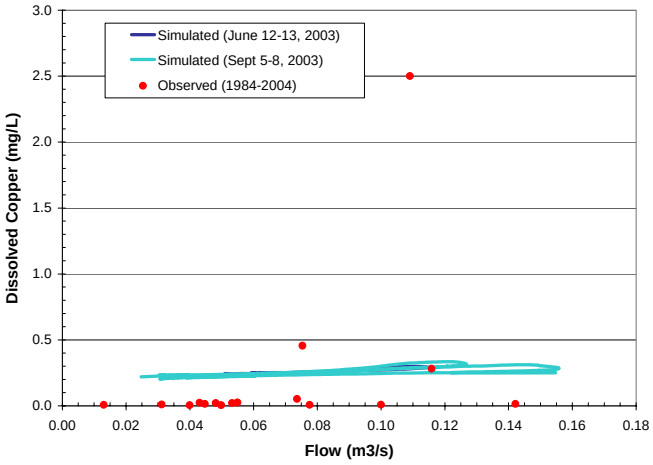

b) Dissolved copper

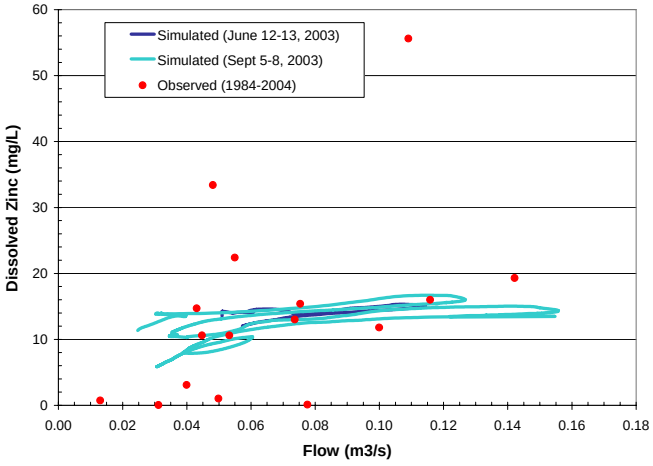

c) Dissolved zinc

Figure C-4. Dissolved chemical calibration and validation at Station CG-6.

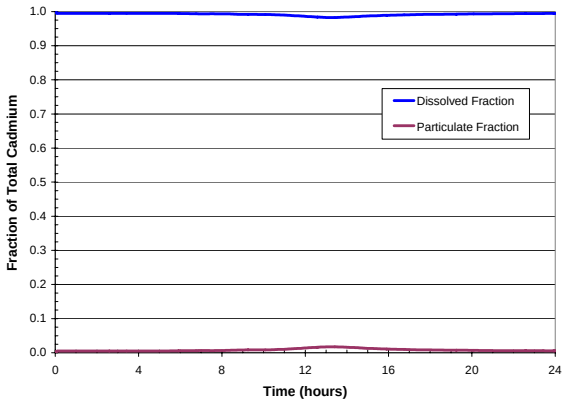

a) Cadmium: June 12-13, 2003

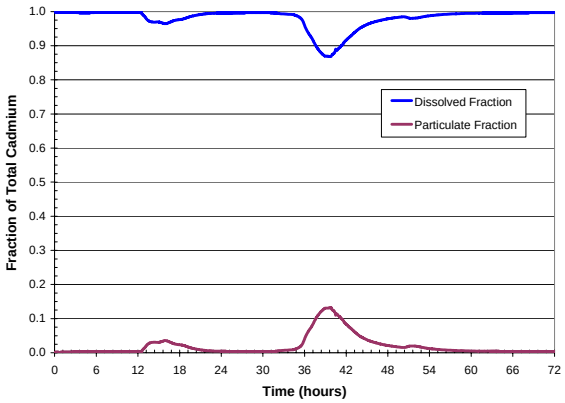

b) Cadmium: September 5-8, 2003

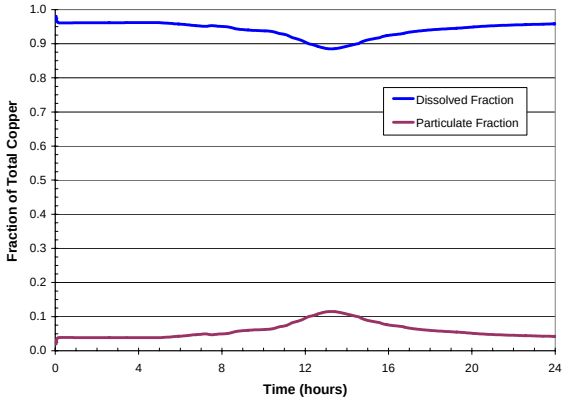

c) Copper: June 12-13, 2003

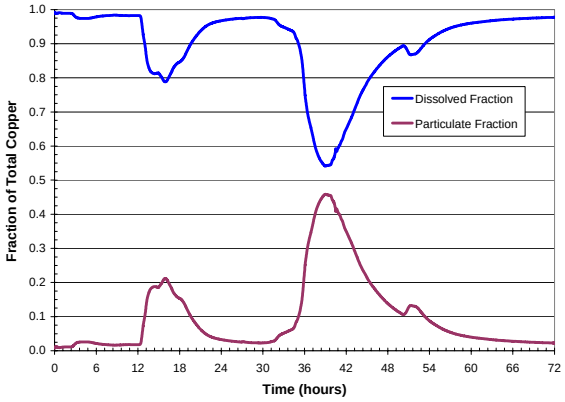

d) Copper: September 5-8, 2003

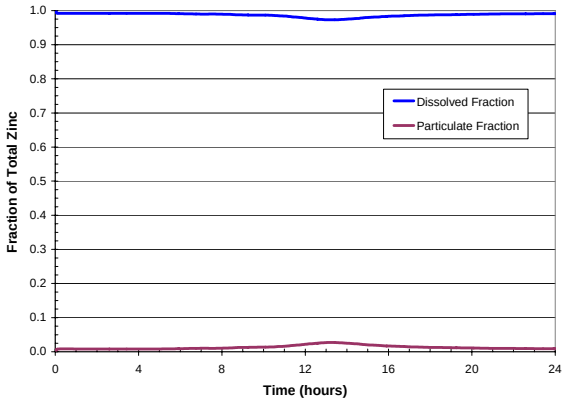

e) Zinc: June 12-13, 2003

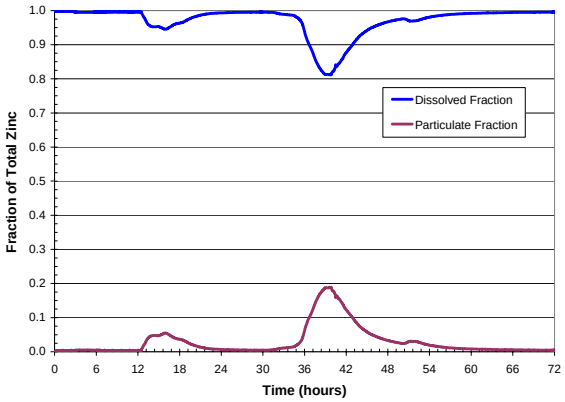

f) Zinc: September 5-8, 2003

Figure C-5. Chemical phase distribution at Station CG-6.

APPENDIX D: MODEL UNCERTAINTY ASSESSMENT SUMMARY

As described in Section 5.5, model sensitivity was explored by parameter perturbation as part of calibration efforts. The most sensitive parameters in the hydrologic model were the effective hydraulic conductivity (K_h) and flow resistance (Manning n). The most sensitive parameters for the sediment transport model were typically the soil erodibility (K) and land cover factor (C). The land management practice factor (P) was not considered to be uncertain because lands in the watershed are not managed for agriculture or as rangelands. The most sensitive parameter for the chemical transport model was the chemical partition coefficient (K_d). During calibration, these parameters were varied within accepted ranges representing the uncertainty of each parameter.

Model uncertainty was estimated using the approach described by Mishra (2001). For each uncertain (sensitive) parameter upper, middle, and lower limits were established to represent the parameter distribution as were presented in Tables 5-8 through 5-10. The upper and lower limits were selected to be representative of the upper and lower 95% confidence interval for each parameter.

Overall model uncertainty envelope bounds were estimated from the combination of individual parameter values that cause the largest increase (upper bound) or decrease (lower bound) in model response. Upper bound conditions occur for maximum surface runoff, maximum soil erosion, and minimum chemical partitioning. Lower bound conditions occur for minimum runoff, minimum erosion, and maximum partitioning. To supplement the results presented in Section 5.5, graphs showing the model uncertainty envelope for total metals concentrations at Stations CG-1, SD-3, and CG-4 are presented in Figures B-1 to B-3. Results for Station CG-6 were presented in Figure 5-23.

The uncertainty assessment suggests that the model hydrologic calibration is reasonable at least for events that produce flows in the range of 0.03 to 0.30 m^3/s (1 to 10 cfs). This range of flows is typical of the observed flow record for California Gulch. The flow uncertainty envelope during the September storm is somewhat wider than estimated for the June storm. Recalling that this analysis only examined parameter uncertainty, it is possible that the wider uncertainty of model results for the September storm reflects the

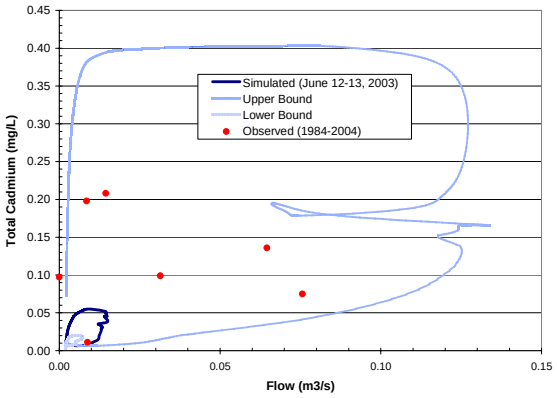

a) Total cadmium: June 12-13, 2003

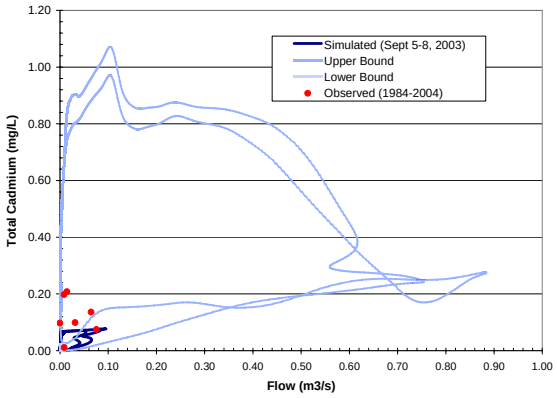

b) Total cadmium: September 5-8, 2003

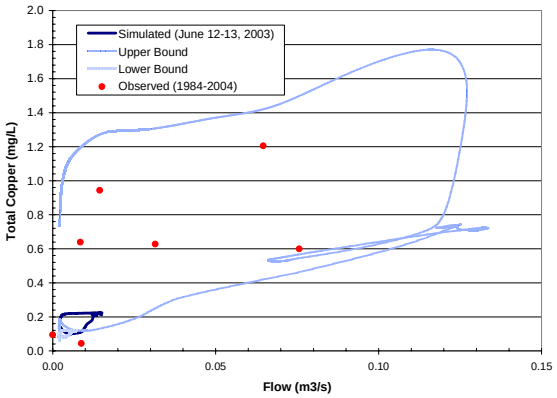

c) Total copper: June 12-13, 2003

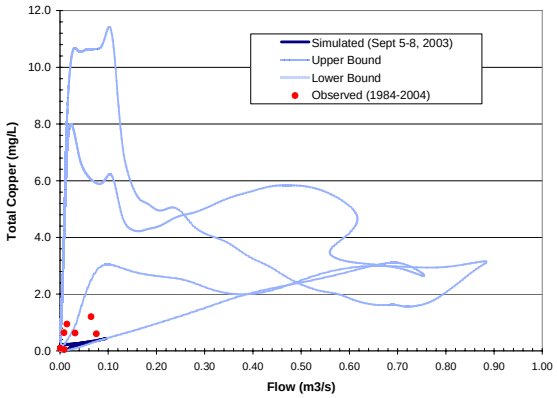

d) Total copper: September 5-8, 2003

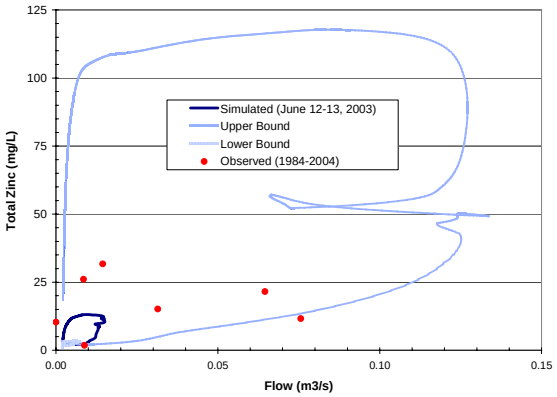

e) Total zinc: June 12-13, 2003

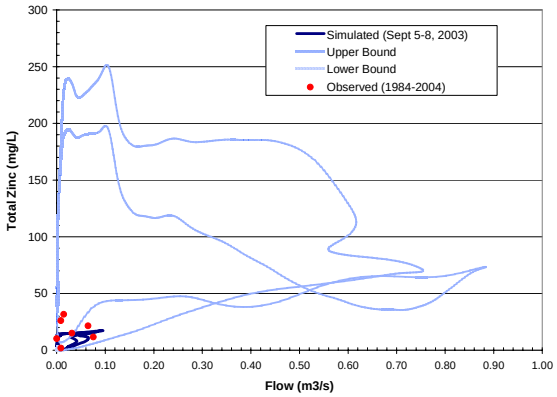

f) Total zinc: September 5-8, 2003

Figure D-1. Chemical transport uncertainty envelope at Station CG-1.

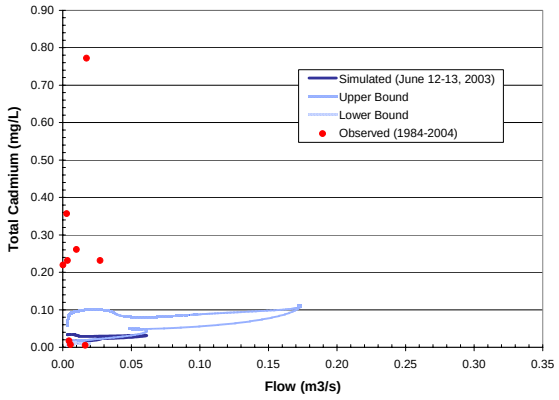

a) Total cadmium: June 12-13, 2003

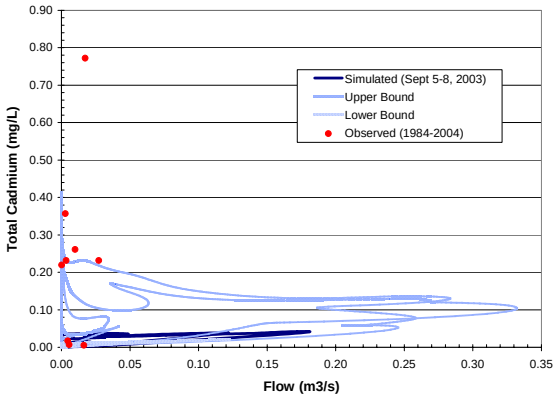

b) Total cadmium: September 5-8, 2003

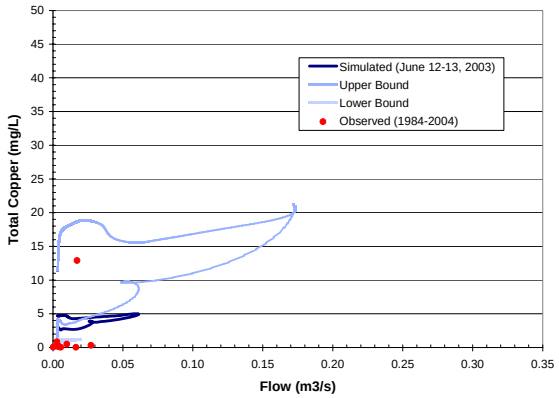

c) Total copper: June 12-13, 2003

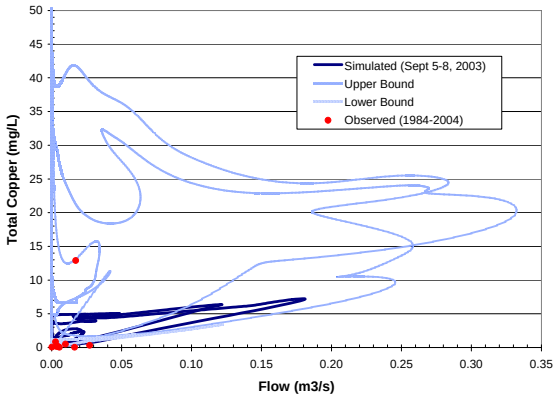

d) Total copper: September 5-8, 2003

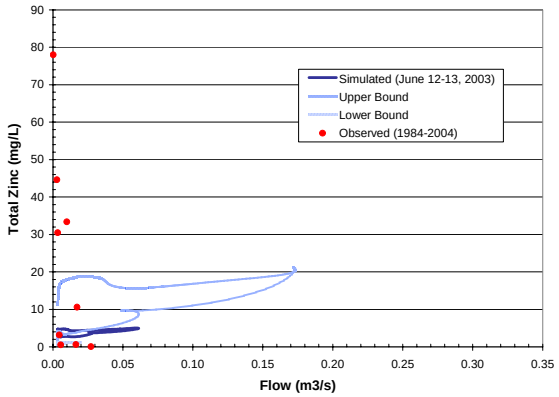

e) Total zinc: June 12-13, 2003

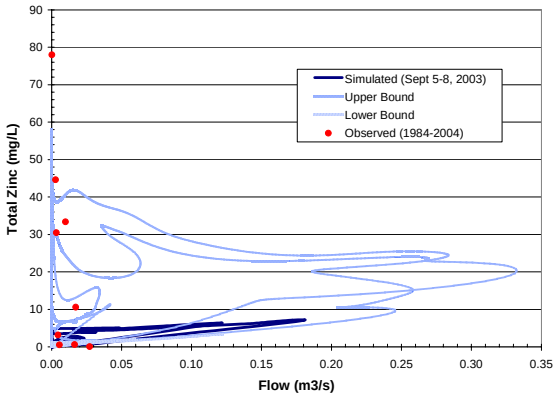

f) Total zinc: September 5-8, 2003

Figure D-2. Chemical transport uncertainty envelope at Station SD-3.

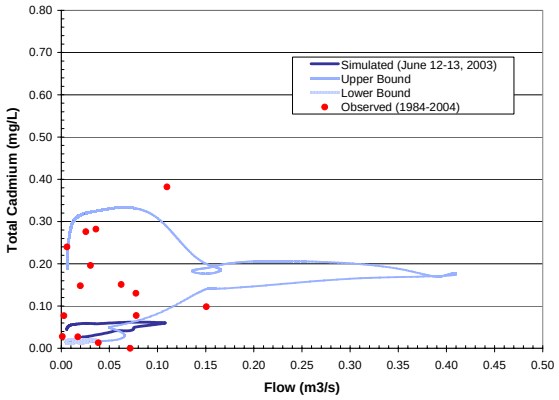

a) Total cadmium: June 12-13, 2003

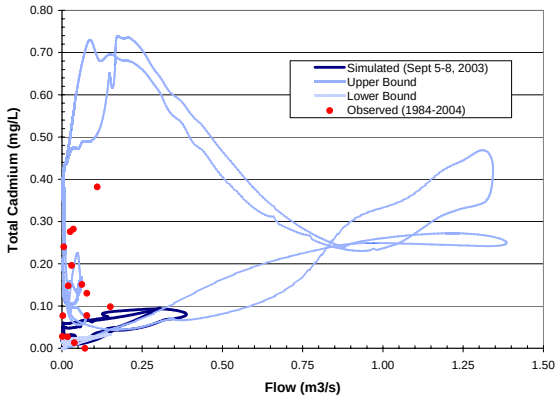

b) Total cadmium: September 5-8, 2003

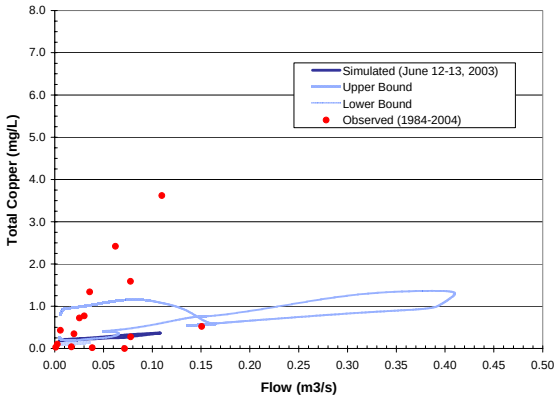

c) Total copper: June 12-13, 2003

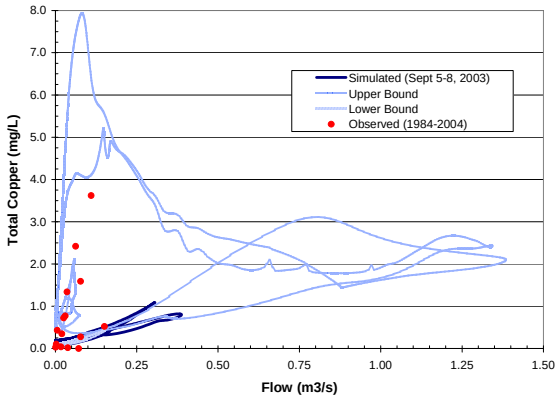

d) Total copper: September 5-8, 2003

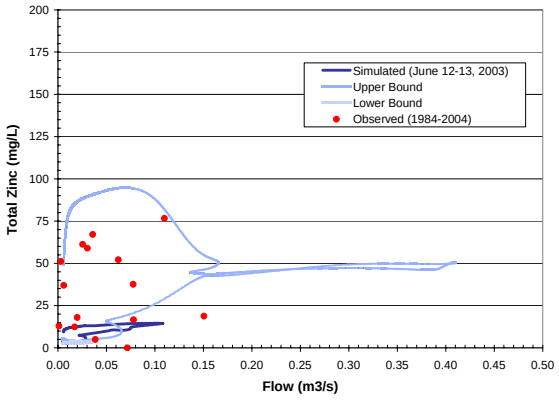

e) Total zinc: June 12-13, 2003

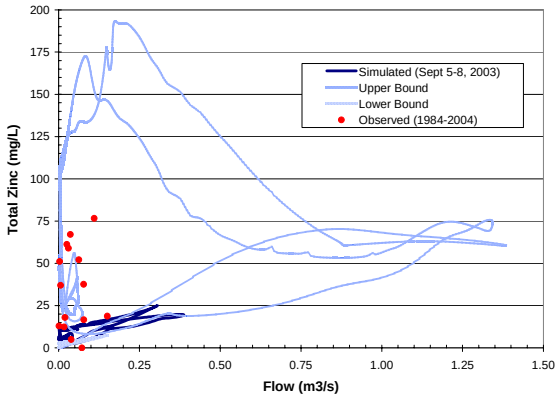

f) Total zinc: September 5-8, 2003

Figure D-3. Chemical transport uncertainty envelope at Station CG-4.

uncharacterized variability and uncertainty in the spatial and temporal distributions of rainfall. Differences between true rainfall conditions and those simulated will cause differences between observed and simulated stream flow. However, upper bound flows at all stations are much more than observed values for both the June and September events. This suggests that effective hydraulic conductivities cannot be much less than calibrated values without introducing a high bias into model results. Similarly, lower bound flows at all stations are considerably less than observed values for both the June and September events. This suggests that effective hydraulic conductivities cannot be much greater than calibrated values without introducing an appreciable low into model results.

The uncertainty assessment for sediment transport is more difficult to evaluate. Recalling that observed TSS concentrations are not paired in time with simulation conditions, it is difficult to make direct comparisons of between observed and simulated TSS values. Also note that the June and September 2003 events generated little overland flow because of the extent of infiltration in upland areas as 98% of all rainfall infiltrated. As a result, overland erosion during these events is very limited and it is difficult to demonstrate the full impact of soil erosion parameter uncertainty for these events. However, the initial fraction of silt and clay particles in stream bed sediments was zero so the presence of silt or clay particles in the stream network is an indications that some particle mass is transferred to streams from the overland plane. Therefore, sediment transport uncertainty can be at least partially characterized by considering the fine particle fraction. For this assessment, the clay fraction was examined. Once detached from the aggregate soil matrix, clay particles are easily transported. For upper bound flow conditions, significant erosion of clay occurs and, given the limited deposition flux for clay, much of clay mass eroded from the overland plane is exported from the watershed. Simulated maximum clay concentrations in stream channels for upper bound flows can exceed 50,000 mg/L at Station CG-1. Simulated maximum upper bound clay concentrations at other stations are less but can still exceed 10,000 mg/L. For lower bound flows, little clay erosion occurs and virtually no clay is exported. Again, since clay-sized particle originate only from the overland plane and are not present in the sediment bed at the start of the simulation, the

variation of simulated clay concentrations in the stream channel demonstrates the impact overland soil erosion parameters have on model results.

The uncertainty assessment for chemical transport is also complicated because observed metals concentrations are not paired in time with simulations conditions. However, where the sediment transport assessment depended largely on overland transport, metals transport depends on both overland and channel sediment transport. This permits a more complete assessment for metals. Model uncertainty envelopes for metals bracket the observed range of concentrations at each station. Note that metals concentrations for some mine waste types in the overland plane exceed initial metals concentrations in the sediment bed. As a result, for locations and conditions where there is significant sediment and metals input from the overland plane, the large variability present in some metals uncertainty envelopes may be a reflection of the impact sediment transport uncertainty has on metals transport. The overall uncertainty assessment nonetheless suggests that the calibration appropriately characterizes metals transport for California Gulch to the limit of available data.

APPENDIX E: EXPANDED DISCUSSION OF MODEL RESULTS

DISCUSSION

Overall model performance was judged to be quite reasonable. High quality data were available to construct and evaluate the hydrologic components of the California Gulch application. Other than the need to account for snow and ice conditions during the calibration period, model parameterization for the June and September 2003 events was identical. In terms of flow volumes, the average relative percent difference between simulated and observed values was -8.6% for the calibration (June) and +11.3% for the validation (September) events. Average model performance for the peak flow and time to peak metrics was also quite good as was summarized in Table 5.5. Data to evaluate the sediment and chemical transport components of the California Gulch application were less strong. Observed total suspended solids (TSS) and total metals concentration observations were collected over a small range of flows across a 20-year period. No time series concentration data are available for direct comparison to model results for the events simulated or any other period of record. Given this limitation of the database, only the range of observed and simulated concentrations could be meaningfully compared. In terms of these broad ranges, model performance was again considered to be quite reasonable. However, the model results suggest a stronger relationship between flow and concentration than is suggested by the observations. Also, chemical transport model performance has a low bias as the model tends to underestimate maximum total metals concentrations. Differences between simulated and observed conditions for hydrology, sediment transport, and chemical transport are related to numerous factors.

Soils within the watershed have very high infiltration capacities. As calibrated, roughly 98% of all rainfall infiltrates and relatively little overland flow is generated. Although the model calibration simulates channel flows well for both events, it is worth noting that calibrated K_h values are less than values that would be expected based on soil texture and grain size considerations alone. Calibrated K_h values range from 1.5×10^{-6} to 2.8×10^{-6} m/s (0.54 to 1.01 cm/hr). Based solely on texture, these values are in the range of sandy loam to silt loam soils (Rawls et al. 1983; Rawls et al. 1993). While generally applicable to the Leadville sandy loam soil type, values for mines areas could be greater due to the presence of larger particle sizes and rock fragments, which are often associated with

increased pore volume and pore size in soils. However, as demonstrated in Figure 5-18 to 5-21 use of larger effective K_h values resulted in simulated flows that were significantly less than observed values.

Several possible explanations for this exist. One possibility is that over time finer soil particles weathered from larger rock fragments have filled the void spaces in the soil matrix such that the infiltration characteristics of the overall soil aggregate are controlled by the finer soil particles. Another possibility is that water infiltrated on steep hillslopes travels through the soil as interflow and returns to the surface at some down gradient point. Considering the very steep slopes in parts of the watershed, this seems very reasonable. A third possibility is that water infiltrated on very porous, mined areas eventually reaches less porous, undisturbed soil layers that force the water to move laterally until it returns to the surface at the base of a waste pile. Given the extent of disturbed soils and mined wastes, this possibility also seems quite reasonable.

One of the challenges associated with the California Gulch model application is the potential for snow and ice. Given the high elevations within the watershed, which reach 3650 m (12,900 ft), it is possible for snow to fall at almost time of year. The Mine Pits and Dumps (MP), Troutville (TrE) and Bross (BrF) soil types are common at high elevations in the watershed. To account for the presence of snow and ice during the June 2003 storm, the effective hydraulic conductivities for these three soil types was reduced by 50%. While reasonable, this parameter adjustment may have been applied over too broad an area. In addition to their occurrence in the upper parts of the watershed, the MP and TrE soil types also occur at lower elevations. As a consequence, it is possible that the peak flow at the watershed outlet for the June storm was overestimated as a result of increased runoff from MP and TrE soil types at lower elevations where snow did not exist. Model performance for future model application efforts to California Gulch could be improved by further dividing the soil types into elevation classes. This would permit more refined application of parameter adjustments to account for snow. The TREX watershed model itself could be enhance by inclusion of a soil temperature index to control infiltration for snow and ice conditions.

Although representative of storm events that typically occur in the watershed, the June and September storm events were both relatively small. As a consequence of limited rainfall and the high infiltration capacity of the soils, little surface runoff is generated outside of urban areas with extensive impervious cover. The corresponding surface soil erosion and chemical transport is small. The model results suggest that most sediment reaching the watershed outlet originated from the sediment bed. Very little of the solids mass transported through the stream was transported from the overland plane and out the watershed outlet during these small events. Results for chemical transport are similar as model results suggest that most of the chemicals mass reaching the watershed outlet originated from the stream bed.

Because most sediment and chemicals transported during the calibration and validation events originate from the sediment bed rather than overland soils, the model is sensitive to the initial grain size and chemical distributions in the sediment bed. Sediment and chemical transport model performance can be improved by more detailed specification of these initial conditions. Unfortunately, compared to upland soils, relatively few sediment samples have been collected over time. Nonetheless, to better define bed grain size distributions, a series of sediment samples were collected in 2004. These samples indicated that grain distributions were highly variable and that no clear patterns existed. Pockets of finer particles (fine gravel, sand, and some smaller particles) were interspersed with coarser materials at some locations. As a result, it may be reasonable to include a greater fraction of finer particles in the initial bed grain size distribution. However, at some sites essentially no finer particles were present. Similarly, metals concentrations have been measured in comparatively few bed sediment samples. The few samples that were collected and analyzed for metals indicate that metals concentrations in sediments vary widely and depend on the extent to which flocs of metal precipitates occur (see WCC, 1993c). Given this degree of heterogeneity, further surveys of bed sediments to more quantitative define grain size and chemical distributions are warranted to improve the model application to the California Gulch site.

Relationships between observed TSS and metals concentration and flow in surface water are complex. Observed TSS values show some structure with flow and generally increase

and flow increases. However, observed metals concentrations show less structure. At least in the case of TSS, high concentrations at the lowest flows may indicate the presence of precipitated flocs of metal oxide or hydroxide compounds depending on pH, metals concentrations, and the concentrations of other ions. Precipitated flocs in suspension would be retained on the filters used to separate solids from whole water samples. In contrast, high metals concentrations could reflect the influx from of metals groundwater. Given that many metals samples were collected during spring snowmelt periods when groundwater inputs to the gulch tend to be largest, this seems reasonable. The possibility of significant groundwater inputs of metals is further supported by the observation that reported dissolved phase metals concentrations often equal total metals concentrations.

Despite the connection between surface water and groundwater and the likely input of metals from groundwater, the metals concentration boundary conditions for base flow were assigned zero concentrations. Because of the complexity of site hydrogeology, it is difficult to determine realistic, *a priori* metals base flow boundary concentrations because observations do not exist for the specific events simulated. Groundwater monitoring data could be used to assign boundary concentrations. However, the uncertainty of boundary values would be large. As a result of sorption and retardation during subsurface flow, concentrations at points of influx to the surface water system can be very different than observed at distant monitoring wells. While use of zero boundary concentrations contributes to the model's low bias for metals transport, this was judged to be preferable to use of alternative, potentially arbitrary non-zero values.

It is worth noting that the model uncertainty assessment was limited to consideration of parameter uncertainty. The additional uncertainty in model results attributable to the propagated uncertainty in forcing functions (such as the spatial and temporal patterns of rainfall) or initial and boundary conditions (like sediment grain size distributions or metals concentrations in base flow) is difficult to assess without a large number of model realizations. However, it should also be noted that uncertainty in forcing functions and boundary and initial conditions can be difficult to evaluate if the underlying spatial and temporal distributions are not known *a priori*.

LIMITATIONS AND RECOMMENDATIONS

While model application efforts were successful, some limitations of the framework are worth noting. In particular, it is worth noting that channel geometries specifiable as model input are limited to prismatic shapes: rectangular, trapezoidal, and triangular. It is also worth noting that only a single Manning n value can be assigned to a channel node or overland cell in the model. In contrast, natural channels often have irregular, compound forms. Significant differences in vegetation or other roughness elements can occur within a channel or adjacent floodplain areas. Further development of TREX to simulate irregular, compound channel cross sections with variable roughness is recommended.

Note that flows within California Gulch are typically small and are conveyed in small rills or low flow conveyance channels (LFCCs) incised within larger channels. During typical flow conditions, stream flow is controlled by the geometry and roughness of the LFCC. During larger floods, stream flow may be controlled by the geometry and roughness of the outer channel. Photographs of showing channel geometries within California Gulch are presented in Figure D-1. It is important to note the nature of chemical geometry and roughness relationships in the channel network because a model calibrated for low flow conditions may not be as accurate when simulating high flow conditions.

Buhman et al. (2002) describe an approach the permits description of irregular channel geometries through a set of power function parameters, Γ, that relate flow depth to cross-sectional area and hydraulic radius in the Manning equation for one-dimensional flow. In general, implementation of the Γ power function parameter set is recommended to further improve and extend the capabilities of the TREX watershed modeling framework. Despite the potential for model improvement, a limitation of the Γ parameter set is that functions for area and hydraulic radius work best for channels that do not have abrupt discontinuities in geometry such as occur in the California Gulch stream network. If TREX is extended to simulate irregular channel geometries, it would be further advisable to account for geometric discontinuities by use of piecewise continuous Γ parameter sets. Using this approach, one Γ set could be specified for flow depths less than the

a) Diffuse flow through low flow channel within a wide channel with armored banks.

b) Shallow flow through low flow channel within wider high flow channel.

c) Low flow channel with heavily vegetated high flow channel

Figure E-1. Compound channel forms within California Gulch.

discontinuity threshold elevation and a second Γ set for depths greater than the threshold. Different roughness (Manning n) values could also be specified for the channel above and below the discontinuity threshold to better represent the effect different substrates along the boundary of different parts of the floodway have on flow.

Beyond channel geometry and roughness considerations, it is worth noting that different algorithms are used to compute sediment transport capacities in the TREX framework.

Table E-1. Comparison of overland and channel sediment transport capacities.

$Q_{channel}$ (m3/s)	$v_{channel}$ (m/s)	h (m)	Engelund and Hansen Cw	Engelund and Hansen q_s (g/s)	$q_{overland}$ (m2/s)	Kilinc-Richardson q_s (kg/m/s)	Kilinc-Richardson q_s (g/s)
0.0001	0.03	0.001	8.83E-05	6.11E-03	2.31E-06	2.35E-04	7.05E+00
0.0004	0.07	0.003	3.17E-04	1.37E-01	1.44E-05	9.73E-03	2.92E+02
0.0032	0.16	0.01	1.28E-03	4.10E+00	1.06E-04	5.72E-01	1.72E+04
0.02	0.33	0.03	4.52E-03	8.91E+01	6.56E-04	2.31E+01	6.94E+05
0.14	0.70	0.1	1.70E-02	2.41E+03	4.67E-03	1.26E+03	3.77E+07
0.78	1.30	0.3	5.05E-02	4.08E+04	2.61E-02	4.16E+04	1.25E+09
4.36	2.18	1	1.25E-01	5.89E+05	1.45E-01	1.38E+06	4.13E+10
17.16	2.86	3	2.00E-01	3.92E+06	5.72E-01	2.23E+07	6.69E+11
23.9	2.99	4	2.16E-01	5.95E+06	7.96E-01	4.37E+07	1.31E+12
Conditions: Engelund and Hansen: $w_{channel}$ =2 m, Manning $n_{channel}$ = 0.05, d_s = 1 mm, S_f = 0.03 Kilinc-Richardson: $w_{overland}$ = 30 m, K = 0.15, C = 1.0, P = 1.0, S_f = 0.03							
Note: $Q_{channel}$ computed from Manning equation, overland unit flow ($q_{overland}$) computed as $Q_{channel}/w_{overland}$							

For the overland plane, including the overland portion of any cell that has a channel in it, the modified Kilinc-Richardson relationship (Eq. 2.26) is used. For channels, the (modified) Engelund and Hansen relationship (Eq. 2.27) is used. As presented in Table D-1, these relationships yield very different results when applied to the same flow conditions. When flooding occurs and flow is transferred from the channel portion of a cell to the overland plane, even a small overland flow can produce a very large transport capacity and lead to significant erosion of the floodplain adjacent to the channel.

As part of their research, Kilinc and Richardson (1973) conducted a series of erosion experiments with bare soils for a range of rainfall-driven flows and slopes. Flows depths were not directly measurable but were inferred based on continuity. The maximum flow depth for these erosion experiments was never more than 1.0 mm. From this it may be reasonable to infer a maximum flow depth condition exists when applying the Kilinc-Richardson relationship. However, it should be noted that flow depth alone may not be an

adequate criterion to guide application of this relationship because transport capacities computed from the Kilinc-Richardson equation depend on unit flow (q) and friction slope (S_f) rather than flow depth.

A more limiting threshold to consider may be the rate at which rainfall or flow can detach individual grains from the bulk soil matrix. In their experimental work, Kilinc and Richardson used bare, disturbed sandy soil as a test substrate. In effect, all erosion experiments were conducted under conditions of infinite sediment supply. In a natural setting, soils may show far more erosion resistance than this test substrate due to vegetative cover, roots, and particle cohesion. If sediment supply is limited, overland soil transport rates will be limited to the rate of grain detachment. Under such supply limited conditions, the transport capacity relationship may not be applicable. Further assessment and identification of limiting conditions or thresholds for application of the Kilinc-Richardson sediment transport capacity relationship are recommended, especially when used in floodplain regions.

Although the model calibration provides a reasonable description of conditions across the California Gulch watershed for the events simulated, it should be recognized this calibration is not necessarily optimal or unique. Because it is fully distributed, each overland cell and channel node within the model can be assigned different values for each model parameter. Within the California Gulch watershed model domain there are 34,002 overland cells and 1,395 channel nodes. Even if limited to the five sensitive parameters identified as part of the uncertainty analysis, across the entire model domain there are more than 170,000 parameters values that can be varied as part of calibration. As a consequence of the overwhelming number of potential parameters involved, tools to automate the parameter estimation process are needed to further explore the robustness of model calibration.

Numerous approaches to estimate optimal model parameters sets exist and include Monte Carlo, Kalman filters, genetic algorithms, and other response gradient search techniques. One tool of particular relevance to parameter estimation is PEST (Doherty, 2001a,b). PEST is a stand-alone parameter estimation tool that can evaluate the optimality of

watershed model applications (Doherty and Johnston, 2003). Calibration optimality is assessed by objective functions defined to quantitatively characterize model performance and predictive error (Loehle, 1997; Loehle and Ice, 2002; Doherty and Johnston, 2003, Moore and Doherty, 2005). Despite the relevance of PEST or other tools, multiple model realizations are typically needed for optimization. This can be problematic when the time required to generate a realization is long. Further, the optimality of any parameterization does not ensure that the calibration is unique as multiple parameterizations that minimize objective function error may exist. Nonetheless, adaptation of PEST to operate with TREX is recommended to provide an improved means to more efficiently calibrate and establish the predictive uncertainty of watershed model applications.

When considering overall model performance, it is important to recall that the goal of the California Gulch application was to demonstrate that the TREX modeling framework can be used to successfully simulate chemical transport at the watershed scale. Independent of specific detail regarding the degree of calibration optimality, the goal of the model application effort was achieved. The model was able to accurately reproduce observed conditions across the site. Where high quality data exist, model performance is excellent. Even where less detailed information exists, the model was nonetheless able to reproduce the range and basic trends of observations for this complex site. The success of the model application demonstrates that TREX is a viable tool for simulating chemical transport at the watershed scale.